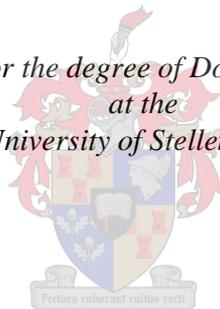# Differential tolerance of a cancer and a non-cancer cell line to amino acid deprivation: mechanistic insight and clinical potential

by
Mark Peter Thomas

Dissertation presented for the degree of Doctor of Philosophy of sciences
at the
University of Stellenbosch

Promoter: Prof. Anna-Mart Engelbrecht
Co-promoter: Prof. Hans Strijdom
Faculty of Science
Department of Physiological sciences

March 2012

Declaration

By submitting this dissertation electronically, I declare that the entirety of the work contained therein is my own, original work, that I am the owner of the copyright thereof (unless to the extent explicitly otherwise stated) and that I have not previously in its entirety or in part submitted it for obtaining any qualification.

March 2012

Abstract

Introduction – Due to spatial separation from the native vascular bed, solid tumours develop regions with limited access to nutrients essential for growth and survival. The promotion of a process known as macroautophagy may facilitate in the maintenance of intracellular amino acid levels, through breakdown of cytoplasmic proteins, so that they remain available for macromolecular biosynthesis and ATP production. Several studies point to the potential ability of some cancers to temporarily increase autophagy and thereby prolong cell survival during metabolic stress. The validity of these claims is assessed when a commonly used breast cancer cell line and an epithelial breast cell line are starved of amino acids in this study. Furthermore, we go on to hypothesize that acute amino acid deprivation during treatment will result in an elevated sensitivity of MDAMB231 cells to doxorubicin toxicity but limit its cytotoxic side-effects in MCF12A cells.

Methods and study design- Human breast cancer cells (MDAMB231) and breast epithelial cells (MCF12A) cultured in complete growth medium were compared to those incubated in medium containing no amino acids. Steady state autophagy levels were monitored using classical protein markers of autophagy (LC3-II and beclin-1) and the acidic compartmentalization in cells (Lysotracker™ red dye) in conjunction with autophagy inhibition (bafilomycin A1 and ATG5 siRNA). Cell viability was monitored using several techniques, including caspase 3/7 activity. ATP levels were assessed using a bioluminescent assay, while mass spectrometry based proteomics was used to quantify cellular amino acid levels. Similar techniques were used to monitor autophagy during doxorubicin treatment, while cellular doxorubicin localization was monitored using immunofluorescence microscopy. Finally, a completely novel GFP-LC3 mouse tumour model was designed to

assess autophagy and caspase activity within tumours *in vivo*, during protein limitation and doxorubicin treatment.

Results - Amino acid deprivation resulted in a transient increase in autophagy at approximately 6 hours of amino acid starvation in MDAMB231 cells. The amino acid content was preserved within these cells in an autophagy-dependent manner, a phenomenon that correlated with the maintenance of ATP levels. Inhibition of autophagy during these conditions resulted in decreased amino acid and ATP levels and increased signs of cell death. MCF12A cells displayed a greater tolerance to amino acid starvation during 24 hours of amino acid starvation. Evidence indicated that autophagy was important for the maintenance of amino acid and ATP levels in these cells and helped prevent starvation-induced cell death. Furthermore, data showed that concomitant amino acid withdrawal resulted in decreased cellular acidity in MDAMB231 cells, and increased acidity in MCF12A cells, during doxorubicin treatment. These changes correlated with evidence of increased cell death in MDAMB231 cells, but a relative protection in MCF12A cells. A novel model was used to apply these techniques *in vivo*, and although mice fed on a low protein diet during high dose doxorubicin treatment had increased mean survival and smaller tumour sizes, evidence suggested that autophagy is protecting a population of cells within these tumours.

Conclusions - This novel approach to tumour sensitization could have several implications in the context of cancer therapy, and given the delicate relationship that autophagy has with the cancer microenvironment, efforts to determine the mechanisms involved in autophagy and sensitization could lead to new and innovative treatment opportunities for cancer management.

Opsomming

Inleiding – As gevolg van hul skeiding van die oorpronklike vaskulêre netwerk, ontwikkel soliede gewasse areas met beperkte toegang tot noodsaaklike voedingstowwe. Die bevordering van „n proses wat as makro-autofagie bekend staan, kan die handhawing van intrasellulêre aminosuur vlakke fasiliteer. Voorafgenoemde proses word waarskynlik deur die afbreek van sitoplasmiese proteïene teweegebring om sodoende vir makro-molekulêre biosintese en ATP produksie beskikbaar te kan wees. Verskeie studies dui daarop dat sommige kankersoorte die vermoë het om autofagie tydelik te verhoog, en daarby sel oorlewing gedurende metaboliese stress te verleng. Die geldigheid van hierdie eise word evalueer wanneer „n algemeen beskikbare borskanker sellyn, en „n borsepiteelsellyn in hierdie studie van aminosure verhonger word. Verder, veronderstel ons dat akute aminosuur ontneming gedurende behandeling „n verhoogde sensitiwiteit van MDAMB231 selle tot doxorubicin toksisiteit tot gevolg sal hê, maar terselfdetyd die middel se sitotoksiese newe-effekte in MCF12A selle sal beperk.

Metodes en studie ontwerp – Menslike borskanker- (MDAMB231) en bors epiteel selle (MCF12A) wat in volledige groeimedium gekweek is, is vergelyk met selle wat in aminosuur vrye medium gekweek is. Basislyn autofagie-vlakke is gemonitor deur die gebruik van klassieke autofagie proteïen merkers (LC3-II en beclin-1) en die asidiese kompartementalisering in selle (Lysotracker™ rooi kleurstof) saam met autofagie inhibisie (bafilomycin A1 and ATG5 siRNA). Sellewensvatbaarheid is deur die gebruik van verskeie tegnieke, insluitend caspase 3/7 aktiwiteit, gemonitor. ATP-vlakke is deur die gebruik van „n bioluminiserende tegniek gemeet, terwyl massa-spektrometrie-gebaseerde "proteomics" gebruik is om sel aminosuur vlakke te kwantifiseer. Soortgelyke tegnieke is gebruik om autofagie gedurende doxorubicin behandeling waar te neem, terwyl sellulêre doxorubicin

lokalisasie deur die gebruik van immunofluoresensie mikroskopie gemonitor is. Ten slotte, is „n unieke GFP-LC3 muismodel in hierdie studie ontwikkel. Hierdie model is gebruik om autofagie en caspase aktiwiteit in gewasse *in vivo* te bestudeer tydens proteïen beperking en doxorubicin behandeling.

Resultate – Aminosuur ontneming het tot „n tydelike verhoging in autofagie na ongeveer 6 ure van aminosuur verhongering in MDAMB231 selle gelei. Die aminosuur inhoud van hierdie selle het op „n autofagie-afhanklike manier behoue gebly. Hierdie verskynsel het met die handhawing van ATP-vlakke gekorreleer. Autofagie inhibisie gedurende hierdie kondisies het „n verlaging in aminosuur en ATP-vlakke teweeggebring, sowel as vermeerderde tekens van seldood tot gevolg gehad. MCF12A selle het „n groter toleransie tot aminosuur verhongering tydens die 24 uur aminosuur verhongeringsperiode getoon. Getuienis het aangedui dat autofagie belangrik vir die handhawing van aminosuur en ATP-vlakke in hierdie selle was, en gehelp het om verhongerings-geïnduseerde seldood te voorkom. Verder het data gewys dat aminosuur ontrekking tot verminderde sellulêre asiditeit in MDAMB231 selle, en verhoogde asiditeit in MCF12A selle gedurende doxorubicin behandeling gelei het. Hierdie veranderinge stem ooreen met getuienis van toenemende seldood in MDAMB231 selle, maar „n relatiewe beskerming in MCF12A selle. „n Unieke model was gebruik om hierdie tegnieke *in vivo* toe te pas. Alhoewel verhoogde oorlewing en kleiner gewasse in muise op „n lae proteïen dieet gedurende hoë dosis doxorubicin behandeling opgemerk is, het bewyse voorgestel dat autofagie „n populasie selle binne die gewasse beskerm.

Gevolgtrekkings – Hierdie unieke benadering tot tumor sensitisering kan verskeie implikasies in die konteks van kanker behandeling hê. Gegewe die delikate verhouding van autofagie met die kanker mikro-omgewing, kan pogings om die meganismes betrokke in autofagie en sensitisering te bepaal, tot nuwe en innoverende behandelings vir kanker lei.

Acknowledgements

I am sincerely indebted to the following (as well as many others not mentioned here).

Primarily to my sweet Celeste. I am grateful mostly for you. Not only for your omnipresent support, but for myriad other small acts and seemingly insignificant instances that ultimately add up to so much more.

P. Thanks for everything, especially your unparalleled selflessness.

The Fouché family for their unwavering support and kindnesses, and my own immediate family and friends, both present and past, for their support.

Special thanks to my supervisor. Anna-Mart, thank you for the countless opportunities and subtle guidance and support. You always displayed true kindness, even when faced with stubborn and all-to unappreciative students.

My friends and colleagues in the department, both current and former, for creating the labs a pleasurable place to spend every day. Particular thanks to Helöise „H‟ Le Roux and Justin Mills for assistance with the animal model, and of course to Clare Springhorn for being such a help (and a burden), but most of all for being a true friend.

For technical assistance and support, acknowledgement must go to:

Dr. Benjamin Loos, Dr. Rob Smith, Lize Bruwer, Dr. Theo Nell, Jamie Imbriolo, Dr. Ruhan Slabbert, Dr. Marietjie Stander, Prof. Barbara Huisamen and Prof. Hans Strijdom,

Table of Contents

Chapter 1

The comparative impact of acute amino acid starvation on growth and survival of a metastatic breast cancer cell line (MDAMB231) and a non-tumourogenic breast cancer cell line (MCF12A).

Chapter 2

Autophagy is vital for the prevention of cell death and growth arrest during the first hours of amino acid starvation in MDAMB231 and MCF12A cells.

Chapter 3

Autophagy is essential for the maintenance of amino acids and ATP levels during acute amino acid starvation in MDAMB231 and MCF12A cells.

Chapter 4

Changes in lysosomal acidity due to amino acid starvation are associated with susceptibility to doxorubicin mediated cell death in MDAMB231 and tolerance in MCF12A cells.

Chapter 5

Development of a novel *in vivo* mouse mammary cancer model to study autophagy in the non-cancer cell population of the tumour and apoptosis within the whole tumour.

Chapter 6

Short term protein starvation results in increased tolerance to high dose chemotherapy but also increased autophagy flux and decreased apoptosis within tumours *in vivo*.

Chapter 7

List of Figures

Chapter 1

Chapter 2

Fig. 2.1 Bafilomycin significantly decreases the capacity of MCF12A cells to reduce MTT to formazan during a 24 hour period of amino acid deprivation.

Fig. 2.2 Bafilomycin (10 nM) significantly diminishes the capacity of MDAMB231 cells to reduce MTT to formazan during only the first 12 hours of total amino acid deprivation.

Fig. 2.3 Bafilomycin (10 nM) has no effect on the capacity of MCF7 cells to reduce MTT to formazan during a 24 hour period of total amino acid deprivation.

Fig. 2.4 Rapamycin ameliorates the drop in the MTT reductive capacity of MDAMB231 cells but not in MCF12A cells during a 24 hour period of total amino acid deprivation.

Fig. 2.5 MDAMB231 cells display significantly increased caspase 3/7 activity at 6 and 12 hours of amino acid starvation if bafilomycin A1 (10 nM) is present during that period.

Fig 2.6 MCF12A cells display significantly increased caspase 3/7 activity at 24 hours of amino acid starvation if bafilomycin (10 nM) is present during that period.

Fig. 2.7 A significant percentage of MDAMB231 cells become trypan blue positive following 6 hours of amino acid deprivation if bafilomycin (10 nM) is present.

Fig. 2.8 A significant percentage of MCF12A cells become trypan blue positive after 24 hours of amino acid deprivation if bafilomycin (10 nM) is present.

Fig. 2.9 Lysosomal acidity peaks at 6 hours of total amino acid deprivation of MDAMB231 cells.

Fig. 2.10 A significant elevation in lysosomal acidity is observed in MCF12A cells during total amino acid deprivation.

Fig. 2.11 A significant elevation in lysosomal acidity is observed in MCF7 cells only after 24 hours of total amino acid deprivation.

Fig. 2.12 Change in protein levels of the autophagy marker LC3 II in MCF12A and MDAMB231 cells after 24 hours of complete amino acid starvation.

Fig. 2.13 Change in protein levels of the autophagy markers LC3 and beclin 1in MCF12A cells during a 24 hour period of amino acid starvation.

Fig. 2.14 Change in protein levels of the autophagy markers LC3 and beclin 1in MDAMB231 cells during a 24 hour period of amino acid starvation.

Fig. 2.15 Change in protein levels of the autophagy markers LC3 and beclin 1in MCF7cells during a 24 hour period of amino acid starvation.

Fig. 2.16 Change in flux of LC3 II in MDAMB231 cells during a 24 hour period of amino acid starvation.

Fig. 2.17 Change in flux of LC3 II in MCF7cells during a 24 hour period of amino acid starvation.

Chapter 4

Fig. 4.13 An elevation in lysosomal acidity is observed in MCF12A cells during a 24 hour treatment with doxorubicin (1 μM).

Fig. 4.14 The elevation in lysosomal acidity observed in MDAMB231cells during a 24 hour treatment with doxorubicin (1 μM) is mostly abolished if amino acids are absent from culture medium.

Fig. 4.15 MCF12A cells treated with doxorubicin (1 μM) are partially protected from apoptosis initiation if amino acids are absent from culture medium during treatment.

Fig. 4.16 Treatment of MDAMB231 cells with doxorubicin (1 μM) results in increased caspase 3/7 activity if amino acids are absent from culture medium for 24 hours but not 12 hours.

Fig. 4.17 Treatment of MCF12A cells with doxorubicin (1 μM) during 24 hours of amino acid deprivation partially prevents alterations to the cell cycle.

Fig. 4.18 Treatment of MDAMB231 cells with doxorubicin (1 μM) during 24 hours of amino acid deprivation leads to an increased g2/m phase and a decreased s phase.

Fig. 4.19 MCF12A cells treated doxorubicin (1 μM) in the absence of amino acids show no signs of increased intracellular doxorubicin but appear to possess areas of increased LAMP-2A pooling.

Fig. 4.20 MDAMB231 cells treated with doxorubicin (1 μM) in culture medium without amino acids or with ATG5 siRNA appear to contain high intracellular levels of doxorubicin.

Fig. 4.21 No changes in lysosomal acidity are observed in MCF7 cells during a 24 hour treatment with doxorubicin (1 μM) with or without amino acids.

Fig 4.22 MCF7 cells do not express caspase 3. Western blots confirm that MCF7 cells do not possess active caspase 3.

Fig. 4.23 Doxorubicin (1 μM) treatment increases apoptosis in MCF7 cells.

Chapter 5

Fig. 5.1 Change in protein levels of the autophagy markers LC3 and beclin 1in E0771cells during a 6hour period of amino acid starvation.

Fig. 5.2 Change in tumour volume.

Fig. 5.3 Internal view of E0771 tumours in GFP-LC3 mice.

Fig. 5.4 Histological sections of a central portion of a E0771 tumour from a C57BL6 mouse and a GFP-LC3 mouse depicting the basal level of GFP LC3 signal.

Fig. 5.5 Basal intratumour GFP signal is lower in C57BL6 mice than in GFP-LC3 mice.

Fig. 5.6 Autophagy response in the gastrocnemius muscles of GFP-LC3 mice that have been placed on a protein free diet.

Fig. 5.7 Intratumour GFP fluorescence signal is significantly increased in GFP-LC3 mice that have been placed on a protein free diet for 24 hours.

Fig. 5.8 Intratumour caspase cleavage is significantly increased in GFP-LC3 mice after being placed on a protein free diet for 24 hours.

Chapter 6

Fig. 6.1 24 hour protein starvation protects against high-dose chemotherapy *in vivo*.

Fig. 6.2 Change in tumour volumes during doxorubicin (10 mg/kg) treatment either with or without proteins in the diet.

Fig. 6.3 Change in tumour volumes after treatment with doxorubicin (10 mg/kg) either with or without proteins in the diet.

Fig. 6.4 Intratumour caspase cleavage is significantly lower if GFP-LC3 mice treated with doxorubicin (10 mg/kg) are placed on a protein free diet during treatment.

Fig. 6.5 Doxorubicin does not interfere with the signal generated from the FLIVO™ caspase dye.

Fig. 6.6 Intratumour autophagy flux increases if GFP-LC3 mice treated with doxorubicin (10 mg/kg) are placed on a protein free diet during treatment.

Fig. 6.7 Change in tumour volumes after treatment with doxorubicin (5 mg/kg) either with or without proteins in the diet.

Fig. 6.8 Intratumour caspase cleavage is significantly lower if GFP-LC3 mice treated with doxorubicin (5 mg/kg) are placed on a protein free diet during treatment.

Fig. 6.9 Intratumour autophagy flux increases if GFP-LC3 mice treated with doxorubicin (5 mg/kg) are placed on a protein free diet during treatment.

Fig. 6.10 Change in tumour volumes after treatment with doxorubicin (10 mg/kg) either with or without a rapamycin (2 mg/kg) injection.

Fig. 6.11 Rapamycin protects against high-dose chemotherapy *in vivo*.

List of Images

Image 5.2 Diagrammatic depiction of experimental procedure and tumour developmental timeline.

Image 5.3 Typical tumour of approximately 230 mm^2 in volume just prior to the initial intervention.

Image 5.4 Tumour in a GFP-LC3 mouse, 33 days after injection with a E0771 cell suspension, illustrating neovascularisation and the position of the second left abdomino-inguinal nipple.

Chapter 6

Image 6.1 Diagrammatic depiction of experimental procedure.

List of Tables

Chapter 4

List of talks and congress contributions

International

Thomas MP, Engelbrecht AM. Sensitization of breast cancer to chemotherapy by means of autophagy manipulation. 8th International AORTIC Conference, Cairo, Egypt, 2011

Thomas MP, Engelbrecht AM. Autophagy as a mechanism for sensitization of breast cancer cells to doxorubicin. Cancer and metabolism: pathways to the future, Edinburgh, Scotland, 2010

Thomas MP. To live or survive by autophagy? University of Bergen: Cardiovascular research group, Bergen, Norway, 2009

National

Thomas MP, Engelbrecht AM. Amino acid deprivation and doxorubicin toxicity in breast cancer. The 39th annual congress of Physiological Society of Southern Africa, Cape Town, South Africa, 2011 (peer reviewed abstract to be published)

Thomas MP, Engelbrecht AM. Autophagy sensitization in breast cancer: Turn it on baby! But how much? 38th annual congress of Physiological Society of Southern Africa, Port Elizabeth, South Africa, 2010

Adam F, **Thomas MP**, Engelbrecht AM. Increased autophagy due to amino acid starvation leads to an increase in free fatty acids and amino acids in human breast cancer cells. The 38th

annual congress of Physiological Society of Southern Africa, Port Elizabeth, South Africa, 2010

Loos B, Engelbrechet AM, **Thomas MP**. Take autophagic flux control and consider what the cell demands. The 37th annual congress of Physiological Society of Southern Africa, Stellenbosch, South Africa, 2009

Thomas MP. Oncology's appeal to autophagy. University of Stellenbosch Medical Campus, Tygerberg, South Africa, 2009

List of abbreviations

18F-FdG PET	Positron-emission tomography imaging with 18fluorodeoxyglucose
2DG	2 Deoxy-Glucose
4E-BP1	4E binding protein
Ala	Alanine
AMP	Adenosine Monophosphate
AMPK	AMP-activated protein kinase
Ang-2	Angiopoietin-2
Arg	Arginine
Asp	Aspartic acid
ATG	Autophagy Related Genes
ATP	Adenosine Triphosphate
BCKDH	Branched chain keto acid dehydrogenase
BCL	B Cell Lymphoma
Con	Control
Cys	Cystein
DAMPs	Damage-Associated Molecular Pattern Molecule(s)
DMEM	Dulbecco‟s Modified Eagle‟s Medium
DNA	Deoxyribonucleic Acid
DSR	Differential Stress Resistance
ECACC	European Collection of Cell Cultures
EDTA	Ethylenediaminetetraacetic Acid
EGF	Endothelial Growth Factor
ER	Endoplasmic Reticulum
ES	Embryonic Stem cells
FACS	Fluorescence-activated cell sorting

FdG	Fluorodeoxyglucose
FITC	Fluorescein isothiocyanate
FLIVO™	FLuorescence in vIVO
GLC	Gas Liquid Chromatography
Gln	Glutamine
Glu	Glutamic acid
Gly	Glycine
HEPES	4-(2-hydroxyethyl)-1-piperazineethanesulfonic acid
HIF	Hypoxic Inducible Factor
His	Histidine
HMGB1	High Mobility Group Box 1
IGF	Insulin-like Growth Factor
IL-3	Interleukin 3
Ile	Isoleucine
LAMP	Lysosomal Associated Membrane Protein
LC3	Light Chain 3
Leu	Leucine
Lys	Lysine
Met	Methionine
mTOR	mammalian Target Of Rapamycin
MTT	3-(4,5-dimethylthiazol-2-yl)-2,5-diphenyltetrazoliumbromide
NAC	N-Acetyl cysteine
NO	Nitric Oxide
PAGE	Polyacrylamide Gel Electrophoresis
PARP	Poly (ADP-ribose) polymerase enzyme
PBS	Phosphate Buffered Saline

PE	Phosphatidylethanolamine
PGE$_2$	Prostaglandin E$_2$
Phe	Phenylalanine
PI3K	Phosphatidylinositol 3-Kinase
PMSF	PhenylMethylSulfonyl Fluoride
Pro	Proline
PTEN	Phosphatase and tensin homologue deleted on chromosome ten
PTP	Permeability Transition Pore
PVDF	Polyvinylidine Fluoride
RAS	RAt Sarcoma
REDD	DNA-damage-inducible transcript
Rheb	Ras homolog enriched in brain
RIPA	Radioimmunoprecipitation
Rpm	revolutions per minute
S6K	S6 kinase
SDS	Sodium Dodecyl Sulphate
SEM	Standard Error of the Mean
Ser	Serine
siRNA	small interfering Ribonucleic Acid
STS	Short Term Starvation
TBS	Tris Buffered Saline
TBS-T	Tris Buffered Saline- Tween20
TCA	The Citric Acid
Thr	Threonine
TOR	Target Of Rapamycin
TSC	Tubular Sclerosis Proteins

Tyr   Tyrosine

UPS   Ubiquitin Proteasome System

UVRAG   UV radiation resistance-associated gene

Val   Valine

V-ATPase   Vacuolar H+ATPase

VEGF   Vascular Endothelial Growth Factor

Preamble _____

It seems a strange concept to me to have to justify my choice of research topic with statistics. Almost everyone of a certain age will be confronted with the spectre of cancer in one of its nefarious guises at some point, either indirectly or, less happily, personally. For women, this will most likely take its form as a breast cancer. Despite many well-intentioned efforts, the number of breast cancer sufferers worldwide appears to be increasing, and breast cancer is now the most prevalent form of cancer in woman today. Cancer is an inevitable corollary to the medical advances that now permit human life-spans to surpass their evolutionarily programmed limits. Women in the United States have a 1 in 8 chance of developing breast cancer at some point in their lifetime, and 1.3 million diagnosed cases of this form of cancer were reported worldwide in 2010 (Breastcancer.org, September 2010). In South Africa, breast cancer has also now taken the lead in the race to be the most prevalent cancer variety, and population forecasts estimate that the incidence of breast cancer in the South African population will have increased by 15.8% in 2015 (UN, World Population prospects, 2008). These statistics are alarming and finding practical solutions to improve breast cancer treatment is imperative.

The studies contained within this thesis are presented in separate chapters, each a product, and contingent on the findings, of the last. Therefore, the layout of this manuscript more or less follows the sequence in which the experimental work (and hence these studies) were performed.

The concept for the first chapter presented here was conceived in the tradition of hypothesis-driven research, which is to say essentially at random, in conjunction with a pragmatic

awareness of the limitations of our laboratory and the resources at our disposal. This initial work characterizes the impact of complete amino acid starvation on a commonly used human breast cancer cell line in comparison to a non-tumourogenic human breast epithelial cell line. Based on the findings from this study, a second study (presented in chapter 2) was undertaken to determine the role of a proteolytic process known as autophagy during these conditions. As increased autophagy is often described (but never directly shown) to preserve amino acid and ATP levels in cancer cells during circumstances of nutrient depletion, a third study (presented in chapter 3) was performed in an attempt to directly demonstrate these phenomena in the context of amino acid deprivation, and thereby pose a mechanism for the autophagy-dependent protection that was revealed in the previous two studies.

Unfortunately, cancer is an actual disease (or more accurately, a cluster of genetic diseases with similar phenotypes), and studies such as those presented in the first three chapters, while scientifically significant, appeal more to those unfortunate enough to have decided to combine their curious nature with more academic interests than those hoping to find real and effective means to combat cancer. With this important reality in mind, and armed with data from our first three studies, our amino acid deprivation protocol was applied in combination with the administration of a chemotherapy drug (doxorubicin) to cancer cells and non-cancer cells. Finally, a novel *in vivo* model was developed (described in chapter 5) and utilized to apply certain aspects of our *in vitro* findings into a living animal with a tumour (described in chapter 6).

2

1 _____

The comparative impact of acute amino acid starvation on growth and survival of a metastatic breast cancer cell line (MDAMB231) and a non-tumourogenic breast cancer cell line (MCF12A)

The genetic diversity of tumour forming cancers is proving to be far greater than first believed, and research investigating approaches that target phenotypic characteristics common to a wide range of cancers could prove beneficial when developing therapeutic regimes aimed at a broader range of malignancies. The safety and apparent effectiveness of strategies employing controlled amino acid starvation of cancer patients has exposed a potentially feasible and reproducible therapeutic intervention approach. The effects of a short term cessation of the external amino acid supply in a tumourogenic and a non-tumourogenic cell culture model are assessed in this chapter. Data presented here demonstrates that a fast growing, metastatic cancer cell line is more sensitive to a dearth of amino acids than a non-tumourogenic line and that short term deprivation of amino acids results in increased cell death and proliferation arrest in these cells.

1   Introduction

Cancer is a cluster of genetic diseases with a phenotype manifesting in unbridled cellular growth, but of the purported hallmarks of cancer, only the metastatic potential of cancerous neoplasms can be used to differentiate malignant from benign tumours. All cancer tumours contain several mutations of low frequency, and recent evidence continues to demonstrate huge variation in number and frequency of cancer mutations (Wadman, 2011) which suggests a need for further development in the field of phenotypic screening to complement the enormous investment placed in targeted drug approaches. Not only is this tactic unconstrained

3

to prior knowledge of biological mechanisms and pathways directing the processes behind cancer, but it has the potential to uncover previously unknown treatment perspectives.

1.2   Targeting breast cancer

Fortunately, advances in early detection using screening and mammography have resulted in significant reductions in mortality rates in breast cancer patients. Despite this progress the lifetime risk of developing breast cancer for western women is approximately one in eight, with approximately 1.3 million newly diagnosed breast cancer cases expected in 2010 (Breastcancer.org, September 2010). Breast cancer is now the most prevalent form of cancer among women, and in the South African context, cancer of the breast is the leading cancer in females in terms of both incidence and mortality. Alarmingly, this trend is set to continue with population forecasts indicating that the future burden of breast cancer in the South African population, in terms of incidence, will have grown by 15.8% in 2015 (extracted from the United Nations, World Population prospects, the 2008 revision).

1.3   Targeting cancer

Current desires to implement personalized medicine for cancer sufferers are hindered by a lack of useful cancer biomarkers. In fact, no new major cancer biomarkers have been validated for clinical use in over two decades (Diamandis, 2010). Technological advances and reduction in the costs associated with genotyping have allowed genome-wide association studies to identify several polymorphisms associated with cancer risk (Hicks et al., 2011). However, while these avenues promise to impact considerabley impact on the future of cancer treatment, the inevitable accumulation of mutations during progression to advanced tumour status confer a level of uniqueness to heterogeneous cancer populations. Unfortunately, it is

this unique nature of tumour genetic profiles that renders personalized approaches to cancer therapy a mere prospective solution at present (Schreiber et al., 2011). Therefore, finding practical solutions to rapidly facilitate improvement of current cancer treatments is imperative. Despite their genetic variability, environmental constraints imposed on fast growing cancers result in characteristic tumour microenvironments and hence analogous features in many tumours. Strategies that focus on these common attributes of solid tumours, and aim at improving our understanding of how cancer tumours manage to maintain exponential growth during times of metabolic stress, could be used to exploit the cancer metabolome and be directed at a broader range of genetically dissimilar cases (Gatenby and Gillies, 2004).

1.3   Amino acid manipulation in the management of tumour progression

Regulation of protein intake is seen as essential both during all stages of cancer progression and following successful treatment (Doyle et al., 2006). This is reflected in the nutritional recommendations from the American Cancer Society which stipulate that those with cancer be placed on diets high in protein content, both during and after treatment, in order to maintain healthy amino acid precursor pools (Lee and Longo, 2011). Indeed, cancer patients are known to present with abnormal plasma free amino acid profiles that appear to vary depending on cancer type (Cascino et al., 1995, Lai et al., 2005). Unfortunately, attempts to characterize the profiles of these amino acid imbalances in order to discriminate between the variants of cancer have not been altogether successful (Maeda et al., 2010).

Biosynthesis of proteins requires that they be constructed in the precise arrangement of amino acids necessary to dictate their folding into functioning molecules. As peptides and proteins represent the major functional and structural proportion of cells, a continuous assimilation of

amino acids from the external environment is necessary for mammalian cells to continue this synthesis. Furthermore, tumour expansion also depends on proteins (and therefore on amino acids) for the production of tumour structural elements and growth factors needed for angiogenesis (Holm et al., 1995). One might therefore consider that the rapid growth of cancerous tumours imposes a need for a precursor pool of amino acids large enough to satisfy their needs during this protein and DNA assemblage.

Conventional therapies for victims of malignant tumours typically involve some combination of ionizing radiation, chemotherapy and surgery, all of which are associated with negative side effects. Utilization of amino acids in a clinical context could provide a safe alternative or adjuvant for the management of cancer metastasis and progression.

1.3.1 Amino acid supplementation in the management of cancer progression

It is evident that fast growing cell populations require a high amino acid supply in order to continue proliferating, and therefore many studies have attempted to starve cancers of amino acids as a potential therapeutic strategy (discussed in the next section). It seems counterintuitive to suggest that maintaining or complementing the amino acid pool of cancer patients by means of supplementation would have a negative impact on amino acid hungry tumours, but several studies have demonstrated that augmenting the levels of specific amino acids do in fact have negative consequences in some cancers. For instance, derivatives of the amino acid L-cysteine are known to impact angiogenesis and tumour invasion (Morini et al., 1999). N-Acetyl cysteine (NAC) causes a decrease in proliferation in several colorectal adenocarcinoma cell lines that is associated with decreased cell surface expression of type one IGF-R, which is important in proliferation and prevention of apoptosis (Kelly et al., 2002).

NAC supplementation also affects cellular mechanisms that are important in contributing to the metastatic potential of melanoma (Tosetti et al., 2002) and bladder cancer cells (Kawakami et al., 2001). NAC has further been shown to reduce tumour size and the presence of angiogenic markers (Albini et al., 2001) and induce apoptosis/necrosis and vascular collapse (Agarwal et al., 2004) in mouse sarcoma and breast tumour xenografts, respectively.

Glutamine is the most abundant amino acid in the body, and it is essential for cellular growth in tumours (Souba, 1993). In fact, some cancers can be described as "glutamine traps" (Souba, 1993) due to the net mobilization of glutamine toward tumour regions (Carrascosa et al., 1984). Therefore, despite the obvious nutritional benefit provided to the host, it might be expected that dietary glutamine supplementation would aid in tumour progression. However, glutamine has been demonstrated to retard tumour growth in breast cancer xenografts (Klimberg et al., 1996), a phenomenon linked to a positive correlation between glutamine levels and glutathione and a negative correlation with the pro-inflammatory prostaglandin PGE_2 (Klimberg et al., 1996). An increased consumption of glutamine by tumours depletes circulating glutamine levels and leads to the impaired activity of natural killer cells. Increased dietary glutamine is believed to restore this function and impede further tumour growth (Yoshida et al., 1995).

Supplementation with certain other amino acids might also be beneficial to some cancer patients. The amino acid arginine is an important precursor of nitric oxide (NO) (Cooke and Dzau, 1997), and increased NO production has been strongly associated with increased apoptosis in many breast cancer cell lines (Simeone et al., 2002) as well as in a head and neck cancer xenographt model (Kawakami et al., 2004). Isoleucine has purported anti-angiogenesis effects in some colon cancers and may prevent liver metastasis and decrease tumour growth through the impairment of vascular endothelial growth factor (Murata and Moriyama, 2007).

Some indirect observations have also provided insight. Cancer patients have relatively increased levels of hydroxyproline in their urine (Okazaki et al., 1992) and reduced levels in cancer tissue (Okazaki et al., 1992). This could result in a proline deficiency in people with cancer. Indeed, supplementation with lysine and proline correlated with decreased migration of breast and ovarian cancer cells and reduced growth of various tumour xenografts (Roomi et al., 2006, Roomi et al., 2005).

1.3.3 Amino acid deprivation in the management of tumour progression

Among their other requirements, cells demand amino acids for cell division and the synthesis of adequate quantities of material necessary to duplicate proteins, peptides and DNA during cell doubling. The process of proliferation in fast dividing cancer cells seems to require increased levels of amino acids to support the protein biosynthesis during these periods of growth (Medina et al., 1992). This is reflected by the observation that the amino acid transporters ASCT2, LAT1 and SLC6A14 exhibit elevated levels of expression in many cancer types. This increased expression has been suggested to play an important role in proliferation and survival of tumour cells (Fuchs and Bode, 2005, Gupta et al., 2006). Indeed, experimental down-regulation of amino acid transporters has been employed to successfully impair cancer cell growth by starving cancer cells of amino acids (Kim et al., 2006a). Moreover, the effectivness of anticancer agents such the compound E7070 has been linked to its ability to inhibit amino acid transport (Tsukahara et al., 2001). This outlines the importance of amino acid redistribution and supply in carcinogenesis and provides an avenue for novel intervention options for patients resistant to other therapies.

Due to the important functions of amino acids in cancer growth, experiments investigating their exclusion or deprivation as treatment for cancer were common as early as the first half of

the last century. These studies took the form of amino acid restriction diets in laboratory animals with cancer. However, these initial investigations failed to establish a link between dietary restriction of amino acids and alterations in tumour growth patterns (Drummond, 1917). In addition, experiments omitting single amino acids such as lysine or cysteine demonstrated few therapeutic benefits. For example, it was observed that the growth rates of spontaneous mammary carcinomas in mice could be curbed for only short periods following omission of lysine from the diet, but that normal rapid growth resumed following prolonged diets free in lysine (Kocher, 1944).

Expectations were rekindled in the latter half of the century when a multitude of studies generated findings showing that amino acid restriction diets could in fact slow tumour development. The first of the studies demonstrating this beneficial property of amino acid starvation treatment in cancer utilized diets deprived only in methionine, valine or isoleucine (Sugimura et al., 1959). Thereafter, it was established that diets deficient in the amino acid phenylalanine could cause reduction in tumour sizes (Lorincz and Kuttner, 1965). Since then it has been demonstrated that limiting tyrosine in addition to phenylalanine leads to impairment in the chemotactic ability and invasiveness (Pelayo et al., 1999) as well as focal adhesion kinase dependent apoptosis in melanomas (Fu et al., 1999), and that tyrosine and phenylalanine restriction also results in metabolically linked cell death of prostate cancer cells (Fu et al., 2010).

As complete and prolonged amino acid restriction was deemed too dangerous to have real clinical relevance, most research expounded on the principle that depleting the circulating levels of single amino acids thought to be critical to tumour growth and development could curb their progression. The enzyme asparaginase catalyzes hydrolysis of asparagine and is used as a treatment for acute lymphoblastic leukaemia based on the premise that these cancers

are unable to synthesize asparagine (Appel et al., 2007), whereas deprivation of the essential amino acid leucine increases sensitivity of melanoma cells with mutations in the RAS/MEK signalling pathway to caspase dependent cell death and inhibits their growth (Sheen et al., 2011). Likewise, valine depletion of tumour bearing rats results in growth inhibition of hepatoma and mammary tumours (Nishihira et al., 1988, Tassa et al., 2003). It has also been demonstrated that selectively restricting amino acids has negative survival implications for prostate cancer cells, and that restricting these cells of phenylalanine/tyrosine, glutamine or methionine caused mitochondrial DNA damage and impacted on mitochondrial function and ATP synthesis (Liu et al., 2011c).

Indirectly depriving cancer cells of amino acids may also prove to be a useful tool. Histidinol (an antagonist to histidine) leads to the functional deprivation of histidine, thereby interrupting the biosynthesis of nucleic acids in a leukaemia cell line (Dehlinger et al., 1977). L-aspartic acid is an essential component of purine and pyramidine ring formation (Ahluwalia et al., 1990). Analogues of this non-essential amino acid interrupt this process, contributing to their well reported antitumour effects (Jayaram et al., 1979, Tyagi and Cooney, 1984). Buthionine sulfoximine, an inhibitor of glutathione synthesis, causes growth inhibition in certain leukaemia, breast and colon carcinoma cell lines (Dorr et al., 1986).

Despite these promising amino acid deprivation studies contradictory observations provide valid cause for caution. Glutamine is a vitally important amino acid for tumour growth, yet some studies have shown that glutamine supplementation is able to repress growth of breast cancer (Klimberg et al., 1996). Conversely, selective restriction of glutamine in prostate cancer results in increased glucose consumption and cell death. Cell death was shown to be partly reversible if cells were also supplemented with pyruvate (Fu et al., 2010). Through duplication of physiological activity of L-glutamine, compounds structurally related to this

amino acid have been shown to interfere with its function and result in antitumour activity of a number of different cancers (Ahluwalia et al., 1990).

Some of the most promising research into amino acid restriction involves deprivation of the essential amino acid methionine. The absence of methionine has repeatedly been shown to correlate with decreased growth of cancer cells without having negative effects on non-cancer cells (Poirson-Bichat et al., 1997, Guo et al., 1993, Epner, 2001), and catabolism of methionine through administration of methioninase inhibits cancer cell and tumour growth (Tan et al., 1999, Yoshioka et al., 1998). This effectiveness could be due to its nature as a methyl donor for methylation events in fast dividing cancer DNA. A hypothesis that is strengthened by evidence indicating that methyl depletion can lead to an increased susceptibility to genomic DNA damage (Pogribny et al., 1995), and that histone methyltransferases might act as effective tumour suppressors (Huang, 2002). Furthermore, clinical studies have demonstrated that dietary methionine restriction is both safe and has potential as an antitumour agent (Epner, 2001).

1.4   Short term dietary restriction and cancer

Long term dietary restriction has been known to correlate positively with a decrease in cancer growth. It has also been shown to significantly extend the lifespan of some species (Heilbronn and Ravussin, 2005) and protect against both spontaneous and induced cancers (Kritchevsky, 2003). These chronic restriction diets typically diminish caloric intake by at least 30%, but the negative implications of associated decreases in weight loss may lessen its attractiveness as a realistic treatment modality for human patients (Raffaghello et al., 2010). The recent discovery that so-called short term starvation (STS) regimes protect healthy cells from various toxins and drug induced toxicities through induction of a differential stress response where

cancer cells seem unable to enjoy the same protection (Lee and Longo, 2011). These restricted diets were demonstrated to be effective if the starvation periods remained relatively brief (approximately 48 hours) and were then followed directly by the toxic insult (Russo and Rizzo, 2008). This protective effect induced by STS has now also been confirmed in human based trials (Safdie et al., 2009).

2 Research problem and experimental aims

2.1 Research problem

Despite decades of research into amino acid starvation therapies, there are few studies that analyse the effect of short term, complete amino acid starvation in cancer. Up to now, most research has investigated the potential of longer term malnourishment of single amino acids, due to predicted side effects of complete depletion regimes. There is also an absence of studies investigating amino acid deprivation in the context of breast cancer. This along with recent interest and success of short term starvation strategies as therapy in the cancer setting has presented a need to investigate the effects of acute deprivation on breast cancer cells.

2.2 Research aims

1. Establish the sensitivity of MDAMB231 cells to acute amino acid deprivation.
2. Determine the time frame at which these cells begin to respond to amino acid deprivation.
3. Confirm the relative contributions of cell death and proliferation (if any) to the responses observed in relation to aims (1) and (2).

3   Methods and materials

Complete step-by step protocols are provided in the appendix.
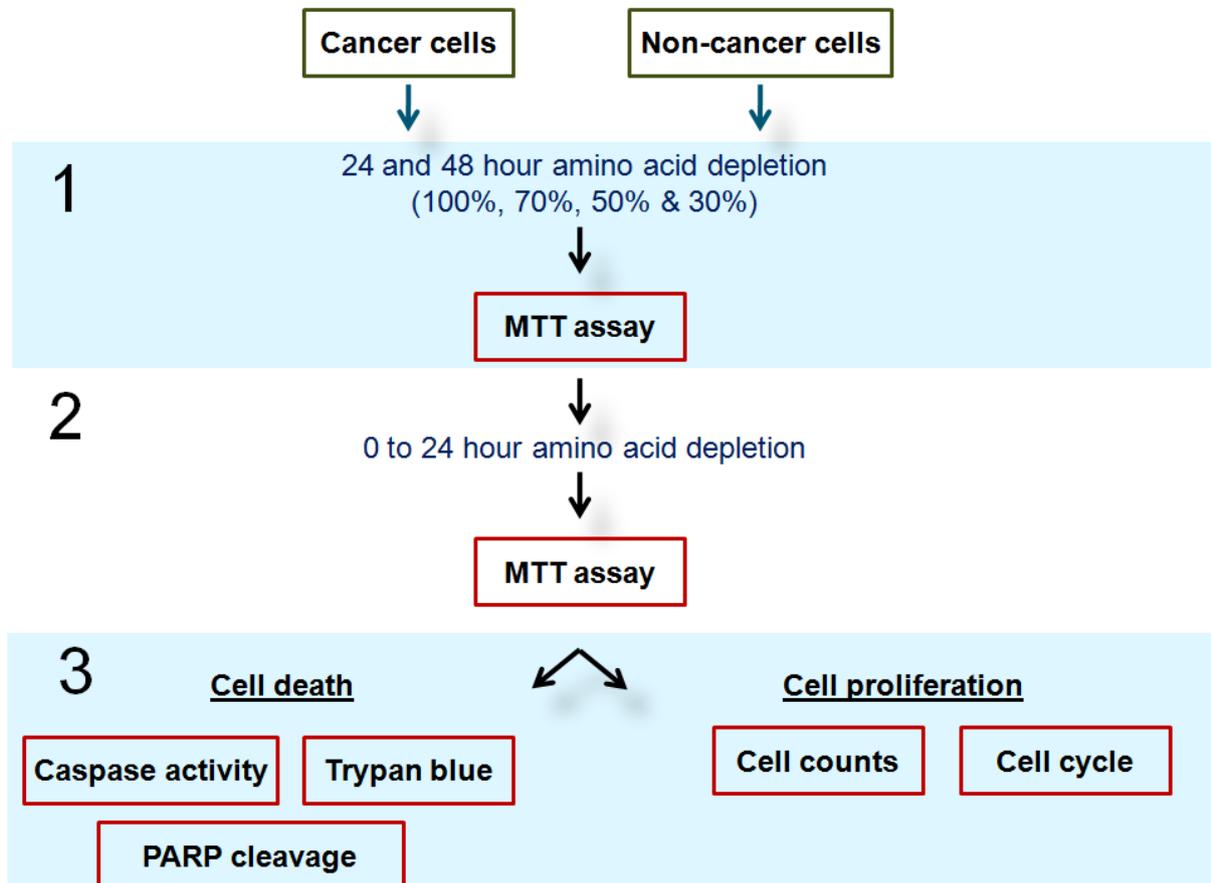
3.1   Study design

Image 1.1 Study design: A metastatic cancer cell line (MDAMB231) and a non-tumourogenic cell line (MCF12A) will be 1. depleted of varying percentages of amino acids and analysed using the MTT assay. 2. Depending on results obtained in 1. these cell lines will be further examined during amino acid starvation over the spectrum of a 24 hour period. 3. Depending on results obtained in 2., both cell lines will be analysed for markers of proliferation and cell death.

3.2   Cell culture

Experiments were performed using the human metastatic mammary carcinoma cell line (MDAMB231) and a human non-tumourogenic breast epithelial cell line (MCF12A). MDAMB231 cells were obtained from American Type Culture Collection (Rockville, MD, USA) and MCF12A cells were obtained from the University of Cape Town. During routine

14

maintenance, cells were grown as monolayers in Glutamax-DMEM (Celtic Molecular Diagnostics, Cape Town, South Africa) supplemented with 10% foetal bovine serum (Sigma Chemical Co., St Louis, MO, USA) at 37°C in a humidified atmosphere of 95% air plus 5% CO_2. MCF12A growth medium was complemented with Ham"s F12 medium (1:1) (Sigma Chemical Co., St Louis, MO, USA), 0.5 µg/ml hydrocortisone (Sigma Chemical Co., St Louis, MO, USA), 10 µg/ml insulin (Sigma Chemical Co., St Louis, MO, USA) and 20 ng/ml EGF (Sigma Chemical Co., St Louis, MO, USA). Cells were first allowed to proliferate in T75 flasks ($75cm^2$ flasks, Greiner Bio One, Germany) until they reached 80% confluence before being split into appropriate treatment plates or dishes. Splitting was accomplished by washing the cell monolayer with warm phosphate buffered saline (PBS) followed by incubation with 4 ml trypsin/EDTA (Sigma Chemical Co., St Louis, MO, USA) at 37°C, with occasional agitation, until cells loosened completely or for a maximum of four minutes. All experiments were performed using exponentially growing cells.

3.2.1 Note on cell confluence

Sub-confluent cell populations were used for all experiments. Plating densities were previously determined for each cell line so that equivalent (sub-confluent) cell populations were always present at the time of treatment.

3.3   MTT assay

The 3-(4,5-dimethylthiazol-2-yl)-2,5-diphenyltetrazoliumbromide (MTT) cell activity assay was used to indicate the percentage of metabolically viable cells post intervention. Absorption measurements were taken to correlate directly with the ability of vital reduction enzymes in the mitochondria of healthy cells to reduce MTT. 10 000 MDAMB231 cells or 15 000

MCF12A cells were plated 48 hours before being treated in 96-well plates using 100 µl of culture medium. Subsequent to treatments, supernatants were discarded and 150 µl of warm PBS and 50 µl of MTT (Sigma Chemical Co., St Louis, MO, USA) solution (0.01 g MTT/ml PBS) was added to each well containing the cell monolayer. The plate was then incubated for 2 hours at 37ºC in a humidified 5% CO_2 atmosphere. Following incubation, supernatants were discarded and 100 µl of isopropanol-HCl/Triton-X-100 (50:1) was added to each well and vigorously agitated for 5 minutes at 300-500 rpm in order to dissolve formazan crystals that had been generated in healthy cells. The suspension was then centrifuged for 2 minutes at 1400 rpm and the supernatant analysed using a plate reader to determine absorbance at a wavelength of 540 nm versus a blank. Groups were analysed in triplicate in at least three separate experiments and absorbance values calculated as a percentage versus untreated controls.

3.4   Caspase 3/7 activity assay

Caspase-3/7 activity was measured using the Caspase-Glo® 3/7 assay (Promega, Madison, WI, USA). 10 000 MDAMB231 cells or 15 000 MCF12A cells were plated 48 hours before being treated in white-walled 96-well plates using 100 µl of culture medium. In experiments where transfection was necessary, cells were reverse transfected during plating. Sub-confluent cells populations were used for all experiments. Tthe Caspase-Glo® 3/7 working buffer reagent was prepared and equilibrated at room temperature and mixed with the lyophilized substrate before the reconstituted buffer was stored at -20°C. Following treatment the working buffer reagent was equilibrated at room temperature for 30 minutes and the 96-well culture plate for 10 minutes prior to assay. 100 µl (1:1) of working reagent was then added to each well containing cells, and the plates mixed at 500 rpm for 30 seconds. The plate was then incubated at 22ºC for 1 hour in the dark. The luminescence was measure in a luminometer.

3.5   Trypan blue assay

Trypan blue cell viability was assessed using the Countess™ Automated Cell Counter (Invitrogen, USA). 100 000 MCF12A cells or 80 000 MDAMB231 cells were plated into 60 mm culture dishes 48 hours prior to treatment. Following treatment cells were trypsinized and pelleted. 10 µl cell suspension was mixed with 10 µl 0.4% trypan blue and 10 µl loaded into a Countess™ chamber slide. The slide was then inserted into the instrument and trypan blue positivity calculated automatically and expressed as the total number of trypan blue positive cells, total number of trypan blue negative cells and absolute total cell number.

3.6   Cell proliferation assay

Cells were harvested from sub-confluent plates and were re-suspended in complete media and plated in 24-well plates at a density of 10 000 cells per well. After 24 h, cells were harvested from the first plate and counted on a hemocytometer.

3.7   Analysis of cell cycle progression

Flow cytometric analysis of the cell cycle was performed using the CycleTEST™ PLUS DNA Reagent kit (Becton Dickinson, California, USA). 200 000 MCF12A cells or 150 000 MDAMB231 cells were plated in T25 culture flasks 48 hours prior to treatment. Prior to analysis, cells were trypsinzed and the cell suspensions centrifuged at 400 x g for 5 minutes at room temperature. Cells were then washed once in PBS. 250 µl of trypsin buffer was added to each tube and allowed to react for 10 minutes at room temperature. Thereafter, 200 µl of trypsin inhibitor and RNase buffer was added to each tube. This solution was again incubated at room temperature for 10 minutes. Finally, 200 µl of ice cold propidium iodide stain

solution was added to each tube, which was incubated on ice in the dark for a further 10 minutes. Samples were filtered through a 50 µm nylon mesh into 12x75 mm tubes. Sample fluorescence was acquired using flow cytometry within 30 minutes. Results were obtained by using the CycleTEST™ PLUS DNA Reagent kit and ModFit LT software (Verity software house, Inc., ME, USA.) on BD FACSAria I. At least 30 000 list-mode data events were acquired for each sample. A 585/42 bandpass filter was used to analyse light emitted between 564 and 606 nm by stained cells.

A.
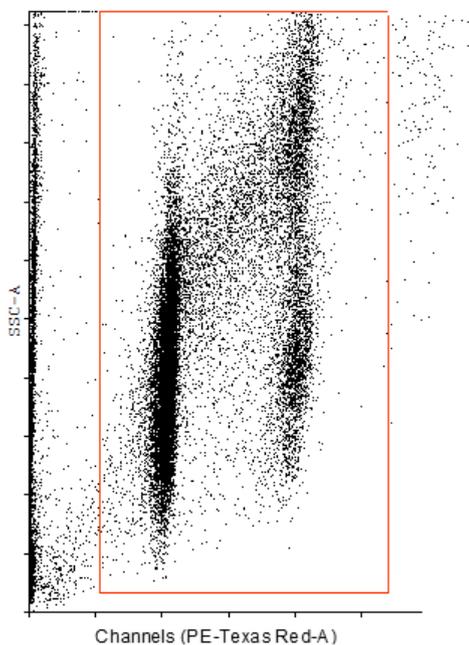
B.
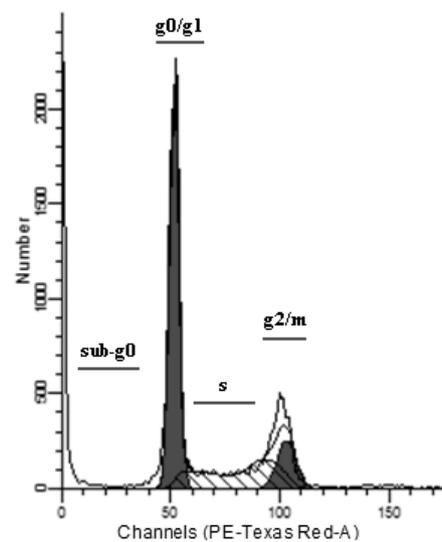
Image 1.2 Acquisition of cell cycle populations. A. Dot plot showing gated cells to exclude aggregates. B. Gated DNA histogram depicting DNA content and the location of g0/g1, s, g2/m and sub-g0 populations. Results were obtained by using the CycleTEST™ PLUS DNA Reagent kit and ModFit LT software on BD FACSAria I. At least 30 000 list-mode data events were acquired for each sample.

ModFit LT software was used to determine the percentage of cells in the g0/g1, s and g2/m phases. The location of these populations, after gating was used to exclude aggregates, is indicated in image 1.2. Mean percentages from three independent experiments were used to perform statistical comparisons.
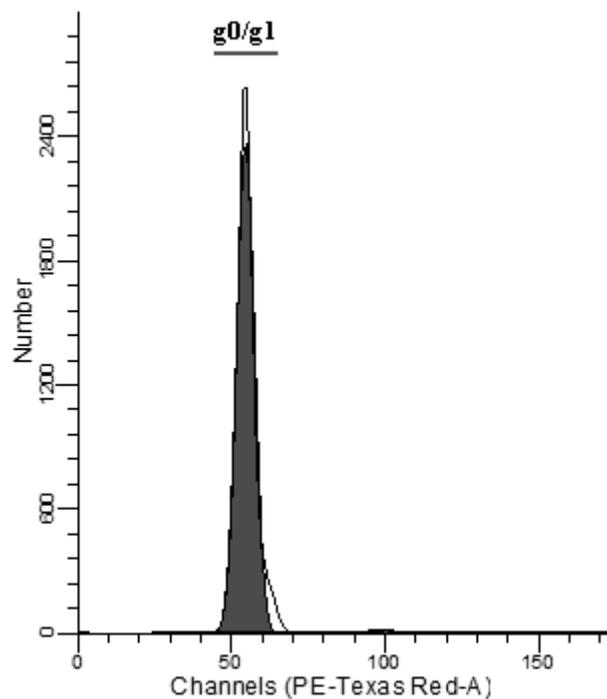
Image 1.3 DNA histogram of peripheral blood mononuclear cells (PBMCs) which has been gated to exclude aggregates. The location of the g0/g1 population is indicated on the graph. Results were obtained by using the CycleTEST™ PLUS DNA Reagent kit and ModFit LT software on BD FACSAria I. At least 30 000 list-mode data events were acquired for each sample.

Peripheral blood mononuclear cells (PBMCs) were isolated from human blood and used as a reference point for determining the location of the g0/g1 peak. An example of such a peak is reproduced in image 1.3.

3.7   PARP Western blots

3.7.1 Protein extraction and quantification

Following treatment, cells immediately had their supernatants discarded and placed on ice. Cell monolayers were then rinsed three times in 5 ml of a pre-lysis buffer (20 mM Tris-HCl, pH 7.4, 137 mM NaCl, 1 mM $CaCl_2$, 1 mM $MgCl_2$ and 0.1 mM sodium orthovanadate). Total cell protein was extracted by incubating cells on ice for 10 minutes in 1 ml of a modified radioimmunoprecipitation (RIPA) buffer, pH 7.4, containing: Tris–HCl 2.5 mM, EDTA 1

19

mM, NaF 50 mM, NaPPi 50 mM, dithiothreitol 1 mM, phenylmethylsulfonyl fluoride (PMSF) 0.1 mM, benzamidine 1 mM, 4 mg/ml SBTI, 10 mg/ml leupeptin, 1% NP40, 0.1% SDS and 0.5% Na deoxycholate. Adherent cells were then harvested from culture dishes by scraping. Whole cell lysates were sonicated in order to disrupt the cell membranes to release their contents before being centrifuged at 4°C and 8000 rpm for 10 minutes. Lysates were then stored at -80°C or had their protein content determined immediately. Protein content was quantified using the Bradford protein determination method (Bradford, 1976), directly before the preparation of cell lysates.

3.7.2 Sample preparation (cell lysates)

Following protein quantification, aliquots diluted in Laemmli sample buffer were prepared for all samples, each containing 40 μg of protein. Aliquots were then stored at -80°C for future analysis by Western blotting.

3.7.3 SDS-PAGE and Western blot analysis

Whole cell lysates were separated on 10% polyacrylamide gels by sodium dodecyl sulphate polyacrylamide gel electrophoresis (SDS-PAGE). A pre-stained protein marker ladder (peqGOLD, PEQLAB Biotechnologie GMBH, Germany) was loaded in the left most well on each gel for orientation and electrophoretic determination of molecular weights of specific bands. Previously prepared protein samples were boiled for 5 minutes and 40 μg of protein (sample preparation described above) was loaded per lane. Gels were run for 60 minutes at 130 V (constant) and 400 mA (Mini Protean System, Bio-Rad, USA). Following SDS-PAGE, proteins were transferred to polyvinylidine fluoride (PVDF) membranes (Immobilon, Millipore, USA) using a semi-dry electrotransfer system (Bio-Rad, USA) for 60 minutes at 15 V and limit 0.5 A. In order to prevent non-specific binding, membranes were blocked in 5% (w/v) fat-free milk in 0.1% Tris Buffered Saline-Tween20 (TBS-T) for 2 hours at room

temperature with gentle agitation. Membranes were then incubated with PARP primary antibody (Cell Signalling, MA, USA) diluted in 5% (w/v) fat-free milk in 0.1% TBS-T (1:1000), overnight at 4°C. The following day, membranes were washed in copious volumes of TBS-T (3X5 minutes) before being incubated in anti-rabbit (Amersham Biosciences, UK, and Dako Cytomation, Denmark) horseradish peroxidase-conjugated secondary antibody for 1 hour at room temperature with gentle agitation. Following the incubation period, membranes were washed a further three times in TBS-T (3x5 minutes), followed by a final 10 minute wash in TBS. Antibodies were detected with the LumiGLO Reserve™ chemiluminescent substrate kit (KPL, Inc., USA) as per the manufacturer's instructions, and bands were exposed to autoradiography film (Hyperfilm, Amersham Biosciences, UK). Exposed bands were visualised and then quantified by densitometry using the UNSCAN-IT© densitometry software (Silk Scientific Corporation, Utah, USA). All bands were expressed as optical density readings relative to a control present on the same blot.

3.8   Amino acid deprived medium

Cells that were incubated without amino acids were incubated in the usual manner except in growth medium that contained no amino acids. Culture medium was designed and prepared to be identical in every way to typical growth medium, apart from the fact that it contained no detectable amino acids. Amino acid free culture medium was prepared by Highveld Biological (Pty) Ltd in association with Dr Elke Bey. Furthermore, dialyzed foetal bovine serum (#A15-107; PAA Laboratories GmbH, Austria) was used in the preparation of this media.

3.9   Statistical analysis

All values are presented as the mean ± standard error of the mean (SEM). Differences between time points and treatment groups were analysed using analysis of variance (ANOVA). The unpaired student‚s t-test was used when comparisons were made between only two groups. Significant changes were further assessed by means of the Bonferroni *post hoc* analysis where appropriate. All statistical analyses were performed using Graphpad Prism version 5.01 (Graphpad Software, Inc, CA, USA). The minimum level of significance accepted was $p < 0.05$.

4   Results

4.1   MDAMB231 cancer cells are more sensitive than MCF12A epithelial cells to acute amino acid starvation

Custom culture medium, designed to be free of amino acids and complemented with dialyzed foetal bovine serum was analyzed for amino acid content using mass spectroscopy based proteomics and found to contain no traces of amino acids (data not shown).
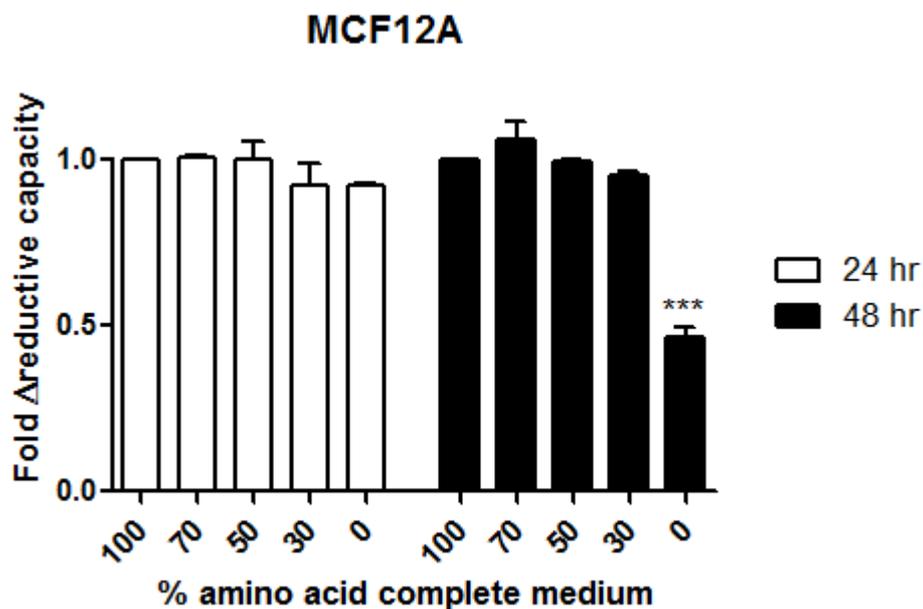
Fig. 1.1 The capacity of MCF12A cells to reduce MTT to formazan is not significantly diminished during 24 hours of amino acid deprivation. Results represent the fold change in MTT reductive capacity. A significant decrease in reductive capacity appeared only following 48 hours incubation in culture medium entirely deficient in amino acids. hr = hours. Each value represents the mean ± SEM of at least three independent determinations. ***, $P < 0.001$ vs. 100% amino acid containing medium.

Initial experiments designed to assess the sensitivity of the cell lines in this study to amino acid deprivation made use of the MTT assay and utilized varying dilutions of growth medium comprised of appropriate ratios of fully complemented growth medium and amino acid free medium. The capacity of the non-tumourogenic (MCF12A) breast epithelial cell line to reduce MTT to formazan was not diminished following a 24 hour incubation in growth medium deficient in amino acids (Fig 1.1). However, 48 hours after converting to amino acid free medium, the MTT reducing capacity of these cells had decreased more than 50%.
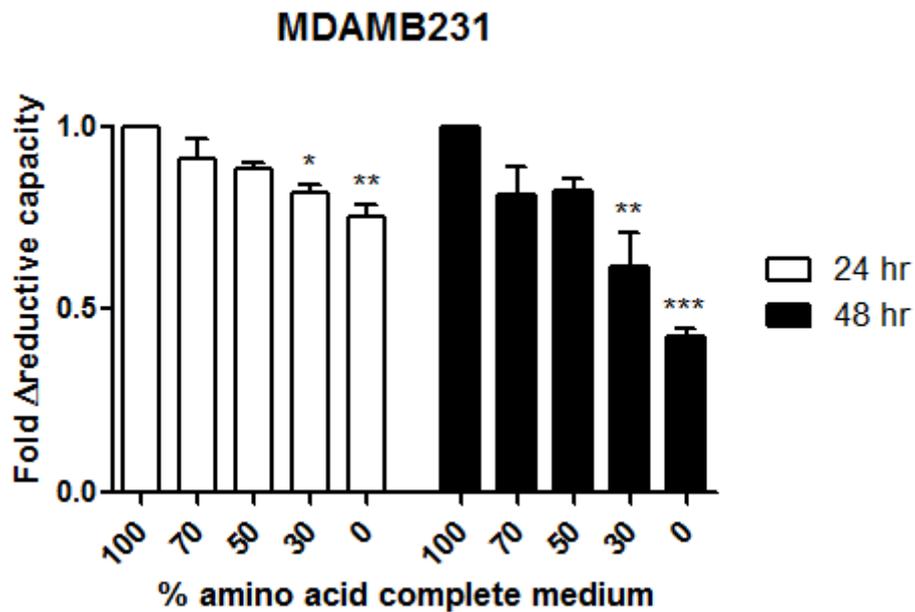
Fig. 1.2 The capacity of MDAMB231 cells to reduce MTT to formazan is significantly diminished during 24 hours of amino acid deprivation even when amino acids are not entirely absent from culture medium. A more pronounced decrease in reductive capacity appears after 48 hours incubation in culture medium deficient in amino acids. hr = hours. Each value represents the mean ± SEM of at least three independent determinations. *, $P < 0.05$; **, $P < 0.01$; ***, $P < 0.001$ vs. 100% amino acid containing medium.

The capacity of the metastatic cancer cell line (MDAMB231) to reduce the MTT to formazan was significantly diminished following a 24 hours incubation in amino acid free medium (Fig 1.2). A significant decrease was observed even when the culture medium was not completely deficient in amino acids. A more pronounced decrease in reductive capacity appeared after 48 hours of amino acid deprivation.
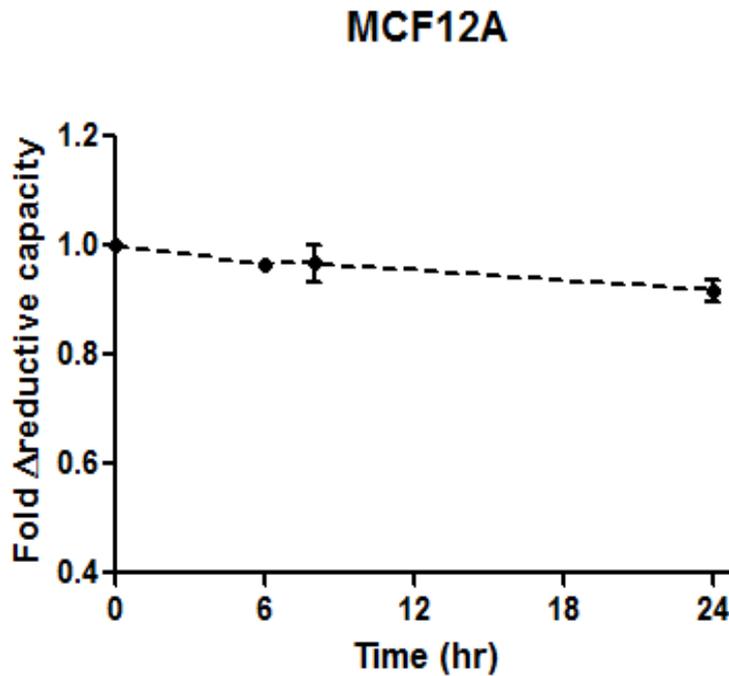
MCF12A

Fig. 1.3 The capacity of MCF12A cells to reduce MTT to formazan is not significantly diminished during a 24 hour period of amino acid deprivation. hr = hours. Results represent the fold change in MTT reductive capacity over time. Each value represents the mean ± SEM of at least three independent determinations.

When analyzed over time, the non-cancer cell line showed no change in reductive capacity over a 24 hour period of amino acid deprivation (Fig 1.3).
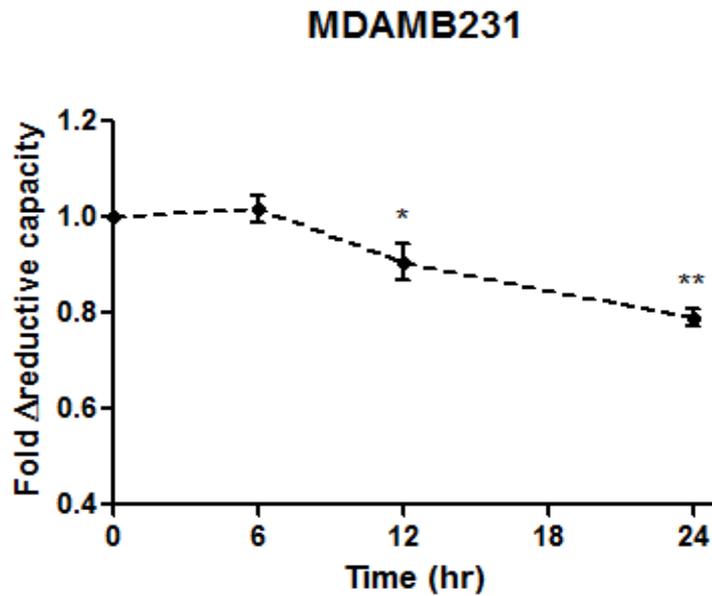
MDAMB231

Fig. 1.4 The capacity of MDAMB231 cells to reduce MTT to formazan is significantly diminished following 12 hours of amino acid deprivation. Results represent the fold change in MTT reductive capacity over time. hr = hours. Each value represents the mean ± SEM of at least three independent determinations. *, $P < 0.05$; **, $P < 0.01$ vs. 0 hr.

A rapid decrease in reductive capacity occurred after only 12 hours, but not before 6 hours, of amino acid deprivation in MDAMB231 cells, during 24 hour period of amino acid deprivation (Fig 1.4).

4.2 MDAMB231 cells (but not MCF12A cells) show increased signs of apoptosis activation during short term amino acid starvation
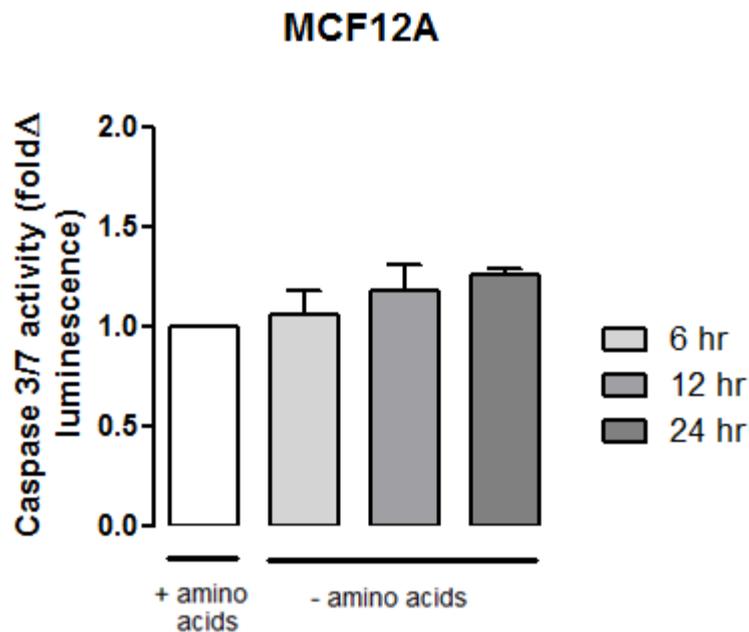
MCF12A

Fig. 1.5 MCF12A show no significant increase in caspase 3/7 activity during a 24 hour period of amino acid starvation. Results represent the fold change in luminescence in cultures depleted of amino acids versus those cultured in medium containing amino acids. Caspase 3/7 activity was taken to be proportionate to produced luminescence intensity. hr = hours. Each value represents the mean ± SEM of at least three independent determinations.

Next, it was determined if programmed cell death was involved in the changes induced by complete amino acid deprivation. Results from a caspase 3/7 activity assay showed that MCF12A cells displayed no significant changes in caspase 3/7 activity in response to amino acid starvation (Fig 1.5).
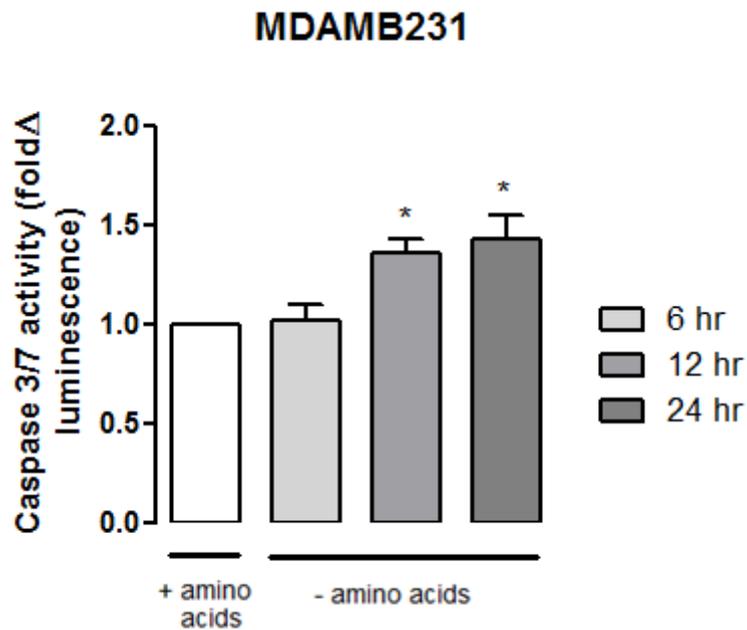
MDAMB231

Fig. 1.6 MDAMB231 cells display significantly increased caspase 3/7 activity at 12 and 24 hours of amino acid starvation. Results represent the fold change in luminescence in cultures depleted of amino acids versus those cultured in medium containing amino acids. Caspase 3/7 activity was taken to be proportionate to produced luminescence intensity. hr = hours. Each value represents the mean ± SEM of at least three independent determinations. *, $P < 0.05$ vs. + amino acids.

MDAMB231 cells had a significant increase in caspase 3/7 activity at 12 and 24 hours following amino acid deprivation (Fig 1.6).

A

MCF12A

— 116 kDa
— 89 kDa

0   24   48

Amino acid deprivation (hr)

B

MDAMB231

— 116 kDa
— 89 kDa

0   24   48

Amino acid deprivation (hr)
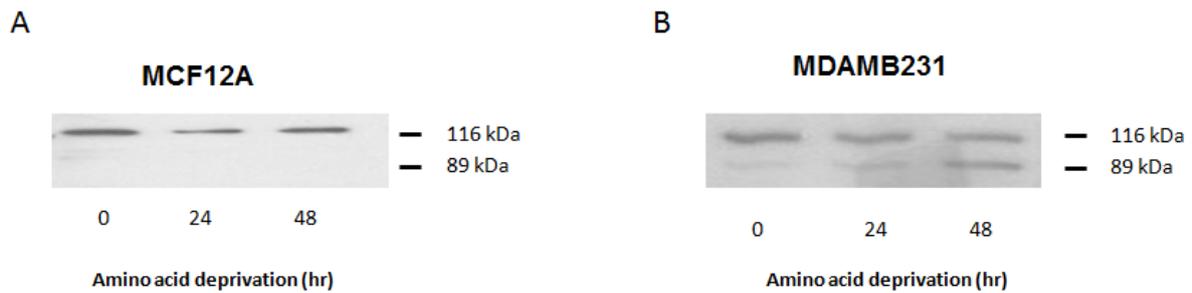
Fig. 1.7 Complete amino acid deprivation of culture medium is associated with the appearance of cleaved PARP at 89 kDa A) No PARP fragments were observed in MCF12A cells. B) in MDAMB231 cells. Images representative of three separate experiments. hr = hours.

PARP, an enzyme involved in DNA damage repair, can be cleaved by both caspase 3 and caspase 7. PARP cleavage is a sensitive indicator of apoptotic cell death, downstream of caspase activity. Western blots displayed detectable PARP fragments at 89 kDa subsequent to 24 or 48 hours of amino acid depletion in the MDA-MB-231 cells but not MCF12A cells (Fig 1.7).
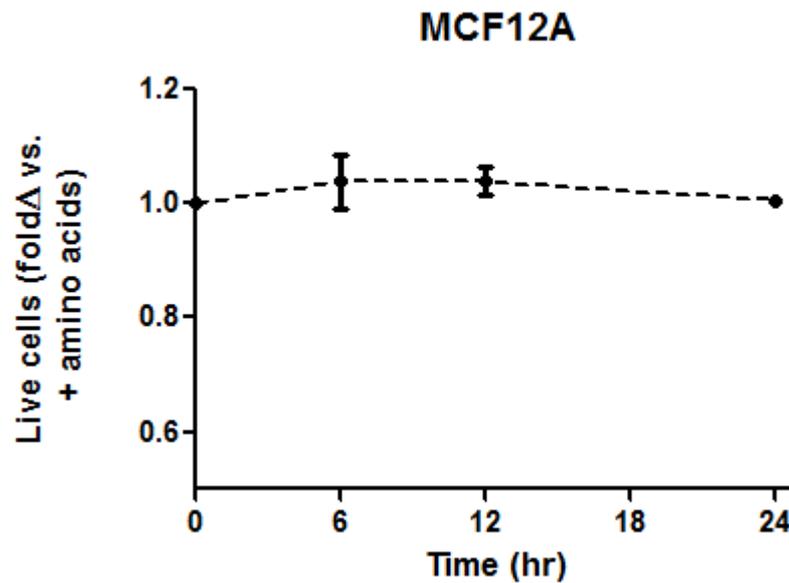
MCF12A

Fig. 1.8 MCF12A cells exclude trypan blue dye during a 24 hour period of amino acid deprivation. Live cells are defined as those that exclude trypan blue dye. Results represent the fold change of live cells over time in culture depleted of amino acids versus those cultured in medium containing amino acids. hr = hours. Each value represents the mean ± SEM of at least three independent determinations.

The trypan blue vital stain is able to traverse only those cell membranes with compromised integrity, and therefore functions as a marker of necrotic and late stage apoptotic cell death and can be used as an indicator of actual cellular impairment following an intervention. MCF12A cells excluded trypan blue dye during a 24 hour period of amino acid deprivation (Fig 1.8).
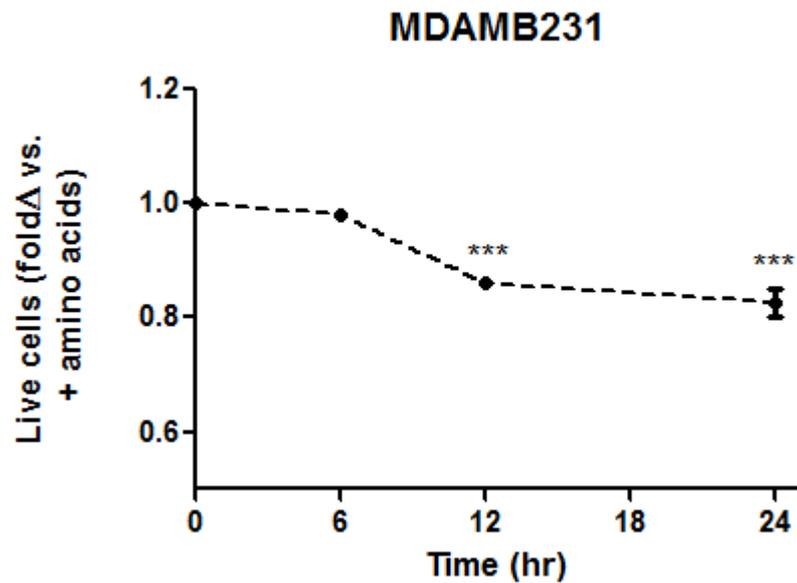
MDAMB231

Fig. 1.9 A significant percentage of trypan blue positive MDAMB231 cells appeared after 12 hours of amino acid deprivation. Live cells are defined as those that exclude trypan blue dye. Results represent the fold change of live cells over time in culture depleted of amino acids versus those cultured in medium containing amino acids. hr = hours. Each value represents the mean ± SEM of at least three independent determinations. ***, $P < 0.001$ vs. 0 hr.

A significant percentage of trypan blue positive MDAMB231 cells appeared after 12 hours of amino acid deprivation (Fig 1.9).

4.3   Analysis of cell proliferation
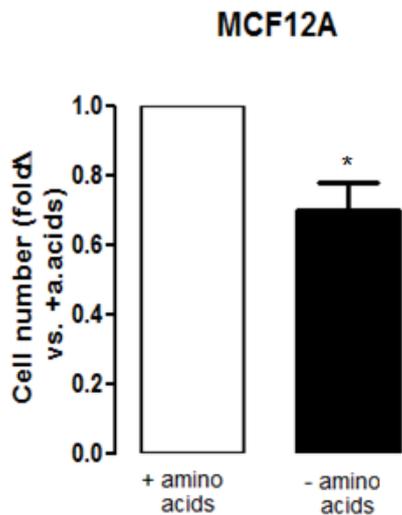
A.   **B.**
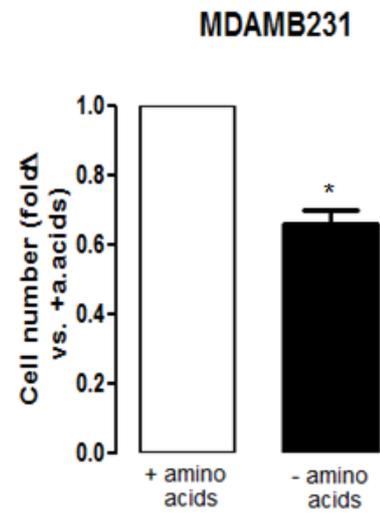
Fig. 1.10 Both MCF12A and MDAMB231 cells display decreased proliferation during amino acid deprivation. Cell proliferation was assessed by cell counts following 24 hour incubation in culture medium either with or without amino acids. hr = hours. Each value represents the mean ± SEM of at least three independent determinations. *, $P < 0.05$ vs. + amino acids.

Removal of amino acids from culture medium for 24 hours results in diminished cell numbers in both the cancer and non-cancer cell lines (Fig 1.10).

4.4   Analysis of the cell cycle

A.

B.
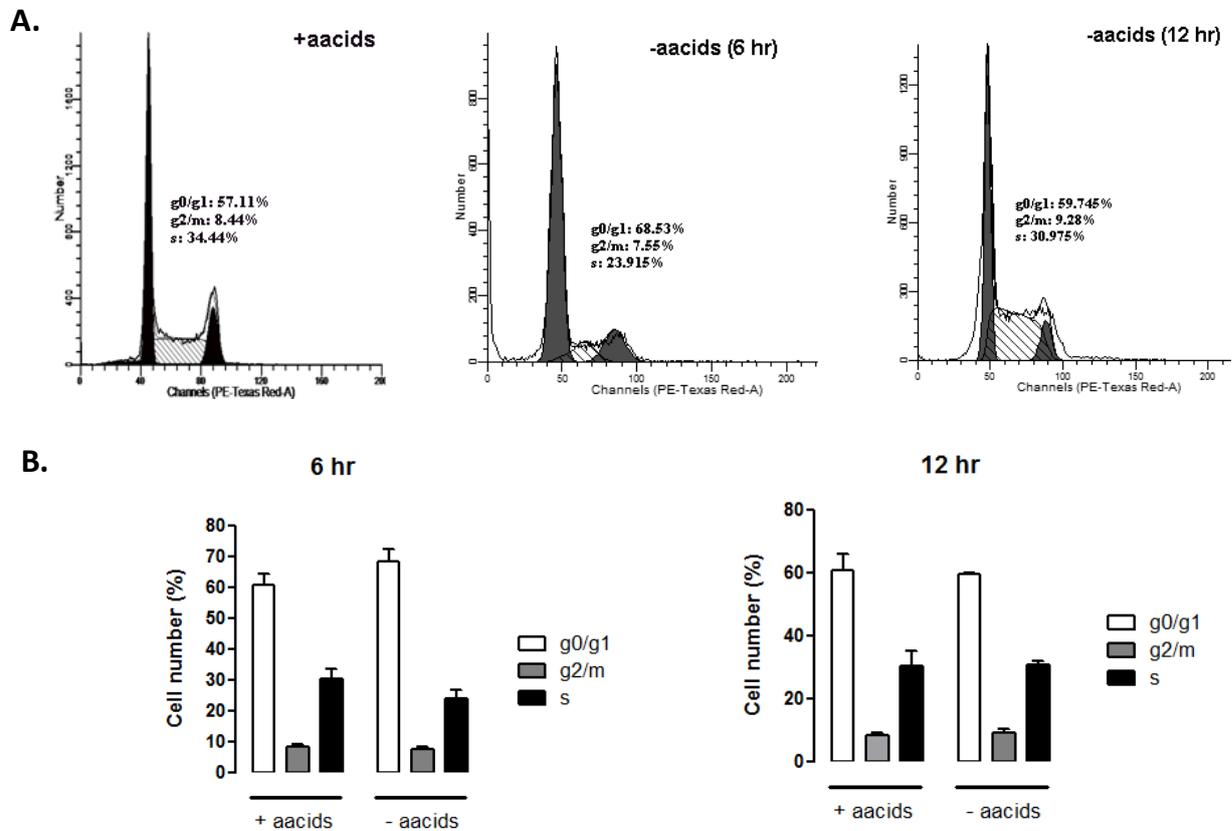
Fig. 1.11 MDAMB231 cells display no change in the cell cycle after 12 hours of amino acid deprivation. Cell cycle progression was assessed using flow cytometry following 6 and 12 hour incubations in culture medium without amino acids and compared with cells incubated for similar durations in culture medium containing amino acids. A. Typical DNA histograms and cell cycle phase percentages. B. Bar graphs representing the mean ± SEM of at least three independent determinations. hr = hours; aacids = amino acids.

The MDAMB231 cell line exhibited no obvious alterations in cell cycle progression at 6 hours or at 12 hours of amino acid starvation (Fig 1.11). Mean percentages from three independent experiments were used to perform statistical comparisons between the same cell cycle phase for the different treatment groups.

33

A.

B.
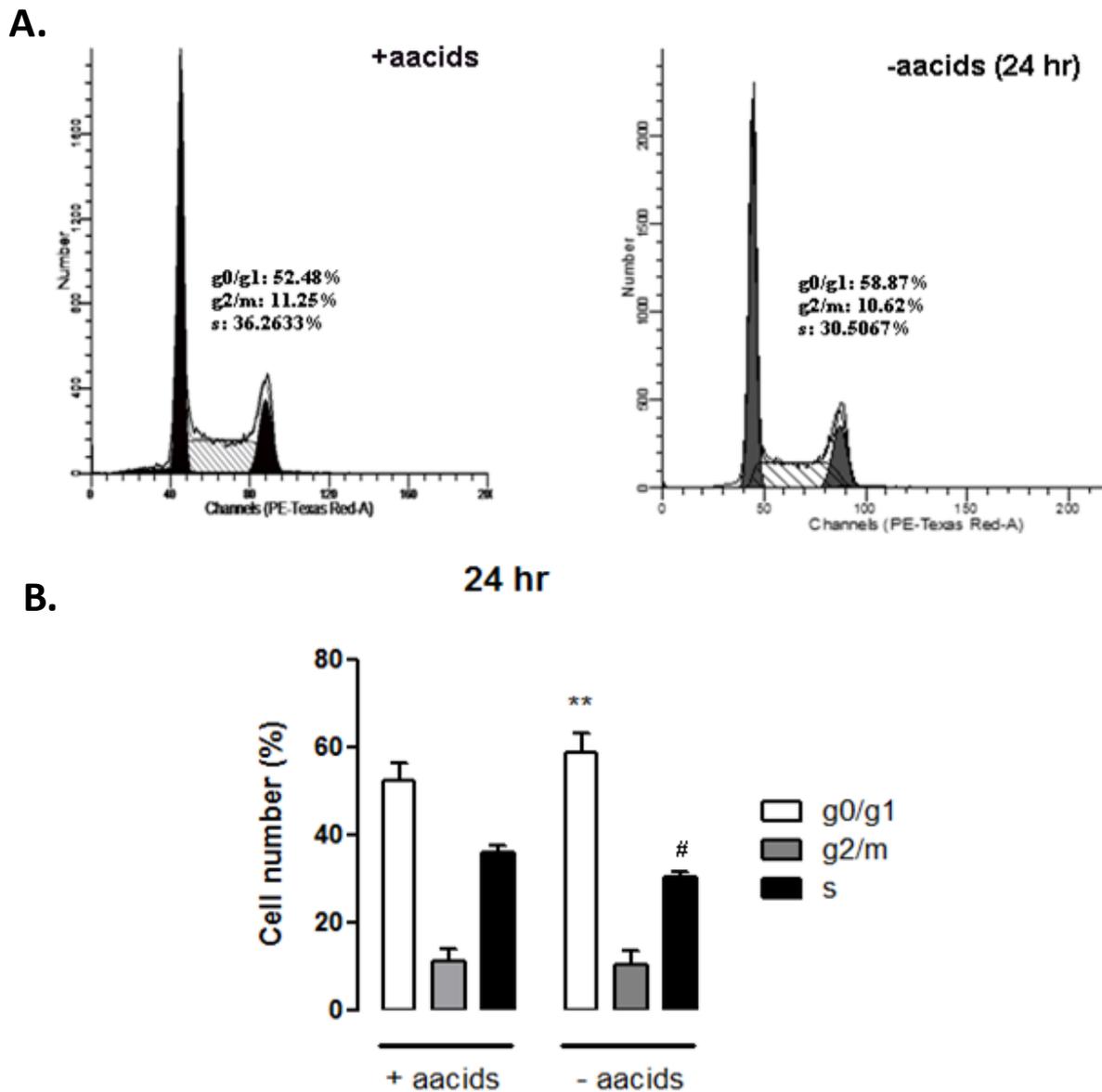
Fig. 1.12 MDAMB231 cells display increased g0/g1 cell cycle arrest following 24 hours of amino acid deprivation. Cell cycle progression was assessed using flow cytometry following a 24 hour incubation in culture medium without amino acids and compared with cells incubated for a similar duration in culture medium containing amino acids. A. Typical DNA histograms and cell cycle phase percentages. B. Bar graphs representing the mean ± SEM of at least three independent determinations. hr = hours; aacids = amino acids. **, $P < 0.01$ vs. + amino acids g0/g1 phase; #, $P < 0.01$ vs. + amino acids s phase.

After 24 hours incubation in amino acid free medium, MDAMB231 cells displayed a significantly increased percentage of cells in the g0/g1 phase of the cell cycle and a significantly decreased percentage of cells in the s phase (Fig 1.12).
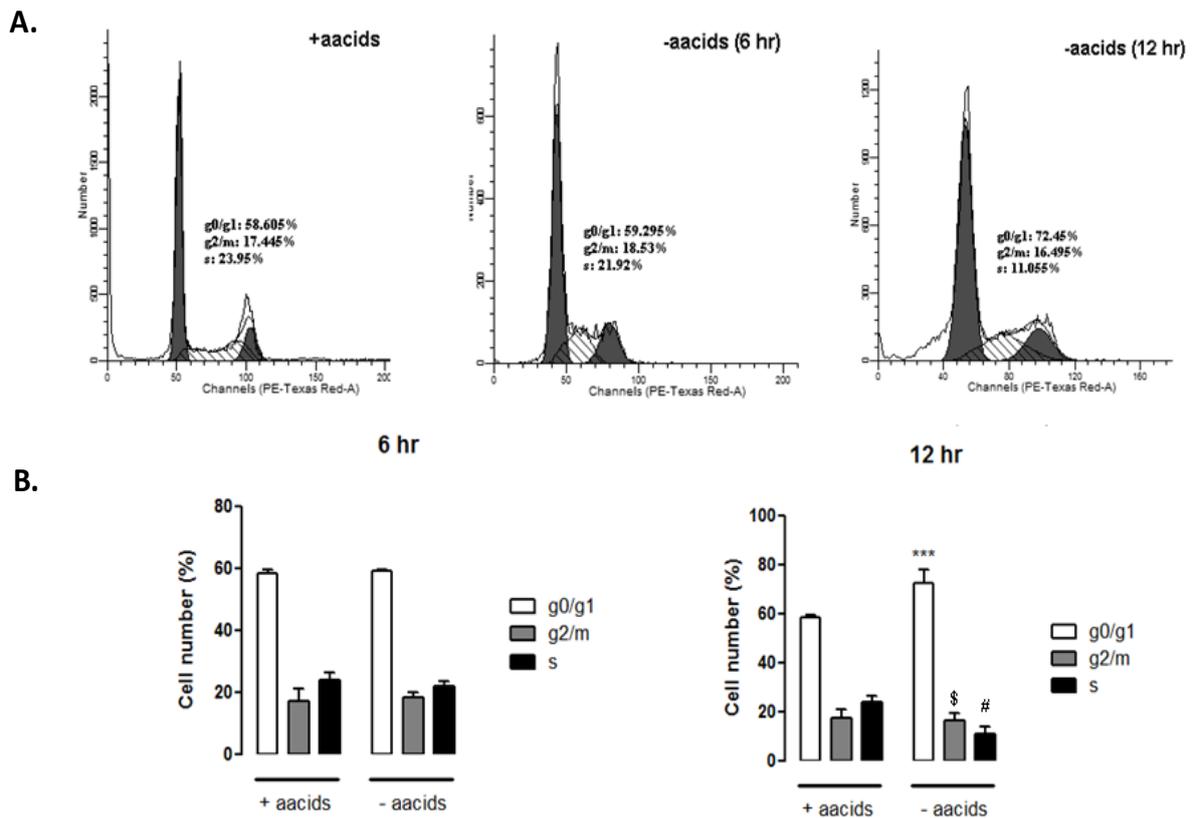
Fig. 1.13 MCF12A cells display increased g0/g1 arrest and decreased s phase after 12 hours of amino acid deprivation. Cell cycle progression was assessed using flow cytometry following 6 and 12 hour incubations in culture medium without amino acids and compared with cells incubated for similar durations in culture medium containing amino acids. A. Typical DNA histograms and cell cycle phase percentages. B. Bar graphs representing the mean ± SEM of at least three independent determinations. hr = hours; aacids = amino acids. ***, $P < 0.001$ vs. + amino acids g0/g1 phase; \$, $P < 0.001$ vs. + amino acids g2/m phase; #, $P < 0.05$ vs. + amino acids s phase.

MCF12A cells displayed a pattern of g0/g1 arrest after 12 hours of starvation (Fig 1.13). While a significantly greater percentage of cells were in the g0/g1 phase after amino acid starvation, significantly fewer cells were present in the g2/m and s phases.

A.

B.
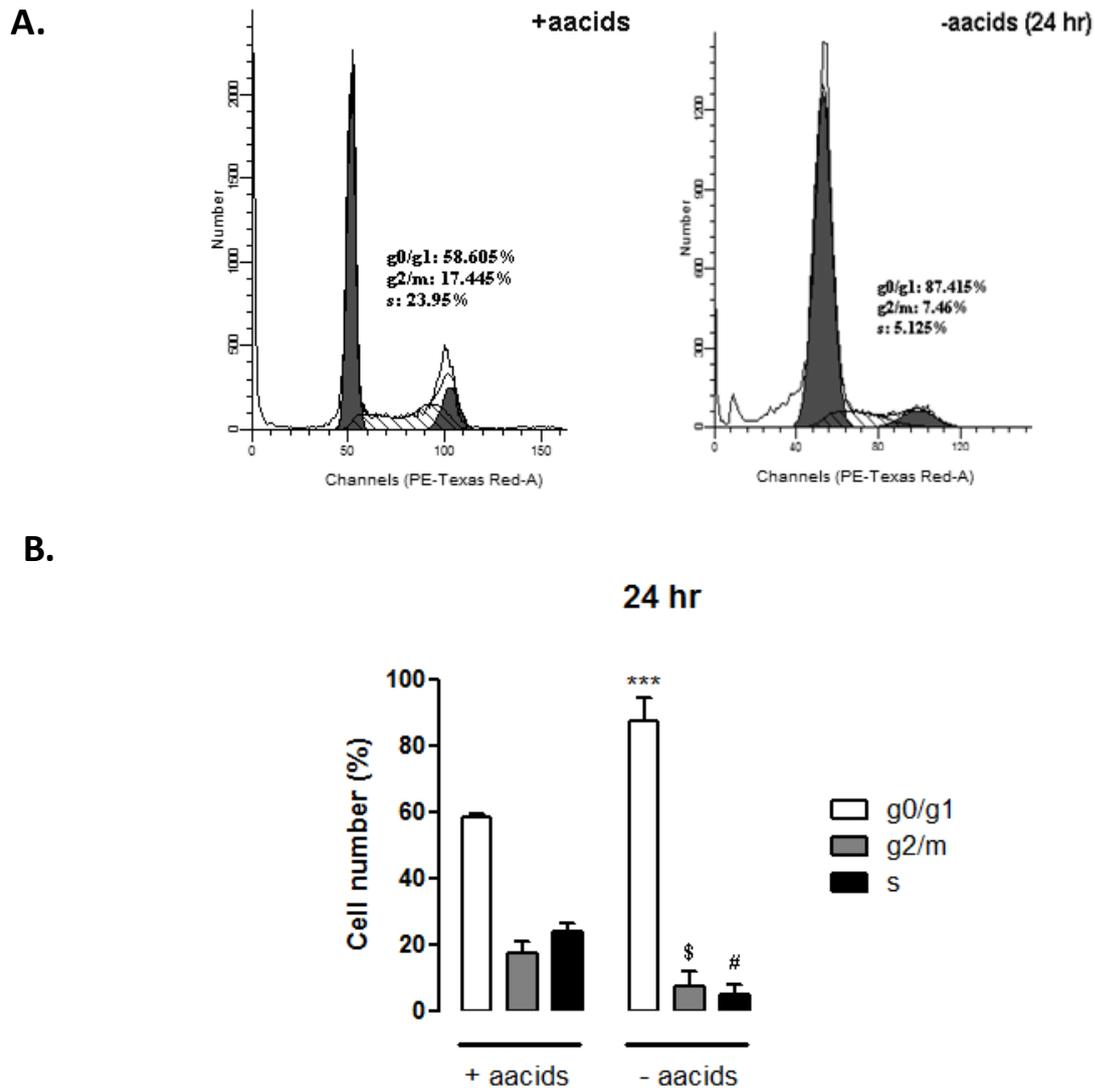
Fig. 1.14 MCF12A cells display increased g0/g1 cell cycle arrest and decrease s phase following 24 hours of amino acid deprivation. Cell cycle progression was assessed using flow cytometry following a 24 hour incubation in culture medium without amino acids and compared with cells incubated for a similar duration in culture medium containing amino acids. A. Typical DNA histograms and cell cycle phase percentages. B. Bar graphs representing the mean ± SEM of at least three independent determinations. hr = hours; aacids = amino acids. ***, $P < 0.001$ vs. + amino acids g0/g1 phase; $, $P < 0.05$ vs. + amino acids g2/m phase; #, $P < 0.001$ vs. + amino acids s phase.

The MCF12A cell lines had a significantly decreased percentage of cells in g2/m and s phases after 24 hours of amino acid starvation (Fig 1.14). A significantly higher percentage of cells were present in the g0/g1 phase of the cell cycle after 24 hours of amino acid starvation.

36

5   Discussion

Breast cancer is the most common neoplasm in women worldwide. Owing to the fact that amino acids are vital to cancer growth, the effects of amino acid deprivation regimens on cancer progression have been investigated for decades, but most research in this area had focused primarily on decreasing or omitting particular amino acids from the microenvironments of cancer cells. Although experimental protocols and outcomes have varied, it is clear that deprivation of specific amino acids can result in decreased invasiveness (Pelayo et al., 1999) and proliferation (Epner, 2001) and increased levels of cell death (Fu et al., 2010) in several cancer cell and xenograft models. Still, there is scant evidence that short-term, total amino acid starvation will produce analogous results. Recent clinical and pre-clinical studies investigating short term starvation protocols during cancer treatment have shown promise (Safdie et al., 2009), indicating that further studies are needed in this area.

The purpose of this observational study was to establish the sensitivity of a commonly used metastatic breast cancer cell line (MDAMB231) to a short term bout of complete amino acid starvation. The MTT cell activity assay assesses the fraction of metabolically viable cells, based on the principle that absorption measurements have been shown to correlate directly with the ability of vital reduction enzymes in the mitochondria of healthy cells to reduce the MTT compound. The MTT assay is utilized as a clonogenic and proliferation (Verma et al., 2010) or cell death assay (Qi et al., 2011) depending on study aims, and despite its lack of specificity is an excellent and useful assay with which to evaluate sensitivity of cultured cells to experimental interventions (by assessing cell viability). Our results indicate that fast growing metastatic MDAMB231 cells are highly sensitive to amino acid deprivation in an *in vitro* experimental model, and that these cells are significantly more sensitive to short periods of amino acid deprivation than a non-tumourogenic breast epithelial line (MCF12A) (Fig 1.1 and Fig 1.2). This is exemplified by an attenuation of MTT reducing capacity even in cultures

only partially deprived of amino acids for 24 hours (Fig 1.2). Cancer cells are known to require amino acids for growth and survival and the rapid proliferation rates of many cancers may depend on high levels of amino acids for protein and DNA synthesis to occur. MDAMB231 cells are highly glycolytic and fast growing (Robey et al., 2005) and may require access to greater concentrations of amino acids in a shorter period of time than slower growing non-cancer cells. Our observation that MTT reduction decreased subsequent to only 12 hours of amino acid depletion in the MDAMB231 cells seems to add credence to that suggestion (Fig 1.4).

It cannot be inferred from MTT reduction data whether changes occur due to alterations in proliferation patterns or simply due to loss of cells through cell death. So, next we wished to establish if decreased MTT activity correlated with cell death. A decrease in amino acid availability might not only impact the progression of biosynthesis pathways but also on metabolic systems in the cell (Bui and Thompson, 2006). Additionally, the pervasiveness throughout the cell and vital significance of amino acids to almost all cellular functions could be a reason why their absence has been shown to trigger programmed cell death mechanisms in some cancers (Fu et al., 1999). We present evidence here that a complete lack of amino acids results in the initiation of cell death mechanisms in the form of increased caspase 3/7 activity in MDAMB231 cells (Fig 1.6), a phenomenon that does not appear in MCF12A cells in our experimental model (Fig 1.5). We also show that caspase cleavage affects the downstream target PARP (Fig 1.7), a protein which undergoes distinct cleavage during caspase dependent apoptosis (Soldani and Scovassi, 2002). Further investigation demonstrated that these molecular changes were accompanied by disruption in membrane integrity in the MDAMB231 cells after only 12 hours of amino acids starvation (Fig 1.9). Together, these data suggest that the high cell turnover and metabolic capacity of the cancer cell line is vitally dependent on amino acids, so much so that their deficiency triggers a cell

death response. The rapid initiation of cell death after only 12 hours in the cancer cells suggests that complete exhaustion of the remaining amino acid pool causes cell death.

Uncontrolled cell proliferation is inherently linked to cancer and is managed by the cell cycle machinery (Collins et al., 1997). Chemotherapeutic agents leading to growth inhibition of MDAMB231 cells act in some instances by eliciting a g0/g1 phase accumulation of these cells (El-Sherbiny et al., 2001, Yan et al., 2006). A g0/g1 arrest in MDAMB231 cells after 24 hours of amino acid deprivation (Fig 1.12) indicates that these cells require the availability of amino acids for growth and proliferation and resort to arrest of these proliferative processes in their absence. A lack of molecular and mechanistic data limits formation of absolute conclusions; here observational evidence showed that a lack of amino acid availability resulted in a decrease in the ability of these cells to proliferate efficiently. Interestingly, while the non-tumourogenic cell line showed no lethal response to acute amino acid deficiency, they had a pronounced g0/g1 cell cycle arrest and a decreased s phase after only 12 hours without externally available amino acids (Fig 1.13). While these slower growing cells did not respond by initiation of immediate cell death like the cancer cells, lower amino acid levels still resulted in a profile of cell cycle arrest. Notably, the changes in the cell cycle were not reflected by the MTT assay.

5.1   Conclusion

Here we present evidence demonstrating that a fast growing metastatic cancer cell line is more sensitive to a dearth of amino acids than a non-tumourogenic line and that short term deprivation of amino acids results in increased initiation of cell death and evidence of proliferation arrest. Slower growing non-cancer cells showed no cell death response and instead appear to exit the cell cycle and arrest growth, presumably in an attempt to conserve

amino acids and ATP and prolong survival in the event that amino acid levels return to normal.

6   References

AGARWAL, A., MUNOZ-NAJAR, U., KLUEH, U., SHIH, S. C. & CLAFFEY, K. P. 2004. N-acetyl-cysteine promotes angiostatin production and vascular collapse in an orthotopic model of breast cancer. *Am J Pathol,* 164**,** 1683-96.

AHLUWALIA, G. S., GREM, J. L., HAO, Z. & COONEY, D. A. 1990. Metabolism and action of amino acid analog anti-cancer agents. *Pharmacol Ther,* 46**,** 243-71.

ALBINI, A., MORINI, M., D'AGOSTINI, F., FERRARI, N., CAMPELLI, F., ARENA, G., NOONAN, D. M., PESCE, C. & DE FLORA, S. 2001. Inhibition of angiogenesis-driven Kaposi's sarcoma tumor growth in nude mice by oral N-acetylcysteine. *Cancer Res,* 61**,** 8171-8.

APPEL, I. M., VAN KESSEL-BAKVIS, C., STIGTER, R. & PIETERS, R. 2007. Influence of two different regimens of concomitant treatment with asparaginase and dexamethasone on hemostasis in childhood acute lymphoblastic leukemia. *Leukemia,* 21**,** 2377-80.

BRADFORD, M. M. 1976. A rapid and sensitive method for the quantitation of microgram quantities of protein utilizing the principle of protein-dye binding. *Anal Biochem,* 72**,** 248-54.

BUI, T. & THOMPSON, C. B. 2006. Cancer's sweet tooth. *Cancer Cell,* 9**,** 419-20.

CARRASCOSA, J. M., MARTINEZ, P. & NUNEZ DE CASTRO, I. 1984. Nitrogen movement between host and tumor in mice inoculated with Ehrlich ascitic tumor cells. *Cancer Res,* 44**,** 3831-5.

CASCINO, A., MUSCARITOLI, M., CANGIANO, C., CONVERSANO, L., LAVIANO, A., ARIEMMA, S., MEGUID, M. M. & ROSSI FANELLI, F. 1995. Plasma amino acid imbalance in patients with lung and breast cancer. *Anticancer Res,* 15**,** 507-10.

COLLINS, K., JACKS, T. & PAVLETICH, N. P. 1997. The cell cycle and cancer. *Proc Natl Acad Sci U S A,* 94**,** 2776-8.

COOKE, J. P. & DZAU, V. J. 1997. Nitric oxide synthase: role in the genesis of vascular disease. *Annu Rev Med,* 48**,** 489-509.

DEHLINGER, P. J., HAMILTON, T. A. & LITT, M. 1977. Amino acid control of stable RNA synthesis in Friend leukemia cells in relation to intracellular purine nucleoside triphosphate levels. *Eur J Biochem,* 77**,** 495-9.

DIAMANDIS, E. P. 2010. Cancer biomarkers: can we turn recent failures into success? *J Natl Cancer Inst,* 102**,** 1462-7.

DORR, R. T., LIDDIL, J. D. & SOBLE, M. J. 1986. Cytotoxic effects of glutathione synthesis inhibition by L-buthionine-(SR)-sulfoximine on human and murine tumor cells. *Invest New Drugs,* 4**,** 305-13.

DOYLE, C., KUSHI, L. H., BYERS, T., COURNEYA, K. S., DEMARK-WAHNEFRIED, W., GRANT, B., MCTIERNAN, A., ROCK, C. L., THOMPSON, C., GANSLER, T. & ANDREWS, K. S. 2006. Nutrition and physical activity during and after cancer treatment: an American Cancer Society guide for informed choices. *CA Cancer J Clin,* 56**,** 323-53.

DRUMMOND, J. C. 1917. A Comparative Study of Tumour and Normal Tissue Growth. *Biochem J,* 11**,** 325-77.

EL-SHERBINY, Y. M., COX, M. C., ISMAIL, Z. A., SHAMSUDDIN, A. M. & VUCENIK, I. 2001. G0/G1 arrest and S phase inhibition of human cancer cell lines by inositol hexaphosphate (IP6). *Anticancer Res,* 21**,** 2393-403.

EPNER, D. E. 2001. Can dietary methionine restriction increase the effectiveness of chemotherapy in treatment of advanced cancer? *J Am Coll Nutr,* 20**,** 443S-449S; discussion 473S-475S.

FU, Y. M., LIN, H., LIU, X., FANG, W. & MEADOWS, G. G. 2010. Cell death of prostate cancer cells by specific amino acid restriction depends on alterations of glucose metabolism. *J Cell Physiol,* 224**,** 491-500.

FU, Y. M., YU, Z. X., PELAYO, B. A., FERRANS, V. J. & MEADOWS, G. G. 1999. Focal adhesion kinase-dependent apoptosis of melanoma induced by tyrosine and phenylalanine deficiency. *Cancer Res,* 59**,** 758-65.

FUCHS, B. C. & BODE, B. P. 2005. Amino acid transporters ASCT2 and LAT1 in cancer: partners in crime? *Semin Cancer Biol,* 15**,** 254-66.

GATENBY, R. A. & GILLIES, R. J. 2004. Why do cancers have high aerobic glycolysis? *Nat Rev Cancer,* 4**,** 891-9.

GUO, H., LISHKO, V. K., HERRERA, H., GROCE, A., KUBOTA, T. & HOFFMAN, R. M. 1993. Therapeutic tumor-specific cell cycle block induced by methionine starvation in vivo. *Cancer Res,* 53**,** 5676-9.

GUPTA, N., PRASAD, P. D., GHAMANDE, S., MOORE-MARTIN, P., HERDMAN, A. V., MARTINDALE, R. G., PODOLSKY, R., MAGER, S., GANAPATHY, M. E. & GANAPATHY, V. 2006. Up-regulation of the amino acid transporter ATB(0,+) (SLC6A14) in carcinoma of the cervix. *Gynecol Oncol,* 100**,** 8-13.

HE, Y. C., CAO, J., CHEN, J. W., PAN, D. Y. & ZHOU, Y. K. 2003. Influence of methionine/valine-depleted enteral nutrition on nucleic acid and protein metabolism in tumor-bearing rats. *World J Gastroenterol,* 9**,** 771-4.

HEILBRONN, L. K. & RAVUSSIN, E. 2005. Calorie restriction extends life span--but which calories? *PLoS Med,* 2**,** e231.

HICKS, C., PANNUTI, A. & MIELE, L. 2011. Associating GWAS Information with the Notch Signaling Pathway Using Transcription Profiling. *Cancer Inform,* 10**,** 93-108.

HOLM, E., HAGMULLER, E., STAEDT, U., SCHLICKEISER, G., GUNTHER, H. J., LEWELING, H., TOKUS, M. & KOLLMAR, H. B. 1995. Substrate balances across colonic carcinomas in humans. *Cancer Res,* 55**,** 1373-8.

HUANG, S. 2002. Histone methyltransferases, diet nutrients and tumour suppressors. *Nat Rev Cancer,* 2**,** 469-76.

JAYARAM, H. N., COONEY, D. A., VISTICA, D. T., KARIYA, S. & JOHNSON, R. K. 1979. Mechanisms of sensitivity or resistance of murine tumors to N-(phosphonacetyl)-L-aspartate (PALA). *Cancer Treat Rep,* 63**,** 1291-302.

KAWAKAMI, K., KAWAKAMI, M. & PURI, R. K. 2004. Nitric oxide accelerates interleukin-13 cytotoxin-mediated regression in head and neck cancer animal model. *Clin Cancer Res,* 10**,** 5264-70.

KAWAKAMI, S., KAGEYAMA, Y., FUJII, Y., KIHARA, K. & OSHIMA, H. 2001. Inhibitory effect of N-acetylcysteine on invasion and MMP-9 production of T24 human bladder cancer cells. *Anticancer Res,* 21**,** 213-9.

KELLY, R. G., NALLY, K., SHANAHAN, F. & O'CONNELL, J. 2002. Type I insulin-like growth factor receptor expression on colorectal adenocarcinoma cell lines is decreased in response to the chemopreventive agent N-acetyl-l-cysteine. *Ann N Y Acad Sci,* 973**,** 555-8.

KIM, C. H., PARK, K. J., PARK, J. R., KANAI, Y., ENDOU, H., PARK, J. C. & KIM DO, K. 2006. The RNA interference of amino acid transporter LAT1 inhibits the growth of KB human oral cancer cells. *Anticancer Res,* 26**,** 2943-8.

KLIMBERG, V. S., KORNBLUTH, J., CAO, Y., DANG, A., BLOSSOM, S. & SCHAEFFER, R. F. 1996. Glutamine suppresses PGE2 synthesis and breast cancer growth. *J Surg Res,* 63**,** 293-7.

KOCHER, R. A. 1944. Effects of a Low Lysine Diet on the Growth of Spontaneous Mammary Tumors in Mice and on the N2 Balance in Man. *Cancer Research,* 4**,** 251-256.

KRITCHEVSKY, D. 2003. Diet and cancer: what's next? *J Nutr,* 133**,** 3827S-3829S.

LAI, H. S., LEE, J. C., LEE, P. H., WANG, S. T. & CHEN, W. J. 2005. Plasma free amino acid profile in cancer patients. *Semin Cancer Biol,* 15**,** 267-76.

LEE, C. & LONGO, V. D. 2011. Fasting vs dietary restriction in cellular protection and cancer treatment: from model organisms to patients. *Oncogene,* 30**,** 3305-16.

LIU, X., FU, Y. M. & MEADOWS, G. G. 2011. Differential effects of specific amino acid restriction on glucose metabolism, reduction/oxidation status and mitochondrial damage in DU145 and PC3 prostate cancer cells. *Oncol Lett,* 2**,** 349-355.

LORINCZ, A. B. & KUTTNER, R. E. 1965. Response of malignancy to phenylalanine restriction. A preliminary report on a new concept of managing malignant disease. *Nebr State Med J,* 50**,** 609-17.

MAEDA, J., HIGASHIYAMA, M., IMAIZUMI, A., NAKAYAMA, T., YAMAMOTO, H., DAIMON, T., YAMAKADO, M., IMAMURA, F. & KODAMA, K. 2010. Possibility of multivariate function composed of plasma amino acid profiles as a novel screening index for non-small cell lung cancer: a case control study. *BMC Cancer,* 10**,** 690.

MEDINA, M. A., SANCHEZ-JIMENEZ, F., MARQUEZ, J., RODRIGUEZ QUESADA, A. & NUNEZ DE CASTRO, I. 1992. Relevance of glutamine metabolism to tumor cell growth. *Mol Cell Biochem,* 113**,** 1-15.

MORINI, M., CAI, T., ALUIGI, M. G., NOONAN, D. M., MASIELLO, L., DE FLORA, S., D'AGOSTINI, F., ALBINI, A. & FASSINA, G. 1999. The role of the thiol N-acetylcysteine in the prevention of tumor invasion and angiogenesis. *Int J Biol Markers,* 14**,** 268-71.

MURATA, K. & MORIYAMA, M. 2007. Isoleucine, an essential amino acid, prevents liver metastases of colon cancer by antiangiogenesis. *Cancer Res,* 67**,** 3263-8.

NISHIHIRA, T., TAKAGI, T., KAWARABAYASHI, Y., IZUMI, U., OHKUMA, S., KOIKE, N., TOYODA, T. & MORI, S. 1988. Anti-cancer therapy with valine-depleted amino acid imbalance solution. *Tohoku J Exp Med,* 156**,** 259-70.

OKAZAKI, I., MATSUYAMA, S., SUZUKI, F., MARUYAMA, K., MARUTA, A., KUBOCHI, K., YOSHINO, K., KOBAYASHI, Y., ABE, O. & TSUCHIYA, M. 1992. Endogenous urinary 3-hydroxyproline has 96% specificity and 44% sensitivity for cancer screening. *J Lab Clin Med,* 120**,** 908-20.

PELAYO, B. A., FU, Y. M. & MEADOWS, G. G. 1999. Inhibition of B16BL6 melanoma invasion by tyrosine and phenylalanine deprivation is associated with decreased secretion of plasminogen activators and increased plasminogen activator inhibitors. *Clin Exp Metastasis,* 17**,** 841-8.

POGRIBNY, I. P., BASNAKIAN, A. G., MILLER, B. J., LOPATINA, N. G., POIRIER, L. A. & JAMES, S. J. 1995. Breaks in genomic DNA and within the p53 gene are associated with hypomethylation in livers of folate/methyl-deficient rats. *Cancer Res,* 55**,** 1894-901.

POIRSON-BICHAT, F., GONFALONE, G., BRAS-GONCALVES, R. A., DUTRILLAUX, B. & POUPON, M. F. 1997. Growth of methionine-dependent human prostate cancer (PC-3) is inhibited by ethionine combined with methionine starvation. *Br J Cancer,* 75**,** 1605-12.

QI, R., SHEN, M., CAO, X., GUO, R., TIAN, X., YU, J. & SHI, X. 2011. Exploring the dark side of MTT viability assay of cells cultured onto electrospun PLGA-based composite nanofibrous scaffolding materials. *Analyst,* 136**,** 2897-903.

RAFFAGHELLO, L., SAFDIE, F., BIANCHI, G., DORFF, T., FONTANA, L. & LONGO, V. D. 2010. Fasting and differential chemotherapy protection in patients. *Cell Cycle,* 9**,** 4474-6.

ROBEY, I. F., LIEN, A. D., WELSH, S. J., BAGGETT, B. K. & GILLIES, R. J. 2005. Hypoxia-inducible factor-1alpha and the glycolytic phenotype in tumors. *Neoplasia,* 7**,** 324-30.

ROOMI, M. W., IVANOV, V., KALINOVSKY, T., NIEDZWIECKI, A. & RATH, M. 2006. Inhibition of matrix metalloproteinase-2 secretion and invasion by human ovarian cancer cell line SK-OV-3 with lysine, proline, arginine, ascorbic acid and green tea extract. *J Obstet Gynaecol Res,* 32**,** 148-54.

ROOMI, M. W., ROOMI, N. W., IVANOV, V., KALINOVSKY, T., NIEDZWIECKI, A. & RATH, M. 2005. Modulation of N-methyl-N-nitrosourea induced mammary tumors in Sprague-Dawley rats by combination of lysine, proline, arginine, ascorbic acid and green tea extract. *Breast Cancer Res,* 7**,** R291-5.

RUSSO, A. & RIZZO, S. 2008. Could starvation minimize chemotherapy-induced toxicities? *Expert Opin Ther Targets,* 12**,** 1205-7.

SAFDIE, F. M., DORFF, T., QUINN, D., FONTANA, L., WEI, M., LEE, C., COHEN, P. & LONGO, V. D. 2009. Fasting and cancer treatment in humans: A case series report. *Aging (Albany NY),* 1**,** 988-1007.

SCHREIBER, H., ROWLEY, J. D. & ROWLEY, D. A. 2011. Targeting mutations predictably. *Blood,* 118**,** 830-1.

SHEEN, J. H., ZONCU, R., KIM, D. & SABATINI, D. M. 2011. Defective regulation of autophagy upon leucine deprivation reveals a targetable liability of human melanoma cells in vitro and in vivo. *Cancer Cell,* 19**,** 613-28.

SIMEONE, A. M., EKMEKCIOGLU, S., BROEMELING, L. D., GRIMM, E. A. & TARI, A. M. 2002. A novel mechanism by which N-(4-hydroxyphenyl)retinamide inhibits breast cancer cell growth: the production of nitric oxide. *Mol Cancer Ther,* 1**,** 1009-17.

SOLDANI, C. & SCOVASSI, A. I. 2002. Poly(ADP-ribose) polymerase-1 cleavage during apoptosis: an update. *Apoptosis,* 7**,** 321-8.

SOUBA, W. W. 1993. Glutamine and cancer. *Ann Surg,* 218**,** 715-28.

SUGIMURA, T., BIRNBAUM, S. M., WINITZ, M. & GREENSTEIN, J. P. 1959. Quantitative nutritional studies with water-soluble, chemically defined diets. IX. Further studies on d-glucosaminecontaining diets. *Arch Biochem Biophys,* 83**,** 521-7.

TAN, Y., SUN, X., XU, M., TAN, X., SASSON, A., RASHIDI, B., HAN, Q., WANG, X., AN, Z., SUN, F. X. & HOFFMAN, R. M. 1999. Efficacy of recombinant methioninase in combination with cisplatin on human colon tumors in nude mice. *Clin Cancer Res,* 5**,** 2157-63.

TOSETTI, F., FERRARI, N., DE FLORA, S. & ALBINI, A. 2002. Angioprevention': angiogenesis is a common and key target for cancer chemopreventive agents. *FASEB J,* 16**,** 2-14.

TSUKAHARA, K., WATANABE, T., HATA-SUGI, N., YOSHIMATSU, K., OKAYAMA, H. & NAGASU, T. 2001. Anticancer agent E7070 inhibits amino acid and uracil transport in fission yeast. *Mol Pharmacol,* 60**,** 1254-9.

TYAGI, A. K. & COONEY, D. A. 1984. Biochemical pharmacology, metabolism, and mechanism of action of L-alanosine, a novel, natural antitumor agent. *Adv Pharmacol Chemother,* 20**,** 69-121.

VERMA, A., PRASAD, K. N., SINGH, A. K., NYATI, K. K., GUPTA, R. K. & PALIWAL, V. K. 2010. Evaluation of the MTT lymphocyte proliferation assay for the diagnosis of neurocysticercosis. *J Microbiol Methods,* 81**,** 175-8.

WADMAN, M. 2011. Fifty genome sequences reveal breast cancer's complexity. *Nature*.

YAN, J., LUO, D., LUO, Y., GAO, X. & ZHANG, G. 2006. Induction of G1 arrest and differentiation in MDA-MB-231 breast cancer cell by boehmeriasin A, a novel compound from plant. *Int J Gynecol Cancer,* 16**,** 165-70.

YOSHIDA, S., KAIBARA, A., YAMASAKI, K., ISHIBASHI, N., NOAKE, T. & KAKEGAWA, T. 1995. Effect of glutamine supplementation on protein metabolism and glutathione in tumor-bearing rats. *JPEN J Parenter Enteral Nutr,* 19**,** 492-7.

YOSHIOKA, T., WADA, T., UCHIDA, N., MAKI, H., YOSHIDA, H., IDE, N., KASAI, H., HOJO, K., SHONO, K., MAEKAWA, R., YAGI, S., HOFFMAN, R. M. & SUGITA, K. 1998. Anticancer efficacy in vivo and in vitro, synergy with 5-fluorouracil, and safety of recombinant methioninase. *Cancer Res,* 58**,** 2583-7.

2 _____

Autophagy is vital for the prevention of cell death and growth arrest during the first hours of amino acid starvation in MDAMB231 and MCF12A cells

Mammalian cells have a remarkable ability to circumvent the deleterious consequences of short term nutrient starvation. Among the most important mechanisms conferring this protection is the ability of cells to generate free amino acids through degradation of intracellular proteins and organelles through the autophagosomal-lysosomal pathway. Some cancer cells have high levels of basal autophagy and may therefore have the capacity to evade some negative consequences of amino acid starvation in an acute setting. This chapter presents evidence that autophagy inhibition using bafilomycin A1 decreases cell survival and reduces proliferation levels during acute amino acid starvation in the K-ras mutant MDAMB231 breast cancer cell line, and then speculates that autophagy is crucial for this tolerance to acute amino starvation.

1   Introduction

Mammalian cells have evolved adaptive and complementary systems of mechanisms to manage fluctuations in cell nutrient levels. These mechanisms are not only vitally important when contending with typical instabilities in nutrient levels but also provide the cell with a way to evade negative consequences in instances of atypical extreme spells of nutrient depletion. These sophisticated systems have developed in such a way as to create a buffer zone in which temporary variations in availability of certain nutrients have little if any effect on cellular function.

Mammalian survival is not normally reliant on constant external energy intake as a considerable fraction of imbibed foodstuffs will be internally stored in well-nourished

46

individuals. As such, the whole organism is well adapted for rapid mobilization of glucose and fat stores during starvation conditions. Much of this is achieved through hormonal regulation, and it is now well established that induced decreases in insulin levels during periods of starvation lead to increased blood glucose levels (Johnston et al., 1982). Furthermore, low levels of insulin are known to stimulate lipid breakdown, while increased levels of circulating glucagon increase gluconeogenesis in the liver (Mortimore and Poso, 1987). At the same time, elevated cortisol secretion stimulates both gluconeogenesis and increases action on fat breakdown (Douyon and Schteingart, 2002).

Amino acids, on the other hand, can't be stored as such, and are effectively stockpiled as functional proteins, especially in the liver and muscle tissue. There exists a rapid equilibrium between the cellular amino acid pool in the tissue and the systemic amino acid pool of plasma protein which can be utilized to yield free amino acids for maintenance of homeostasis. A cell is therefore able to acquire amino acids from the plasma as required for processes such as protein synthesis, and the plasma amino acid pool can then be replenished by the degradation of proteins elsewhere in the body, such as the liver or muscle. This degradation is achieved through hormonal control of protein catabolism stimulated by increased glucagon (Mortimore and Poso, 1987) and cortisol levels (Douyon and Schteingart, 2002) and by depleted levels of insulin (Johnston et al., 1982). A complementary decrease in protein synthesis in the absence of insulin stimulation prevents biosynthesis of non-vital proteins and aids preservation of intracellular amino acid levels (Dice, 1988).

During a bout of short term starvation cells utilize two broadly defined mechanisms that function together to extract amino acids from intracellular proteins; a non-lysosomal proteolytic pathway by means of the multi-enzymatic proteosome system or degradation

pathways characterized by lysosomal proteases typified by the autophagosomal-lysosmal system.

1.1   Proteolytic responses to short-term amino acid starvation

Amongst the tumultuous rhythm and microscopic fervour of the cytosol reside the functional units of the cell, the proteins. Proteins measure in their tens of thousands by variety in any given cell, and of this assortment, approximately a thousand occur in great abundance and comprises the majority of a cell"s operational contents. These complex structures are the molecular products of a predetermined assemblage of amino acids, strung together in a genetically pre-programmed order. In times of short term amino acid supply-drought cells must acquire these fundamental components for certain vital processes and functions. It accomplishes this feat through an act of self-sufficiency when it catabolises resident proteins and recycles the building blocks for use in vital functions elsewhere in the cell. The two principal mechanisms whereby a cell is able to do this are described below.

1.1.1 Degradation by the ubiquitin proteasome system (UPS)

During starvation mammalian cells activate proteolytic systems that are able to enzymatically liberate amino acids for use in protein biosynthesis or energy production. Proteins destined for degradation by this system must first undergo several rounds of covalent tagging on their lysine residues with small peptides called ubiqutin, literally marking them for destruction. They are then shuttled into the central cavity of a cylindrical complex known as the 26S proteasome. Here the tagged proteins are unfolded before proteolytic enzymes located on the luminal wall of the proteasome reduce them to oligopeptides that are eventually broken down to amino acids following further enzyme action (Tisdale, 2005). This ATP dependent system

is accountable for most of the amino acids liberated from skeletal muscle during starvation and is known to be induced during short term amino acid depletion (Mitch and Goldberg, 1996). Amino acids liberated from skeletal muscle in this way are then available for use as energy substrates or for conversion to glucose in the liver. In this way, the amino acid and nitrogen needs of cells are partially met through proteosomal degradation during the first hours of starvation (Finn and Dice, 2006). The ubiquitin-proteasome pathway is also activated in a number of disease states, and is thought to be crucial for survival during short term amino acid starvation in some cancers, including breast cancer (Mizrachy-Schwartz et al., 2010). Furthermore, increased proteasome function is known to occur in skeletal muscle during cancer cachexia (Lecker et al., 1999).

1.1.2 Degradation by the autophagosomal-lysosomal system

Autophagy broadly describes the genetically controlled transference and delivery of bulk cytoplasmic materials to endosomal and lysosomal compartments for degradation. Autophagy has been classed into three distinct ATP dependent types that differ in some functioning and mechanistic activation (Mizushima, 2007). Macroautophagy (referred to simply as autophagy henceforth) is the most well described of these, the other less understood forms designated as microautophagy and chaperone-mediated autophagy. Almost all eukaryotic cells possess low levels of autophagy at resting state (Mizushima et al., 2004). The function of this basal autophagy pertains mainly to the bulk ingestion of cell cytoplasm which results in the removal of cellular „junk‟ in the form of redundant organelles and macromolecules. In fact, autophagy is the only known eukaryotic system able to degrade intracellular materials that are too large to be broken down by the proteasome. This property of organelle and protein quality control is crucial to cellular homeostasis and autophagy deficiency produced though genetically engineered ATG5 or ATG7 knock-outs results in pathological neurodegeneration or prenatal

death (Cataldo et al., 1996, Kuma et al., 2004). Although described as a bulk degradation process, autophagy can behave selectively under some circumstances (Yu et al., 2008). This selective autophagy is supervised by specific protein regulators such as parkin (Mizushima and Levine, 2010) and substrates selectively degraded in this way are known to influence cell survival and death dynamics (Onodera and Ohsumi, 2004).

Autophagy, first described in the 1960˅s (Stromhaug and Klionsky, 2001), is characterised by the development of specialized double membrane autophagosomes that engulf organelles and other cellular components such as proteins before attaining their lytic enzymes through fusion with lysosomes or endosomes. It is this union that confers the ability for mass catabolism and proteolysis of ingested materials (Lockshin and Zakeri, 2004). Exactly how the autophagosome forms and develops is only partly understood, but the discovery that these processes are regulated by over thirty autophagy related genes (ATG) has played a significant role in furthering understanding (Nakatogawa et al., 2009). It has become clear that formation of the autophagosome relies on the endoplasmic reticulum (ER) (Yla-Anttila et al., 2009), and that amino acid starvation results in recruitment of the mammalian target of rapamycin (mTOR) to regions located proximal to or perhaps even physically on the ER (Hayashi-Nishino et al., 2009). Other membrane sites have now also been implicated as potential autophagosome precursors (Webber and Tooze, 2010). Recruitment of mTOR is followed by conscription of a complex of class III phosphatidylinositol-3-OH kinase (PI3K) which includes Beclin-1 and ATG14, proteins coded for by the ATG (Matsunaga et al., 2009). Subsequent to the recruitment and oligomerization of additional proteins, structures known as omegasomes are ultimately formed, and it is from these structures that development of bilayered isolation membranes, precursors of autophagosomes, is founded (Axe et al., 2008). Isolation membranes lengthen and surround intracellular cargo before the ends of the membrane meet and encapsulate the material now destined to become contents of the

autophagosome. The major protein complexes responsible for this series of events are coded for by ATG; these enzymatically catalyse reactions producing the conjugate ATG12-ATG5 (Fujita et al., 2008) and the solubilisation and conjugation of LC3 to phosphatidylethanolamine (PE) to yield the lipidated variant of LC3 (ATG8), an important component of the autophagosome (Weidberg et al., 2010). Finally, autophagosomes fuse with lysosomes generating autolysosomes (or autophagolysosomes if endosomal fusion predated fusion with a lysosome). Finally, the inner membrane of the autophagosome, along with the cargo contained within it, becomes degraded by lysosomal hydrolases.

Autophagy is believed to have evolved in response to cellular stress, primarily nutrient starvation, hypoxia, ATP depletion and signals prompting cellular remodelling where it has been demonstrated to have signalling pathway overlap (Meijer and Codogno, 2004). Although often described as programmed cell death type II in the past (Lockshin and Zakeri, 2004), contemporary models depict autophagy more accurately as a cell survival mechanism that acts alongside cell death in many instances (Tsujimoto and Shimizu, 2005). The relationship between apoptosis and autophagy is complex and many of the same mechanisms responsible for activation of apoptosis are also known to activate autophagy. As both systems are important during a stress response it is plausible that coevolution has lead to a degree of pathway overlap.
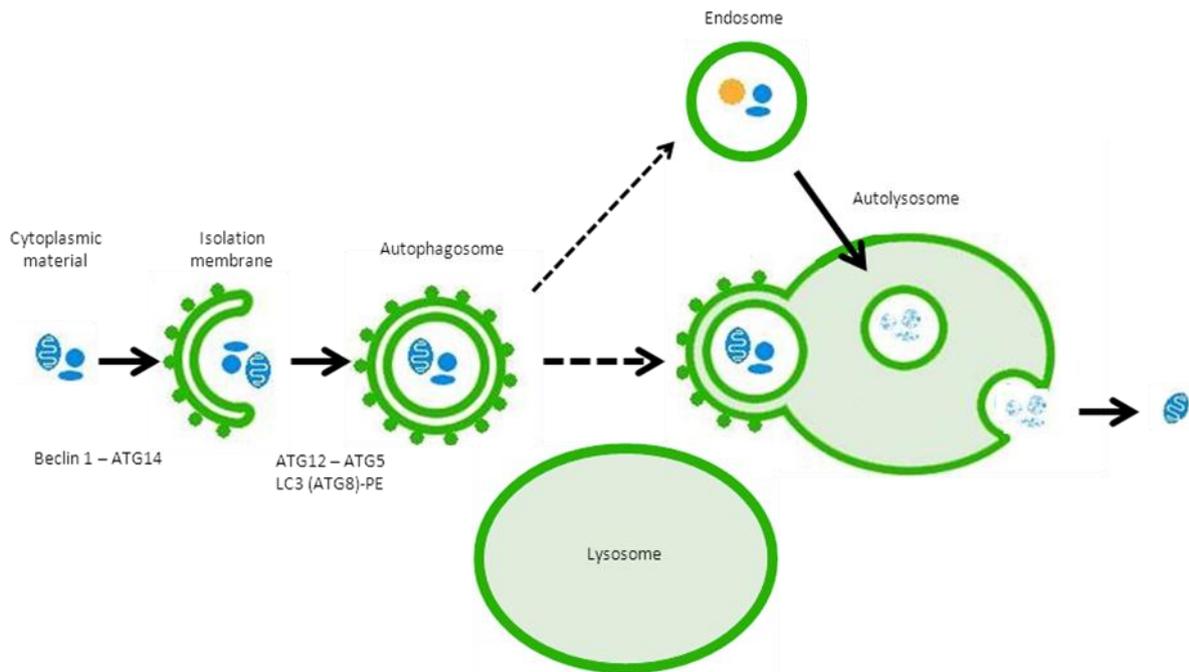
Image 2.1 Schematic depicting degradation by means of macroautophagy and the autophagasomal-lysosomal system. Subsequent to the recruitment of ATG proteins, development of bilayered membrane proteins occurs. This is followed by engulfment of a mass of cytoplasmic material with the aid of other ATG proteins. Resultant autophagosomes translocate to and fuse with lysosomes to form autolysosomes. Here lysosomal hydrolases degrade delivered material breaking it down to basic constituents.

The most well defined function of autophagy is during starvation, particularly amino acid deprivation, and it is well known that autophagy is transiently activated during the first twenty four hours following a starvation incident (Mizushima et al., 2004). Leucine deficiency appears to be the most potent trigger for autophagy induction, but in order for autophagy to become fully activated many other amino acids including tyrosine, phenylalanine, glutamine, alanine, proline and methionine must be lacking as well (Finn and Dice, 2006). Interestingly, although it has been shown that the amino acid that must be lacking in order for protein degradation to occur depends on tissue type, leucine shortage is necessary in all cases (Tischler et al., 1982). The end-products of lysosomal degradation following autophagy are not precisely known, but it is assumed that the basic building blocks of proteins and organelles (amino and fatty acids) are among them. This system also represents an important quality control mechanism whereby proteins are metabolised and recycled (Klionsky, 2007).

Hydrolysis of peptide bonds by lysosomal proteases yields protein degradation products in the form of peptides and amino acids which are then released into the cytosol by way of dedicated transport systems. Although the exact fate of these digestion products is not completely understood, it is most likely the case that the resulting amino acids enter back into the ribosomal system immediately to form new proteins, buffer the intracellular free amino acid pool, enter the blood and move to other tissues and organs or are eventually lost into the urine.

1.3   Amino acid signalling in the control of autophagy

It is essential that cellular growth and proliferation be coordinated with signals informing the cell factory of the nutrient availability status. This is vital to ensure that important energy consuming processes such as protein synthesis and maintenance remain in equilibrium with the nutrient supply. In addition to their critical function in metabolism and as compositional elements in cellular material, amino acids can also function as signalling molecules. The predominant signalling assignment of amino acids (leucine in particular (Blommaart et al., 1997) is their ability to control signal transduction pathway activity that is integral to autophagy regulation. Autophagy has been conclusively demonstrated to occur *in vivo* in almost all tissues following nutrient starvation (Mizushima et al., 2004), and one perspective is that accessibility to sufficient levels of amino acids results in the inhibition of autophagy.

It has been known for over thirty years that amino acids are able to inhibit autophagosome formation (Mortimore and Schworer, 1977). Inhibition of autophagy by amino acids was shown to be accompanied by increased stimulation of protein synthesis and an associated increase in the phosphorylation of a ribosomal protein designated S6 (Blommaart et al., 1995). S6 is partly responsible for ribosomal recruitment to mRNA (Meyuhas, 2000) and is an

important component for cellular growth (Mamane et al., 2004). Positioned directly upstream of this phosphorylation event is a serine/threonine protein kinase, mTOR, which is at the centre of an important signalling network that moderates the rate and type of protein synthesis occurring in response to signals informing it of the cellular nutrient status. By balancing nutrient input with its usage, mTOR prevents cellular energy expenditure from outstripping the cell‟s capacity for nutrient acquisition and energy production (Shintani and Klionsky, 2004).

1.3.2 mTOR

mTOR is controlled by a complex interplay of growth factor and nutrient signals acting at various levels of the mTOR pathway (Wullschleger et al., 2006). It is negatively regulated by a heterodimer consisting of the tubular sclerosis proteins (TSC1 and TSC2), which decrease mTOR signalling, by acting through a small GTP-binding protein (Rheb), during circumstances of diminished nutrients (Inoki et al., 2005). Insulin and growth factors act through PI3K/Akt and Ras, where increased growth factor signalling is converted into pleiotropic effects of growth and mitogenesis (Plas and Thompson, 2005). In this way, pathway communications during typical conditions result in phosphorylation of the TSC1/TSC2 complex and relief of inhibition downstream on mTOR allowing protein synthesis (and energy consumption) to continue unabated (Tee et al., 2002). However, mTOR has been shown to sense nutrient accessibility independently of these upstream mitogenic and growth factor signals and respond directly to alterations in amino acid, oxygen and ATP levels (Hay and Sonenberg, 2004). It has been proposed that hypoxia (Brugarolas et al., 2004) and increasing AMP/ATP ratios (Inoki et al., 2003) act at mTOR or TSC1/TSC2 to diminish pathway activity during times of stress.

54

1.3.3 mTOR, amino acid sensing and autophagy

mTOR is extremely sensitive to changes in nutrients, and in particular to decreased concentrations of amino acids (Gu et al., 2006). The antifungal compound rapamycin inhibits mTOR directly and was shown to be able to reverse the amino acid deprivation induced phosphorylation of S6 (Shintani and Klionsky, 2004). This finding contributed to the hypothesis that amino acid dependent signalling and control of protein synthesis both acted through the mTOR pathway. Furthermore, amino acids stimulate mTOR signalling even in the absence of upstream signals from PI3K/Akt (Blommaart et al., 1995), indicating a potential for the presence of a devoted sensing mechanism. Current evidence indicates that an intracellular amino acid receptor (Beugnet et al., 2003) regulates Rheb binding to mTOR (Long et al., 2005), but it remains inconclusive whether mTOR itself is acting as the amino acids senor or if a third party inhibitor is involved in some way. Inhibition of mTOR signalling preserves homeostasis not only by regulating protein synthesis levels but also by stimulating rapid protein breakdown through concomitant autophagy regulation. It is believed that increasing autophagy during periods of amino acid depletion allows cells to utilize the break-down products of autophagic degradation as energy sources and for synthesis of survival proteins. How mTOR activation influences the intensity of cellular autophagy is unknown, but experiments involving yeast have given some insight. TOR is important during the starvation or rapamycin treatment of yeast cells when the dephosphorylation of the autophagy protein ATG1 enhances its kinase activity (Kamada et al., 2000), which is thought to be important for autophagosome development. TOR is also thought to be important in increasing phosphorylation of ATG13 in the presence of amino acids, resulting in decreased binding with ATG1 (Kabeya et al., 2005), a conjugation step necessary for ATG1 activity. Importantly, it is also now known that amino acid deprivation increases class III PI3K-Beclin1 complex formation and therefore autophagy (Tassa et al., 2003), which provides an

additional indirect mechanism whereby a decreased concentration of amino acids can alter mTOR activity. Finally, activation of S6 might regulate a negative feedback interaction upstream of mTOR, possibly to prevent autophagy overstimulation (Klionsky et al., 2005).
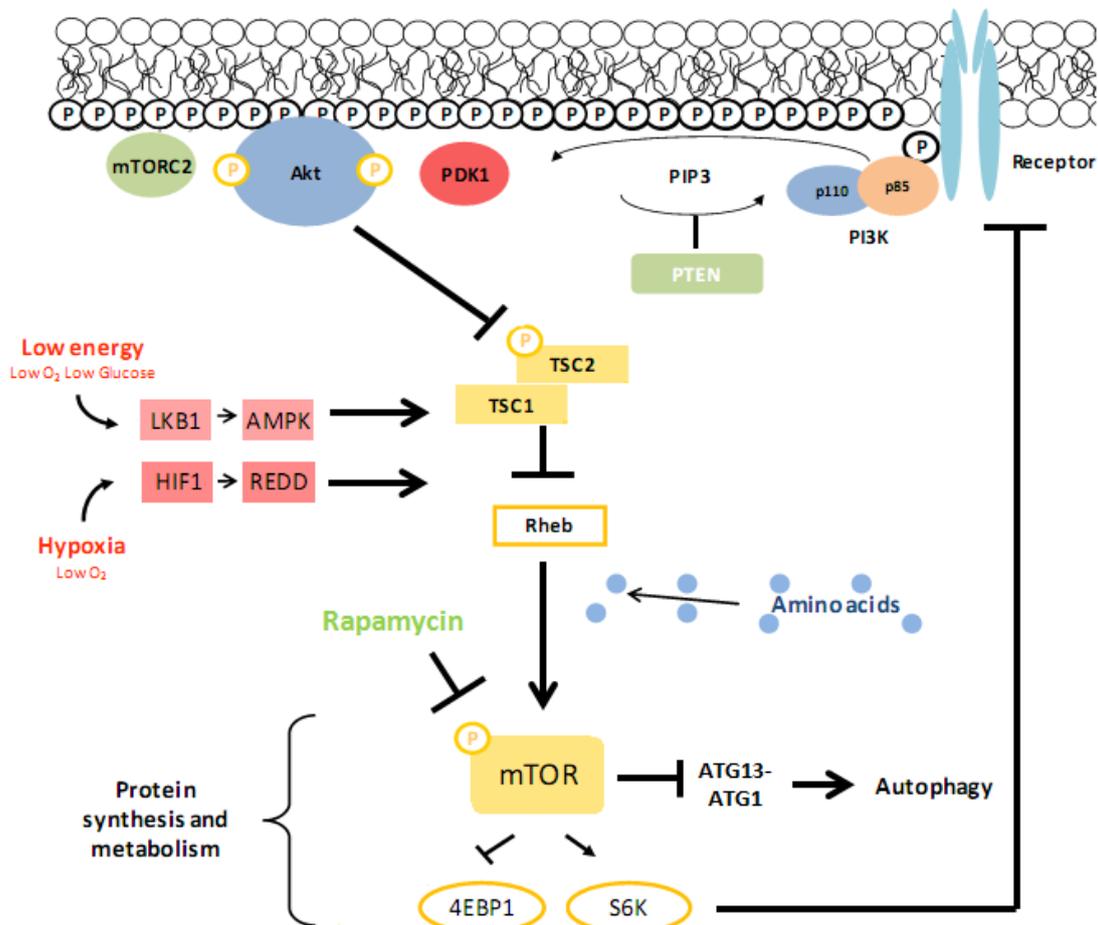
Image 2.2 Schematic depicting regulation of mTOR pathway signalling and regulation of autophagy during nutrient starvation. Low energy or oxygen acts through the TSC1/TSC2 complex or Rheb to induce autophagy, while amino acids inhibit autophagy induction through a sensing mechanism located at mTOR. This is discussed in more detail in the text. PI3K, phosphatidylinositol 3-kinase, REDD, DNA-damage-inducible transcript ,PDK1, phosphoinositide-dependent kinase-1, AMPK, AMP-activated protein kinase, HIF1, hypoxia inducible factor 1,TSC, tuberous sclerosis complex, Rheb, Ras homologue enrich in brain, mTOR mammalian target of rapamycin, S6K 70kD S6 kinase.

1.4   Autophagy and tumourogenesis

Many cancers are able to avoid apoptosis in the stressful cancer microenvironment. Cell death through autophagy has been suggested as a primary mechanism of tumour suppression in cancer cells lacking apoptosis machinery (Liang et al., 1999, Jin and White, 2008), but whether autophagy leads to tumour formation or suppression is still a matter of controversy (Eisenberg-Lerner and Kimchi, 2009). Growing tumours develop regions with limited access to nutrients, due to spatial separation from the native vascular bed. The manner in which tumour cells obtain nutrients in these scenarios is still under intense investigation (Sato et al., 2007).

As the understanding of autophagy mechanisms has developed, and its intimate relationship with maintenance of cellular homeostasis (through the attenuation of metabolic stress) slowly appreciated, interest in the role of autophagy in development of pathogenesis has emerged. Following from this, a large body of data supporting the links between the cancer microenvironment and autophagy has developed and the literature is now replete with studies investigating ties between cancer and autophagy. Through these studies a paradox has emerged, and autophagy is now often described as a double-edged sword in the literature (Shintani and Klionsky, 2004) due to its ability both to act as a tumour suppressor and to be vital to tumour progression (Eisenberg-Lerner and Kimchi, 2009).

1.4.1 Autophagy as cancer suppressor

Disruption of autophagy can promote cancer development, potentially through loss of prevention of DNA damage and instability, through removal of protein aggregates and damaged organelles and perhaps even by limiting cell growth (Mathew et al., 2009). Beclin1

57

(the mammalian homologue of yeast ATG6) is a component of the PI3K VPS34 complex required for autophagy and its importance to a functional autophagy response has been demonstrated in many species including humans (Furuya et al., 2005). Beclin1 was first identified as a Bcl2 interacting protein (Liang et al., 1998), an interaction that leads to the inhibition of autophagy, which is diminished during starvation (Liang et al., 1999). Some cancer cells have been shown to have lower levels of Beclin1 than epithelial cells derived from the same origin, and the characterization of Beclin1 as a haploinsufficient tumour suppressor leads to the first substantial association between autophagy and cancer (Liang et al., 1999). The allelic deletion of Beclin1 has now been strongly tied with cancer progression and much of the research linking autophagy and tumourogenesis deals with this association. Beclin1 expression levels were found to be decreased in 18 of 32 tested breast cancers and have also been implicated in development of other human cancers including those of the prostate, brain, colon and ovaries (Liang et al., 1999, Aita et al., 1999, Miracco et al., 2007). Furthermore, conditional ATG7 deletion in the liver of mice results in tumour formation (Takamura et al., 2011). It is clear from this evidence that autophagy dysfunction is associated with the development of cancer under some circumstances. Indeed, the monoallelic deletion of Beclin1 leads to spontaneous lymphomas as well as lung, breast and liver cancers in mice (Yue et al., 2003, Qu et al., 2003), while the over-expression of Beclin1 in culture inhibits cancer progression (Liang et al., 1999). The subsequent discovery that regulators of autophagy proteins are important in cancer development and progression also emphasizes the role of autophagy as a tumour suppressor. UVRAG, which interacts with the Beclin1 PI3K complex, is essential for autophagosame formation (Liang et al., 2006), while Bif-1 interacts with Beclin1 through UVRAG (Takahashi et al., 2007). Both have been implicated in tumourogenesis (Liang et al., 2006, Lee et al., 2006). Furthermore, well known tumour suppressor genes such as PTEN and TSC are known to repress mTOR activity and thereby induce autophagy (Arico et al., 2001, Feng et al., 2005). Additionally, oft recurring mutations

58

in cancer such as p53 (Feng et al., 2005) and DAPk (Inbal et al., 2002) have both been described to have roles in the induction of autophagy in some circumstances.

1.4.1 Autophagy in cancer progression

Despite the large body of data demonstrating a role for autophagy in tumour suppression, autophagy also appears to be vital for tumour survival during times of metabolic stress. Indeed, several cancers have been shown to have high basal autophagy activity (White and DiPaola, 2009, Guo et al., 2011, Yang et al., 2011), and numerous studies have demonstrated that autophagy inhibition can result in the activation of a programmed cell death response in certain cancers (Mathew et al., 2009). Furthermore, autophagy has been directly linked to the tolerance that some cancer cells display in response to nutrient deprivation (Sato et al., 2007). Also, certain genes that are frequently mutated in many cancers are known to influence autophagy activity. For example, Akt and class I PI3K are known to stimulate mTOR activity and thereby inhibit autophagy (Lum et al., 2005), while cytoplasmic p53 is now also thought to obstruct autophagy activation (Tasdemir et al., 2008). However, mutant p53 has not yet been shown to alter autophagy activity in human cancer. Together the evidence seems to indicate that autophagy has dual roles in cancer progression and development depending on the context (White and DiPaola, 2009).

Although a detectable level of autophagy occurs *in vivo* in many tissues, almost all cells have the capacity to increase autophagy in response to nutrient starvation, although the degree to which it becomes elevated during these circumstances appears to be tissue type specific (Mizushima et al., 2004). Interestingly, increased autophagy is prominent in poorly vascularised regions of tumours but not those regions that have adequate access to the host blood supply (Karantza-Wadsworth et al., 2007, Degenhardt et al., 2006). Therefore,

autophagy as a response to nutrient deficiency in these tumour microenvironments could be essential for survival of some cancers (Mathew et al., 2009). Pancreatic cancer cells and primary tumour samples, having especially pronounced levels of basal autophagy, were confirmed to require autophagy for survival during periods of deprivation of essential nutrients (Yang et al., 2011). Furthermore, inhibition of autophagy with chloroquine reduced tumour size and lengthened survival. Failure to adapt to episodes of nutrient starvation would result in a metabolic catastrophe and therapeutic starvation regimes being used to target the cancer metabolome are proving insightful. Indications are that autophagy may protect cancer cells during nutrient depletion, and therapeutic starvation models mimicking glucose deprivation have shown a Beclin1-dependent increased autophagy in prostate cancer (DiPaola et al., 2008). Autophagy inhibition during nutrient starvation leads to cell death in cervical cancer (Boya et al., 2005) as well as lymphocytes from patients with chronic lymphocytic leukaemia. Liver, gastric and pancreatic cancer cell lines are able to withstand removal of glucose, serum or amino acids from culture medium for substantially longer periods than normal human fibroblasts (Izuishi et al., 2000). This tolerance to amino acid deprivation by cancer cells was linked to protective autophagy by the same authors in a colorectal cancer culture model (Sato et al., 2007). A possible reason for the conflicting roles for autophagy could be linked to the recently revealed mechanism by which colon cancers are able to resist the negative effects of prolonged nutrient starvation due to the presence of p53 and its role in autophagy regulation (Scherz-Shouval et al., 2010).

High levels of basal autophagy may also be required for cancer survival in nutrient rich conditions, and several tumour lines are now known to be dependent on autophagy for normal growth. Human cancers with mutations in H-ras or K-ras may require autophagy for tumour survival (Guo et al., 2011), and data from recent studies suggest that pancreatic (Yang et al., 2011) and other Ras-driven tumours (Lock et al., 2011) require autophagy for sustained

growth. This recently reported autophagy-addiction of some tumours could represent an avenue of autophagy inhibition as an effective anticancer strategy in this setting.

2 Hypothesis and experimental aims

2.1 Research problem

Autophagy is essential for cell survival during times of metabolic stress, and is known to become activated during times of amino acid starvation. However, whether autophagy leads to cancer progression or suppression is still a matter of controversy. While most evidence indicates that autophagy acts as a tumour suppressor, many cancer cell lines display high levels of basal autophagy activity. However, it is unclear whether these cancers have a survival advantage during times of amino acid deprivation. Few studies have investigated the effects of short term amino acid deprivation in this context and studies investigating a protective role for autophagy under these conditions in breast cancer are completely absent.

2.2 Study rationale

Observations from previous experiments (outlined in the previous chapter) demonstrated that the non-tumourogenic breast epithelial cell line MCF12A showed few detrimental effects after being incubated in culture medium bereft of any amino acids for 24 hours. On the other hand, the commonly utilized metastatic breast adenocarcinoma cell line MDAMB231 showed greater sensitivity to amino acid exclusion from culture media and displayed a sudden increase in cell death and a profile of cell cycle arrest after only twelve hours of amino acid starvation. As these cells are known to have high *ras* activation and high basal autophagy levels, and autophagy is thought to be an important factor in tolerance to nutrient deprivation, the aim of this study was to investigate whether autophagy is in fact an important survival mechanism during short term amino acid starvation in these cells.

2.3 Hypothesis

The *ras* mutant MDAMB231 cell line relies on a pre-existing high basal autophagy for survival and tolerance during the first hours of amino acid starvation but not thereafter.

2.4 Experimental aims

1. Use the lysomotropic reagent bafilomycin A1 as an autophagy inhibitor to determine if autophagy is necessary for survival and cell cycle maintenance during the first hours of amino acid starvation in MDAMB231 cells and compare this to non-tumourogenic MCF12A cells.

2. Determine if any observed changes during amino acid starvation are associated with alterations in lysosomal acidity or markers of autophagy.

3   Methods and materials

Complete step-by step protocols are provided in the appendix.
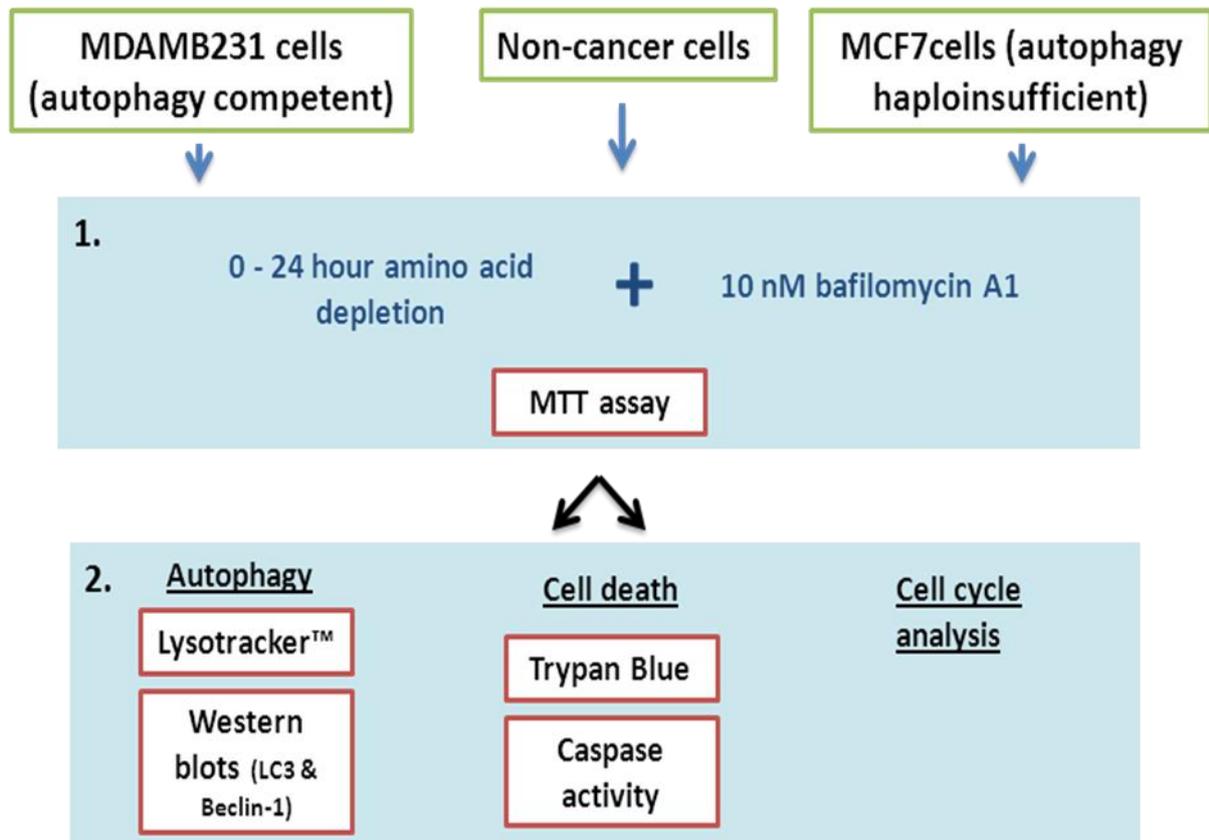
3.1   Study design

Image 2.3 Study design: A metastatic cancer cell line (MDAMB231), an autophagy haploinsufficient cell line (MCF7) and a non-tumourogenic cell line (MCF12A) will be cultured in the absence of amino acids and in the presence of the autophagy inhibitor bafilomycin A1 (10 nM) for a period of 24 hours and analysed at several time periods using the MTT assay. MDAMB231 and MCF12A cell lines will be further examined during amino acid starvation with bafilomycin A1 over the spectrum of a 24 hour period using assays for apoptosis, necrosis and autophagy. Finally the cell cycle will be assessed. Continuation to phase 2 is contingent on the results obtained in phase 1.

3.2   Cell culture

Experiments were performed using the human metastatic mammary carcinoma cell line MDAMB231 which were obtained from American Type Culture Collection (Rockville, MD, USA) and the human non-tumourogenic breast epithelial cell line MCF12A that was obtained from the University of Cape Town. The MCF7 cell line, also used in some experiments, was a donation from the University of the Western Cape. During routine maintenance, cells were grown as monolayers in Glutamax-DMEM (Celtic Molecular Diagnostics, Cape Town, South Africa supplemented with 10% foetal bovine serum (Sigma Chemical Co., St Louis, MO, USA) at 37°C in a humidified atmosphere of 95% air plus 5% CO_2. MCF12A growth medium was complemented with Ham's F12 medium (1:1) (Sigma Chemical Co., St Louis, MO, USA), 0.5 µg/ml hydrocortisone (Sigma Chemical Co., St Louis, MO, USA), 10 µg/ml insulin (Sigma Chemical Co., St Louis, MO, USA) and 20 ng/ml EGF (Sigma Chemical Co., St Louis, MO, USA). Cells were first allowed to proliferate in T75 flasks (75cm^2 flasks, Greiner Bio One, Germany) until they reached 80% confluence before being split into appropriate treatment plates or dishes. Splitting was accomplished by washing the cell monolayer with warm phosphate buffered saline (PBS) followed by incubation with 4 ml trypsin/EDTA (Sigma Chemical Co., St Louis, MO, USA) at 37°C, with occasional agitation, until cells loosened completely or for a maximum of four minutes. All experiments were performed using exponentially growing cells. Bafilomycin A1 from *Streptomyces griseus* (B1793, Sigma Chemical Co., St Louis, MO, USA) was dissolved in DMSO in ready to use aliquots to avoid freeze-thaw cycles, and was stored at -20°C. Rapamycin from *Streptomyces hygroscopicus* (R0395, Sigma Chemical Co., St Louis, MO, USA) was dissolved in DMSO in ready to use aliquots to avoid freeze thaw cycles, and was stored at -20°C.

3.3   MTT assay

The protocol for the MTT assay performed in this study is described in the materials and methods section in the previous chapter. 10 000 MCF7 cells were plated 48 hours before being treated in 96-well plates using 100 µl of culture medium.

3.4   Caspase 3/7 activity assay

The protocol for the Caspase-3/7 activity assay (Caspase-Glo® 3/7 assay) performed in this study is described in the materials and methods section in the previous chapter.

3.5   Trypan blue assay

The protocol for the trypan blue assay performed in this study is described in the materials and methods section in the previous chapter. 80 000 MCF7 cells were plated into 60 mm culture dishes 48 hours prior to treatment.

3.6   Analysis of cell cycle progression

The protocol for the flow cytometric analysis of the cell cycle performed in this study (CycleTEST™ PLUS DNA Reagent kit) is described in the materials and methods section in the previous chapter. 50 000 MCF7 cells were plated into T25 culture flasks 48 hours prior to treatment.

3.7   LC3 and Beclin-1 Western blots

3.7.1 Protein extraction and quantification

Following treatment, cells immediately had their supernatants discarded and were placed on ice. Cell monolayers were then rinsed three times in 5 ml of a pre-lysis buffer (20 mM Tris-HCl, pH 7.4, 137 mM NaCl, 1 mM $CaCl_2$, 1 mM $MgCl_2$ and 0.1 mM sodium orthovanadate). Total cell protein was extracted by incubating cells on ice for 10 minutes in 1 ml of a modified radioimmunoprecipitation (RIPA) buffer, pH 7.4, containing: Tris–HCl 2.5 mM, EDTA 1 mM, NaF 50 mM, NaPPi 50 mM, dithiothreitol 1 mM, phenylmethylsulfonyl fluoride (PMSF) 0.1 mM, benzamidine 1 mM, 4 mg/ml SBTI, 10 mg/ml leupeptin, 1% NP40, 0.1% SDS and 0.5% Na deoxycholate. Adherent cells were then harvested from culture dishes by scraping. Whole cell lysates were sonicated in order to disrupt the cell membranes to release their contents before they were centrifuged at 4°C and 8000 rpm for 10 minutes. Lysates were then stored at -80°C or had their protein content determined immediately. Protein content was quantified using the Bradford protein determination method (Bradford, 1976), directly before the preparation of cell lysates

3.7.2 Sample preparation (cell lysates)

Following protein quantification, aliquots diluted in Laemmli sample buffer were prepared for all samples, each containing 40 μg of protein. Aliquots were then stored at -80°C for future analysis by western blotting.

3.7.3 SDS-PAGE and Western blot analysis

Whole cell lysates were separated on 12% polyacrylamide gels for LC3 II and 10% polyacrylamide gels for beclin 1 by sodium dodecyl sulphate polyacrylamide gel electrophoresis (SDS-PAGE). A pre-stained protein marker ladder (peqGOLD, Austria) was loaded in the left most well on each gel for orientation and electrophoretic determination of molecular weights of specific bands. Previously prepared protein samples were boiled for 5 minutes and 40 μg of protein (sample preparation described above) was loaded per lane. Gels were run for 60 minutes at 130 V (constant) and 400 mA (Mini Protean System, Bio-Rad, USA). Following SDS-PAGE, proteins were transferred to polyvinylidine fluoride (PVDF) membranes (Immobilon, Millipore, USA) using a semi-dry electrotransfer system (Bio-Rad, USA) for 60 minutes at 15 V and limit 0.5 A. In order to prevent non-specific binding, membranes were blocked in 5% (w/v) fat-free milk in 0.1% Tris Buffered Saline-Tween20 (TBS-T) for 2 hours at room temperature with gentle agitation. Membranes were then incubated with LC3B primary antibody (Cell Signalling, MA, USA) or beclin 1 primary antibody (Cell Signalling, MA, USA) diluted in 0.1% TBS-T (1:1000), overnight at 4°C. The following day, membranes were washed in copious volumes of TBS-T (3X5 minutes) before being incubated in anti-rabbit (Amersham Biosciences, UK, and Dako Cytomation, Denmark) horseradish peroxidase-conjugated secondary antibody for 1 hour at room temperature with gentle agitation. Following the incubation period, membranes were washed a further three times in TBS-T (3x5 minutes), followed by a final 10 minute wash in TBS. Antibodies were detected with the LumiGLO Reserve™ chemiluminescent substrate kit (KPL, Inc., USA) as per the manufacturer‟s instructions, and bands were exposed to autoradiography film (Hyperfilm, Amersham Biosciences, UK). Exposed bands were visualised and then quantified by densitometry using the UNSCAN-IT© densitometry software (Silk Scientific Corporation,

Utah, USA). All bands were expressed as optical density readings relative to a control present on the same blot.

3.8   Assessment of acidic compartmentalization

3.8.1 Lysotracker™ and Hoechst staining (imaging)

100 000 MCF12A cells or 80 000 MDAMB231 or MCF7 cells were plated into 60 mm culture dishes containing pre-autoclaved coverslips, 48 hours prior to treatment. Cell monolayers were rinsed three times with sterile PBS and incubated in 1:10000 Lysotracker™/PBS solution for 10 minutes at room temperature. Cell monolayers were then rinsed three times with sterile PBS and fixed and permeabilised with an ice-cold 1:1 methanol/acetone mixture for 10 minutes at 4ºC. After being left to air dry for 20 minutes in the dark, cells were, once more, washed three times in sterile PBS and enough Hoechst 3342 (10 mg/ml in a 1:200 dilution) was then added to cover the entire cell monolayer. This was left to incubate for 10 minutes at 4ºC. Thereafter, cells were washed five times in sterile PBS and images were immediately acquired with an Olympus IX81 microscope fitted with CellR® software. A minimum of three randomly chosen fields, of at least 3 independent experiments per experimental condition were prepared.

3.8.2 Lysotracker™ (flow cytometry)

200 000 MCF12A cells or 150 000 MDAMB231 or MCF7 cells were plated into T25 culture flasks 48 hours prior to treatment. Prior to analysis, cells were trypsinzed and the cell suspensions centrifuged at 400 x g for 5 minutes at room temperature. Cells were then washed once in PBS. Lysotracker™ (Invitrogen™, USA) was prepared in PBS (1:10 000)

immediately before use. Cell suspensions were centrifuged at 400 x g for 5 minutes at room temperature and the pellets re-suspended in 250 µl fresh Lysotracker™/PBS and incubated for 10 minutes at room temperature before analysis using flow cytometry (BD FACSAria I). At least 10 000 cells were collected using a 488 nm laser and 610LP, 616/23BP emission filters.

3.9 ATG5 siRNA transfections

Cells were transfected using a reverse transcription protocol into 60 mm petri dishes. 20 pmol of ATG5 siRNA duplex (Cell Signalling, MA, USA, lSilence® Atg5 siRNA I #6345) was diluted into 250 µl of transfection medium (containing no antibiotics or serum). 2 µl of Lipofectamine™ RNAiMAX (13778075; Invitrogen™, USA) was gently mixed and added to this. 250 µl of this suspension was then added to each petri dish and allowed to incubate for 20 minutes. 100 000 MCF12A cells or 80 000 MDAMB231 cells were then plated into the culture dishes containing the RNAi duplex-Lipofectamine RNAiMAX complexes to have a final volume of 2 ml and gently mixed. Cells were incubated at 37°C until ready to treat (24-48 hours later). Stealth RNAi (STEALTH RNAI NEG CTL MED GC, 12935300; Invitrogen™, USA) was used as a negative control, as suggested by the manufacturer. Cells were treated 48 hours later.

3.9.1 RNA extraction, cDNA synthesis and RTPCR

Total RNA was extracted and purified using the PureLink™ RNA Mini Kit (12183018A; Invitrogen™, USA) as per the manufacturer's instructions. RNaseOUT™ Recombinant Ribonuclease Inhibitor (10777019; Invitrogen™, USA) was then added to samples before they were stored at -40°C. cDNA was then synthesised using the SuperScript® III First-

Strand Synthesis SuperMix (18080051; Invitrogen™,USA) as per the manufacturer‟s instructions. Gene expression was analyzed using realtime-PCR that was performed using the 96-well cycler StepOnePlus™ Real-Time PCR System and SYBR® Green dye. Analysis was performed by the Central Analytical Facility of Stellenbosch University, DNA Sequencing Facility located in the Department of Genetics under the supervision of Dr Ruhan Slabbert. The following primers were selected and purchased through the Central Analytical Facility with the assistance of Dr Ruhan Slabbert.:

ATG5 autophagy 5-like [Homo sapiens]. PrimerBank ID 4757798a1. Amplicon size 171. Primer sequence (5' → 3'). Forward primer (TTGACGTTGGTAACTGACAAAGT), reverse primer (TGTGATGTTCCAAGGAAGAGC). Heat-shock 90kD protein-1, beta [Homo sapiens]. PrimerBank ID 2014949594a1. Amplicon size 247. Primer sequence (5' → 3'). Forward primer (TGGTGTGGTTGACTCTGAGGA), reverse primer (GGAGGTATGATAGCGCAGCA). NADH dehydrogenase (ubiquinone) 1 alpha subcomplex. PrimerBank ID 4758770a1. Amplicon size 102. Primer sequence (5' → 3'). Forward primer (GGACTGGCTACTGCGTACATC), reverse primer (GCGCCTATCTCTTTCCATCAGA). β-cytoskeletal actin [Homo sapiens]. PrimerBank ID 4501885a1. Amplicon size 250. Primer sequence (5' → 3'). Forward primer (CATGTACGTTGCTATCCAGGC), reverse primer (CTCCTTAATGTCACGCACGAT).

3.10 Statistical analysis

All values are presented as the mean ± standard error of the mean (SEM). Differences between time points and treatment groups were analysed using one or two way analysis of variance (ANOVA). Significant changes were further assessed by means of the Bonferroni *post hoc* analysis where appropriate. All statistical analyses were performed using Graphpad

Prism version 5.01 (Graphpad Software, Inc, CA, USA). The minimum level of significance accepted was p < 0.05.

4   Results

4.1   Bafilomycin A1 (10 nM) decreases cell viability during acute amino acid starvation in MDAMB231 cells and to a lesser degree in MCF12A cells but not in MCF7 cells.
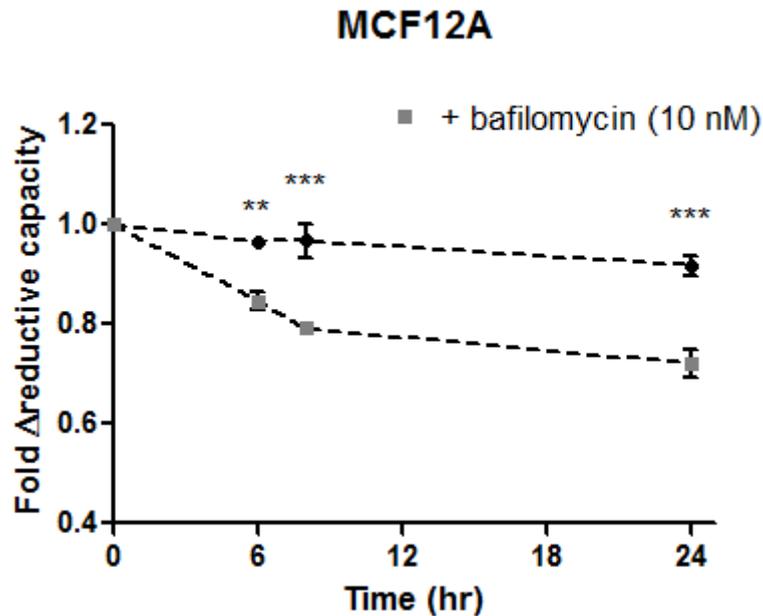
Fig. 2.1 Bafilomycin significantly decreases the capacity of MCF12A cells to reduce MTT to formazan during a 24 hour period of amino acid deprivation. Results represent the fold change in MTT reductive capacity over time. Bafilomycin A1 (10 nM) was added to culture medium 6 hours prior to analysis (and was therefore present during the entire experiment at the 6 hour time point). hr = hours. Each value represents the mean ± SEM of at least three independent determinations. **, $P < 0.01$; ***, $P < 0.001$ vs. time-matched + bafilomycin (10 nM) treatments.

MCF12A cells were incubated in culture medium completely depleted of amino acids for a period of 24 hours, with or without 10 nM of bafilomycin A1 (Fig 2.1). Bafilomycin A1 inhibits acidification inside lysosomes and thereby prevents autophagosome-lysosome fusion, effectively inhibiting autophagy progression. The capacity for MCF12A cells to reduce MTT to formazan was significantly diminished at all time points tested if bafilomycin A1 (10 nM) was added to culture medium 6 hours prior to analysis (Fig 2.1). This is a strong indication that the metabolic viability of these cells is impaired.
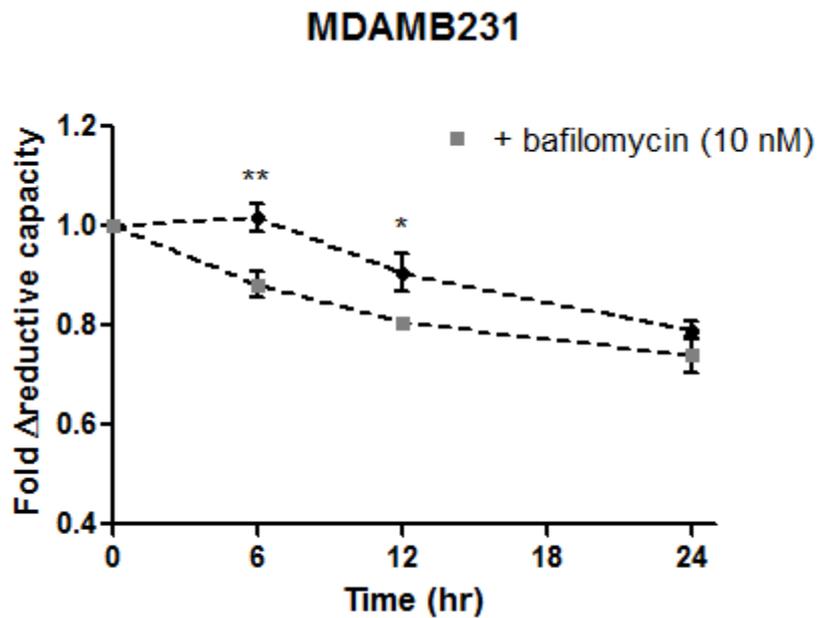
73

MDAMB231

Fig. 2.2 Bafilomycin (10 nM) significantly diminishes the capacity of MDAMB231 cells to reduce MTT to formazan during only the first 12 hours of total amino acid deprivation. Results represent the fold change in MTT reductive capacity over time. Bafilomycin A1 (10 nM) was added to culture medium 6 hours prior to analysis (and was therefore present during the entire experiment at the 6 hour time point). hr = hours. Each value represents the mean ± SEM of at least three independent determinations. *, $P < 0.05$; **, $P < 0.01$ vs. time-matched + bafilomycin (10 nM) treatments.

MDAMB231 cells displayed a significant decrease in their ability to reduce MTT only after 12 hours of incubation in amino acid free medium. However, if this medium was supplemented with bafilomycin A1 (10 nM) then their reductive capacity was significantly lower at 6 and 12 hours (Fig 2.2). Interestingly, bafilomycin did not alter MTT reducing capacity at 24 hours of amino acid deprivation.
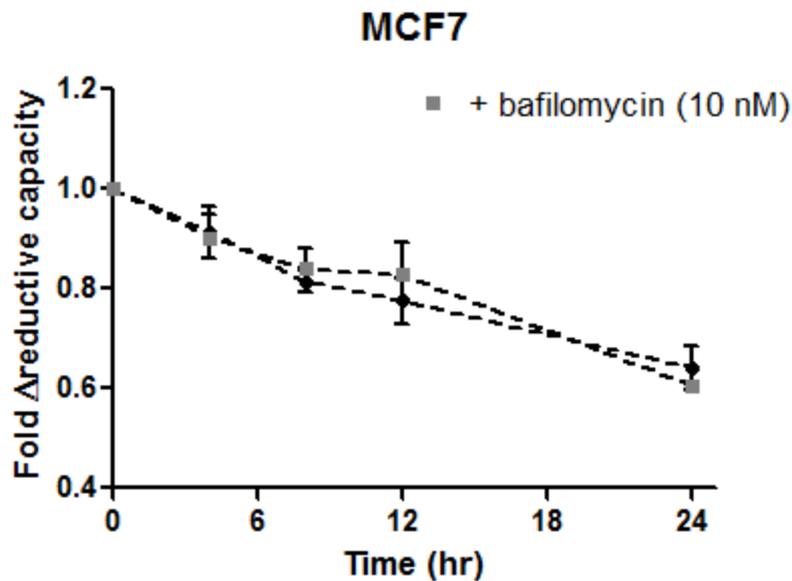
74

Fig. 2.3 Bafilomycin (10 nM) has no effect on the capacity of MCF7 cells to reduce MTT to formazan during a 24 hour period of total amino acid deprivation. Results represent the fold change in MTT reductive capacity over time. Bafilomycin A1 (10 nM) was added to culture medium 6 hours prior to analysis (and was therefore present during the entire experiment at the 6 hour time point). hr = hours. Each value represents the mean ± SEM of at least three independent determinations.

The MCF7 breast cancer cell line is beclin 1 haploinsufficient and therefore partially autophagy incompetent. Amino acid deprivation lead to an approximately 40% lower MTT reducing capacity after 24 hours when compared to 0 hours (cell incubated in amino acid complete medium) (Fig 2.3), indicating that these cells are sensitive to amino acid deprivation. The presence of bafilomycin A1 (10 nM) did not alter the ability of these cells to reduce MTT.
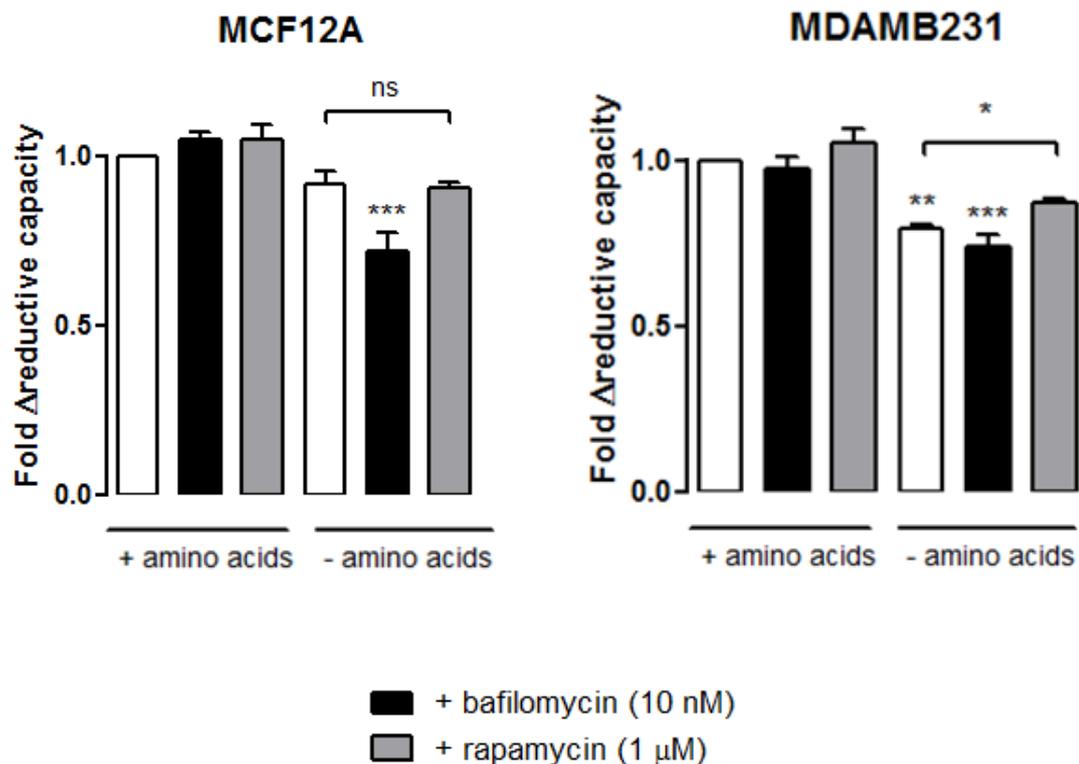
Fig. 2.4 Rapamycin ameliorates the drop in the MTT reductive capacity of MDAMB231 cells but not in MCF12A cells during a 24 hour period of total amino acid deprivation. Results represent the fold change in MTT reductive capacity over time. Rapamycin (1 μM) was present in culture medium during the 24 hour incubation with amino acid free medium where indicated (no bafilomycin was present in these treatments). Bafilomycin A1 (10 nM) was added to culture medium 6 hours prior to analysis. Each value represents the mean ± SEM of at least three independent determinations. **, $P < 0.01$ vs. + amino acids; ***, $P < 0.001$ vs. + amino acids + bafilomycin (10 nM). *, $P < 0.05$; ns = no significance.

The antifungal compound rapamycin inhibits mTOR directly and is thereby able promote the induction of autophagy. By including rapamycin (1 μM) in culture medium we were able to ameliorate the drop in MTT reductive capacity observed during a 24 hour period of starvation in MDAMB231 cells (Fig 2.4). The slight increase in MTT reducing capacity seen in MDAMB231 cells was not detected when MCF12A cells were subjected to a similar protocol of amino acid starvation in the presence of rapamycin (1 μM).
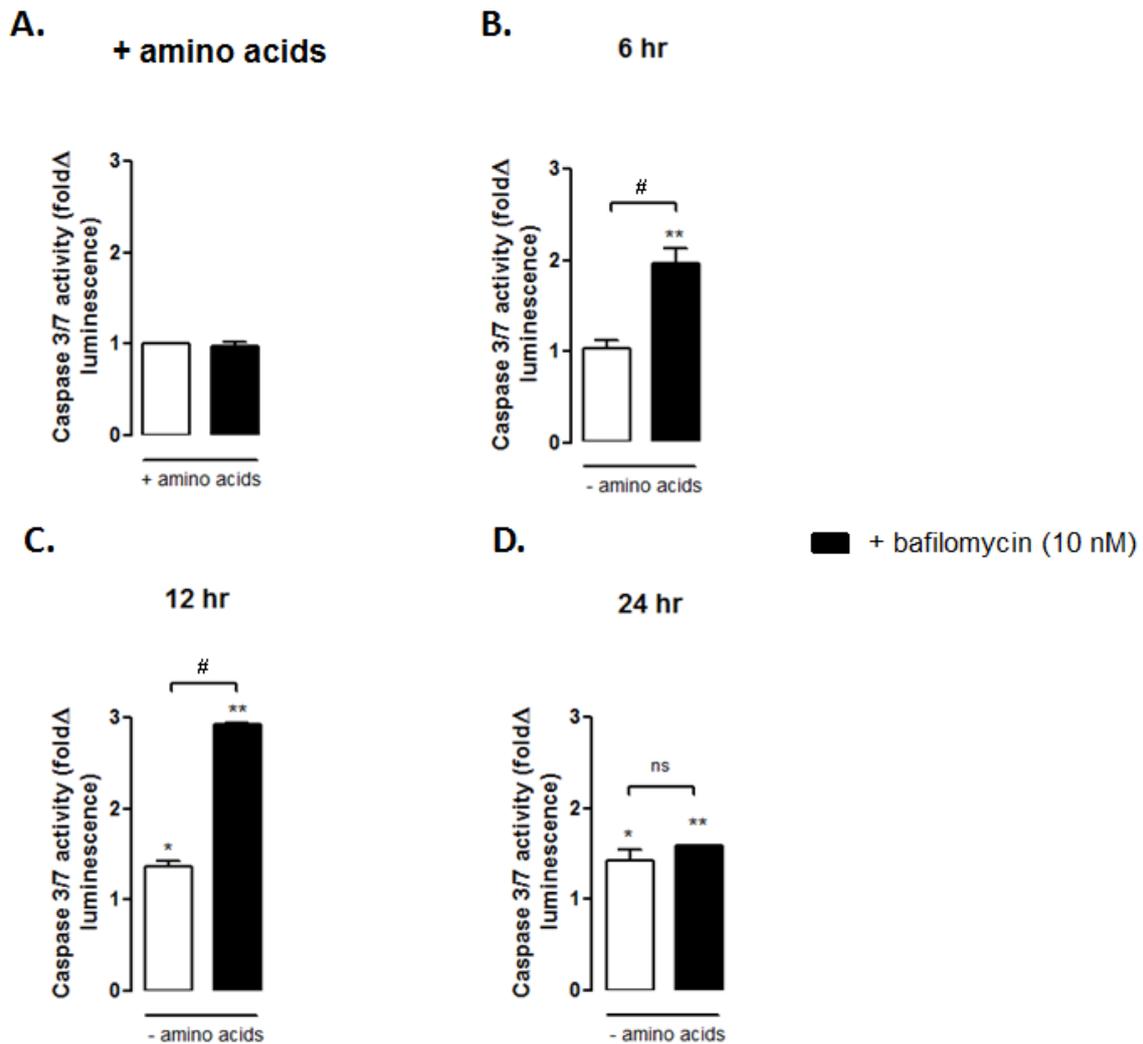
76

Fig. 2.5 MDAMB231 cells display significantly increased caspase 3/7 activity at 6 and 12 hours of amino acid starvation if bafilomycin A1 (10 nM) is present during that period. This phenomenon is not observed if caspase activity is measured after 24 hours of a similar treatment. Results represent the fold change in luminescence in cultures depleted of amino acids versus those cultured in medium containing amino acids. Caspase 3/7 activity was taken to be proportionate to produced luminescence intensity. Bafilomycin A1 (10 nM) was added to culture medium 6 hours prior to analysis. Each value represents the mean ± SEM of at least three independent determinations. *, $P <$ 0.05 vs. + amino acids; **, $P <$ 0.01 vs. + amino acids + bafilomycin (10 nM). #, $P <$ 0.001 ; ns = no significant difference.

Incubation of MDAMB231 cells with bafilomycin A1 (10 nM) for 6 hours in amino acid complete medium did not result in any detectable changes in caspase 3/7 activity (Fig 2.5a). However, the presence of bafilomycin A1 (10 nM) during amino acid starvation resulted in significant increases in caspase 3/7 activity in cells starved for 6 and 12 hours (Fig 2.5, b + c). No difference in caspase 3/7 activity was observed in MDAMB231 cells that were amino acid starved for 24 hours, either with or without bafilomycin (10 nM).
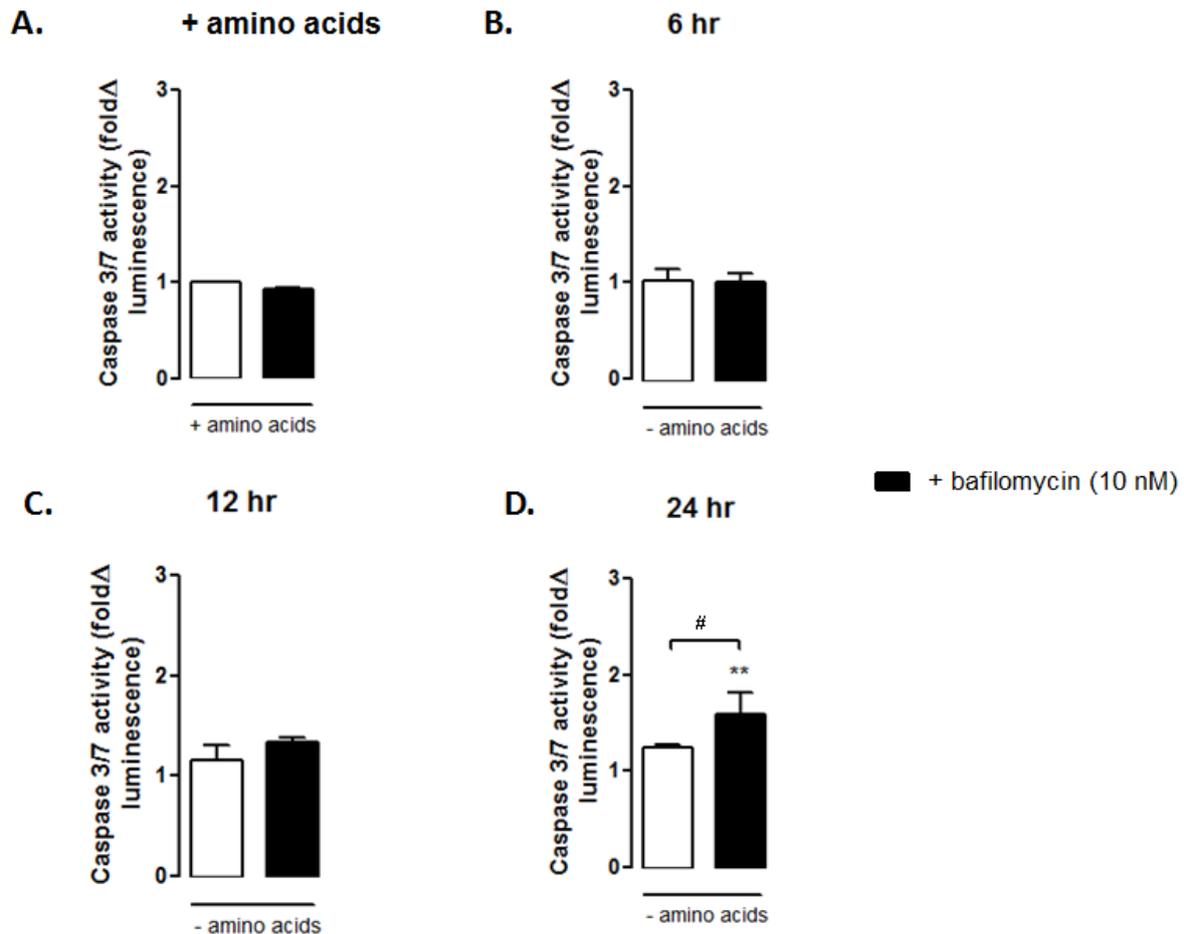
77

Fig 2.6 MCF12A cells display significantly increased caspase 3/7 activity at 24 hours of amino acid starvation if bafilomycin (10 nM) is present during that period. This phenomenon is not observed if caspase activity is measured before 24 hours of a similar treatment. Results represent the fold change in luminescence in cultures depleted of amino acids versus those cultured in medium containing amino acids. Caspase 3/7 activity was taken to be proportionate to produced luminescence intensity. Bafilomycin A1 (10 nM) was added to culture medium 6 hours prior to analysis. Each value represents the mean ± SEM of at least three independent determinations. **, $P < 0.01$ vs. + amino acids + bafilomycin (10 nM). #, $P < 0.001$.

Incubation of MCF12A cells with bafilomycin A1 (10 nM) for 6 hours in amino acid complete medium did not result in any detectable changes in caspase 3/7 activity (Fig 2.6). Furthermore, the presence of bafilomycin A1 (10 nM), in amino acid free medium, did not result in significant increases in caspase 3/7 activity in cells starved for 6 and 12 hours either. However, a significant increase in caspase 3/7 activity was observed if MCF12A cells were amino acid starved for 24 hours in the presence of bafilomycin A1 (10 nM).
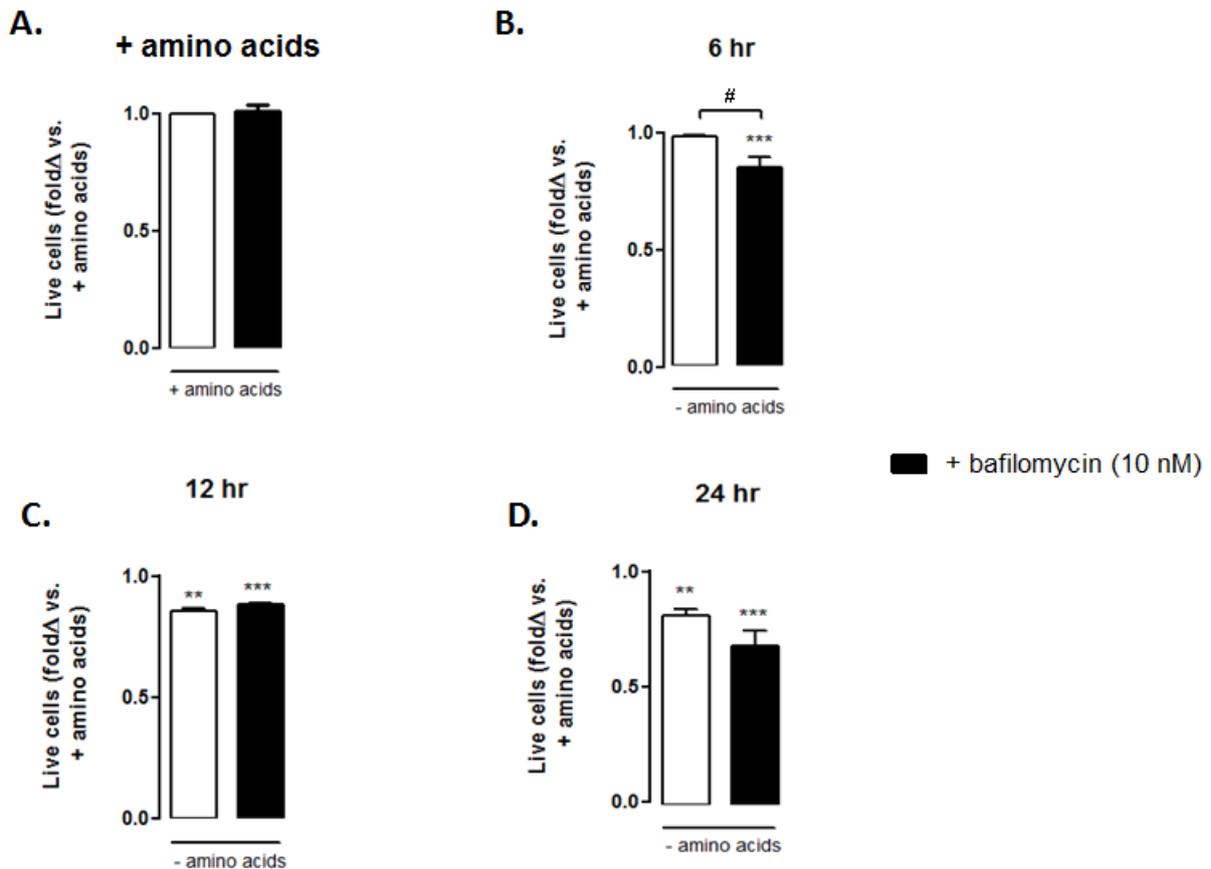
Fig. 2.7 A significant percentage of MDAMB231 cells become trypan blue positive following 6 hours of amino acid deprivation if bafilomycin (10 nM) is present. Similar results are not observed at later timepoints. Live cells are defined as those that exclude trypan blue dye. Results represent the fold change of live cells over time in culture depleted of amino acids versus those cultured in medium containing amino acids. Bafilomycin A1 (10 nM) was added to culture medium 6 hours prior to analysis. Each value represents the mean $\pm$ SEM of at least three independent determinations. **, $P < 0.01$ vs. + amino acids; ***, $P < 0.001$ vs. + amino acids + bafilomycin (10 nM). #, $P < 0.01$.

The trypan blue vital stain is able to traverse only those cell membranes with compromised integrity, and therefore functions as a marker of necrotic and late stage apoptotic cell death and can be used as an indicator of actual cellular impairment following an intervention. MDAMB231 cells excluded trypan blue dye in the presence of bafilomycin A1 (10 nM) in amino acid complete medium (Fig 2.7). However, MDAMB231 cells became trypan blue positive to significant levels after 6 hours of deprivation in amino acid free medium only if supplemented with bafilomycin A1 (10 nM). Bafilomycin A1 (10 nM) did not exacerbate trypan blue positive staining at 12 or 24 hours of amino acid deprivation.
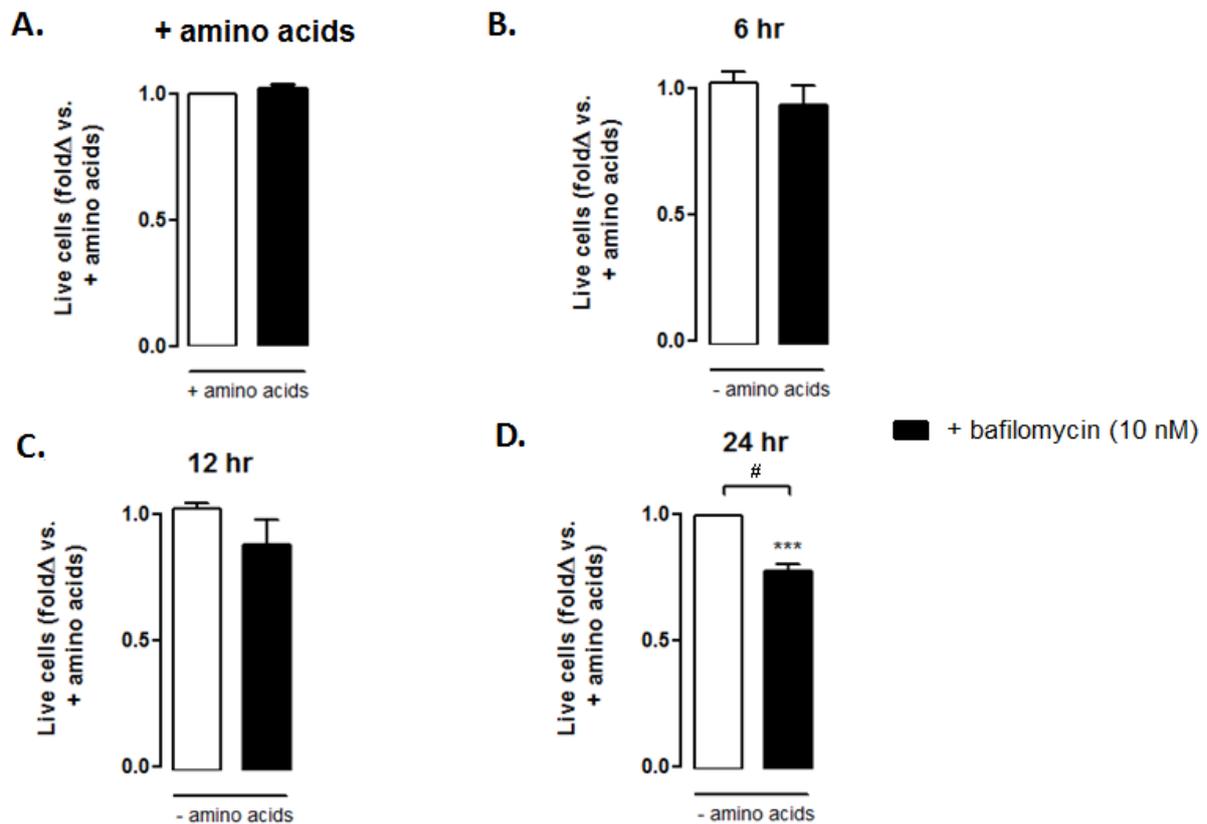
Fig. 2.8 A significant percentage of MCF12A cells become trypan blue positive after 24 hours of amino acid deprivation if bafilomycin (10 nM) is present. Live cells are defined as those that exclude trypan blue dye. Results represent the fold change of live cells over time in culture depleted of amino acids versus those cultured in medium containing amino acids. Bafilomycin A1 (10 nM) was added to culture medium 6 hours prior to analysis. Each value represents the mean ± SEM of at least three independent determinations. ***, $P < 0.001$ vs. + amino acids + bafilomycin (10 nM). #, $P < 0.001$.

MCF12A cells excluded trypan blue dye in the presence of bafilomycin A1 (10 nM), in amino acid complete medium (Fig 2.8). These cells did not become trypan blue positive to significant levels after 6 or 12 hours of deprivation in amino acid free medium. Membrane integrity was not significantly compromised if medium was supplemented with bafilomycin A1 (10 nM). However, significantly greater numbers of trypan blue positive cells (cells with impaired membrane integrity) were detectable in MCF12A cells starved of amino acids for 24 hours with bafilomycin A1 (10 nM). This indicates that the presence of bafilomycin caused increased membrane permeability in MCF12A cells only at 24 hours of amino acid starvation.

4.2   Short term amino acid deprivation causes comparatively differential shifts in the lysosomal acidity in MCF12A, MDAMB231 and MCF7 cells.
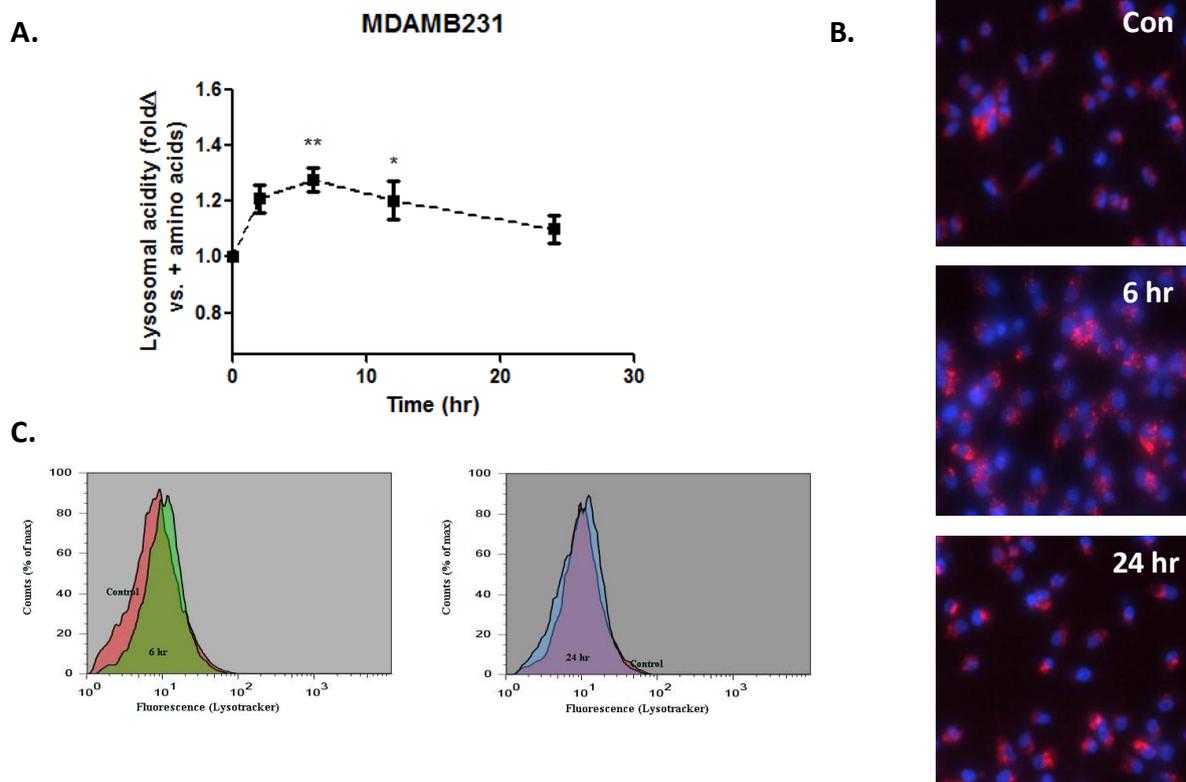
A.

B.

C.

Fig. 2.9 Lysosomal acidity peaks at 6 hours of total amino acid deprivation of MDAMB231 cells. Lysosomal acidity was monitored using a Lysotracker dye and flow cytometry. A) Lysosomal acidity plotted as fold change compared to cells cultured in amino acid complete medium versus a function of time in hours. B) Images depicting stained acidic compartments (red) and nuclei (blue) C) Peak shifts of mean fluorescent intensity (lysotracker) at 6 and 24 hours of amino acid deprivation represented in A. hr = hours. Values are expressed as mean ± SEM of at least three independent determinations. *, $P < 0.05$; **, $P < 0.01$ vs. 0 hr.

The use of dyes to monitor the activity of lysosomes is sometimes utilized as a measure of autophagy. Although controversial, they can be used in combination with other techniques as an indicator of autophagy flux. In the MDAMB231 cell line, with high basal autophagy, lysosomal acidic compartmentalization increased and peaked at 6 hours after amino acid starvation (Fig 2.9a). Thereafter, lysosomal acidity decreased back to baseline levels after 24 hours. These findings were confirmed qualitatively by means of imaging with Lysotracker™ dye, or quantitatively with flow cytometry in conjunction with Lysotracker™.
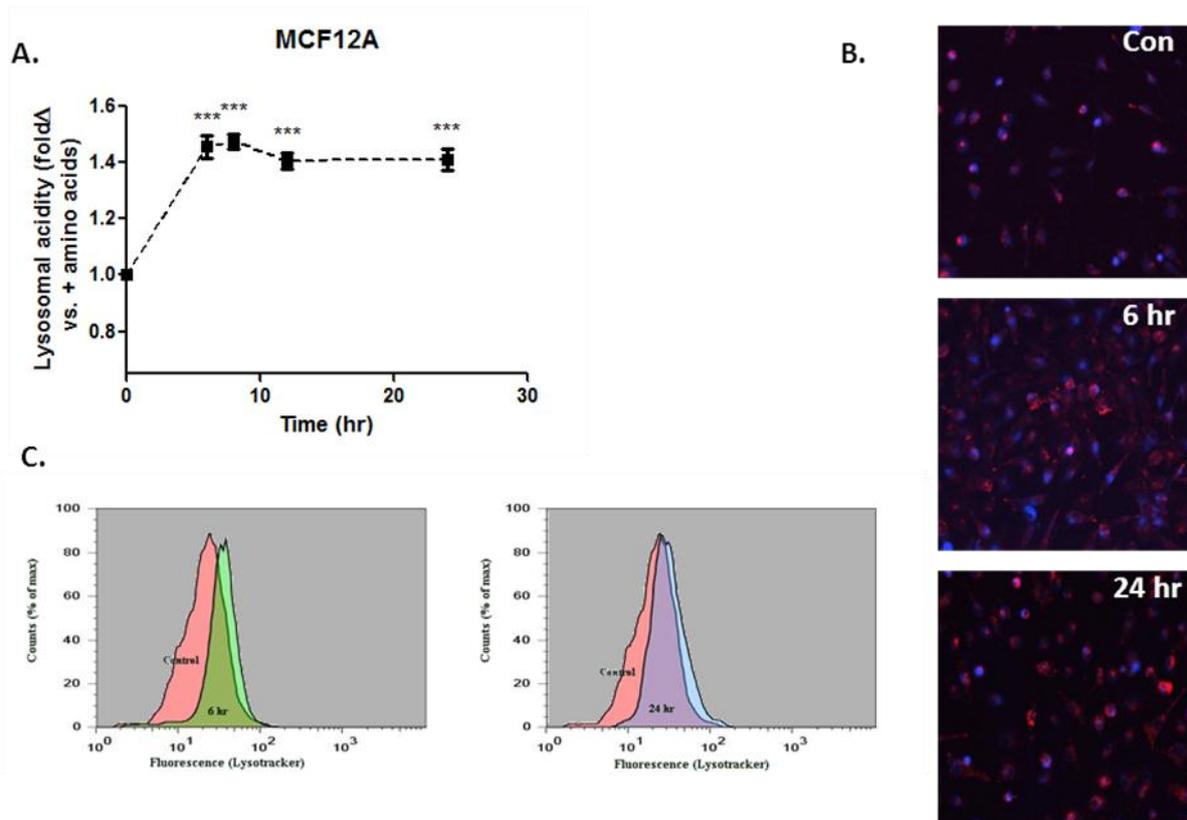
81

Fig. 2.10 A significant elevation in lysosomal acidity is observed in MCF12A cells during total amino acid deprivation. Lysosomal acidity was monitored using a Lysotracker dye and flow cytometry. A) Lysosomal acidity plotted as fold change compared to cells culture in amino acid complete medium versus a function of time in hours. B) Images depicting stained acidic compartments (red) and nuclei (blue) C) Peak shifts of mean fluorescent intensity (lysotracker) at 6 and 24 hours of amino acid deprivation. hr = hours. Values are expressed as mean ± SEM of at least three independent determinations. ***, $P < 0.001$ vs. 0 hr.

In the MCF12A cell line, lysosomal acidic compartmentalization was shown to display a sustained increase after six hours of amino acid starvation that was maintained up to 24 hours thereafter (Fig 2.10). These findings were confirmed visually by means of imaging and with flow cytometry in conjunction with the Lysotracker™ dye.

A.

B.

C.

Fig. 2.11 A significant elevation in lysosomal acidity is observed in MCF7 cells only after 24 hours of total amino acid deprivation. Lysosomal acidity was monitored using a Lysotracker dye and flow cytometry. A) Lysosomal acidity plotted as fold change compared to cells culture in amino acid complete medium versus a function of time in hours. B) Images depicting stained acidic compartments (red) and nuclei (blue) C) Peak shifts of mean fluorescent intensity (lysotracker) at 6 and 24 hours of amino acid deprivation represented in A. hr = hours. Values are expressed as mean $\pm$ SEM of at least three independent determinations. **, $P < 0.01$ vs. 0 hr.

In the MCF7 cell line, lysosomal acidic compartmentalization was observed to increase during amino acid starvation. This increase became statistically significant after 24 hours of amino acid starvation (Fig 2.10). These findings were confirmed visually by means of imaging and with flow cytometry in conjunction with the Lysotracker™ dye.

4.3   MDAMB231 cells have a higher basal autophagy than MCF12A cells and display a higher autophagic flux than MCF7 cells when starved of amino acids.
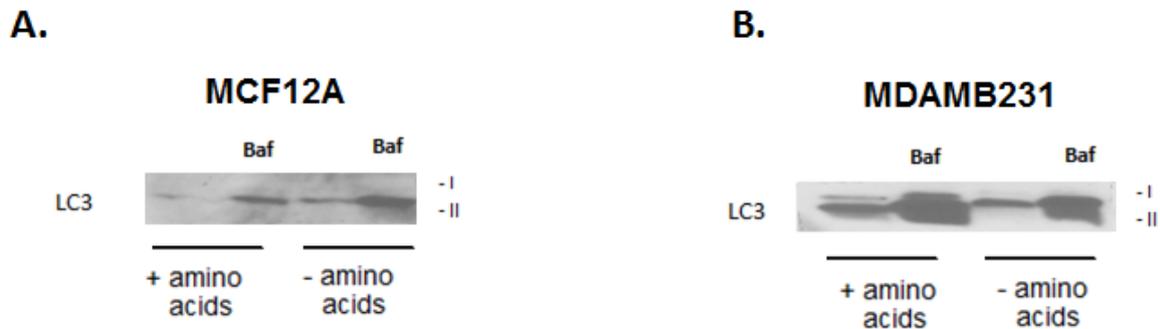
Fig. 2.12 Change in protein levels of the autophagy marker LC3 II in MCF12A and MDAMB231 cells after 24 hours of complete amino acid starvation. Representative western blots showing increased LC3 II protein levels at 24 hours of complete amino acid deprivation following addition of the lysomotropic reagent bafilomycin A1 (10 nM). A. MCF12A cells have increased levels of LC3 II following amino acid starvation, indicating increased conversion of LC3 I to LC3 II. This is exacerbated if bafilomycin A1 (10 nM) is present. B. MDAMB231 cells display high basal levels of LC3 II. Bafilomycin A1 was added to culture medium 6 hours prior to cell harvesting for analyses.

LC3 II is the most common marker for the measurement of autophagy activity. However, LC3 II is degraded by autophagy itself, and therefore high autophagy levels can lead to decreased LC3 II in some circumstances of high autophagy flux. If cells are incubated with an agent that impairs lysosomal acidification (such as bafilomycin A1) then the accumulation of LC3 II can be used to determine the true level of autophagy. Blocking autophagosome degradation in this way can be used to distinguish between these possibilities and assess autophagy levels by the „amount" of LC3 II protein that accumulates as a result. MDAMB231 cells have a much higher basal level of autophagy than corresponding MCF12A cells (Fig 2.12). However, whereas 24 hours of amino acid starvation lead to increased levels of LC3 II in MCF12A cells, a similar increase was not observed in MDAMB231 cells incubated in similar conditions. Furthermore, inhibition of autophagosome degradation using bafilomycin A1 (10 nM) resulted in high autophagic flux in both cell lines during starvation, but again did not demonstrate a relative increase in autophagy in MDAMB231 cells compared to cells incubated in amino acid complete medium.
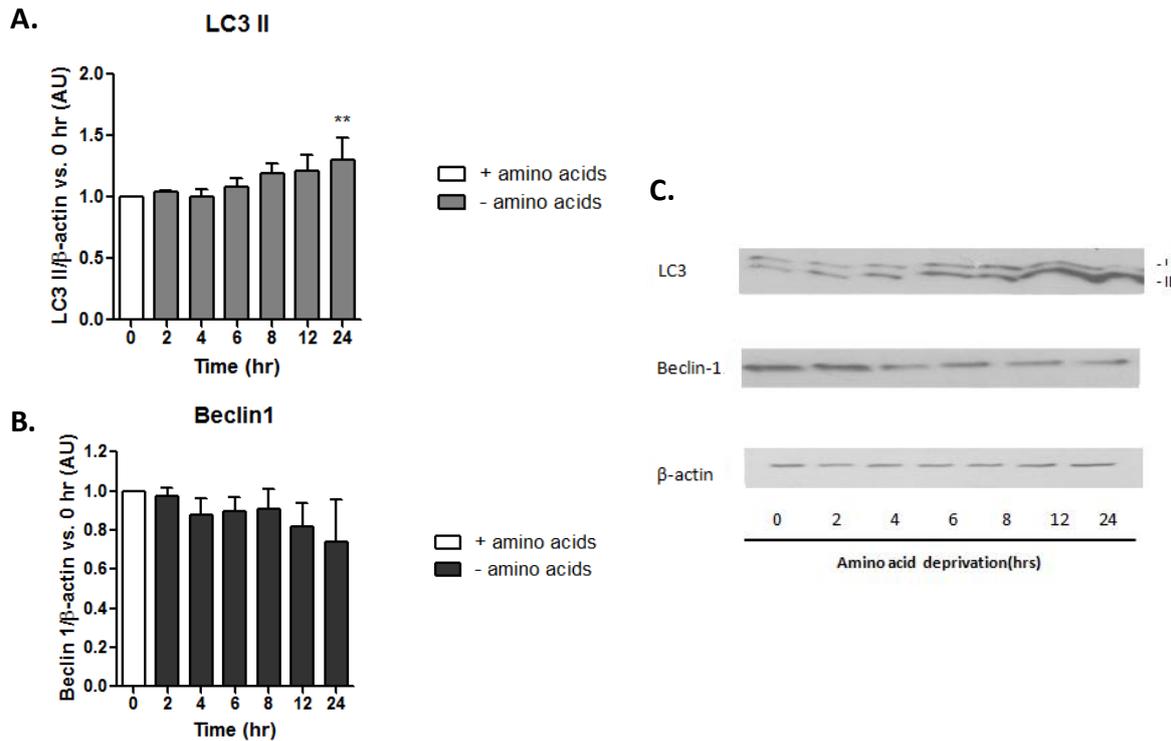
Fig. 2.13 Change in protein levels of the autophagy markers LC3 and beclin 1in MCF12A cells during a 24 hour period of amino acid starvation. Bar graphs show a densitometric representation of A) LC3-II and B) beclin 1 protein levels (normalized to β-actin vs. 0 hours of amino acid starvation) C) Representative western blots showing increased LC3 II protein levels at 24 hours of complete amino acid deprivation. hr = hours; AU = Arbitrary Units. No significant changes to beclin 1 levels were detected. Values are expressed as mean ± SEM. **, $P < 0.01$ vs. 0 hr.

Induction of autophagy generates a lipidated variant of LC3 (namely LC3 II) that is commonly used to gauge the level of autophagy within a cell. Amino acid starvation caused an increase in the protein level of LC3 II in MCF12A cells that corresponded with increasing time spent in amino acid deprived medium (Fig 2.13a). The autophagy protein beclin 1 is vital for autophagy induction, but no significant change in the protein levels of this marker were detected in MCF12A cells incubated in amino acid free medium.
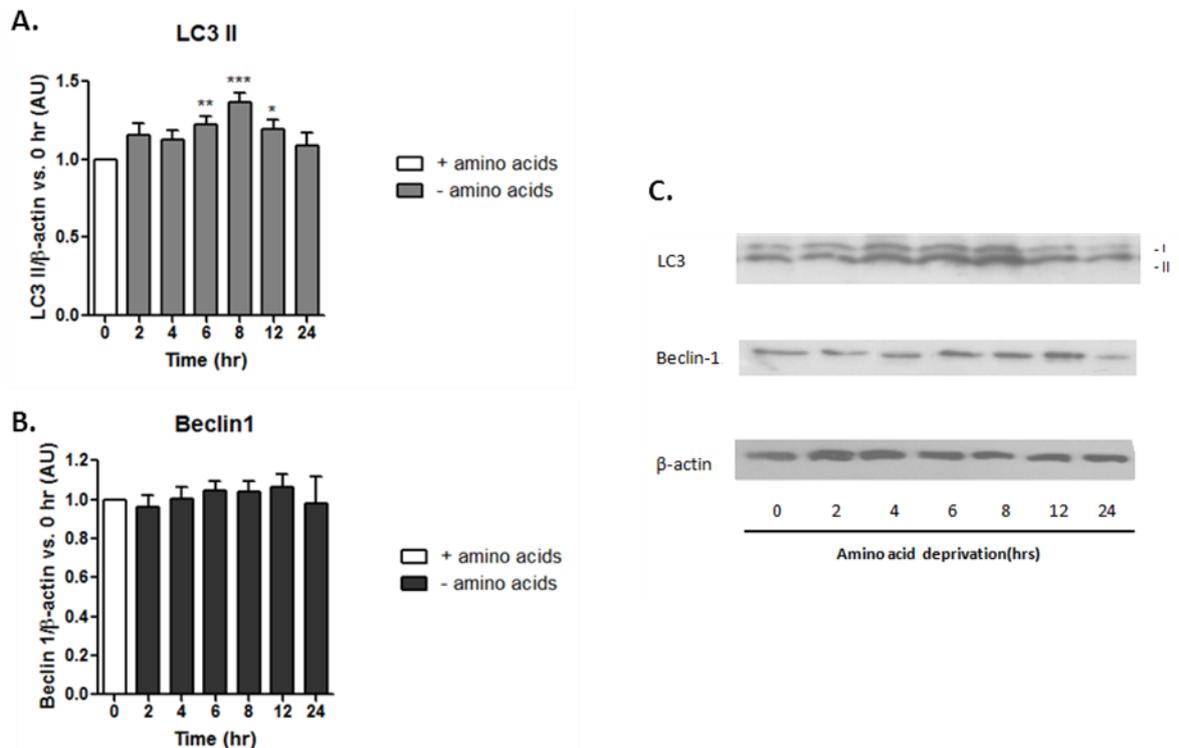
85

Fig. 2.14 Change in protein levels of the autophagy markers LC3 and beclin 1 in MDAMB231 cells during a 24 hour period of amino acid starvation. Bar graphs show a densitometric representation of A) LC3-II and B) beclin 1 protein levels (normalized to β-actin vs. 0 hours of amino acid starvation) C) Representative western blots showing increasing LC3 II protein levels during the first 8 hours of complete amino acid deprivation. No significant changes to beclin 1 levels were detected. hr = hours; AU = Arbitrary Units. Values are expressed as mean ± SEM. *, $P < 0.05$; **, $P < 0.01$; ***, $P < 0.001$ vs. 0 hr.

MDAMB231 cells were demonstrated to have increased levels of LC3 II within the first 8 hours of amino acid starvation (Fig 2.14a). These findings (as well as those for MCF12A cells) corresponded with the level of acidic compartmentalization in cells treated in a similar manner. LC3 II levels decreased and were no different than control levels after 24 hours of amino acid starvation. Beclin 1 levels did not change significantly either.
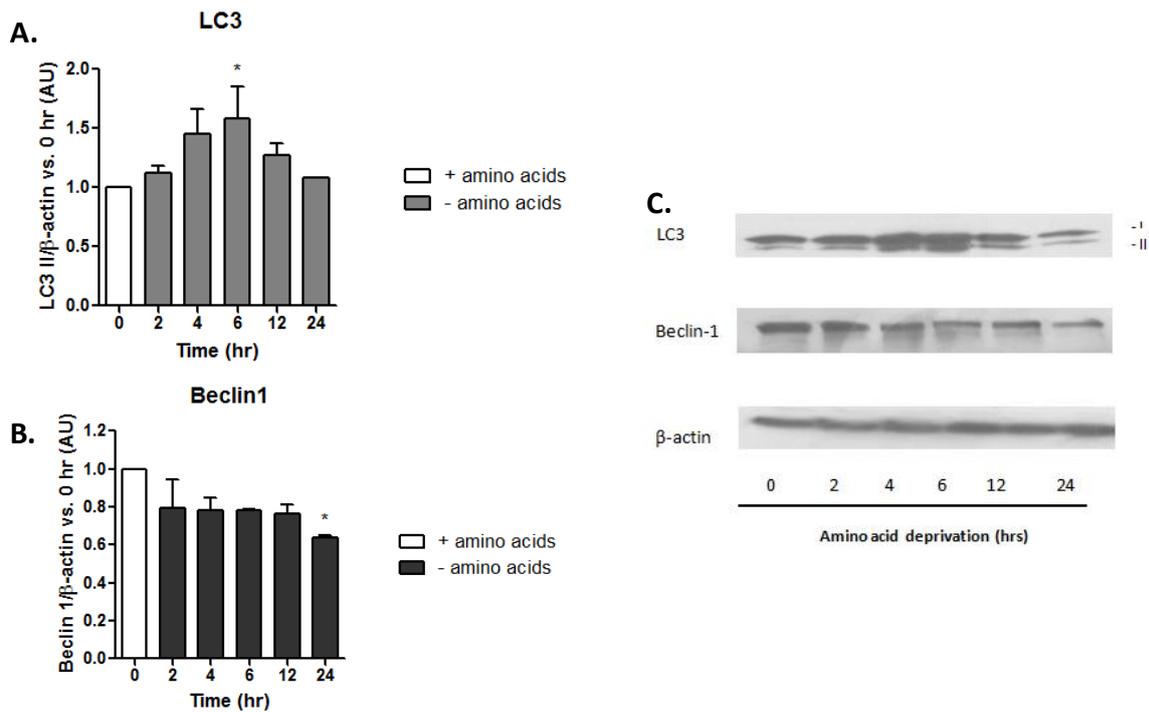
Fig. 2.15 Change in protein levels of the autophagy markers LC3 and beclin 1in MCF7cells during a 24 hour period of amino acid starvation. Bar graphs show a densitometric representation of A) LC3-II and B) beclin 1 protein levels (normalized to β-actin vs. 0 hours of amino acid starvation) C) Representative western blots showing increasing LC3 II protein levels during the first 6 hours of complete amino acid deprivation. A significant decrease to beclin 1 levels were detected after 24 hours of complete amino acid starvation. hr= hours; AU = Arbitrary Units. Values are expressed as mean ± SEM. *, $P < 0.05$ vs. 0 hr.

MCF7 cells were demonstrated to increase levels of LC3 II within the first 6 hours of amino acid starvation (Fig 2.15a), similar to those observed for the MDAMB231 cell line. However, these findings did not correspond with levels of lysosomal acidity. LC3 II protein levels decreased and were no different than control levels after 24 hours of amino acid starvation. Beclin 1 levels were shown to decrease significantly by 24 hours of amino acid starvation.
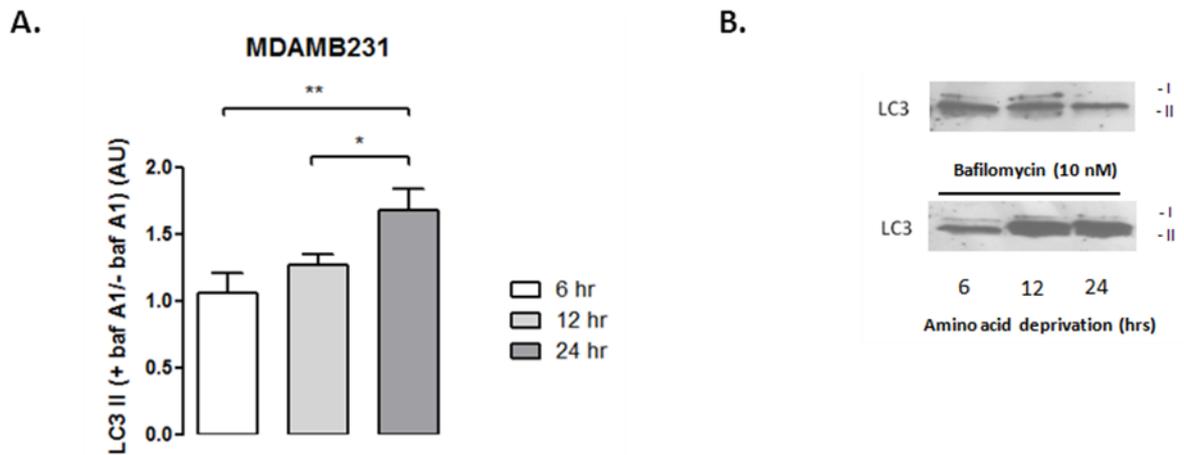
A.

B.

Fig. 2.16 Change in flux of LC3 II in MDAMB231 cells during a 24 hour period of amino acid starvation. A) Bar graphs showing densitometric representation of LC3-II protein levels. Values for LC3 II flux were calculated by dividing LC3 II protein levels in the presence lysomotropic reagent bafilomycin A1 (10 nM) by levels in its absence. B) Representative western blots showing LC3 II protein levels during 6, 12 and 24 hours of complete amino acid deprivation. hr = hours; AU = Arbitrary Units. Values are expressed as mean ± SEM of at least three independent determinations. *, $P < 0.05$; **, $P < 0.01$.

Autophagy flux measurements are a good indication of autophagy levels at any given time. To assess autophagy flux, cells were treated and then supplemented with 10 nM of bafilomycin A1 6 hours prior to harvesting for analysis. Values for flux were calculated from LC3 II protein levels obtained from western blot analysis. LC3 II levels in the presence of bafilomycin were divided by LC3 II levels from cells starved for the same time period without bafilomycin A1 (10 nM). In this way, it was determined that autophagy flux increased in MDAMB231 cells from 6 to 24 hours of amino acid starvation (Fig 2.16).
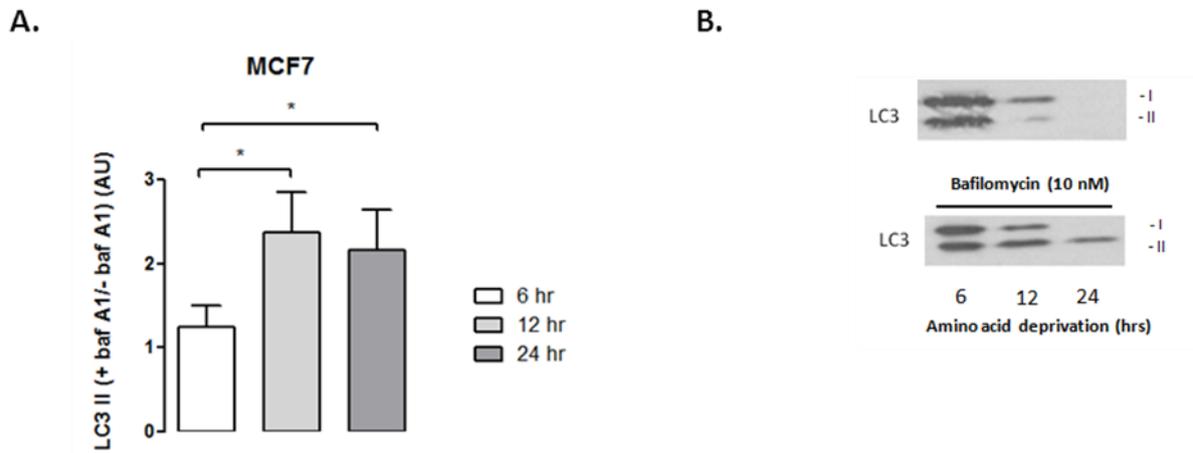
A.

B.

Fig. 2.17 Change in flux of LC3 II in MCF7cells during a 24 hour period of amino acid starvation. A) Bar graphs showing densitometric representation of LC3-II protein levels. Values for LC3 II flux were calculated by dividing LC3 II protein levels in the presence lysomotropic reagent bafilomycin A1 (10 nM) by levels in its absence. B) Representative western blots showing LC3 II protein levels during 6, 12 and 24 hours of complete amino acid deprivation. hr = hours; AU = Arbitrary Units. Values are expressed as mean ± SEM of at least three independent determinations. *, $P < 0.05$.

Even though MCF7 cells are known to be autophagy haploinsufficient, amino acid starvation appeared to increase autophagy flux when cells were starved from 6 to 24 hours by omitting amino acid from the culture medium (Fig 2.17). Importantly, some measures of autophagy flux only take treatments with blocked autophagy into account and by that measure MCF7 cells have decreasing autophagy flux while MDAMB231 cells still have increasing flux.

89

4.4 Autophagy is important for the maintenance of normal cell cycle progression during amino acid starvation in MDAMB231 cells but not in MCF12A cells.
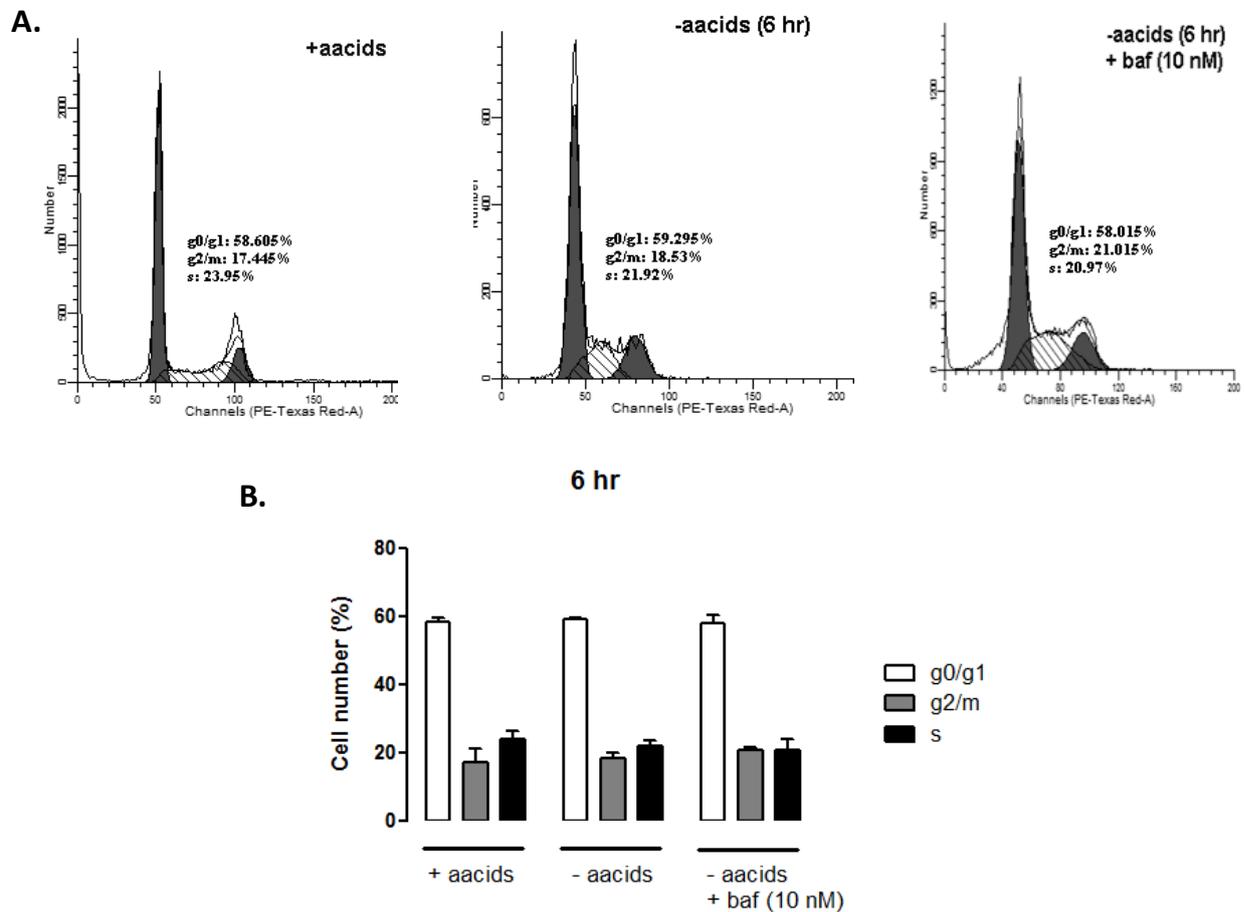
Fig. 2.18 Autophagy inhibition in MCF12A cells with bafilomycin A1 does not result in any cell cycle changes following 6 hours of amino acid deprivation. Cell cycle progression was assessed using flow cytometry following a 6 hour incubation in culture medium without amino acids and compared with cells incubated for similar durations in culture medium containing amino acids. Addition of bafilomycin A1 (10 nM) resulted in no significant changes to cell cycle parameters. Bafilomycin A1 (10 nM) was added to culture medium 6 hours prior to analysis. A. Typical DNA histograms and cell cycle phase percentages. B. Bar graphs representing the mean ± SEM of at least three independent determinations. hr = hours; aacids = amino acids.

MCF12A cells displayed no change in cell cycle progression after 6 hours of amino acid starvation, either with or without bafilomycin (10 nM) (Fig 2.18).
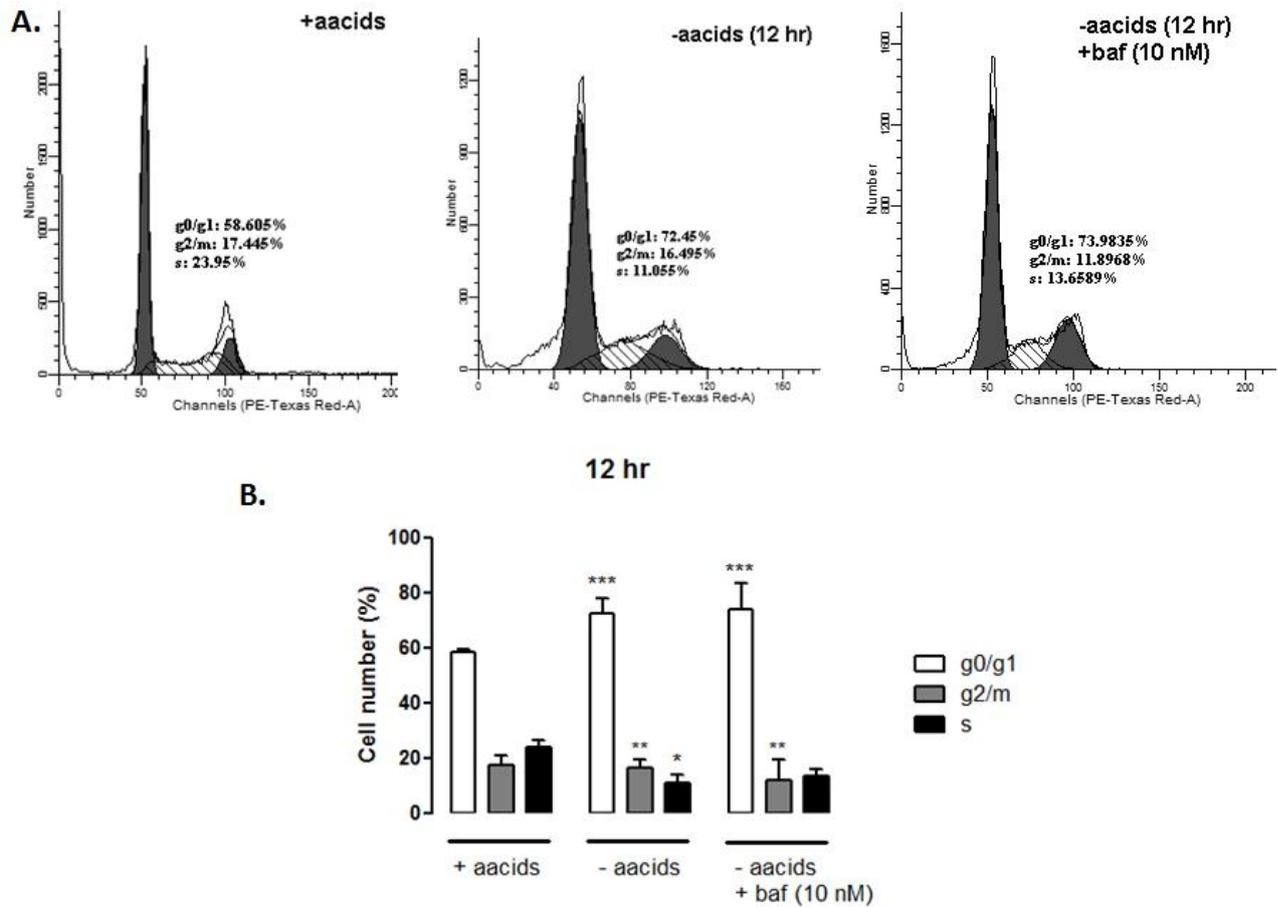
Fig. 2.19 Autophagy inhibition in MCF12A cells with bafilomycin A1 leads does not result in any cell cycle changes following 12 hours of amino acid deprivation. Cell cycle progression was assessed using flow cytometry following a 12 hour incubation in culture medium without amino acids and compared with cells incubated for similar durations in culture medium containing amino acids. Addition of bafilomycin A1 (10 nM) resulted in no significant changes to cell cycle parameters. Bafilomycin A1 (10 nM) was added to culture medium 6 hours prior to analysis. A. Typical DNA histograms and cell cycle phase percentages. B. Bar graphs representing the mean ± SEM of at least three independent determinations. hr = hours; aacids = amino acids. *, $P < 0.05$ vs. + amino acids s phase; ***, $P < 0.001$ vs. + amino acids g0/g1 phase; **, $P < 0.001$ vs. + amino acids g2/m phase.

Although, MCF12A cells displayed a pronounced pattern g0/g1 arrest after 12 hours of starvation, bafilomycin A1 did not alter cell cycle progression in response to amino acid starvation (Fig 2.19).
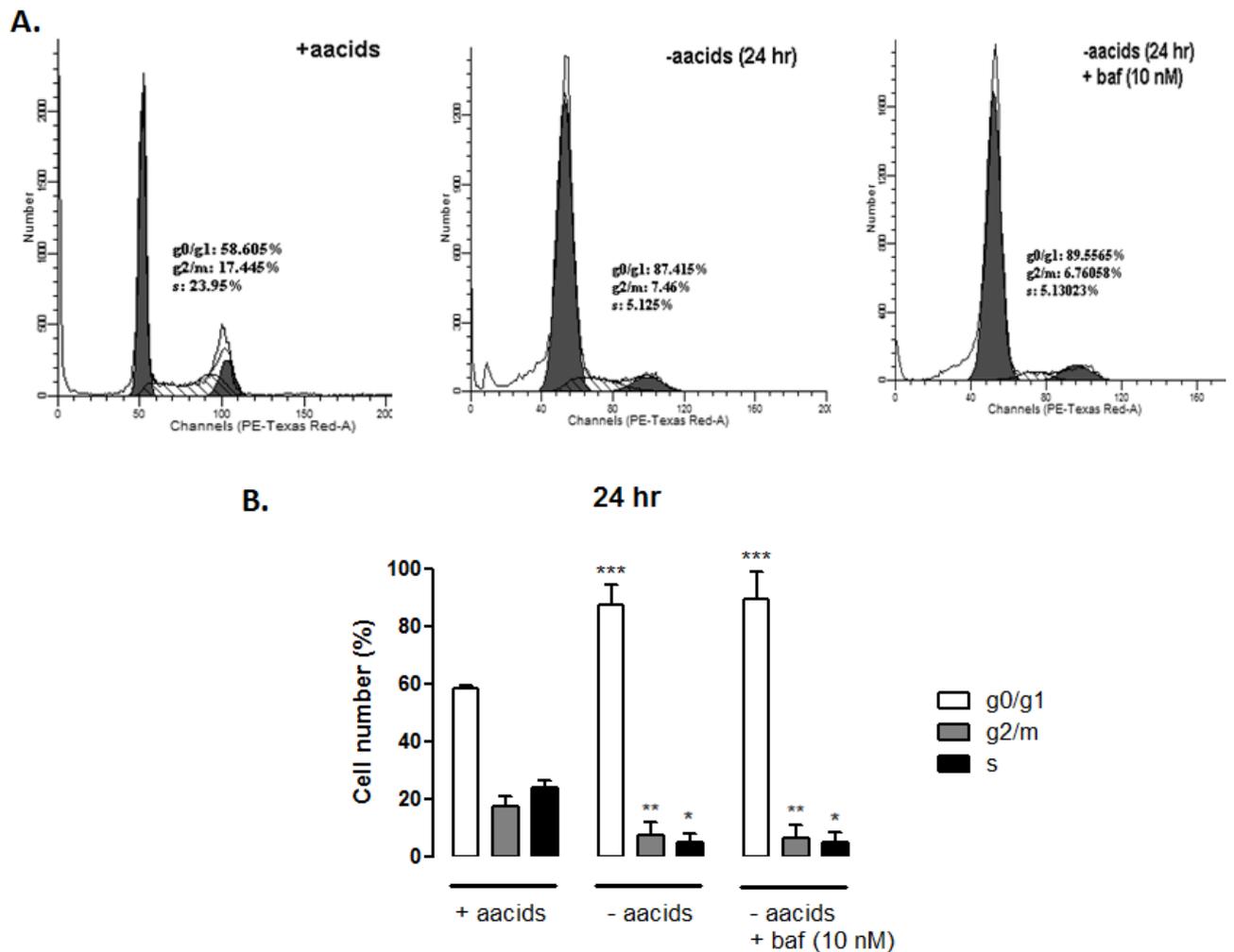
Fig. 2.20 Autophagy inhibition in MCF12A cells with bafilomycin A1 leads does not result in any cell cycle changes following 24 hours of amino acid deprivation. Cell cycle progression was assessed using flow cytometry following a 24 hour incubation in culture medium without amino acids and compared with cells incubated for similar durations in culture medium containing amino acids. Addition of bafilomycin A1 (10 nM) resulted in no significant changes to cell cycle parameters. Bafilomycin A1 (10 nM) was added to culture medium 6 hours prior to analysis. A. Typical DNA histograms and cell cycle phase percentages. B. Bar graphs representing the mean ± SEM of at least three independent determinations. hr = hours; aacids = amino acids. *, $P < 0.001$ vs. + amino acids s phase; ***, $P < 0.001$ vs. + amino acids g0/g1 phase; **, $P < 0.05$ vs. + amino acids g2/m phase.

Bafilomycin A1 did not alter cell cycle progression in response to 24 hours of amino acid starvation in MCF12A cells (Fig 2.20), or MCF7 cells (data not shown).
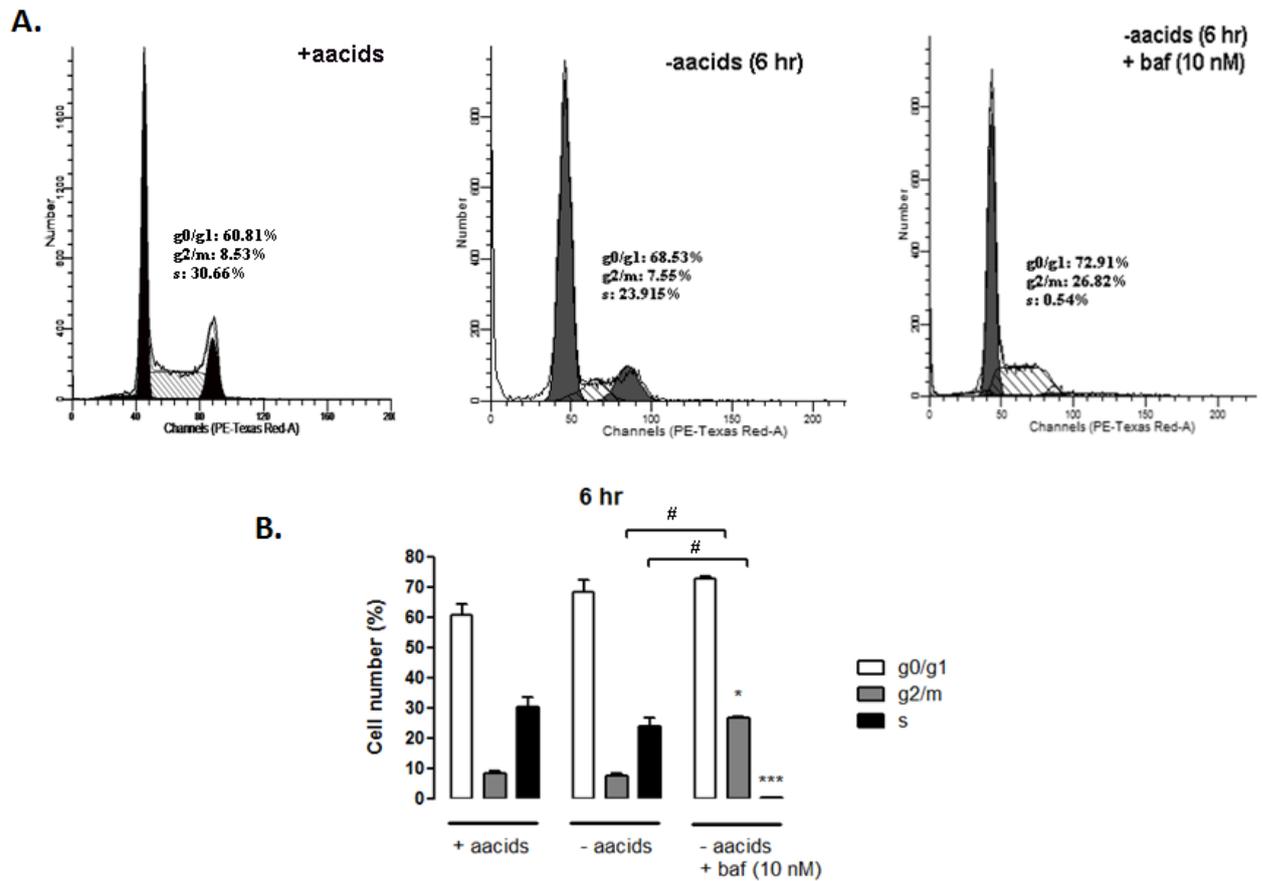
Fig. 2.21 Autophagy inhibition in MDAMB231 cells with bafilomycin A1 following 6 hours of amino acid deprivation leads to an increased g2/m phase and a decreased s phase. Cell cycle progression was assessed using flow cytometry following a 6 hour incubation in culture medium without amino acids and compared with cells incubated for similar durations in culture medium containing amino acids. Addition of bafilomycin A1 (10 nM) resulted in significant changes to g2/m and s phases of the cycle. Bafilomycin A1 (10 nM) was added to culture medium 6 hours prior to analysis. A. Typical DNA histograms and cell cycle phase percentages. B. Bar graphs representing the mean ± SEM of at least three independent determinations. hr = hours; aacids = amino acids. *, $P < 0.05$ vs. + amino acids g2/m phase; ***, $P < 0.001$ vs. + amino acids s phase; #, $P < 0.05$.

As in MCF12A cells, MDAMB231 cells exhibited no obvious alterations in cell cycle progression after 6 hours of amino acid starvation (Fig 2.21). Interestingly, inhibition of autophagy with bafilomycin A1 (10 nM) resulted in a significant g2/m arrest and an associated decrease in s-phase.

93

A.

B.
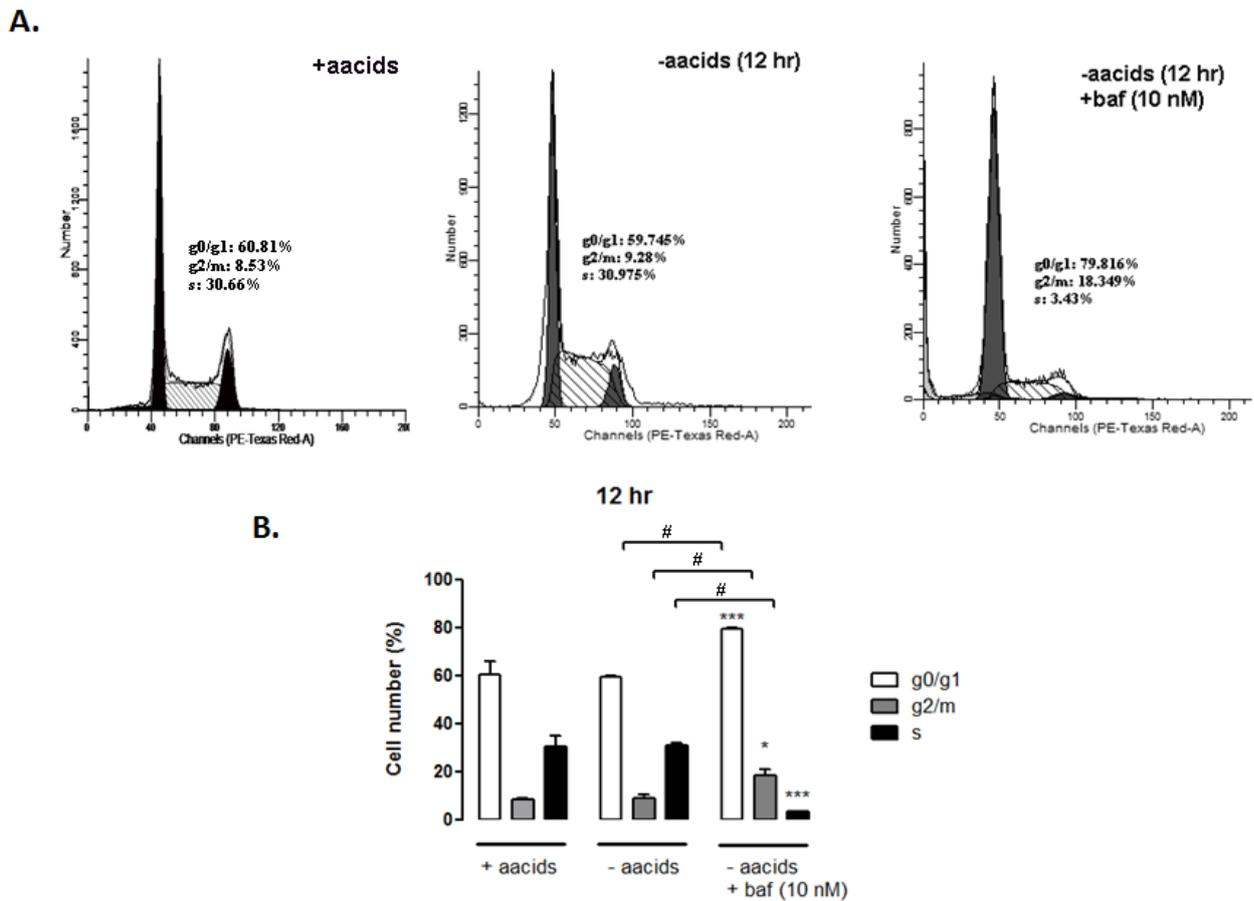
Fig. 2.22 Autophagy inhibition in MDAMB231 cells with bafilomycin A1 following 12 hours of amino acid deprivation leads to increased g0/g1 and g2/m phases and a decreased s phase. Cell cycle progression was assessed using flow cytometry following a 12 hour incubation in culture medium without amino acids and compared with cells incubated for similar durations in culture medium containing amino acids. Addition of bafilomycin A1 (10 nM) resulted in significant changes to g1/g0, g2/m and s phases of the cycle. Bafilomycin A1 (10 nM) was added to culture medium 6 hours prior to analysis. A. Typical DNA histograms and cell cycle phase percentages. B. Bar graphs representing the mean ± SEM of at least three independent determinations. hr = hours; aacids = amino acids. *, $P < 0.05$ vs. + amino acids g2/m phase; ***, $P < 0.001$ vs. + amino acids s phase; #, $P < 0.05$.

Inhibition of autophagy with bafilomycin A1 (10 nM) resulted in a significant g0/g1 and g2/m arrest and an associated decrease in s-phase in MDAMB231 cells after 12 hours of amino acid starvation (Fig 2.22).

94
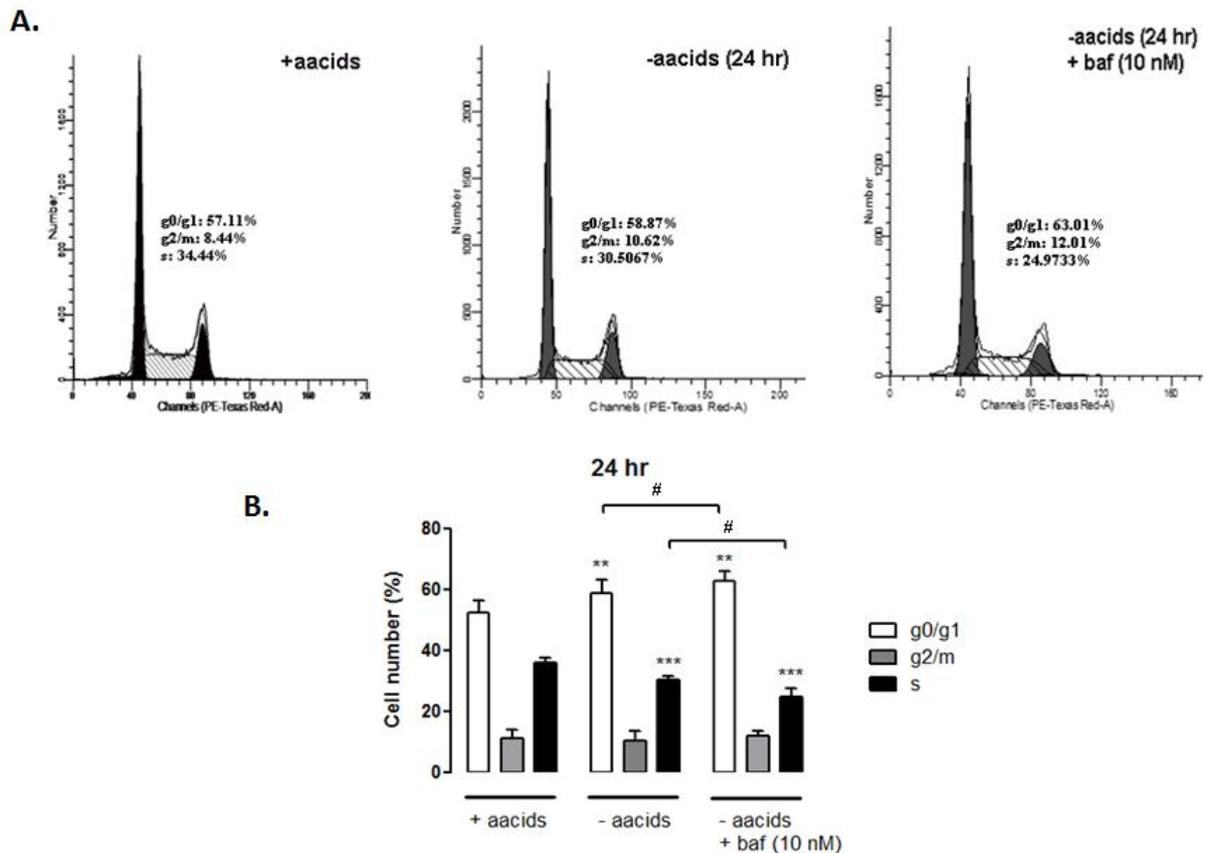
Fig. 2.23 Autophagy inhibition in MDAMB231 cells with bafilomycin A1 following 24 hours of amino acid deprivation leads to an increased g0/g1 phase and a decreased s phase. Cell cycle progression was assessed using flow cytometry following a 24 hour incubation in culture medium without amino acids and compared with cells incubated for similar durations in culture medium containing amino acids. Addition of bafilomycin A1 (10 nM) resulted in significant changes to g1/g0 and s phases of the cycle. Bafilomycin A1 (10 nM) was added to culture medium 6 hours prior to analysis. A. Typical DNA histograms and cell cycle phase percentages. B. Bar graphs representing the mean ± SEM of at least three independent determinations. hr = hours; aacids = amino acids. **, $P < 0.01$ vs. + amino acids g0/g1 phase; ***, $P < 0.01$ vs. + amino acids s phase; #, $P < 0.05$.

Inhibition of autophagy with bafilomycin A1 (10 nM) resulted in a significant g0/g1 arrest and an associated decrease in s-phase in MDAMB231 cells after 24 hours of amino acid starvation (Fig 2.23).

4.5 Autophagy inhibition with ATG5 siRNA during 24 hours of amino acid deprivation leads to increased caspase 3/7 activity in MDAMB231 cells and MCF12A cells
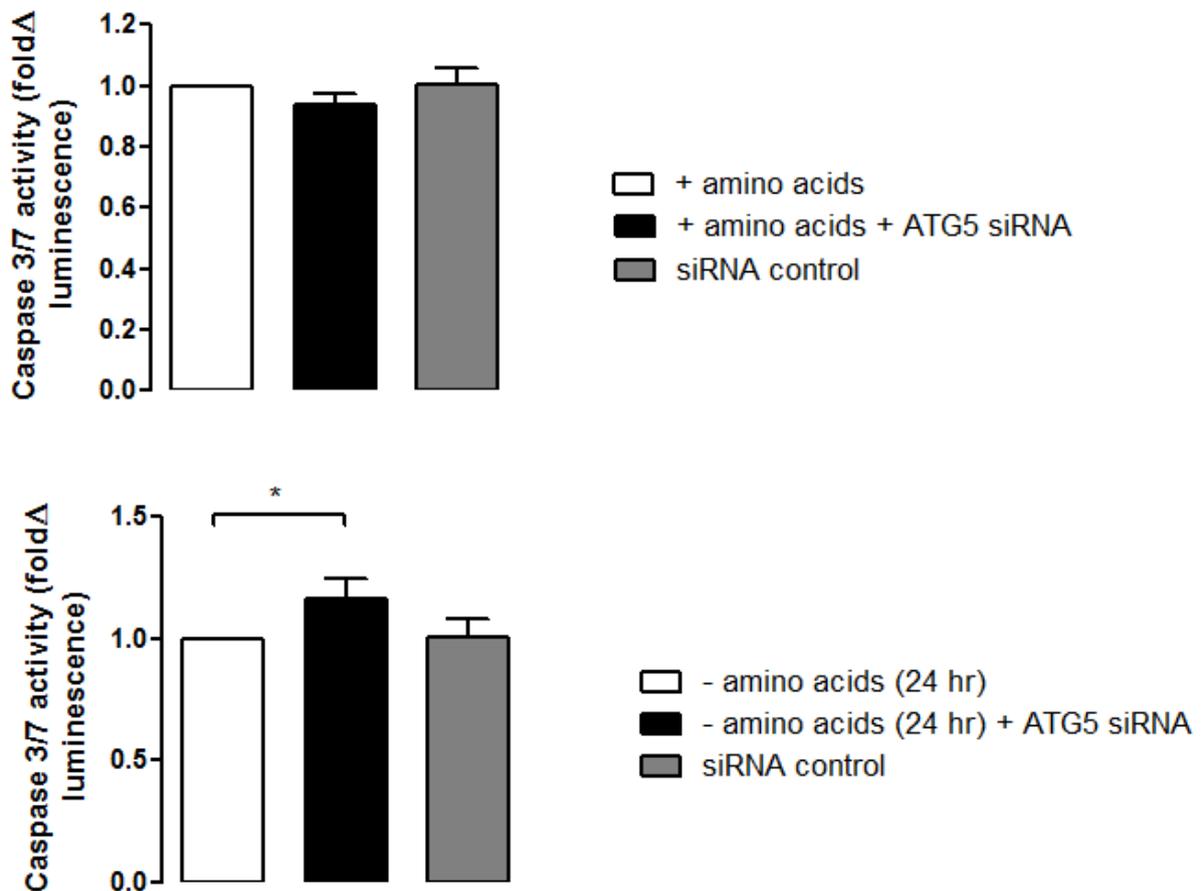
Fig. 2.24 Autophagy inhibition with ATG5 siRNA in MDAMB231 cells causes an increase caspase 3/7 activity at 24 hours of amino acid starvation. Results represent the fold change in luminescence in cultures depleted of amino acids versus either those cultured in medium containing amino acids or depleted of amino acids for 24 hours. Transfection with ATG5 siRNA alone and prior to amino acid starvation did not lead to significant increases in caspase 3/7 cleavage. Caspase 3/7 activity was taken to be proportionate to produced luminescence intensity. hr = hours. Each value represents the mean ± SEM of at least three independent determinations. Significance markers depict comparisons versus cells treated for 24 hours with amino acid free medium. *, $P < 0.05$

Direct inhibition of autophagy using ATG5 siRNA resulted in increased caspase 3/7 cleavage in MDAMB231 cells incubated in culture medium without amino acids for 24 hours (Fig 2.24). ATG5 siRNA did not cause increased caspase 3/7 activity if present in amino acid complete medium for an equivalent period of time.
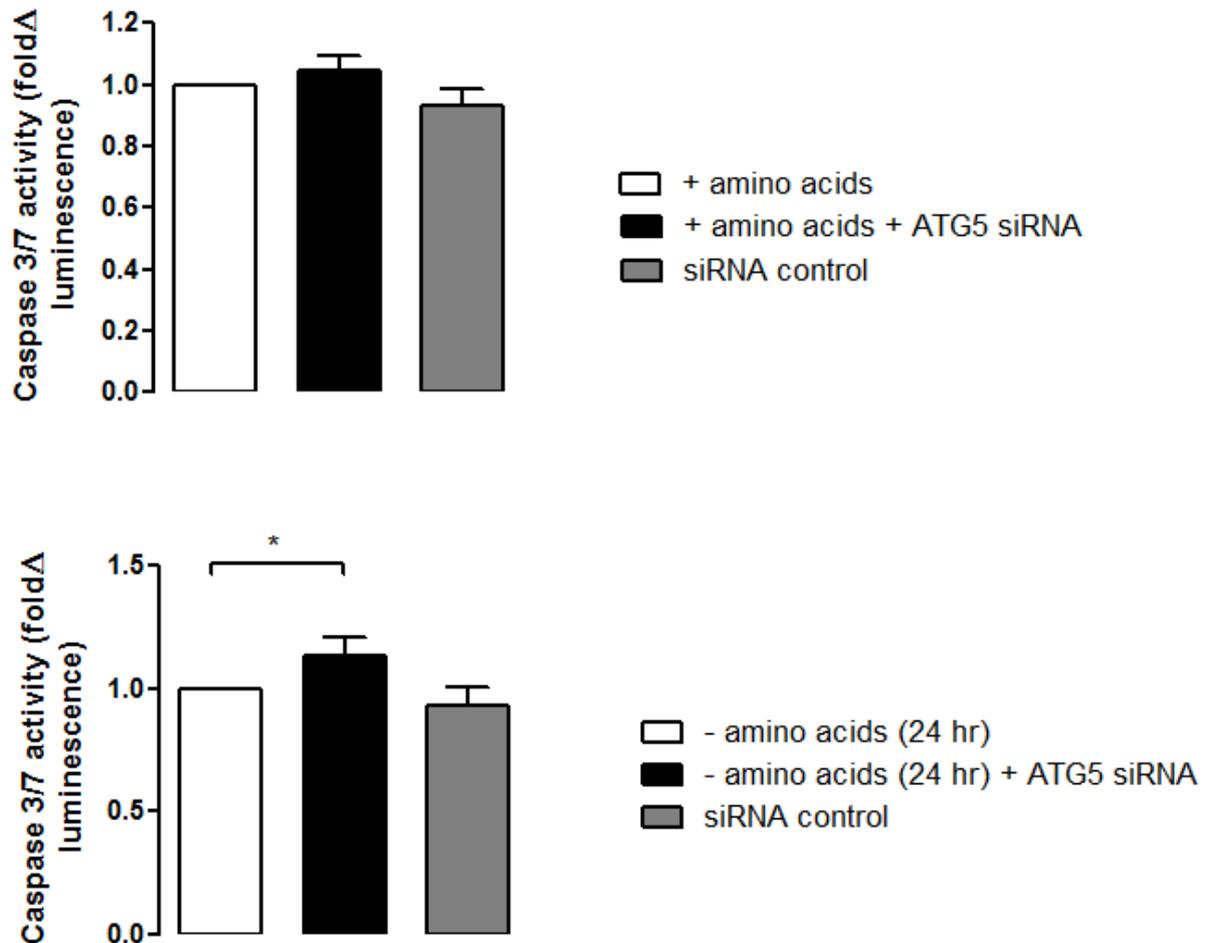
Fig. 2.25 Autophagy inhibition with ATG5 siRNA in MCF12A cells causes an increase caspase 3/7 activity at 24 hours of amino acid starvation. Results represent the fold change in luminescence in cultures depleted of amino acids versus either those cultured in medium containing amino acids or depleted of amino acids for 24 hours. Transfection with ATG5 siRNA alone and prior to amino acid starvation did not lead to significant increases in caspase 3/7 cleavage. Caspase 3/7 activity was taken to be proportionate to produced luminescence intensity. hr = hours. Each value represents the mean ± SEM of at least three independent determinations. Significance markers depict comparisons versus cells treated for 24 hours with amino acids free medium. *, $P < 0.05$

Direct inhibition of autophagy using ATG5 siRNA resulted in increased caspase 3/7 cleavage in MCF12A cells incubated in culture medium without amino acids for 24 hours (Fig 2.25). ATG5 siRNA did not cause increased caspase 3/7 activity if present in amino acid complete medium for an equivalent period of time.

4.6   An apparent activation of an autophagy related gene occurs during amino acid starvation of MDAMB231 cells
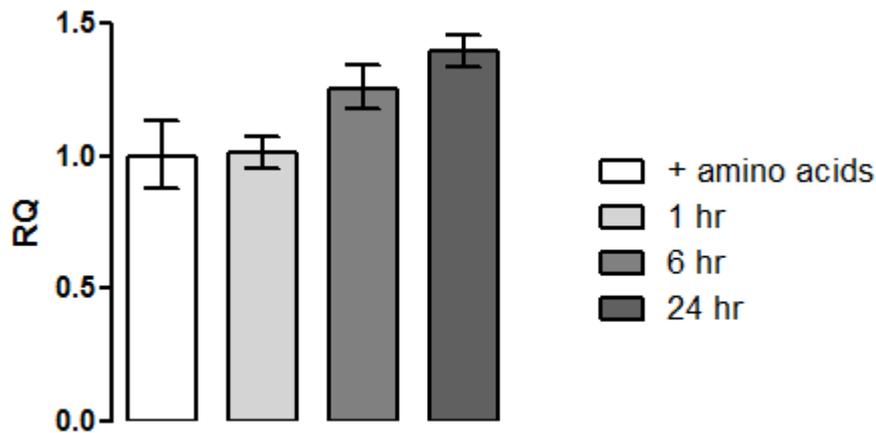
Fig. 2.26 Relative induction values of ATG5 mRNA during amino acid starvation in MDAMB231 cells. ATG5 mRNA levels increase during amino acid starvation of MDAMB231 cells. Results represent quantification values of the amount of target ATG5 cDNA, normalized to an endogenous control (90 kDa), and relative to a calibrator (+ amino acids; RQ = 1.00). Error bars are representative of RQ min and RQ max values. hr = hours.

A moderate induction of ATG5 was observed in MDAMB231 cells starved of amino acids (Fig 2.26). Using relative quantification based on data acquired from the Real-Time PCR assay, a moderate induction of ATG5 was observed at 6 and 24 hours during amino acid starvation of MDAMB231 cells.

A.
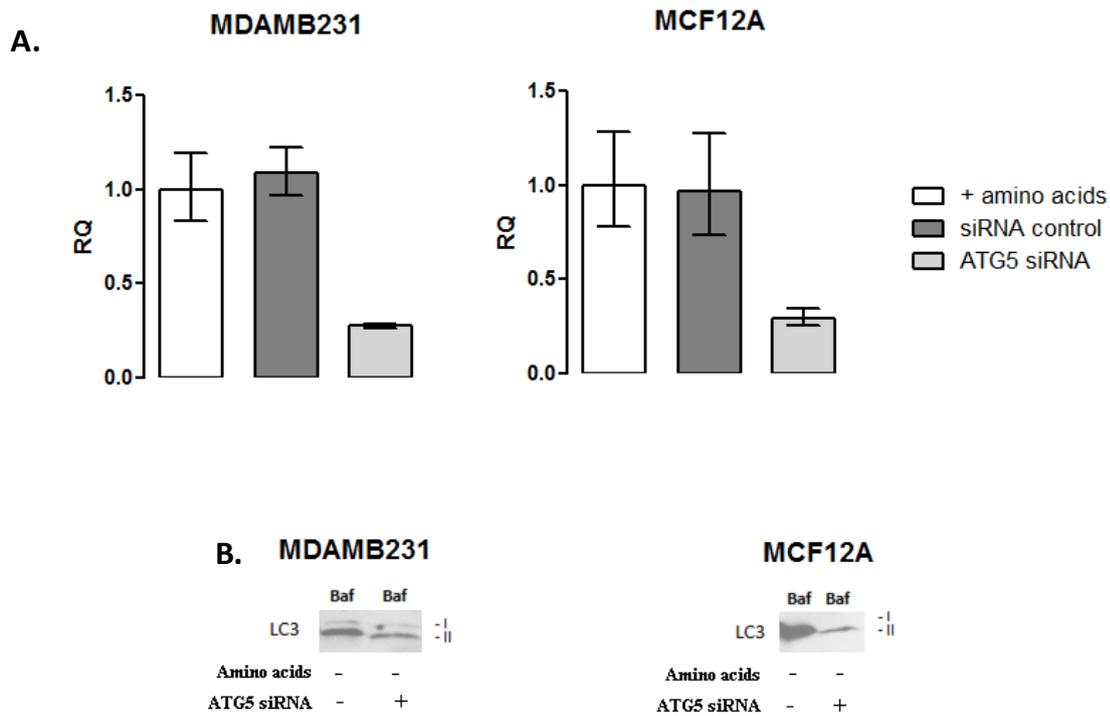
Fig. 2.27 Validation experiments confirmed a prominent down-regulation of ATG5 expression and protein levels in both cell lines after transfection with ATG5 siRNA. Addition of a scrambled siRNA negative control did not have any effect on expression of ATG5. A) Bar graphs representing quantification values of the amount of target ATG5 cDNA, normalized to an endogenous control (90 kDa), and relative to a calibrator (+ amino acids; RQ = 1.00). Error bars are representative of RQ min and RQ max values. B) Western blots indicating a decreased accumulation of LC3 II during 24 hours of amino acid starvation in the presence of bafilomycin A1 (10 nM) during ATG5 silencing.

Relative quantification based on data acquired from the Real-Time PCR assay confirmed silencing of ATG5 through down-regulation of ATG5 expression in both MDAMB231 and MCF12A cells (Fig 2.27). Western blotting illustrated that protein levels of LC3 II declined following ATG5 silencing. This experiment serves as a validation that ATG5 expression levels are blunted by ATG5 siRNA in our experimental model.

5   Discussion

Although autophagy is known to become activated in response to metabolic stress, such as during times of amino acid starvation, it appears as though many cancer cell lines display high levels of autophagy activity even in nutrient rich conditions (Yang et al., 2011). Furthermore, the tumour microenvironment is prone to episodes of short term nutrient depletion due to poorly defined vascular systems (Tredan et al., 2007). Autophagy is initiated in these circumstances and is believed to confer a survival advantage during nutrient depletion. However, it not clear how cancer cells with already high basal autophagy levels will tolerate short term bouts of low nutrient levels. In addition, studies investigating the effects of acute amino acid deprivation in the context of breast cancer with high basal autophagy are almost completely absent.

In general, there is a paucity of research investigating nutrient starvation in cancer, particularly studies considering the breast cancer setting. In fact, few studies exist for any cell types (cancer or otherwise) where amino acids or proteins are depleted with all other nutrients kept constant, and studies investigating the acute depletion of nutrients (less than 24 hours) are almost totally missing from the literature. In addition, data from the few studies that have been performed are equivocal and autophagy has been shown to either protect cells or lead to their death depending on the context. In a rare instance, rat hepatoma cells (H4IIE) were starved of amino acids with or without the autophagy inhibitor bafilomycin A1 (Wang et al., 2009), and autophagy was monitored and found to increase rapidly following starvation. Cell survival was maintained in an autophagy dependent manner for the first 6 hours of amino acid starvation in this model, and viability was rescued by bafilomycin A1 after 12 hours of starvation. The authors postulated that protective autophagy occurs during the acute stages of amino acids starvation in these cells whereas destructive autophagy occurs at later stages.

Amino acid starvation was also induced during short term starvation of PC-12 cells (Sadasivan et al., 2006). Even though autophagy was markedly increased at six hours, various viability assays confirmed decreased survival during amino acid starvation. Starvation in the presence of the autophagy inhibitor 3-methyladenine alleviated amino acid starvation associated cell death leading the authors to conclude that these cells were undergoing an autophagy cell death (type-II) response.

It has recently become clear that several cancer lines are dependent on autophagy for normal growth, and that human cancer with mutations in H-*ras* or K-*ras* may require autophagy for tumour survival (Guo et al., 2011). Some pancreatic (Yang et al., 2011) and other Ras-driven tumours (Lock et al., 2011) have also been shown to require autophagy for sustained growth. This so-called autophagy-addiction that is now thought to be characteristic of some cancers could represent an important avenue for development of new anticancer strategies. Although genetic *ras* mutations are infrequent in breast cancer, Ras was shown to be highly and abnormally activated in over 50% of tested cancers in one study (von Lintig et al., 2000). This increased Ras activity was attributed to the over-expression of growth factor receptors in many of these breast cancers. It is therefore important that breast cancer with high Ras activity be studied in association with autophagy.

Observations from previous experiments (described in chapter 1) demonstrated that the non-tumourogenic breast epithelial cell line MCF12A showed few detrimental effects after being incubated in culture medium bereft of any amino acids for 24 hours. On the other hand, the commonly utilized metastatic breast adenocarcinoma cell line MDAMB231 showed greater sensitivity to amino acid exclusion from culture media and displayed a sudden increase in cell death and a profile of cell cycle arrest after only 12 hours of amino acid starvation. As these cells are known to have high *ras* activation and high basal autophagy levels (Ogata et al.,

2001), and autophagy is thought to be an important factor in tolerance to nutrient deprivation, the aim of this study (presented in this chapter) was to investigate if autophagy is in fact an important survival mechanism during short term amino acid starvation in these cells.

Bafilomycin A1, a specific inhibitor of vacuolar H^+ATPase (V-ATPase) (Yoshimori et al., 1991), was used in this study. Bafilomycin is now known to rapidly and reversibly inhibit fusion between autophagosomes and lysosomes, if administered for short time periods (Klionsky et al., 2008), acting through the mechanism of inhibiting lysosomal acidification (Yamamoto et al., 1998). This is a similar mechanism of autophagy inhibition as the clinically relevant choloroquine. It is clear from the data presented in this chapter that both the tumourogenic cancer cell line and the non-tumourogenic cell line in our model rely on a process inhibited by bafilomycin A1 for survival during short term amino acid starvation.

Data in this chapter illustrates that autophagy activity increases significantly above basal levels during the first 6 hours of amino acid starvation in MDAMB231 cells. Increased lysosomal acidity (Fig 2.9) and high levels of the autophagy marker LC3 II (Fig 2.14) both signify an increased autophagy response at this time point. Indeed, MDAMB231 cells displayed no signs of apoptosis (Fig 2.5 & chapter 1) or membrane impairment (Fig 2.7 & chapter 1) after being incubated in the absence of amino acids for 6 hours. Furthermore, cells appeared to have normal cell cycle progression and retained the ability to reduce MTT. The MCF12A cell line showed similarly high lysosomal acidity (Fig 2.10) and increasing LC3 II levels (Fig 2.13) after 6 hours of amino acid deprivation and no signs of cell death or cell cycle disruption either. On the other hand, the beclin 1 haploinsufficient (partially autophagy deficient) MCF7 cell line presented with indications of decreased viability compared to cells incubated in amino acid complete medium (Fig 2.3) that corresponded with high levels of lysosomal acidity (Fig 2.11), despite having high levels of LC3 II after 6 hours of amino acid

starvation (Fig 2.15). Inhibition of autophagy with 10 nM of bafilomycin A1 was able to reverse tolerance to amino acid deprivation at 6 hours in MDAMB231 cells. When bafilomycin was present in the culture medium, these cells underwent increased apoptosis (Fig 2.5) and had signs of increased membrane permeability (Fig 2.7). Furthermore, if autophagy was inhibited, amino acid starved MDAMB231 cells presented with a significantly decreased s-phase and appearance of a profile of g2/m cell cycle arrest (Fig 2.21). Interestingly, although MCF12A cells showed a decreased MTT reducing capacity (Fig 2.1) with bafilomycin, they did not display any increased caspase 3/7 cleavage (Fig 2.5) or significantly increased membrane permeability (Fig 2.8) in response to acute amino acid starvation. Tellingly, these cells also did not show changes in their cell cycle parameters if bafilomycin was present during 6 hours of amino acid starvation (Fig 2.18). As expected, bafilomycin also had no influence on the MCF7 cells (Fig 2.3). Together, these results indicate that increased autophagy activity in MDAMB231 cells after only 6 hours of amino acid deprivation seems to be protective and vital for tolerance to stress during these first few hours of amino acid depletion. Although MCF12A cells are not completely unchanged by 6 hours of amino acid depletion, they do not experience any serious negative effects due to starvation, even if autophagy is inhibited with bafilomycin. Presumably this is because they are much slower growing and do not require access to as high concentrations of amino acids as the more aggressive adenocarcinoma cell line. This is further illustrated by assessment of the cell cycle parameters during the first 12 hours of amino acid starvation. Importantly, results indicate that autophagy is vital for normal cell cycle progression in MDAMB231 cells, but not MCF12A cells. This is a good indicator that nutrient levels have fallen too low to support typical growth and cellular functioning in the faster growing cancer cells.

MDAMB231 cells have an existing high basal autophagy activity, even in nutrient rich conditions (Fig 2.12). Still, they are unable to tolerate amino acid depletion for more than a

few hours in our model. This is evidenced by increased cell death after only 12 hours of amino acid depletion (Fig 2.5c). Nonetheless, these cells do respond to acute amino acid starvation by increasing their autophagy activity, which appears to aid them in tolerating amino acid deprivation for the initial 6 hours in our model. However, without autophagy, MDAMB231 cells are unable to maintain survival for even a few short hours. Importantly, the presence of a high basal autophagy activity in MDAMB231 cells, even in nutrient rich conditions, could signify that they require autophagy for normal functioning. The fact that the addition of bafilomycin to normal (amino acid complete) medium did not decrease cell viability indicates that these cells are able to survive during 6 hours without autophagy, provided that sufficient nutrients are available. Efficient and pronounced down regulation of ATG5 in MDAMB231 cells and MCF12A cells (Fig 2.27) resulted in a statistically significant increase in caspase 3/7 activity during 24 hours of amino acid starvation in both cell lines (Fig 2.24 and Fig 2.25). This serves to illustrate that down-regulation of autophagy prior to the protective increase in autophagy at 6 hours amino acid starvation in MDAMB231 cells leads to an increase in activation of programmed cell death pathways.

The expression of the autophagy marker LC3 II clearly increased to a peak at 6 and 8 hours in MDAMB231 cells (Fig 2.14a). However, despite relatively decreased LC3 II levels at 12 and 24 hours of amino acid starvation, autophagy flux was higher than at 6 hours (Fig 2.16) and corresponded to levels of baseline flux (Fig 2.12b). LC3 II protein levels are known to decrease during high autophagy flux due to its increased degradation following lysosomal fusion (Mizushima et al., 2010). In our model, the status of autophagy flux corresponded inversely to the level of lysosomal acidity in MDAMB231 cells (Fig 2.9a). It is plausible that higher autophagy flux results in increased lysosomal turnover and therefore a decreased level of acidity in MDAMB231 cells. Notably, this phenomenon was observed to occur conversely

104

for MCF12A cells, which displayed high autophagy flux levels in association with increased cellular acidity.

It is clear that a surging autophagy response occurs at 6 hours in the MDAMB231 cells, and that this amplification of autophagy is necessary for the maintenance of cell survival during this period. Results indicate that protective autophagy is lost after 6 hours and that by 24 hours of amino acid starvation autophagy is playing little or no role in the maintenance of survival, even though autophagy flux, lysosomal acidity and LC3 II protein levels are high (but equivalent to levels at baseline). At this point, a sudden increase in cell death and a profile of cell cycle arrest after only 12 hours of amino acid starvation becomes apparent. MCF12A cells remained remarkably tolerant to amino acid deprivation. However, after 24 hours of starvation, MCF12A cells also had significantly increased levels of autophagy. This is inferred from the high autophagy flux (2.12a) and significantly increased LC3 II protein levels (2.13). Furthermore, lysosomal acidity was also significantly elevated in these cells at this point. Importantly, if autophagy was then inhibited with bafilomycin A1, these cells began to display indications of increased cell death (Fig 2.6) and membrane permeability (Fig 2.8). These results are in accordance with the hypothesis that increases in autophagy are protective due to the enhanced generation of amino acids through lysosomal degradation. Importantly, as these cells are slower growing (and presumably require access to lower amino acid concentrations than the MDAMB231 cells) they only begin to possess an enhanced autophagy response at a later point of starvation (24 hours in our model).

Notably, bafilomycin was added only 6 hours prior to analysis of various parameters. Therefore, while bafilomycin was present during the entire period of starvation for the 6 hour amino acid deprivation experiments, it was only administered at hour 18 for the 24 hour amino acid deprivation experiments. This factor is important in interpreting results in light of

the fact that MDAMB231 cells display a protective surge at around six hours of starvation. Therefore, if autophagy is inhibited during this period, then its protective effect would not be realised. Conversely, if autophagy is blocked after this 6 hour protective surge (such as at hour 18 during the 24 hour amino acid starvation experiments) then the substrates generated at 6 hours would presumably elicit a protective effect during the later stages of amino acid deprivation.

LC3 II protein levels, and not autophagy flux, appear to be a more reliable indicator of the ability of MDAMB231 cells (with high basal autophagy) to withstand amino acid deprivation through autophagy. Despite a clear increase in autophagy flux of the MCF7 cell line, lysosomal acidity was not significantly higher until 24 hours of amino acid starvation. Therefore, caution should be taken when utilizing lysosomal acidity or autophagy flux measurements independently of other markers of autophagy to assess survival in response to nutrient deprivation. Also, high basal autophagy in MDAMB231 cells does not support survival in the face of amino acid deprivation. In fact is seems reasonable to postulate that it may be due to resident high autophagy activity (and constant turnover of intracellular material) that these cells require greater access to free amino acids.

Additionally, it is conceivable that reliance on high basal autophagy necessitates that MDAMB231 cells cannot increase autophagy levels further for too long periods during metabolic stress. It is possible that a feedback mechanism prevents overstimulation of this process as a safeguard. This notion is supported by evidence that the autophagy promoter rapamycin was able to partly rescue MTT reductive capacity during 24 hours of amino acid depletion (Fig 2.4). These results indicate that MDAMB231 cells are still capable of increasing autophagy at this time point of amino acid starvation in spite of their apparent failure to effectively (and protectively) do so in the absence of rapamycin. This implies that

these cells will only be able to withstand shorter periods of stress in the abscence of intervention, such as that sometimes associated with the intermittent nutrient supply in cancer tumours. In order to investigate this possibility, expression levels of the autophagy related gene ATG5 were analysed (Fig 2.26). This experiment demonstrated that MDAMB231 cells appear to initiate autophagy in response to starvation, even at 24 hours of amino acid depletion. Whether autophagy activation is prevented in some other manner is unknown. The fact that MDAMB231 breast cancer cells are so reliant on autophagy in the way described in this chapter presents an interesting and novel anticancer strategy that requires further exploration. The recent desire to employ fasting regimes in patients receiving anticancer treatment (Raffaghello et al., 2010, Safdie et al., 2009, Lee and Longo, 2011) has presented a need for continued investigation of the effects of acute nutrient deprivation in cancer cells.

5.1 Conclusions

It is clear that autophagy is an important mechanism for short term tolerance to nutrient deprivation in MCF12A and MDAMB231 cells. However, probably due to an already high basal level of autophagy activity, MDAMB231 cells are unable to sustain this protection for more than a few hours. On the other hand, MCF12A cells remain protected by increasing autophagy levels. Despite indications that MCF7 cells do respond to amino acid starvation by increasing autophagy activity, there is no indication that this is protective in these cells. Autophagy is typically assessed after only at least 24 hours in many studies. If this had been the case in this study then conclusions would have differed and it would have been inferred that autophagy is protective in MCF12A cells, but that high autophagy flux levels of MDAMB231 cells are unable to save these cells from negative impact of nutrient deprivation. This indicates the importance of dynamic assessment of autophagy, something clearly lacking in most published findings.

107

This study provides important and original insights into how a breast cancer cell line with high basal autophagy is able to respond to an acute bout of nutrient deprivation. However, no mechanistic support is provided for how autophagy is accomplishing this protective feat. It is often assumed that by generating substrates from the degradation of cytoplasmic material, autophagy is able to buffer any losses owing to the unavailability of (or inaccessibility to) nutrients. However, support for this idea has only rarely been offered. Our model provides an opportunity to assess this hypothesis. As only amino acids have been eliminated from the cell medium (and thereby forcing limited cellular access) in our model, assessment of the amino acid content and the consequences to energy production during amino acid starvation would provide great insight into the mechanism whereby autophagy is able to aid in survival during a starvation event.

6   References

AITA, V. M., LIANG, X. H., MURTY, V. V., PINCUS, D. L., YU, W., CAYANIS, E., KALACHIKOV, S., GILLIAM, T. C. & LEVINE, B. 1999. Cloning and genomic organization of beclin 1, a candidate tumor suppressor gene on chromosome 17q21. *Genomics,* 59**,** 59-65.

ARICO, S., PETIOT, A., BAUVY, C., DUBBELHUIS, P. F., MEIJER, A. J., CODOGNO, P. & OGIER-DENIS, E. 2001. The tumor suppressor PTEN positively regulates macroautophagy by inhibiting the phosphatidylinositol 3-kinase/protein kinase B pathway. *J Biol Chem,* 276**,** 35243-6.

AXE, E. L., WALKER, S. A., MANIFAVA, M., CHANDRA, P., RODERICK, H. L., HABERMANN, A., GRIFFITHS, G. & KTISTAKIS, N. T. 2008. Autophagosome formation from membrane compartments enriched in phosphatidylinositol 3-phosphate and dynamically connected to the endoplasmic reticulum. *J Cell Biol,* 182**,** 685-701.

BEUGNET, A., TEE, A. R., TAYLOR, P. M. & PROUD, C. G. 2003. Regulation of targets of mTOR (mammalian target of rapamycin) signalling by intracellular amino acid availability. *Biochem J,* 372**,** 555-66.

BLOMMAART, E. F., LUIKEN, J. J., BLOMMAART, P. J., VAN WOERKOM, G. M. & MEIJER, A. J. 1995. Phosphorylation of ribosomal protein S6 is inhibitory for autophagy in isolated rat hepatocytes. *J Biol Chem,* 270**,** 2320-6.

BLOMMAART, E. F., LUIKEN, J. J. & MEIJER, A. J. 1997. Autophagic proteolysis: control and specificity. *Histochem J,* 29**,** 365-85.

BOYA, P., GONZALEZ-POLO, R. A., CASARES, N., PERFETTINI, J. L., DESSEN, P., LAROCHETTE, N., METIVIER, D., MELEY, D., SOUQUERE, S., YOSHIMORI, T., PIERRON, G., CODOGNO, P. & KROEMER, G. 2005. Inhibition of macroautophagy triggers apoptosis. *Mol Cell Biol,* 25**,** 1025-40.

BRADFORD, M. M. 1976. A rapid and sensitive method for the quantitation of microgram quantities of protein utilizing the principle of protein-dye binding. *Anal Biochem,* 72**,** 248-54.

BRUGAROLAS, J., LEI, K., HURLEY, R. L., MANNING, B. D., REILING, J. H., HAFEN, E., WITTERS, L. A., ELLISEN, L. W. & KAELIN, W. G., JR. 2004. Regulation of mTOR function in response to hypoxia by REDD1 and the TSC1/TSC2 tumor suppressor complex. *Genes Dev,* 18**,** 2893-904.

CATALDO, A. M., HAMILTON, D. J., BARNETT, J. L., PASKEVICH, P. A. & NIXON, R. A. 1996. Properties of the endosomal-lysosomal system in the human central nervous system: disturbances mark most neurons in populations at risk to degenerate in Alzheimer's disease. *J Neurosci,* 16**,** 186-99.

DEGENHARDT, K., MATHEW, R., BEAUDOIN, B., BRAY, K., ANDERSON, D., CHEN, G., MUKHERJEE, C., SHI, Y., GELINAS, C., FAN, Y., NELSON, D. A., JIN, S. & WHITE, E. 2006. Autophagy promotes tumor cell survival and restricts necrosis, inflammation, and tumorigenesis. *Cancer Cell,* 10**,** 51-64.

DICE, J. F. 1988. Microinjected ribonuclease A as a probe for lysosomal pathways of intracellular protein degradation. *J Protein Chem,* 7**,** 115-27.

DIPAOLA, R. S., DVORZHINSKI, D., THALASILA, A., GARIKAPATY, V., DORAM, D., MAY, M., BRAY, K., MATHEW, R., BEAUDOIN, B., KARP, C., STEIN, M., FORAN, D. J. & WHITE, E. 2008. Therapeutic starvation and autophagy in prostate cancer: a new paradigm for targeting metabolism in cancer therapy. *Prostate,* 68**,** 1743-52.

DOUYON, L. & SCHTEINGART, D. E. 2002. Effect of obesity and starvation on thyroid hormone, growth hormone, and cortisol secretion. *Endocrinol Metab Clin North Am,* 31**,** 173-89.

EISENBERG-LERNER, A. & KIMCHI, A. 2009. The paradox of autophagy and its implication in cancer etiology and therapy. *Apoptosis,* 14**,** 376-91.

FENG, Z., ZHANG, H., LEVINE, A. J. & JIN, S. 2005. The coordinate regulation of the p53 and mTOR pathways in cells. *Proc Natl Acad Sci U S A,* 102**,** 8204-9.

FINN, P. F. & DICE, J. F. 2006. Proteolytic and lipolytic responses to starvation. *Nutrition,* 22**,** 830-44.

FUJITA, N., ITOH, T., OMORI, H., FUKUDA, M., NODA, T. & YOSHIMORI, T. 2008. The Atg16L complex specifies the site of LC3 lipidation for membrane biogenesis in autophagy. *Mol Biol Cell,* 19**,** 2092-100.

FURUYA, N., YU, J., BYFIELD, M., PATTINGRE, S. & LEVINE, B. 2005. The evolutionarily conserved domain of Beclin 1 is required for Vps34 binding, autophagy and tumor suppressor function. *Autophagy,* 1**,** 46-52.

GU, J., YAMAMOTO, H., OGAWA, M., NGAN, C. Y., DANNO, K., HEMMI, H., KYO, N., TAKEMASA, I., IKEDA, M., SEKIMOTO, M. & MONDEN, M. 2006. Hypoxia-induced up-regulation of angiopoietin-2 in colorectal cancer. *Oncol Rep,* 15**,** 779-83.

GUO, J. Y., CHEN, H. Y., MATHEW, R., FAN, J., STROHECKER, A. M., KARSLI-UZUNBAS, G., KAMPHORST, J. J., CHEN, G., LEMONS, J. M., KARANTZA, V., COLLER, H. A., DIPAOLA, R. S., GELINAS, C., RABINOWITZ, J. D. & WHITE, E. 2011. Activated Ras requires autophagy to maintain oxidative metabolism and tumorigenesis. *Genes Dev,* 25**,** 460-70.

HAY, N. & SONENBERG, N. 2004. Upstream and downstream of mTOR. *Genes Dev,* 18**,** 1926-45.

HAYASHI-NISHINO, M., FUJITA, N., NODA, T., YAMAGUCHI, A., YOSHIMORI, T. & YAMAMOTO, A. 2009. A subdomain of the endoplasmic reticulum forms a cradle for autophagosome formation. *Nat Cell Biol,* 11**,** 1433-7.

INBAL, B., BIALIK, S., SABANAY, I., SHANI, G. & KIMCHI, A. 2002. DAP kinase and DRP-1 mediate membrane blebbing and the formation of autophagic vesicles during programmed cell death. *J Cell Biol,* 157**,** 455-68.

INOKI, K., OUYANG, H., LI, Y. & GUAN, K. L. 2005. Signaling by target of rapamycin proteins in cell growth control. *Microbiol Mol Biol Rev,* 69**,** 79-100.

INOKI, K., ZHU, T. & GUAN, K. L. 2003. TSC2 mediates cellular energy response to control cell growth and survival. *Cell,* 115**,** 577-90.

IZUISHI, K., KATO, K., OGURA, T., KINOSHITA, T. & ESUMI, H. 2000. Remarkable tolerance of tumor cells to nutrient deprivation: possible new biochemical target for cancer therapy. *Cancer Res,* 60**,** 6201-7.

JIN, S. & WHITE, E. 2008. Tumor suppression by autophagy through the management of metabolic stress. *Autophagy,* 4**,** 563-6.

JOHNSTON, D. G., PERNET, A., MCCULLOCH, A., BLESA-MALPICA, G., BURRIN, J. M. & ALBERTI, K. G. 1982. Some hormonal influences on glucose and ketone body metabolism in normal human subjects. *Ciba Found Symp,* 87**,** 168-91.

KABEYA, Y., KAMADA, Y., BABA, M., TAKIKAWA, H., SASAKI, M. & OHSUMI, Y. 2005. Atg17 functions in cooperation with Atg1 and Atg13 in yeast autophagy. *Mol Biol Cell,* 16**,** 2544-53.

KAMADA, Y., FUNAKOSHI, T., SHINTANI, T., NAGANO, K., OHSUMI, M. & OHSUMI, Y. 2000. Tor-mediated induction of autophagy via an Apg1 protein kinase complex. *J Cell Biol,* 150**,** 1507-13.

KARANTZA-WADSWORTH, V., PATEL, S., KRAVCHUK, O., CHEN, G., MATHEW, R., JIN, S. & WHITE, E. 2007. Autophagy mitigates metabolic stress and genome damage in mammary tumorigenesis. *Genes Dev,* 21**,** 1621-35.

110

KLIONSKY, D. J. 2007. Autophagy: from phenomenology to molecular understanding in less than a decade. *Nat Rev Mol Cell Biol,* 8**,** 931-7.

KLIONSKY, D. J., ELAZAR, Z., SEGLEN, P. O. & RUBINSZTEIN, D. C. 2008. Does bafilomycin A1 block the fusion of autophagosomes with lysosomes? *Autophagy,* 4**,** 849-950.

KLIONSKY, D. J., MEIJER, A. J. & CODOGNO, P. 2005. Autophagy and p70S6 kinase. *Autophagy,* 1**,** 59-60; discussion 60-1.

KUMA, A., HATANO, M., MATSUI, M., YAMAMOTO, A., NAKAYA, H., YOSHIMORI, T., OHSUMI, Y., TOKUHISA, T. & MIZUSHIMA, N. 2004. The role of autophagy during the early neonatal starvation period. *Nature,* 432**,** 1032-6.

LECKER, S. H., SOLOMON, V., MITCH, W. E. & GOLDBERG, A. L. 1999. Muscle protein breakdown and the critical role of the ubiquitin-proteasome pathway in normal and disease states. *J Nutr,* 129**,** 227S-237S.

LEE, C. & LONGO, V. D. 2011. Fasting vs dietary restriction in cellular protection and cancer treatment: from model organisms to patients. *Oncogene,* 30**,** 3305-16.

LEE, J. W., JEONG, E. G., SOUNG, Y. H., NAM, S. W., LEE, J. Y., YOO, N. J. & LEE, S. H. 2006. Decreased expression of tumour suppressor Bax-interacting factor-1 (Bif-1), a Bax activator, in gastric carcinomas. *Pathology,* 38**,** 312-5.

LIANG, C., FENG, P., KU, B., DOTAN, I., CANAANI, D., OH, B. H. & JUNG, J. U. 2006. Autophagic and tumour suppressor activity of a novel Beclin1-binding protein UVRAG. *Nat Cell Biol,* 8**,** 688-99.

LIANG, X. H., JACKSON, S., SEAMAN, M., BROWN, K., KEMPKES, B., HIBSHOOSH, H. & LEVINE, B. 1999. Induction of autophagy and inhibition of tumorigenesis by beclin 1. *Nature,* 402**,** 672-6.

LIANG, X. H., KLEEMAN, L. K., JIANG, H. H., GORDON, G., GOLDMAN, J. E., BERRY, G., HERMAN, B. & LEVINE, B. 1998. Protection against fatal Sindbis virus encephalitis by beclin, a novel Bcl-2-interacting protein. *J Virol,* 72**,** 8586-96.

LOCK, R., ROY, S., KENIFIC, C. M., SU, J. S., SALAS, E., RONEN, S. M. & DEBNATH, J. 2011. Autophagy facilitates glycolysis during Ras-mediated oncogenic transformation. *Mol Biol Cell,* 22**,** 165-78.

LOCKSHIN, R. A. & ZAKERI, Z. 2004. Apoptosis, autophagy, and more. *Int J Biochem Cell Biol,* 36**,** 2405-19.

LONG, X., ORTIZ-VEGA, S., LIN, Y. & AVRUCH, J. 2005. Rheb binding to mammalian target of rapamycin (mTOR) is regulated by amino acid sufficiency. *J Biol Chem,* 280**,** 23433-6.

LUM, J. J., BAUER, D. E., KONG, M., HARRIS, M. H., LI, C., LINDSTEN, T. & THOMPSON, C. B. 2005. Growth factor regulation of autophagy and cell survival in the absence of apoptosis. *Cell,* 120**,** 237-48.

MAMANE, Y., PETROULAKIS, E., RONG, L., YOSHIDA, K., LER, L. W. & SONENBERG, N. 2004. eIF4E--from translation to transformation. *Oncogene,* 23**,** 3172-9.

MATHEW, R., KARP, C. M., BEAUDOIN, B., VUONG, N., CHEN, G., CHEN, H. Y., BRAY, K., REDDY, A., BHANOT, G., GELINAS, C., DIPAOLA, R. S., KARANTZA-WADSWORTH, V. & WHITE, E. 2009. Autophagy suppresses tumorigenesis through elimination of p62. *Cell,* 137**,** 1062-75.

MATSUNAGA, K., SAITOH, T., TABATA, K., OMORI, H., SATOH, T., KUROTORI, N., MAEJIMA, I., SHIRAHAMA-NODA, K., ICHIMURA, T., ISOBE, T., AKIRA, S., NODA, T. & YOSHIMORI, T. 2009. Two Beclin 1-binding proteins, Atg14L and Rubicon, reciprocally regulate autophagy at different stages. *Nat Cell Biol,* 11**,** 385-96.

MEIJER, A. J. & CODOGNO, P. 2004. Regulation and role of autophagy in mammalian cells. *Int J Biochem Cell Biol,* 36**,** 2445-62.

MEYUHAS, O. 2000. Synthesis of the translational apparatus is regulated at the translational level. *Eur J Biochem,* 267**,** 6321-30.

MIRACCO, C., COSCI, E., OLIVERI, G., LUZI, P., PACENTI, L., MONCIATTI, I., MANNUCCI, S., DE NISI, M. C., TOSCANO, M., MALAGNINO, V., FALZARANO, S. M., PIRTOLI, L. & TOSI, P. 2007. Protein and mRNA expression of autophagy gene Beclin 1 in human brain tumours. *Int J Oncol,* 30**,** 429-36.

MITCH, W. E. & GOLDBERG, A. L. 1996. Mechanisms of muscle wasting. The role of the ubiquitin-proteasome pathway. *N Engl J Med,* 335**,** 1897-905.

MIZRACHY-SCHWARTZ, S., COHEN, N., KLEIN, S., KRAVCHENKO-BALASHA, N. & LEVITZKI, A. 2010. Amino acid starvation sensitizes cancer cells to proteasome inhibition. *IUBMB Life,* 62**,** 757-63.

MIZUSHIMA, N. 2007. Autophagy: process and function. *Genes Dev,* 21**,** 2861-73.

MIZUSHIMA, N. & LEVINE, B. 2010. Autophagy in mammalian development and differentiation. *Nat Cell Biol,* 12**,** 823-30.

MIZUSHIMA, N., YAMAMOTO, A., MATSUI, M., YOSHIMORI, T. & OHSUMI, Y. 2004. In vivo analysis of autophagy in response to nutrient starvation using transgenic mice expressing a fluorescent autophagosome marker. *Mol Biol Cell,* 15**,** 1101-11.

MIZUSHIMA, N., YOSHIMORI, T. & LEVINE, B. 2010. Methods in mammalian autophagy research. *Cell,* 140**,** 313-26.

MORTIMORE, G. E. & POSO, A. R. 1987. Intracellular protein catabolism and its control during nutrient deprivation and supply. *Annu Rev Nutr,* 7**,** 539-64.

MORTIMORE, G. E. & SCHWORER, C. M. 1977. Induction of autophagy by amino-acid deprivation in perfused rat liver. *Nature,* 270**,** 174-6.

NAKATOGAWA, H., SUZUKI, K., KAMADA, Y. & OHSUMI, Y. 2009. Dynamics and diversity in autophagy mechanisms: lessons from yeast. *Nat Rev Mol Cell Biol,* 10**,** 458-67.

OGATA, H., SATO, H., TAKATSUKA, J. & DE LUCA, L. M. 2001. Human breast cancer MDA-MB-231 cells fail to express the neurofibromin protein, lack its type I mRNA isoform and show accumulation of P-MAPK and activated Ras. *Cancer Lett,* 172**,** 159-64.

ONODERA, J. & OHSUMI, Y. 2004. Ald6p is a preferred target for autophagy in yeast, Saccharomyces cerevisiae. *J Biol Chem,* 279**,** 16071-6.

PLAS, D. R. & THOMPSON, C. B. 2005. Akt-dependent transformation: there is more to growth than just surviving. *Oncogene,* 24**,** 7435-42.

QU, X., YU, J., BHAGAT, G., FURUYA, N., HIBSHOOSH, H., TROXEL, A., ROSEN, J., ESKELINEN, E. L., MIZUSHIMA, N., OHSUMI, Y., CATTORETTI, G. & LEVINE, B. 2003. Promotion of tumorigenesis by heterozygous disruption of the beclin 1 autophagy gene. *J Clin Invest,* 112**,** 1809-20.

RAFFAGHELLO, L., SAFDIE, F., BIANCHI, G., DORFF, T., FONTANA, L. & LONGO, V. D. 2010. Fasting and differential chemotherapy protection in patients. *Cell Cycle,* 9**,** 4474-6.

SADASIVAN, S., WAGHRAY, A., LARNER, S. F., DUNN, W. A., JR., HAYES, R. L. & WANG, K. K. 2006. Amino acid starvation induced autophagic cell death in PC-12 cells: evidence for activation of caspase-3 but not calpain-1. *Apoptosis,* 11**,** 1573-82.

SAFDIE, F. M., DORFF, T., QUINN, D., FONTANA, L., WEI, M., LEE, C., COHEN, P. & LONGO, V. D. 2009. Fasting and cancer treatment in humans: A case series report. *Aging (Albany NY),* 1**,** 988-1007.

SATO, K., TSUCHIHARA, K., FUJII, S., SUGIYAMA, M., GOYA, T., ATOMI, Y., UENO, T., OCHIAI, A. & ESUMI, H. 2007. Autophagy is activated in colorectal cancer cells and contributes to the tolerance to nutrient deprivation. *Cancer Res,* 67**,** 9677-84.

SCHERZ-SHOUVAL, R., WEIDBERG, H., GONEN, C., WILDER, S., ELAZAR, Z. & OREN, M. 2010. p53-dependent regulation of autophagy protein LC3 supports cancer cell survival under prolonged starvation. *Proc Natl Acad Sci U S A,* 107**,** 18511-6.

SHINTANI, T. & KLIONSKY, D. J. 2004. Autophagy in health and disease: a double-edged sword. *Science,* 306**,** 990-5.

STROMHAUG, P. E. & KLIONSKY, D. J. 2001. Approaching the molecular mechanism of autophagy. *Traffic,* 2**,** 524-31.

TAKAHASHI, Y., COPPOLA, D., MATSUSHITA, N., CUALING, H. D., SUN, M., SATO, Y., LIANG, C., JUNG, J. U., CHENG, J. Q., MULE, J. J., PLEDGER, W. J. & WANG, H. G. 2007. Bif-1 interacts with Beclin 1 through UVRAG and regulates autophagy and tumorigenesis. *Nat Cell Biol,* 9**,** 1142-51.

TAKAMURA, A., KOMATSU, M., HARA, T., SAKAMOTO, A., KISHI, C., WAGURI, S., EISHI, Y., HINO, O., TANAKA, K. & MIZUSHIMA, N. 2011. Autophagy-deficient mice develop multiple liver tumors. *Genes Dev,* 25**,** 795-800.

TASDEMIR, E., MAIURI, M. C., GALLUZZI, L., VITALE, I., DJAVAHERI-MERGNY, M., D'AMELIO, M., CRIOLLO, A., MORSELLI, E., ZHU, C., HARPER, F., NANNMARK, U., SAMARA, C., PINTON, P., VICENCIO, J. M., CARNUCCIO, R., MOLL, U. M., MADEO, F., PATERLINI-BRECHOT, P., RIZZUTO, R., SZABADKAI, G., PIERRON, G., BLOMGREN, K., TAVERNARAKIS, N., CODOGNO, P., CECCONI, F. & KROEMER, G. 2008. Regulation of autophagy by cytoplasmic p53. *Nat Cell Biol,* 10**,** 676-87.

TASSA, A., ROUX, M. P., ATTAIX, D. & BECHET, D. M. 2003. Class III phosphoinositide 3-kinase--Beclin1 complex mediates the amino acid-dependent regulation of autophagy in C2C12 myotubes. *Biochem J,* 376**,** 577-86.

TEE, A. R., FINGAR, D. C., MANNING, B. D., KWIATKOWSKI, D. J., CANTLEY, L. C. & BLENIS, J. 2002. Tuberous sclerosis complex-1 and -2 gene products function together to inhibit mammalian target of rapamycin (mTOR)-mediated downstream signaling. *Proc Natl Acad Sci U S A,* 99**,** 13571-6.

TISCHLER, M. E., DESAUTELS, M. & GOLDBERG, A. L. 1982. Does leucine, leucyl-tRNA, or some metabolite of leucine regulate protein synthesis and degradation in skeletal and cardiac muscle? *J Biol Chem,* 257**,** 1613-21.

TISDALE, M. J. 2005. The ubiquitin-proteasome pathway as a therapeutic target for muscle wasting. *J Support Oncol,* 3**,** 209-17.

TREDAN, O., GALMARINI, C. M., PATEL, K. & TANNOCK, I. F. 2007. Drug resistance and the solid tumor microenvironment. *J Natl Cancer Inst,* 99**,** 1441-54.

TSUJIMOTO, Y. & SHIMIZU, S. 2005. Another way to die: autophagic programmed cell death. *Cell Death Differ,* 12 Suppl 2**,** 1528-34.

VON LINTIG, F. C., DREILINGER, A. D., VARKI, N. M., WALLACE, A. M., CASTEEL, D. E. & BOSS, G. R. 2000. Ras activation in human breast cancer. *Breast Cancer Res Treat,* 62**,** 51-62.

WANG, J., WHITEMAN, M. W., LIAN, H., WANG, G., SINGH, A., HUANG, D. & DENMARK, T. 2009. A non-canonical MEK/ERK signaling pathway regulates autophagy via regulating Beclin 1. *J Biol Chem,* 284**,** 21412-24.

WEBBER, J. L. & TOOZE, S. A. 2010. New insights into the function of Atg9. *FEBS Lett,* 584**,** 1319-26.

WEIDBERG, H., SHVETS, E., SHPILKA, T., SHIMRON, F., SHINDER, V. & ELAZAR, Z. 2010. LC3 and GATE-16/GABARAP subfamilies are both essential yet act differently in autophagosome biogenesis. *EMBO J,* 29**,** 1792-802.

WHITE, E. & DIPAOLA, R. S. 2009. The double-edged sword of autophagy modulation in cancer. *Clin Cancer Res,* 15**,** 5308-16.

WULLSCHLEGER, S., LOEWITH, R. & HALL, M. N. 2006. TOR signaling in growth and metabolism. *Cell,* 124**,** 471-84.

113

YAMAMOTO, A., TAGAWA, Y., YOSHIMORI, T., MORIYAMA, Y., MASAKI, R. & TASHIRO, Y. 1998. Bafilomycin A1 prevents maturation of autophagic vacuoles by inhibiting fusion between autophagosomes and lysosomes in rat hepatoma cell line, H-4-II-E cells. *Cell Struct Funct,* 23**,** 33-42.

YANG, S., WANG, X., CONTINO, G., LIESA, M., SAHIN, E., YING, H., BAUSE, A., LI, Y., STOMMEL, J. M., DELL'ANTONIO, G., MAUTNER, J., TONON, G., HAIGIS, M., SHIRIHAI, O. S., DOGLIONI, C., BARDEESY, N. & KIMMELMAN, A. C. 2011. Pancreatic cancers require autophagy for tumor growth. *Genes Dev,* 25**,** 717-29.

YLA-ANTTILA, P., VIHINEN, H., JOKITALO, E. & ESKELINEN, E. L. 2009. 3D tomography reveals connections between the phagophore and endoplasmic reticulum. *Autophagy,* 5**,** 1180-5.

YOSHIMORI, T., YAMAMOTO, A., MORIYAMA, Y., FUTAI, M. & TASHIRO, Y. 1991. Bafilomycin A1, a specific inhibitor of vacuolar-type H(+)-ATPase, inhibits acidification and protein degradation in lysosomes of cultured cells. *J Biol Chem,* 266**,** 17707-12.

YU, L., STRANDBERG, L. & LENARDO, M. J. 2008. The selectivity of autophagy and its role in cell death and survival. *Autophagy,* 4**,** 567-73.

YUE, Z., JIN, S., YANG, C., LEVINE, A. J. & HEINTZ, N. 2003. Beclin 1, an autophagy gene essential for early embryonic development, is a haploinsufficient tumor suppressor. *Proc Natl Acad Sci U S A,* 100**,** 15077-82.

3 ━━━━━━━━━━━━━━━━━━━━━━━━

Autophagy is essential for the maintenance of amino acids and ATP levels during acute amino acid starvation in MDAMB231 and MCF12A cells

Tumour cells are able to survive in a harsh microenvironment that is associated with aberrant nutrient supply. Autophagy has been frequently implicated as a potential survival mechanism in these tumours, based on the premise that the degradation products released following autophagy-mediated breakdown of cytoplasmic material can be utilized for protein synthesis or as substrates for ATP production. Unfortunately, there is little direct evidence to support this hypothesis in cancer cells. This chapter presents evidence that the autophagy inhibitor bafilomycin A1 reduces amino acid content and ATP levels during short term amino acid starvation, and implicates autophagy related processes in the generation of amino acids and fatty acids during short term starvation of a tumourogenic cancer cell line with high basal autophagy.

1 Introduction

All cells within the body require constant access to nutrients and a means for the steady removal of waste. These two requirements are assured due to the close cellular proximity of an intricate network of blood vessels and capillaries. Solid tumours are heterogeneous and structurally complex, and in contrast to non-tumour tissues the neoplastic stroma is associated with an altered extracellular matrix and an increased number of fibroblasts that produce growth factors, adhesion molecules and chemokines necessary for tumour development and progression (Aznavoorian et al., 1990). As a solid tumour grows, some of the cells within the mass will inevitably become physically separated from the host tissue's native vascular stroma, and nutrient and oxygen delivery to those cells located farthest away become diffusion limited (Kerbel, 2000). Tumours must therefore rely on existing vasculature for the

115

supply of nutrients in order to survive or they must contrive to generate new blood vessels to facilitate their continued growth. The concept that a growing mass of tumour cells must recruit its own blood supply for the preservation of oxygen and other nutrient levels, called angiogenesis, became accepted in the 1970s (Folkman, 1971). It has since been discovered that tumour cells send out signals that initiate the formation of new vessels in an adaptive process of neoangiogenesis, which is amplified within solid tumours.

1.2   Tumour angiogenesis

VEGF-A is expressed in most cells under basal conditions, but as a survival cytokine in cancer it attracts sprouting neovessels into hypoxic regions of the tumour mass throughout the life of the neoplasm (Forsythe et al., 1996). The expression of VEGF relies on the fact that fast growing, hypovascular tumours rapidly develop local regions of hypoxia. These low oxygen levels result in the stabilization and activation of the hypoxic inducible factor HIF-1 which is followed by its translocation to the nucleus where it can bind to the *vegf* promoter and lead to expression of VEGF-A (Pouyssegur et al., 2006). Angiopoietin-2 (Ang-2) is a receptor ligand that is limited to endothelial cells and allows vessel remodelling (Hegen et al., 2004), and its expression is also under hypoxic control in solid tumours (Gu et al., 2006). The co-expression of VEGF and Ang-2 destabilizes capillaries and allows them to move out of their dormant state. This then initiates sprouting angiogenesis from native vessels into the hypoxic regions of tumours (Pouyssegur et al., 2006). In this way, hypoxia in solid tumour regions can directly lead to increased angiogenesis and improved access to blood.

Despite neoangiogenesis, fast growing tumours quickly develop microenvironments that are nutrient limited. Tumours that outstrip the capacity for neovascularisation consequently become hypoxic and develop characteristic nutrient starved areas. Furthermore, new tumour

vessels show structural malformations that produce transient episodes of chaotic blood flow and local regions of ischemia (Tredan et al., 2007). The rapid development of new vasculature can leave these vessels unable to sufficiently and continuously provide needed nutrients. Also, the high demand of such metabolically active cells such as those within tumours could surpass the supply capacity of these new vessels. Hence, tumour cells must necessarily possess or attain some other method of survival during these times of nutrient depression. Indeed, cultured cancer cells display increased levels of survival during short (48 hours) periods of nutrient starvation compared to non-cancer control cells of similar origin (Izuishi et al., 2000). In order to understand or exploit this capability for survival, researchers must appreciate how these cells are able to utilize various substrates during energy metabolism.
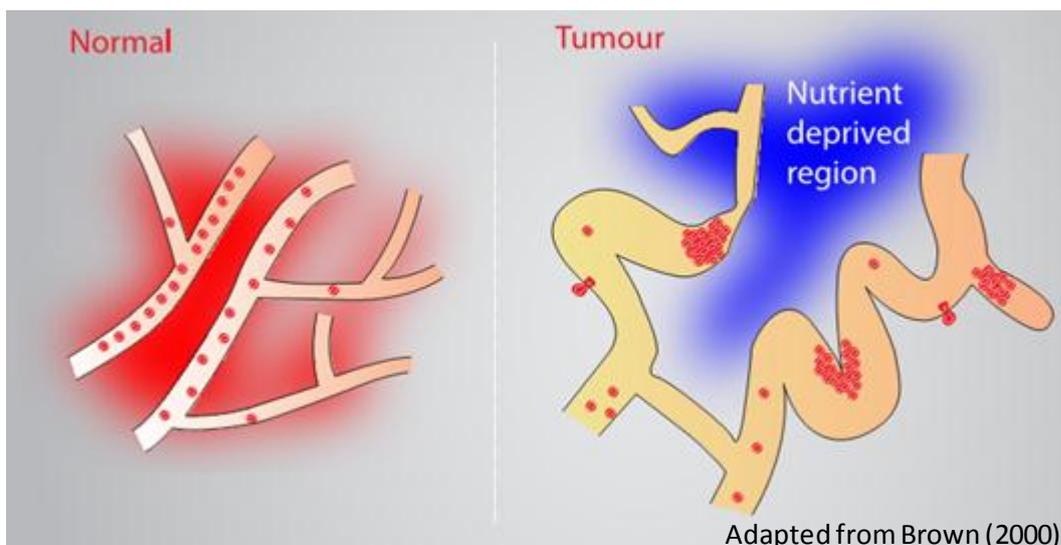
Image 3.1 Blood vessels in normal tissue are well formed and are sufficiently close together to ensure that all cells in the surrounding area are within the diffusion distance of valuable nutrients. On the other hand, tumour vasculature is abnormal and chaotic and is characterized by regions displaying transient episodes of nutrient deprivation. Tumour vessels have blind eyes, ateriovenous shunts, wall breaks and occlusions. This image is adapted from Brown (2000).

117

1.3   Tumour metabolism

As glucose has a greater diffusion limit than that of oxygen, and many tumour cells reside in hypoxic microenvironments (Vaupel et al., 1989), some cancer cells must use non-oxidative metabolic pathways to convert sugars into energy. Glycolysis is normally inhibited in the presence of oxygen, allowing mitochondria to continue with pyruvate oxidation. This so-called Pasteur effect ensures that the more efficient oxidative phosphorylation is utilized, generating eighteen times more ATP per mole of glucose in the process (Racker, 1974). However, Otto Warburg was the first to argue that the tumour cells (subjected to his analysis) used aerobic glycolysis with reduced mitochondrial oxidative phosphorylation for glucose metabolism (Warburg, 1956). He then went on to postulate (incorrectly) that cancer was a consequence of defects in oxidative phosphorylation in mitochondria that forced cancer cells to revert to glycolysis as the predominant form of energy generation. We now know that cancer is a result of key genetic mutations or defects occurring in proto-oncogenes or tumour suppressors, but even though the Warburg hypothesis has proved to be incorrect, Warburg‟s observation that cancers display increased aerobic glycolysis had been repeatedly verified. In fact, this phenomenon is used clinically in the technique of Positron-emission tomography imaging with 18fluorodeoxyglucose (18F-FdG PET) where a fluorodeoxyglucose (FdG) tracer (a glucose analogue) becomes trapped and phosphorylated by hexokinases.   The resultant radiolabelling is used to facilitate in the location of tissues with high rates of glucose uptake, in order to identify possible cancers (Pauwels et al., 2000). Various genetic and biochemical origins of enhanced glycolytic flux in tumour cells have now been identified (Hsu and Sabatini, 2008), and is now appreciated to be a *bona fide* hallmark of cancer (Hanahan and Weinberg, 2011). However, it is now believed that oxidizable substrates do in fact contribute significantly to ATP generation in many cancer cell types, in spite of high glycolysis rates.

The assumption of negligible oxidative phosphorylation in cancers now seems to be a tenuous one, and the perception that cancer cells largely utilize aerobic glycolysis for fuel equivocal. For example, mass balance analysis has revealed that HeLa (Reitzer et al., 1979, Rodriguez-Enriquez et al., 2006) and MCF7 (Guppy et al., 2002) human tumour cell lines both utilize oxidative and non-oxidative metabolism for ATP generation, while in other breast and lung cancers oxidative phosphorylation can be the predominant mode of energy metabolism (Kallinowski et al., 1989). In fact, it seems that despite extremely high rates of glycolysis in fast growing tumours, the contribution of glucose to ATP generation is measured at only approximately 10% in some instances (Zu and Guppy, 2004). Current conjecture is that the distinct microenvironment produced by high levels of glycolysis might grant a survival advantage to cancer cells, while at the same time not necessarily being the chief source for the generation of energetic intermediates as previously assumed (Gillies et al., 2008, Semenza, 2008). These recent clarifications are important in the context of autophagy research as oxidative phosphorylation is the principal method by which lysosomal breakdown products can be converted to ATP.

1.4   Metabolic fate of autophagy degradation products

There is a well known incongruity between cell growth and the rate of proliferation in solid tumours. Data from *in vitro* studies and analysis of cell cycle parameters *in vivo* reveal that typical tumour cells possess the capacity for extremely rapid proliferation rates (Friberg and Mattson, 1997). However, the time it takes for tumours to double in size is relatively protracted, in the order of months or even years in some cases (Rew and Wilson, 2000). It is possible that the sacrificing of cell contents or even whole cells by means of autophagy in order to utilize the constituents for continued tumour growth and survival could be occurring. During starvation, the organism is able to sustain itself for rather long periods through contact

119

with many different tissues that are able to sacrifice large quantities of carbohydrates, fats and even proteins for energy (Finn and Dice, 2006). However, those cells subjected to ischemic conditions or those that have impaired nutrient availability (such as cancer cells) will have little or no contact with the systemic nutrient pool. Blood vessels and capillaries serve as conduits to supply valuable nutrients, but are diffusion limited to only a few micrometers. During these conditions of decreased nutrient supply cells must therefore rely solely on their own intracellular environment (and possibly that of their close neighbours) for energy substrates.

Experimental evidence suggests that tumour cells exist under hypoxic conditions at a distance of about $100 - 400$ μm from blood vessels, implying that hypoxic regions are commonly established in tumours of only approximately 0.5 mm in diameter (Brown, 2000). Interestingly, increased autophagy is prominent in poorly vascularised regions of tumours but not those regions that have adequate access to the host blood supply (Karantza-Wadsworth et al., 2007), a phenomenon strongly associated with oxygen levels. Autophagy as a response to nutrient deficiency could be essential for survival of some cancers in these cases (Degenhardt et al., 2006).

It seems widely accepted that, in times of need, mammalian cells survive starvation by utilizing the break-down products of autophagy degradation as energy sources and for synthesis of survival proteins, and that in this way autophagy acts as a provider that replenishes the cellular amino acid pool during stressful times (Kuma and Mizushima, 2010, Mizushima, 2007). However, little direct evidence exists to support these claims. On the other hand, maintenance of amino acid levels has been demonstrated to be autophagy-dependent during starvation (Kuma et al., 2004), and autophagy is also known to be induced in response

to decreases in ATP or amino acids and increased by hypoxia acting through mTOR, and AMPK.

1.4.1 Autophagy and gluconeogenesis

Global starvation will result in rapid depletion of carbohydrate provisions. It has been suggested that gluconeogenesis in the liver could be fuelled by lysosomal breakdown products, perhaps by utilizing the glucose-alanine cycle (Kuma and Mizushima, 2010). In the liver, selected amino acids are able to be converted into glucose or fatty acids by gluconeogenesis or ketogenesis respectively, but before amino acids can be used for this purpose they must have their amine group removed. The presence of increased lysosomal degradation products leads to activation of aminotransferases and the subsequent deamination of the amino acids. Following deamination, the resulting keto acids are thought to be used for energy through gluconeogenesis. Although there is little evidence to suggest this claim as yet, alanine liberated through autophagy could be converted into glucose in this way. Compelling recent data showing that blood glucose levels are lower during starvation when an autophagy inhibitor is present adds strength to this idea (Kanamori et al., 2009). In addition, starvation leads to the largest protein loss in the liver (Yin et al., 2008), and up to 40% of liver protein can be lost in rodent livers after 48 hours of starvation. This protein loss appears to be sourced mostly from cytosolic material, and cellular volume can decrease by as much as 25% after 24 hours of starvation as a result (Mortimore and Poso, 1987). Deletion of liver specific ATG7 in mice leads to increased serum alanine aminotransferase and aspartate aminotransferase (Komatsu et al., 2005), and glycogen degradation is facilitated by autophagy during starvation in the muscle and liver (Kotoulas et al., 2006). Together, these findings indicate that increased autophagy in this organ is important for amino acid balance and homeostasis.

121

1.4.2 Autophagy and the contribution of TCA cycle intermediates

Maintenance of the amino acid pool during extremely short term starvation is managed by the proteasome (Vabulas and Hartl, 2005), but during starvation that persists into a few hours, autophagy becomes the predominant amino acids supplier. Amino acids resulting from autophagosomal-lysosomal degradation are often cited as potential substrates for metabolism through the TCA cycle and eventual production of energy. Certainly, the catabolism of amino acids can be used to form gluconoegenic and ketogenic precursors (Owen et al., 2002). These can then be used in anaplerotic and cataplerotic pathways to be terminally oxidized in the mitochondria for use in the production of energetic intermediates. During aerobic respiration, energy is garnered following degradation of glucose, fatty acids and certain amino acids in the mitochondria in pathways associated with the TCA cycle. Here, oxidation of the acetyl group of acetyl coenzyme A to carbon dioxide is coupled to the reduction of electron transporting coenzymes. Electrons transferred from these coenzymes to oxygen through the electron transport chain yield energy in the form of ATP (Da Poian, 2010). Although amino acids are not considered a good fuel source, certain amino acids can be used to generate energy in this way.

In order to be used for this purpose, amino acids must be catabolised by having their nitrogen groups removed to form their ketogenic precursors. This is accomplished by one of two enzymatically catalyzed processes, namely deamination and transamination. In transamination, amino groups are transferred to α-ketoacids by aminotransferases, while in deamination the amino group is lost as ammonia (Da Poian, 2010). Proteolysis and amino acid catabolism result in ketogenic amino acids that can be used as intermediates at various points in the TCA cycle directly or following conversion to pyruvate or acetyl-CoA (Image 3.2).
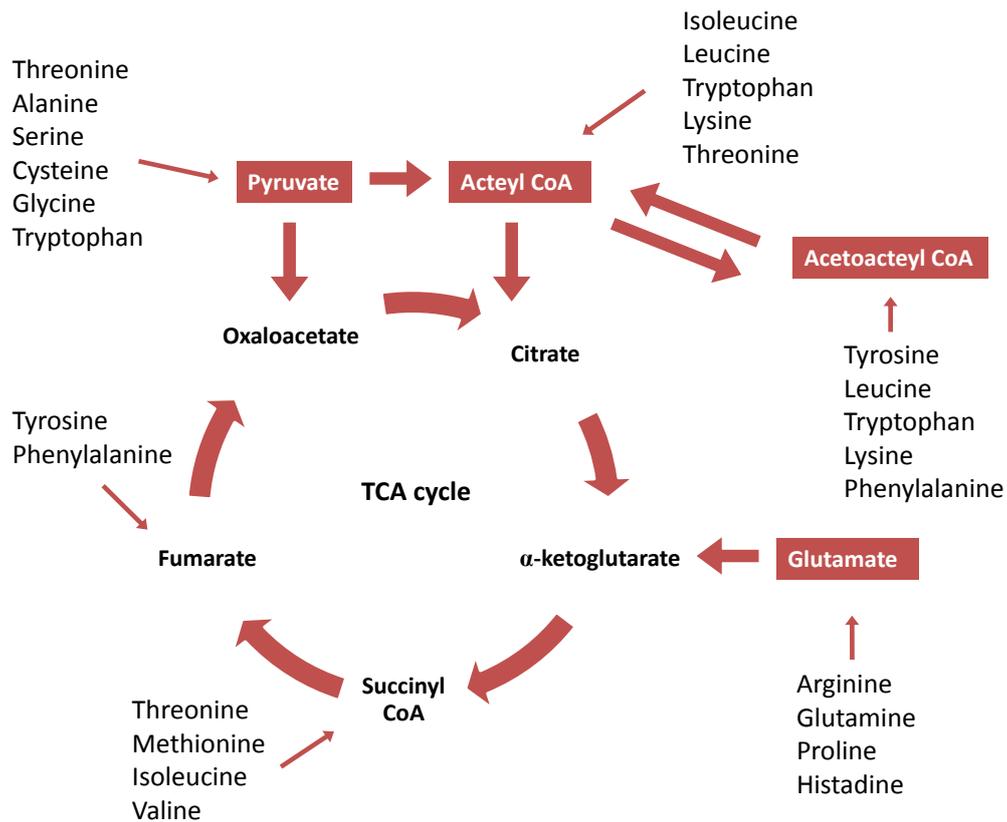
Image 3.2 Schematic showing the various points at which the carbon skeleton of the amino acids can be introduced into the citric acid (TCA).

The branched-chain amino acids in particular can be catabolised in tissues besides the liver, and, following deamination, their keto acids can enter the TCA cycle at various points to generate reducing equivalents and produce ATP through oxidative phosphorylation (Image 3.2). In fact, there is some evidence to support the hypothesis that substrates generated by autophagy help to maintain the ATP steady state. The fact that the activity of the aminotransferase enzyme branched-chain α-ketoacid dehydrogenase is up-regulated in starvation is also strong evidence that autophagy is contributing to the generation of ATP by increasing the cellular generation of branched chain amino acids to be used for fuel (Harris et al., 1989).

Although ATP levels are rarely measured in the context of autophagy some studies have provided evidence that ATP is generated intracellularly in an autophagy dependent manner. For instance, it was demonstrated that signs of low ATP levels in ES cells lacking autophagic ability could be reversed by methylpyruvate, a membrane-permeable derivative of pyruvate that serves as a substrate for the TCA cycle (Qu et al., 2007). It was also shown that supplementation with methylpyruvate could rescue an autophagy-deficient variant of an IL-3 dependent cell line from metabolic stress-induced cell death (Lum et al., 2005). Furthermore, starved mice present with increased autophagy and decreased myocardial ATP (Kanamori et al., 2009). Inclusion of the autophagy inhibitor bafilomycin A1 lead to a further decrease in ATP content as well as a decrease in amino acid content and cardiac function in these animals. Other inhibitors of autophagy have also been shown to reduce ATP content in glucose starved rat cardiomyoctes (Matsui et al., 2007), while the autophagy inducer rapamycin has been shown to attenuate this reduction (Maruyama et al., 2008). Additionally, shorter periods of glucose deprivation of cardiomyocytes show similar reductions in ATP in the presence of autophagy inhibition (Han et al., 2011). Despite a lack of data, it appears that cancer cells may also be able to generate ATP in a similar manner (Katayama et al., 2007, Cheng et al., 2010).

Indirect indications of the importance of autophagy breakdown products to energy maintenance can also be found upon assessment of signals controlling autophagy. Increased autophagy due to mTOR inhibition (Brugarolas et al., 2004) and increasing AMP/ATP ratios (Inoki et al., 2003) is observed during hypoxia. Sensing of intracellular ATP levels is accomplished through the activation of AMP-activated protein kinase (AMPK). Conditions of hypoxia, ischemia and exercise as well as other situations that decrease circulating amino acid or glucose levels lead to the activation of AMPK through escalating cellular AMP and phosphorylation of the catalytic subunit (Tokunaga et al., 2004). AMPK activation due to low

124

energy levels up-regulates catabolic processes and decreases unnecessary energy consuming processes (Hardie, 2007). AMPK activation owing to withdrawal of nutrients or decreases in oxygen levels is involved in the activation of autophagy (Liang et al., 2007). Therefore, AMPK promotion of autophagy occurs most likely in an effort to maintain cellular ATP levels.

An overlooked role of autophagy is in the regulation of lipid metabolism. Autophagy inhibition in the liver results in increased triglyceride storage in the form of lipid droplets (Komatsu et al., 2005), and it is believed that macrolipophagy may be responsible for autophagy mediated degradation of these lipid droplets (Singh et al., 2009). During starvation, this form of triglyceride storage is decreased upon autophagy inhibition (Shibata et al., 2009), and evidence now indicates that autophagy regulation during nutrient deprivation is associated with hydrolysis of triglycerides to generate free fatty acids for β-oxidation (Singh et al., 2009).

Collectively, the lysosomal mediated decomposition of organelle membranes, lipids and proteins, in response to metabolic stress in harsh tumour microenvironments, yields fatty acids and amino acids that could potentially be oxidized in the electron transport chain for ATP production (Image 3.3).

1.5   Autophagy and protein synthesis

Proteins recycled during autophagy are released from lysosomes as amino acids and are then available to immediately enter back into the ribosomal system to form new proteins. Although protein synthesis is energetically expensive, certain proteins are important during the stress response and must therefore be synthesised anyway. Synthesis of some proteins does

continue, but in cells with deficient autophagy machinery, protein synthesis is decreased further than in autophagy competent controls (Onodera and Ohsumi, 2005), while the synthesis of important starvation-induced proteins is also decreased in these autophagy mutants (Tsukada and Ohsumi, 1993). Additional compelling evidence that autophagy supports protein synthesis in post-fertilization development, was recently obtained from an oocyte-specific autophagy deficient mouse model (Tsukamoto et al., 2008).
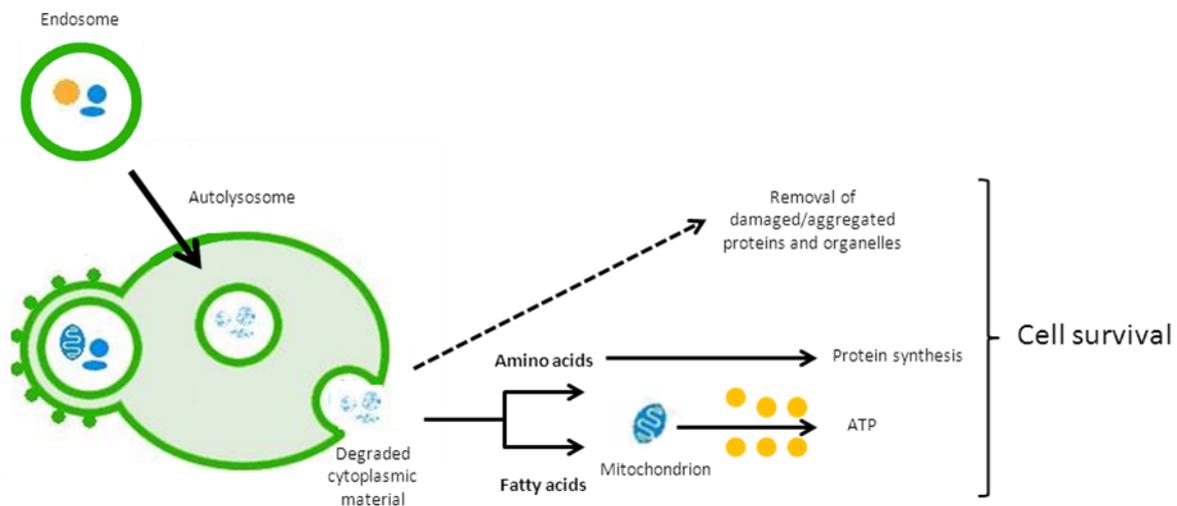
Image 3.3 Autophagy is believed to promote cell survival during stressful conditions through the generation of substrates for energy production, amino acids for synthesis of survival proteins or by removing damaged or aggregated proteins and organelles. Cytoplasmic material containing proteins and organelles is delivered to lysosomes by endosomes or autophagasomes where it is broken down by lysosomal enzymes.

1.6   Role of autophagy in cancer energy homeostasis

Prolonged cellular stress typically initiates programmed cell death, but cancer cells have been consistently shown to have defects in their apoptotic pathway intermediates that are thought to aid in tumour survival and metastasis (Nelson et al., 2004). In the absence of apoptosis, cells have the ability to divert to alternate cell death modes such as necrosis (Zong and

126

Thompson, 2006). However, autophagy induction has been repeatedly shown to have cytoprotective effects in cancer cells undergoing metabolic stress. In cells with defective apoptosis, activation of autophagy is implicated as a survival mechanism that also prevents the onset of necrotic cellular morphology (Karantza-Wadsworth et al., 2007, Mathew et al., 2007b), whereas cells defective in both autophagy and apoptosis inevitably undergo necrosis in response to surmounting metabolic stress conditions (Degenhardt et al., 2006). Also, if metabolic stress is eventually alleviated, and autophagy levels again depressed, normal cellular growth and activity is promptly restored (Mathew et al., 2007a). Therefore, in cells undergoing stress with no means of committing to controlled cell death (such as cancer cells) autophagy may be a mechanism for temporary asylum from their demise. Autophagy may also be partly responsible for a reversible state of dormancy following a metabolic stress in cancer cells (Lu et al., 2008).

How autophagy protects cancer cells from becoming necrotic is not precisely known. As inadequate energy reserves result in the loss of cellular membrane integrity and eventual cell permeability and death (Zong and Thompson, 2006), it seems likely that many cancers are able to produce substrates through increased autophagy in order to maintain ATP levels (Lum et al., 2005, Katayama et al., 2007, Degenhardt and White, 2006) and this could ameliorate metabolic stresses and delay cell death. In support of this idea, in a colorectal cancer cell line that displayed decreased ATP levels when incubated under hypoxia, compared to untreated normoxic cells, ATP levels were almost completely abolished if autophagy was inhibited (Frezza et al., 2011). This decrease in ATP corresponded with a similar decrease in cell viability following autophagy inhibition. More studies such as this are needed if the direct impact of autophagy on energy generation and cellular survival during metabolic stress is to be understood.

2   Hypothesis and experimental aims

2.1   Research problem

Throughout the literature autophagy is implicated as a survival mechanism whereby cancer cells are able to overcome metabolically stressful conditions and avoid cell death though its activation. It is presumed that autophagy mediated consumption of cellular material within cancer cells increases the availability of amino acids for use in protein synthesis and in ATP generation. Currently, data for direct measurements of amino acids in nutrient starved cancer cells are completely absent. Furthermore, direct assessment of ATP levels are almost never published, particularly in association with cancer studies. Therefore assessment of amino acid levels during short term starvation and correlation with ATP levels under these conditions is a vital next step if therapeutic interventions are to be designed on the basis that autophagy increases survival through generation of substrates for energy production.

2.2   Hypothesis

MDAMB231 cells are able to maintain amino acid levels during short term amino acid starvation through a mechanism that can be inhibited by bafilomycin A1 (10 nM).

2.3 Experimental aims

1. Assess the capacity of MDAMB231 cells and MCF12A cells to maintain amino acid levels during short term amino acid starvation by quantifying amino acid content during amino acid deprivation in the presence and absence of bafilomycin A1 (10 nM).
2. Assess ATP levels during similar conditions.

128

3. Analyse glucose consumption during amino acid starvation in order to assess whether glucose uptake is altered.

4. Assess the branched chain amino acid content within both cell lines during amino acid deprivation in the presence and absence of bafilomycin A1 (10 nM).

5. Use BCKDH siRNA in conjunction with ATG5 siRNA to assess the accumulation of branched chain amino acids during starvation.

6. Analyse the free fatty acid content of MDAMB231 cells during short term amino acid starvation.

3   Methods and materials

The materials and methods describing the cell culture procedures utilized in this study can be found in previous chapters. (+)-Etomoxir sodium salt hydrate (E1905; Sigma Chemical Co., St Louis, MO, USA) was prepared fresh in culture medium immediately prior to administration.

3.1   Study design
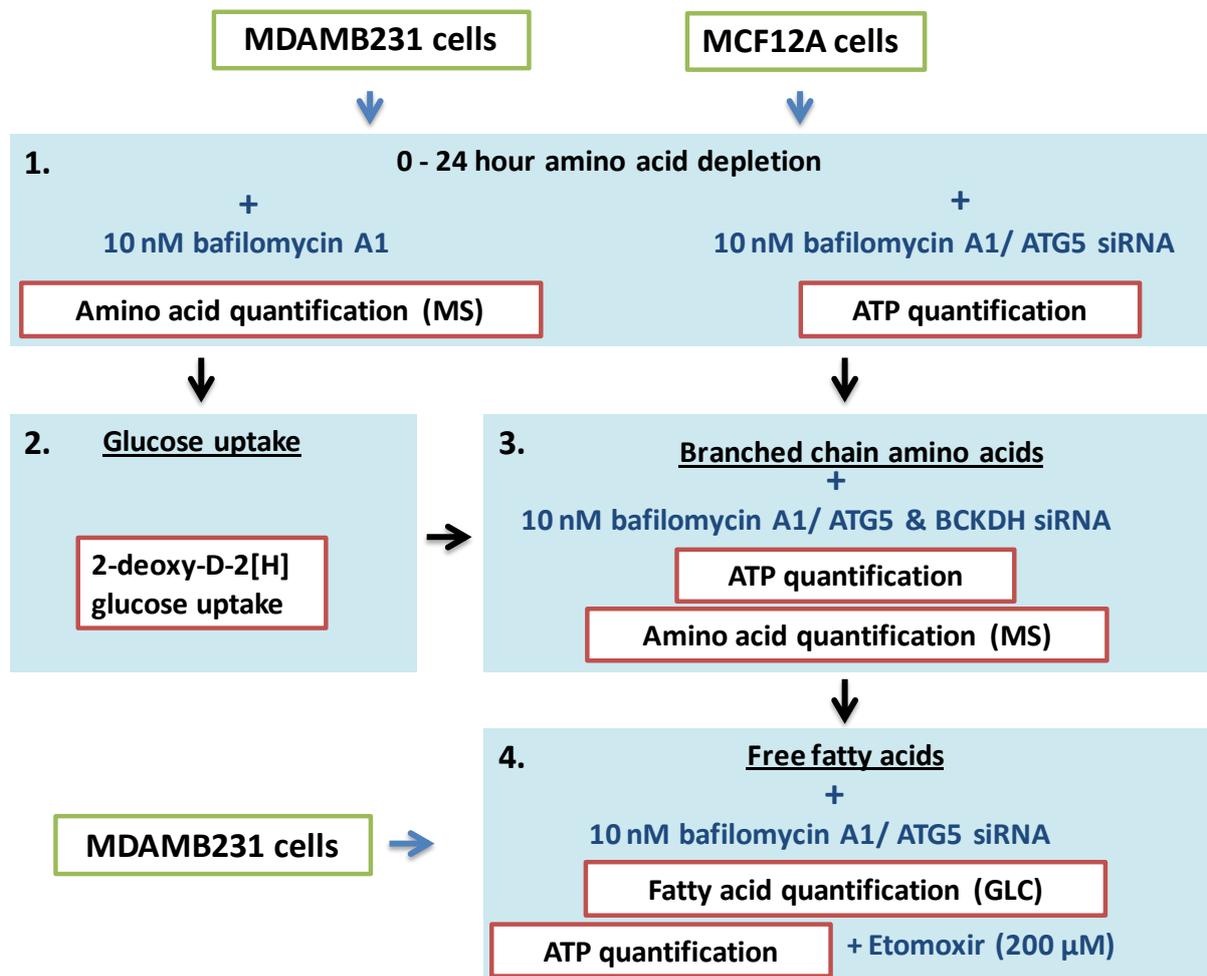
Image 3.4 Study design: MDAMB231 cells and MCF12A cells will be cultured in the absence of amino acids in the presence of the autophagy inhibitor bafilomycin A1 (10 nM) for a period of 24 hours and ATP and amino acid content analysed. **2.** Glucose uptake in MDAMB231 and MCF12A cell lines will be further examined during amino acid starvation. **3.** Branched chain amino acids will be analysed and ATP levels determined in the presence of the autophagy inhibitor bafilomycin A1 (10 nM) or ATG5 or BCKDH siRNA. **4.** Free fatty acid content will be analysed in MDAMB231 cells in the presence of the autophagy inhibitor bafilomycin A1 (10 nM) or β-oxidation inhibitor etomoxir (200 μM). Continuation to phase **4** is contingent on the results obtained in phase **1 and 3.** BCKDH = Branched chain keto acid dehydrogenase

3.2   Determination of 2-deoxy-D-2[H] glucose uptake

100 000 MCF12A cells or 80 000 MDAMB231 cells were plated into 60 mm culture dishes 48 hours prior to treatment. 2DG uptake was measured as previously described (Donthi et al., 2000). Cells were cultured to reach ~70% confluency prior to amino acid deprivation. Cells were then washed twice with an equilibrating solution which contained in mM: KCl 6, Na_2HPO_4 1, NaH_2PO_4 0.2, $MgSO_4$ 1.4, NaCl 128, HEPES 10, $CaCl_2$ 1.25 and 2% free fatty acid BSA. Cells were then deprived of all substrates present in the culture medium for 1 hour, by incubation at 37˚C in a humidified atmosphere in 2 ml of this solution. After 1 hour the cells were incubated with 1.5 µCi/ml 2DG (PerkinElmer, Boston, USA) in a final concentration of 1.8 µM deoxyglucose for 30 minutes. The solution containing the 2DG was then aspirated. Cells were washed twice with a basic buffer that contained in mM: KCl 6, 51 Na2HPO4 1, $MgSO_4$ 1.4, NaH_2PO_4 0.2, NaCl 128 and HEPES 10. Cells were lysed with 250 µl of 1 M NaOH overnight at room temperature. The following day the cell lysates were vortexed and diluted in 250 µl dH_2O to yield a concentration of 0.5 M NaOH. To determine the cell-associated radioactivity, 100 µl of the cell lysates was mixed with 3 ml scintillation fluid and left in the dark for 2 hours. All measurements were prepared in duplicate. A liquid scintillation counter (Beckman Coulter Inc., USA) was used for counting radioactivity. The remaining 200 µl of the cell lysates was used for determination of protein content with the use of the Lowry method (Lowry et al., 1951).

3.3   Amino acid analysis

Amino acid analysis was performed using the Waters AccQ Tag Ultra Derivatization Kit. 100 000 MCF12A cells or 80 000 MDAMB231 cells were plated into 60 mm culture dishes 48 hours prior to treatment. Cells were washed twice in room temperature PBS. Cells were then scraped in 500 µl of PBS and transferred to centrifugal filter units (Amicon Ultra; Millipore, MA, USA). Tubes were centrifuged for 15 min at 1400 rpm to obtain a filtrate. Samples were analysed at the Mass Spec lab (Department of Biochemistry, Stellenbosch) for amino acid quantification using the Waters API Quattro Micro. Mass Spec conditions were as follows: Capillary voltage: 3.5kV, Cone voltage: 1V, Source: 100 ºC, Desolvation Temp: 350 ºC, Desolvation gas: 350 L/h, Cone gas: 50 L/h. The analysis was carried out by MS analyst M. Adonis.

3.3.1 Sample preparation

10 µl of the undiluted sample was added to the Waters AccQ Tag Kit constituents and placed in a heating block at a temperature of 55°C, for ten minutes.

EZ:Faast derivatization and solid phase extraction

EZ:Faast consists of a solid phase extraction step followed by a derivatization step and a liquid-liquid extraction step to get rid of interfering compounds in the matrix. In the solid phase extraction step the samples are pulled through a sorbent tip that binds the amino acids while the remaining interfering compounds flow through. The amino acids are then extruded and derivatized, allowing them to migrate to the organic layer, which is removed, dried, re-dissolved and subject to LCMS analysis. In addition a stable daughter ion is formed that makes LCMSMS analysis possible.

Standards:

Labelled Homoarginine, Methionine-D3 and homophenylalanine were included as internal standards, part of the EZ:Faast kit. EZ:Faast LC method (with EZ:Faast column): The method was used as described in the EZ:Faast user's guide. Injection: 5 µl. Source: ESI +. Solvents A1 and A2: Eluent A2 (100 ml Eluent A concentrate and 900 ml Water). Solvents B1 and B2: Eluent B (Supplied by AccQ Tag Kit). Column: AccQ Tag C18, 1.7um, 2.1x100 mm.
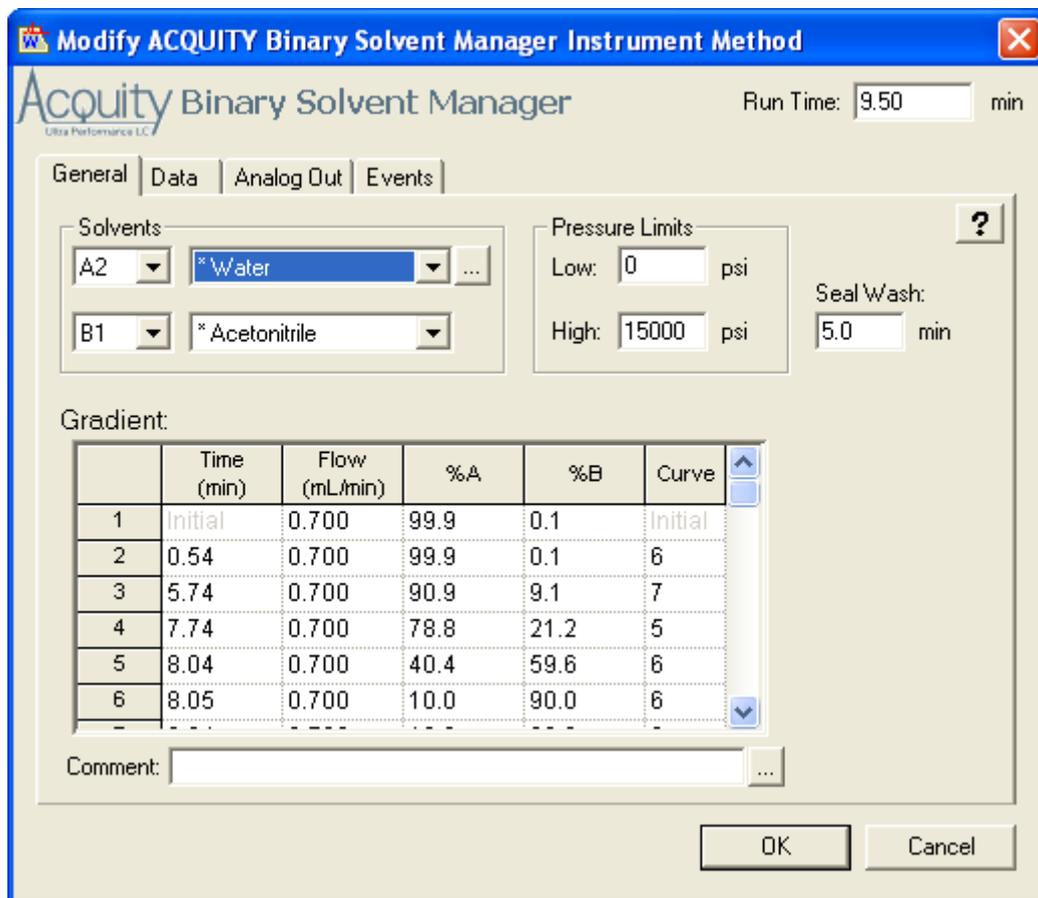
Image 3.5 Print Screen of amino acid analysis. Solvent A: 10 mM ammonium formate in water

3.4   ATP analysis

ATP levels were determined using the ATP Bioluminescence detection kit (ENLITEN®, Promega, Madison, WI, USA). 100 000 MCF12A cells or 80 000 MDAMB231 cells were plated into 60 mm culture dishes 48 hours prior to treatment. Cells were detached by incubation with 4 ml trypsin/EDTA (Sigma Chemical Co., St Louis, MO, USA) at 37°C, with occasional agitation, until cells loosened completely or for a maximum of four minutes. Cells were then centrifuged at 4°C and 1500 rpm and the pellet washed in sterile PBS. The resulting suspension was centrifuged at 4°C and 1500 rpm. The pellet was then resuspended in 50 µl ice-cold lysis buffer (100 mM Tris-HCl and 4 mM EDTA, pH 7.75), which was immediately followed by the addition of 150 µl of boiling lysis buffer (Essmann et al., 2003). Samples were then incubated for 2 minutes at 99°C. Lysates were centrifuged at 10 000 rpm at 4°C for 1 minute. Supernatants were collected for ATP detection and protein determination. 50 µl of supernatant and 50 µl luciferase reagent were used and chemiluminescence was immediately acquired in a luminometer (Glomax-96 luminometer; Promega, Madison, WI, USA).

3.5   Fatty acid analysis

Free fatty acid and total phospholipid fatty acids were separated and analysed using Gas Liquid Chromatography (GLC). Analysis was performed by J. Van Wyk at the MRC nutritional research unit for fatty acid analysis. 100 000 MCF12A cells or 80 000 MDAMB231 cells were plated into 60 mm culture dishes 48 hours prior to treatment. After treatment, cells were washed twice in room temperature saline (0.9 mM Sodium Chloride). Cells were then scraped in 500 µl of saline, sonicated for 10 seconds each in order to disrupt cell membranes, and sent for analysis.

3.5.1 Analysis protocol

Neutral lipids were separated from phospholipids by TLC on silica gel plates (10x 10 cm). Lipid bands were visualised with ultraviolet light after spraying plates with chloroform containing BBOT (2.5-bis (5''-tert,-butylbenzoxazolyl-[2'']thiophene; 10 mg/100 ml). Lipids were incubated in 5% H_2SO_4/methanol at 70°C for 2 hours to induce transmethyalation. After cooling fatty acid methyl esters (FAME) were extracted using with 1ml water and 2ml *n*-hexane. The top layer was evaporated and redissolved in CS_2 and analysed by GLC (Varian Model 3300 equipped with flame ionization detection) using 30 m fused silica megabore DB-225 columns of 0.53mm diameter (J & W Scientific, Folsom California, USA). Gas flow rates were: hydrogen 25 ml/minutes; air 250 ml/minutes and hydrogen (carrier gas) 5-8 ml/minutes. Temperature increases during analysis was 4 °C/minutes, initial temperature 160 °C, final temperature 220 °C, injector temperature 240 °C and detector temperature 250 °C. FAME were identified by retention time comparison to standard FAME mixture (Nu-Check-Prep Inc., Elysian, MI, USA).

3.6   BCKHD siRNA transfection and analysis

Cells were transfected using a reverse transcription protocol into 60 mm petri dishes. An extended protocol can be found in the materials and methods section of the previous chapter or in the appendix. 20 pmol of BCKDHB - branched chain keto acid dehydrogenase E1, beta polypeptide (HSS100949; Invitrogen™, USA) was used per petri dish. The following primers were selected and purchased through the Central Analytical Facility with the assistance of Dr Ruhan Slabbert.:

Branched chain keto acid dehydrogenase E1, beta polypeptide precursor; 2-oxoisovalerate dehydrogenase beta subunit; BCKDH E1-b. PrimerBank ID 34101272a3. Amplicon size 179.

Primer sequence (5'→3'). Forward primer (GCAGGTGGCTCATTTTACTTTCC), reverse (CAACAGTGCATCTAAAGACTCCA). Heat-shock 90kD protein-1, beta [Homo sapiens]. PrimerBank ID 2014949594a1. Amplicon size 247. Primer sequence (5' → 3'). Forward primer (TGGTGTGGTTGACTCTGAGGA), reverse primer (GGAGGTATGATAGCGCAGCA). NADH dehydrogenase (ubiquinone) 1 alpha subcomplex. PrimerBank ID 4758770a1. Amplicon size 102. Primer sequence (5' → 3'). Forward primer (GGACTGGCTACTGCGTACATC), reverse primer (GCGCCTATCTCTTTCCATCAGA). β-cytoskeletal actin [Homo sapiens]. PrimerBank ID 4501885a1. Amplicon size 250. Primer sequence (5' → 3'). Forward primer (CATGTACGTTGCTATCCAGGC), reverse primer (CTCCTTAATGTCACGCACGAT). Stealth RNAi (Invitrogen™, STEALTH RNAI NEG CTL MED GC, 12935300) was used as a negative control, as suggested by the manufacturer.

3.7   Statistical analysis

All values are presented as the mean ± standard error of the mean (SEM). Differences between time points and treatment groups were analysed using one or two factorial analysis of variance (ANOVA). Significant changes were further assessed by means of the Bonferroni *post hoc* analysis where appropriate. All statistical analyses were performed using Graphpad Prism version 5.01 (Graphpad Software, Inc, CA, USA). The minimum level of significance accepted was $p < 0.05$.

4   Results

4.1   Evidence of a transient and robust generation of amino acids at 6 hours of amino acid deprivation in MDAMB231 cells and MCF12A cells

A.

B.
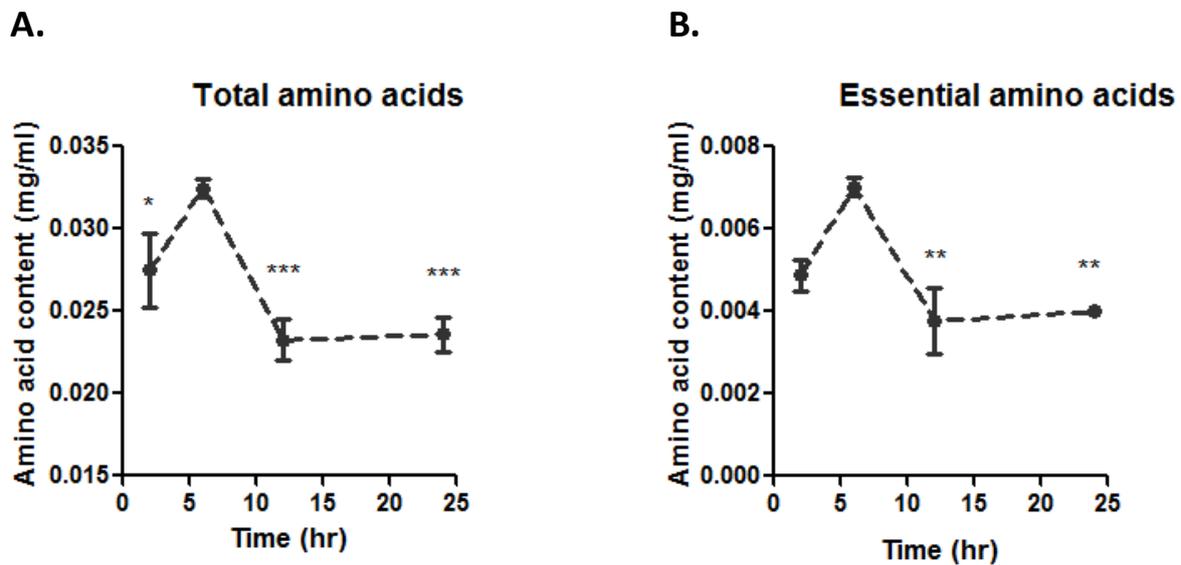
Fig. 3.1 Change in cellular amino acid concentrations in MDAMB231 cells during a 24 hour period of amino acid starvation. Amino acid concentrations were measured at 2, 6, 12 and 24 hours of complete amino acid deprivation from culture medium. An increase in the level of both total and essential amino acids is observed at 6 hours of starvation. A. 'Total amino acids' indicates the sum of the Asp, Thr, Ser, Asn, Glu, Gln, Pro, Gly, Ala, Val, Cys, Met, Ile, Leu, Tyr, Phe, Lys, His and Arg concentrations. B. 'Essential amino acids' indicates the sum of Thr, Val, Met, Ile, Leu, Phe, Lys, His and Arg concentrations. hr = hours. Each value is the mean ± SEM of at least three independent determinations. *, $P < 0.05$; **, $P < 0.01$; ***, $P < 0.001$ vs. 6 hours.

The total amino acid content (Asp, Thr, Ser, Asn, Glu, Gln, Pro, Gly, Ala, Val, Cys, Met, Ile, Leu, Tyr, Phe, Lys, His and Arg) of MDAMB231 cells was determined after incubating these cells in culture medium free of any amino acids. A significant increase in the total amino acid content of these cells was observed between 2 and 6 hours of amino acid starvation (Fig 3.1). Thereafter amino acid levels decreased to a low level that was sustained at 24 hours of amino acid starvation. The content of „essential amino acids‟ (Thr, Val, Met, Ile, Leu, Phe, Lys, His and Arg) displayed a similar pattern over time (Fig 3.1).
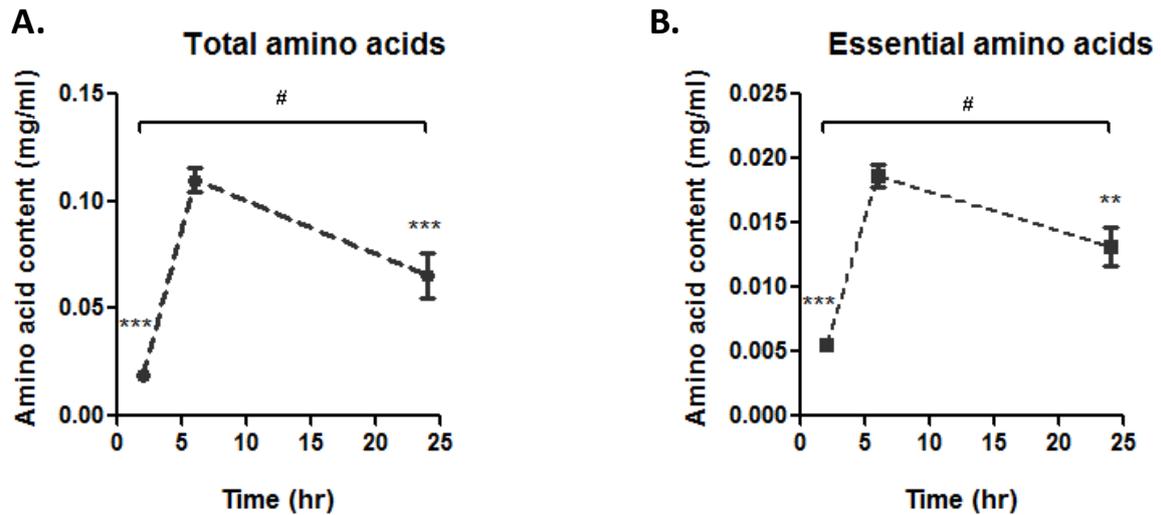
Fig. 3.2 Cellular amino acid concentrations in MCF12A cells during a 24 hour period of amino acid starvation. Amino acid concentrations were measured at 2, 6 and 24 hours of complete amino acid deprivation from culture medium. An increase in the level of both total and essential amino acids is observed at 6 hours of starvation. A. 'Total amino acids' indicates the sum of the Asp, Thr, Ser, Asn, Glu, Gln, Pro, Gly, Ala, Val, Cys, Met, Ile, Leu, Tyr, Phe, Lys, His and Arg concentrations. B. 'Essential amino acids' indicates the sum of Thr, Val, Met, Ile, Leu, Phe, Lys, His and Arg concentrations. hr = hours. Each value is the mean ± SEM of at least three independent determinations. **, $P < 0.01$; ***, $P < 0.001$ vs. 6 hours. #, $P < 0.001$ 2 hours vs. 24 hours.

The total amino acid content of MCF12A cells also increased significantly between 2 and 6 hours of amino acid starvation (Fig 3.2). Although total amino acid levels were observed to have decreased significantly by 24 hours of starvation, the total amino acid content of MCF12A cells remained significantly higher than those at 2 hours of amino acid starvation. The content of cellular essential amino acids displayed a similar pattern to that of total amino acids over time (Fig 3.2).

138

4.2 Amino acid starvation causes a decrease in the ATP content of MDAMB231 but not MCF12A cells
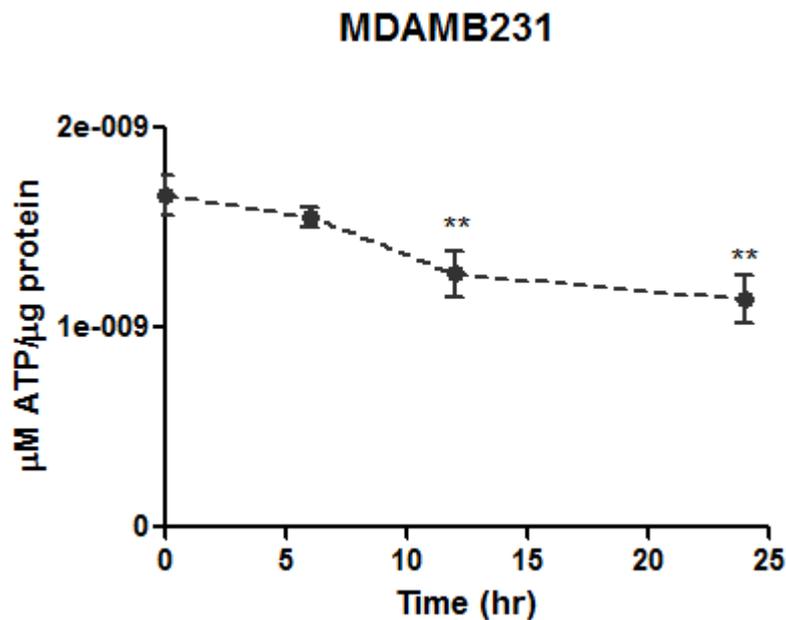
Fig. 3.3 ATP content in MDAMB231 cells following complete amino acid depletion. ATP levels are observed to be significantly lower by twelve hours of amino acid deprivation. ATP levels were measured at 0, 6, 12 and 24 hours of incubation in total amino acid deprived culture medium. hr = hours. Each value is the mean ± SEM of at least three independent determinations. **, $P < 0.01$ vs. 0 hr.

The ATP content of MDAMB231 cells was measured following 0, 6, 12 and 24 hours of incubation in amino acid deprived culture medium that was completely free of amino acids (Fig 3.3). ATP levels did not change during the first 6 hours of starvation but were observed to have decreased significantly by 12 hours of amino acid deprivation. ATP levels remained low at 24 hours of starvation as well.

139
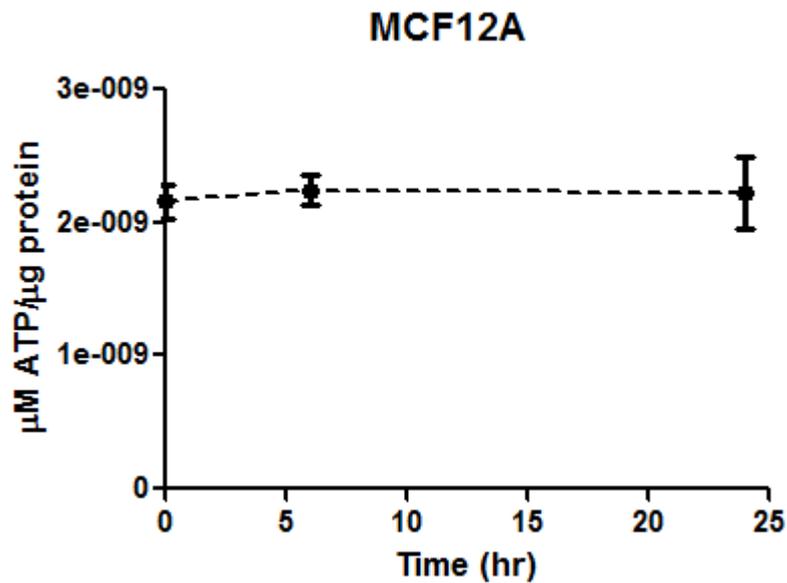
MCF12A

Fig. 3.4 ATP content in MCF12A cells following complete amino acid depletion. No changes in ATP levels are observed during amino acid deprivation. ATP levels were measured at 0, 6, and 24 hours of incubation in total amino acid deprived culture medium. hr = hours. Each value is the mean ± SEM of at least three independent determinations.

The ATP content of MCF12A cells was measured following 0, 6, and 24 hours of incubation in amino acid deprived culture medium (Fig 3.4). ATP levels did not change during the observed period of amino acid deprivation (Fig 3.4).

4.3   Maintenance of amino acid levels at 6 hours of amino acid depletion is prevented by bafilomycin A1 (10 nM)
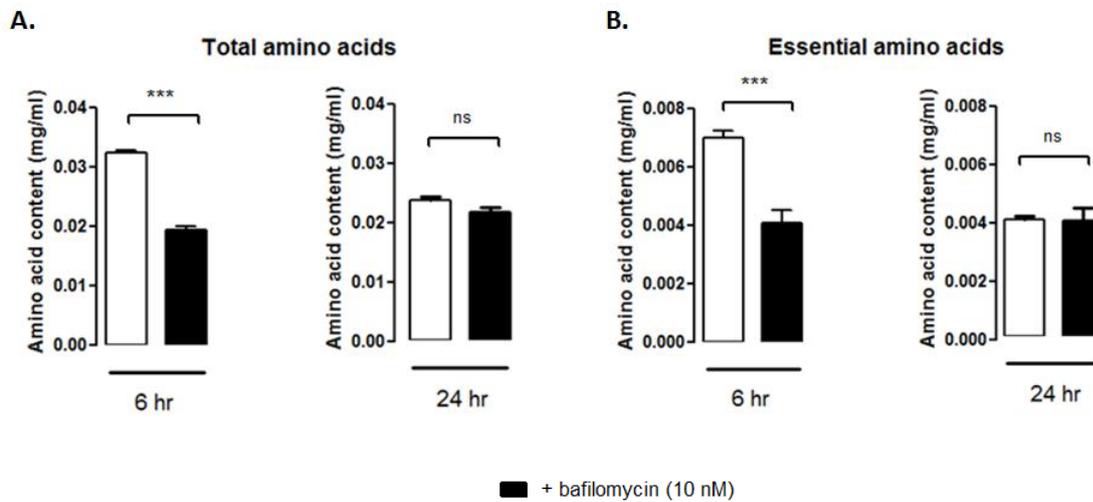
Fig. 3.5 Bafilomycin (10 nM) significantly lowers amino acid content in MDAMB231 cells after 6 but not 24 hours of amino acid starvation. Amino acid concentrations were measured at 6 and 24 hours of complete amino acid deprivation from culture medium. A. 'Total amino acids' indicates the sum of the Asp, Thr, Ser, Asn, Glu, Gln, Pro, Gly, Ala, Val, Cys, Met, Ile, Leu, Tyr, Phe, Lys, His and Arg concentrations. B. 'Essential amino acids' indicates the sum of Thr, Val, Met, Ile, Leu, Phe, Lys, His and Arg concentrations. Bafilomycin A1 (10 nM) was added to culture medium 6 hours prior to analysis. hr = hours. Each value is the mean ± SEM of at least three independent determinations. ***, $P < 0.001$. ns = no significance.

Bafilomycin A1 inhibits fusion of autophagosomes with lysosomes, effectively blocking autophagy, and this should theoretically prevent the degradation of proteins engulfed through this process. Bafilomycin A1 (10 nM) was added to culture medium 6 hours prior to analysis and resulted in significantly lower total amino acid content in MDAMB231 cells after 6 but not 24 hours of amino acid starvation (Fig 3.5). Similar results were obtained when the essential amino acids were analysed in the same samples. These results indicate that bafilomycin (10 nM) prevented maintenance of amino acid levels during 6 hours of amino acid starvation.

A.

B.

Total amino acids

Essential amino acids
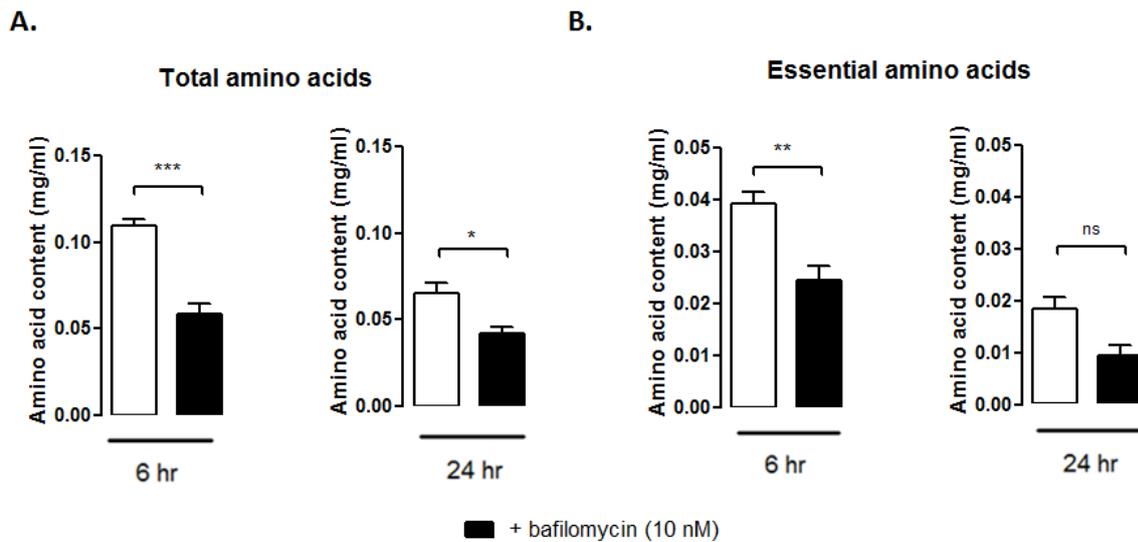
+ bafilomycin (10 nM)

Fig. 3.6 Bafilomycin (10 nM) significantly lowers the total amino acid content in MCF12A cells after 6 and 24 hours of amino acid starvation. Amino acid concentrations were measured at 6 and 24 hours of complete amino acid deprivation from culture medium. A. 'Total amino acids' indicates the sum of the Asp, Thr, Ser, Asn, Glu, Gln, Pro, Gly, Ala, Val, Cys, Met, Ile, Leu, Tyr, Phe, Lys, His and Arg concentrations. B. 'Essential amino acids' indicates the sum of Thr, Val, Met, Ile, Leu, Phe, Lys, His and Arg concentrations. Bafilomycin A1 (10 nM) was added to culture medium 6 hours prior to analysis. hr = hours. Each value is the mean ± SEM of at least three independent determinations. *, $P < 0.05$; **, $P < 0.01$; ***, $P < 0.001$. ns = no significance.

The addition of bafilomycin A1 (10 nM) to culture medium 6 hours prior to analysis resulted in significantly lower total amino acid content in MCF12A cells after both 6 and 24 hours of amino acid starvation (Fig 3.6). Although results for the essential amino acids showed a similar trend, amino acid levels were significantly lower only at 6 (and not 24) hours of amino acid starvation.

4.4   Maintenance of ATP levels at 6 hours of amino acid depletion is prevented by bafilomycin (10 nM) and ATG5 siRNA in MDAMB231 cells
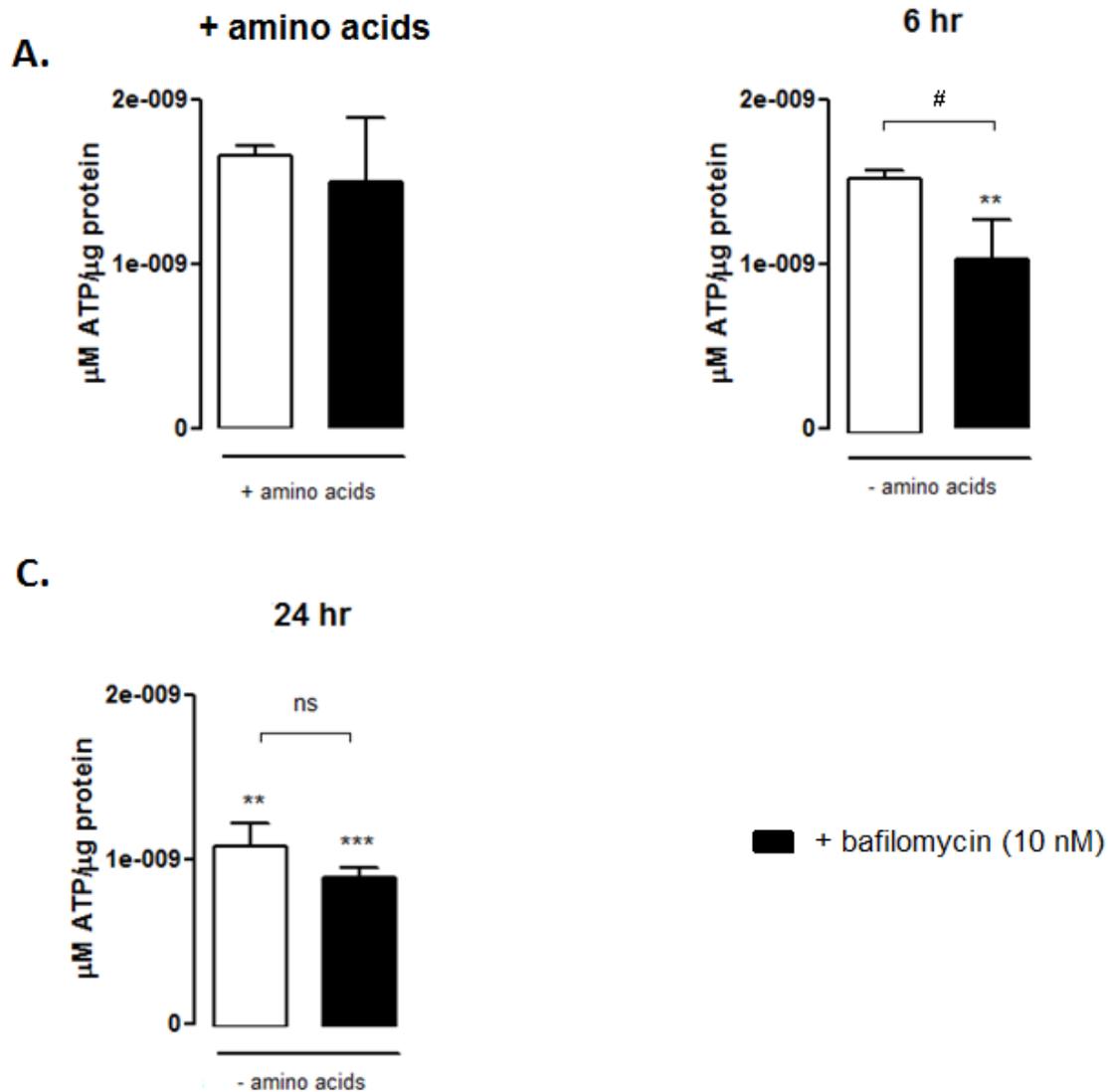
Fig. 3.7 Bafilomycin (10 nM) lowers the ATP content in MDAMB231 cells at 6 but not 24 hours of amino acid depletion. ATP levels are observed to be significantly lower at 6 hours of amino acid deprivation if bafilomycin (10 nM) is supplemented. ATP levels were measured at 0, 6 and 24 hours of incubation in total amino acid deprived culture medium. Bafilomycin A1 (10 nM) was added to culture medium 6 hours prior to analysis. hr = hours. Each value is the mean ± SEM of at least three independent determinations. **, $P < 0.01$; ***, $P < 0.001$ vs. + amino acids. #, $P < 0.01$. ns = no significance.

The addition of bafilomycin A1 (10 nM) to culture medium 6 hours prior to analysis resulted in a significantly lower ATP content in MDAMB231 cells after 6 hours of amino acid starvation (Fig 3.7). However, a similar decrease in ATP was not observed if cells were incubated in amino acid free medium for 24 hours with bafilomycin (10 nM).

143
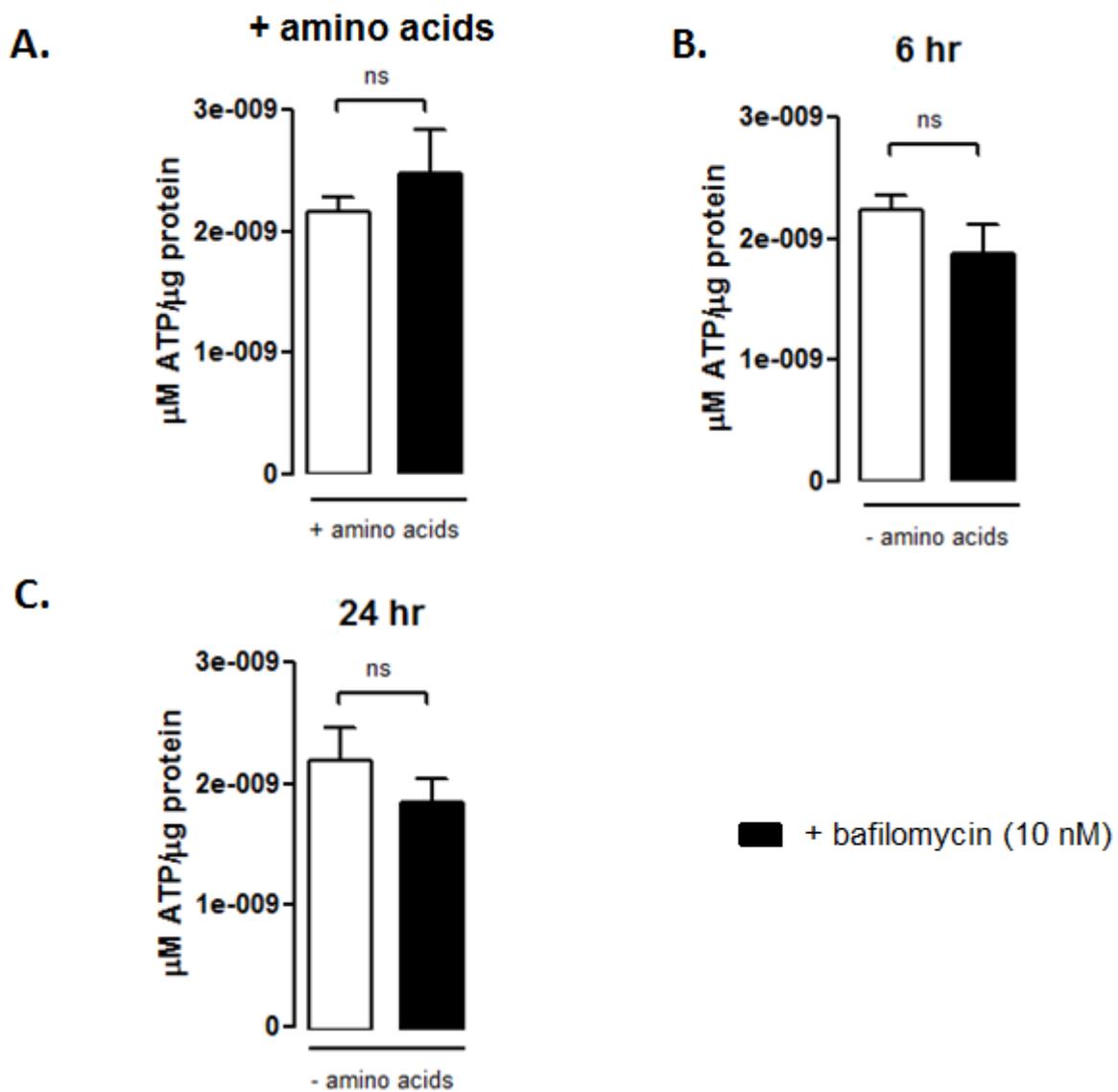
Fig. 3.8 Bafilomycin (10 nM) does not significantly lower the ATP content in MCF12A cells at 6 or 24 hours of amino acid depletion. ATP levels are observed to remain constant at 6 and 24 hours of amino acid deprivation if bafilomycin (10 nM) is supplemented. ATP levels were measured at 0, 6 and 24 hours of incubation in total amino acid deprived culture medium. Bafilomycin A1 (10 nM) was added to culture medium 6 hours prior to analysis. hr = hours. Each value is the mean ± SEM of at least three independent determinations. ns = no significance.

The addition of bafilomycin A1 (10 nM) to culture medium 6 hours prior to analysis resulted in a no significant changes in ATP content in MCF12A cells after 6 or 24 hours of amino acid starvation (Fig 3.8).
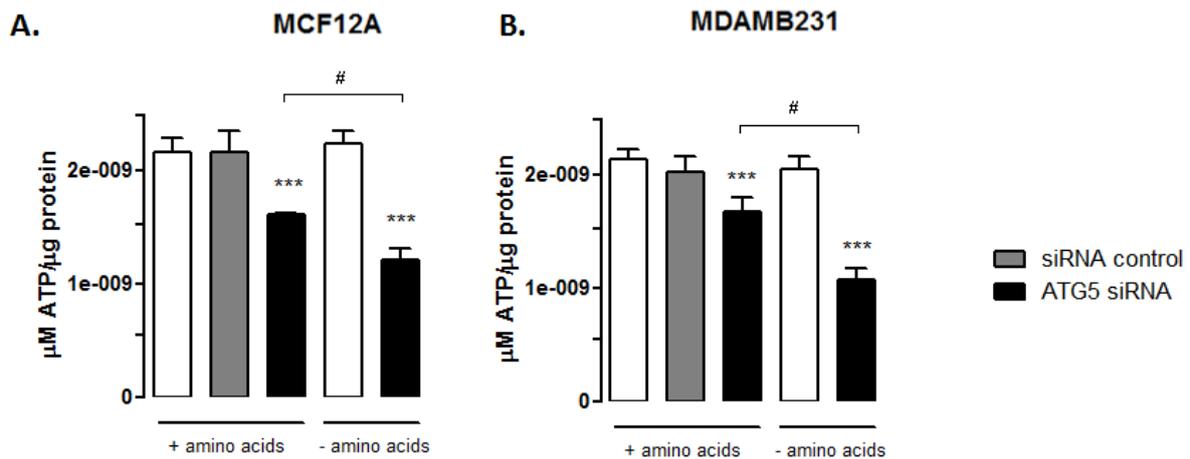
Fig. 3.9 ATP content in the presence or absence of amino acids after ATG5 siRNA transfection. A. MCF12A cells and B. MDAMB231 cells were incubated in amino acid free medium for a period of 6 hours. ATP levels are observed to be significantly lower in ATG5 siRNA transfected cells. ATP levels measured after 6 hours of complete amino acid deprivation were significantly lower than those in normal culture medium. Cells were reverse transfected 48 hours prior to treatment. Control siRNA did not affect ATP content in either cell line. Each value is the mean ± SEM of at least three independent determinations. ***, $P < 0.001$ vs. untreated cells. #, $P < 0.05$.

To investigate if the decreases in ATP observed when bafilomycin A1 was added to culture medium (Fig 3.7 and 3.8) was due to decreased autophagy, MDAMB231 and MCF12A cells were transfected with ATG5 siRNA, prior to their incubation in amino acid free medium. Cells were incubated in amino acid free medium for a period of 6 hours. The ATP levels of cells in normal or amino acid free medium were observed to be significantly lower if the cells had been transfected with ATG5 siRNA. Furthermore, ATP levels were significantly diminished in both cell lines when they were incubated in the absence of amino acids compared to when they were incubated with amino acids (black bars in Fig 3.9). Both cell lines were reverse transfected, 48 hours prior to treatment.

4.5 Amino acid depletion results in increased glucose uptake in MDAMB231 cells but not in MCF12A cells
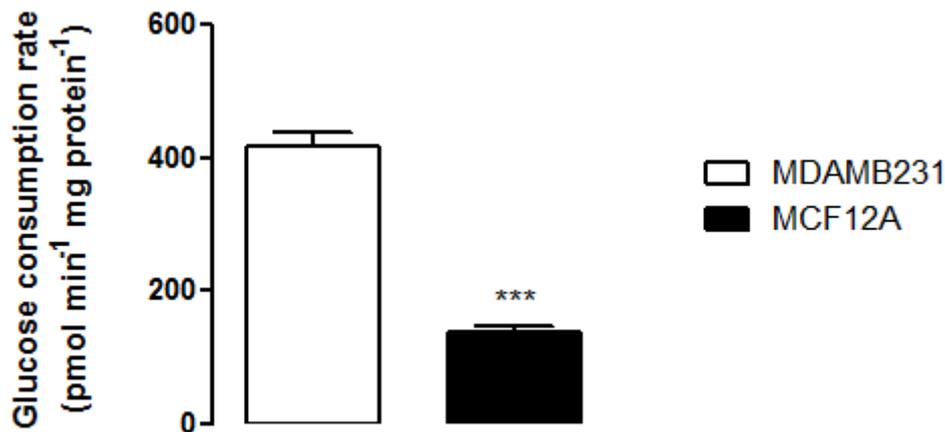
Fig. 3.10 Glucose uptake is significantly higher in MDAMB231 adenocarcinoma cells than in MCF12A breast epithelial cells. MDAMB231 cells display a higher rate of 2-deoxy-D-2[H] glucose uptake than MCF12A cells during a 30 minute incubation in radiolabled deoxyglucose (1.8 µM). Each value is the mean ± SEM of at least three independent determinations. ***, $P < 0.001$ vs. MDAMB231 cells.

Cancers are believed to rely principally on glucose for energy production. Therefore, MDAMB231 and MCF12A cells were incubated with radiolabled deoxyglucose (1.8 µM) for 30 minutes to assess glucose uptake. The aggressive, metastatic MDAMB231 adenocarcinoma cell line displayed a significantly higher rate of 2-deoxy-D-2[H] glucose uptake than non-tumourogenic MCF12A breast epithelial cells, indicating that they have a higher rate of basal glucose consumption during the normal proliferation phase (Fig 3.10).

A.

MDAMB231

B.

MCF12A

Legend:
- □ Untreated control
- ■ 6 hr
- ▨ 24 hr
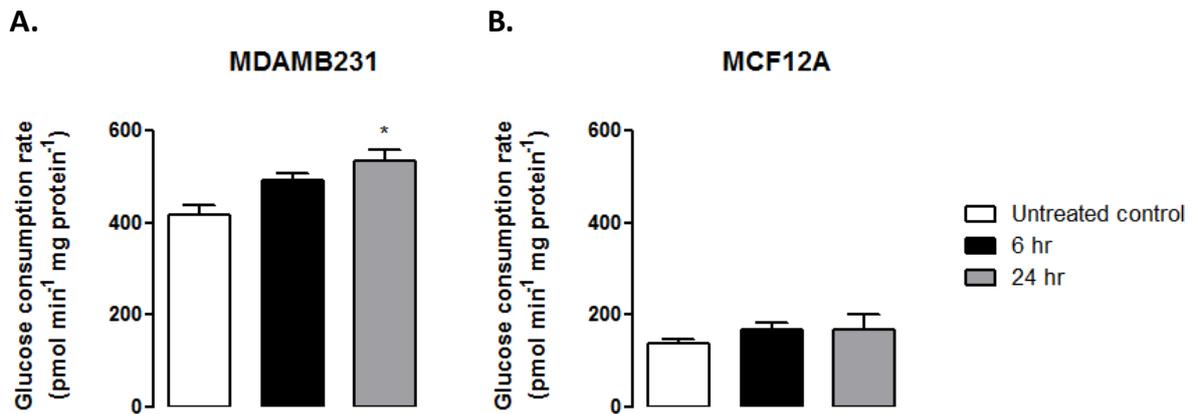
Fig. 3.11 Glucose uptake increases in MDAMB231 cells but not in MCF12A during amino acid starvation. A. MDAMB231 cells display an increased rate of 2-deoxy-D-2[H] glucose uptake after 24 hours of amino acid starvation. After 6 hours or 24 hours of amino acid starvation both cell lines were exposed to radiolabled deoxyglucose (1.8 μM) for 30 minutes. B. No changes were observed for MCF12A cells. Each value is the mean ± SEM of at least three independent determinations. *, $P < 0.05$ vs. untreated control.

MDAMB231 and MCF12A cells were incubated in amino acid free medium before being exposed to radiolabled deoxyglucose (1.8 μM) for 30 minutes. Cells displayed an increased rate of 2-deoxy-D-2[H] glucose uptake that reached significance at 24 hours of starvation (Fig 3.11). Glucose uptake did not increase in MCF12A starved of amino acids for 6 or 24 hours (Fig 3.11b).

4.6 Amino acid depletion results in a transient generation of branched chain amino acids at 6 hours of amino acid deprivation in MDAMB231 cells and MCF12A cells
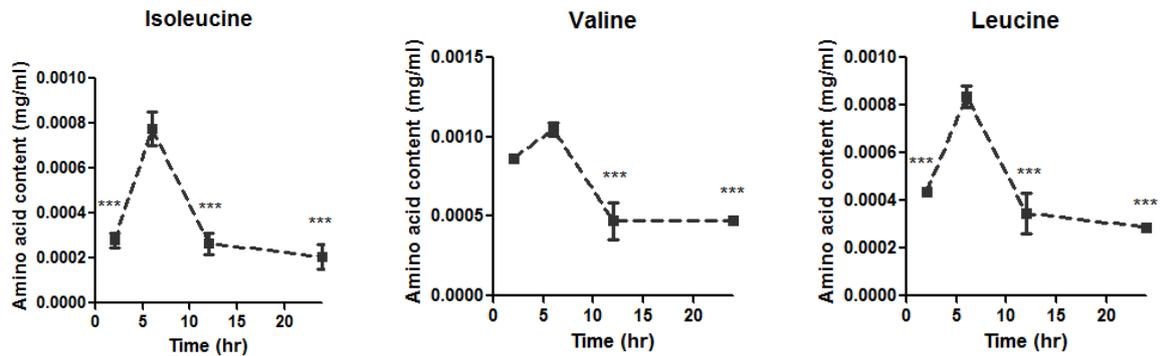
Fig. 3.12 Change in cellular branched chain amino acid content in MDAMB231 cells during a 24 hour period of amino acid starvation. Amino acid concentrations were measured after 2, 6, 12 and 24 hours of complete amino acid deprivation. A sudden increase in the content of isoleucine and leucine is observed at 6 hours of amino acid starvation. hr = hours. Each value is the mean ± SEM of at least three independent determinations. ***, $P < 0.001$ vs. 6 hours.

A significant increase in the cellular content of branched chain amino acids was observed between 2 and 6 hours of amino acid starvation in MDAMB231 cells. However, the level of valine was not significantly lower at 2 hours compared to 6 hours of starvation. Levels of all three branched chain amino acids decreased significantly from 6 to 12 hours and remained low at 24 hours of amino acid starvation (Fig 3.12).
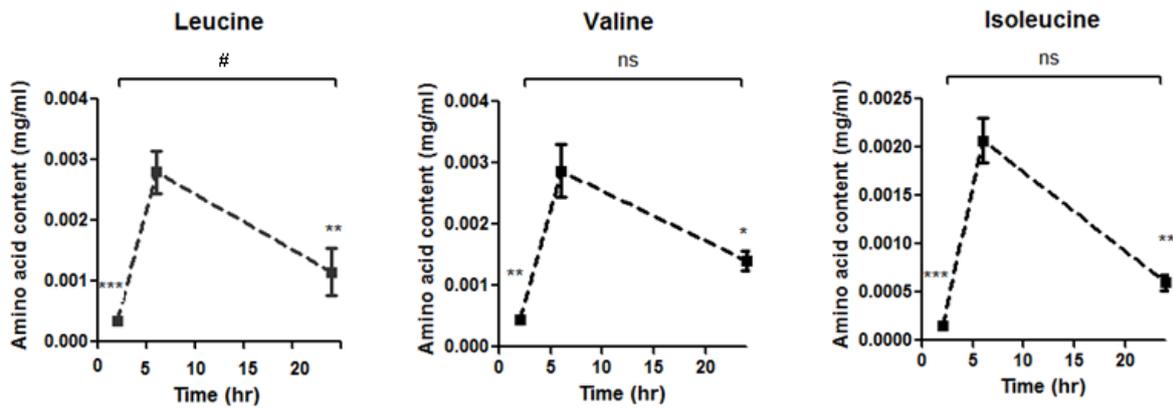
Fig. 3.13 Cellular branched chain amino acid concentrations in MCF12A cells during a 24 hour period of amino acid starvation. Amino acid concentrations were measured after 2, 6 and 24 hours of complete amino acid deprivation. Amino acid content was highest at 6 hours of amino acid deprivation. Each value is the mean ± SEM of at least three independent determinations. *, $P < 0.05$; **, $P < 0.01$; ***, $P < 0.001$ vs. 6 hours. # , $P < 0.01$ 2hours vs. 24 hours. ns = no significance.

MCF12A cells have significantly higher levels of detectable branched chain amino acids at 6 hours compared to 2 hours of amino acid starvation (Fig 3.13). Although the levels of all of the branched chain amino acids were significantly decreased at 24 hours of starvation, these levels remained higher than at 2 hours. In particular, there was significantly more leucine at 24 hours than at 2 hours of amino acid starvation.

4.7 Maintenance of the branched chain amino acids is prevented by bafilomycin (10 nM) at 6 hours but not 24 hours of amino acid depletion
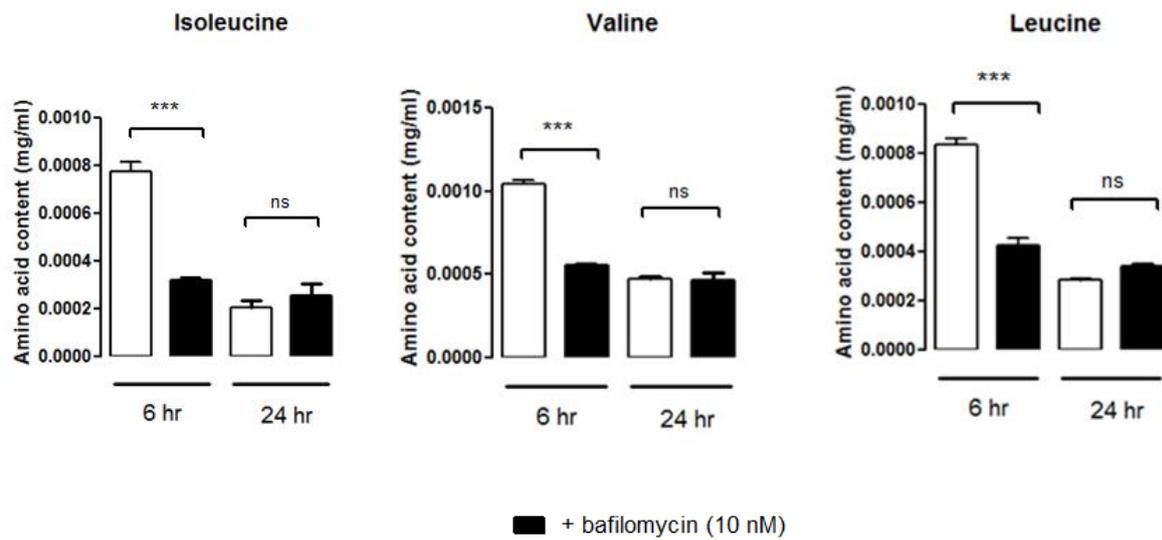
Fig. 3.14 Bafilomycin (10 nM) significantly lowers branched chain amino acid content in MDAMB231 cells at 6 but not 24 hours of amino acid starvation. Amino acid concentrations were measured at 6 and 24 hours of complete amino acid deprivation Bafilomycin A1 (10 nM) was added to culture medium 6 hours prior to analysis. hr = hours. Each value is the mean ± SEM of at least three independent determinations. ***, $P < 0.001$. ns = no significance.

In similar results to those shown previously (Fig 3.5), the presence of bafilomycin A1 (10 nM) also prevented the maintenance of cellular branched chain amino acid levels during 6 hours but not 24 hours of amino acid starvation in MDAMB231 cells (Fig 3.14).
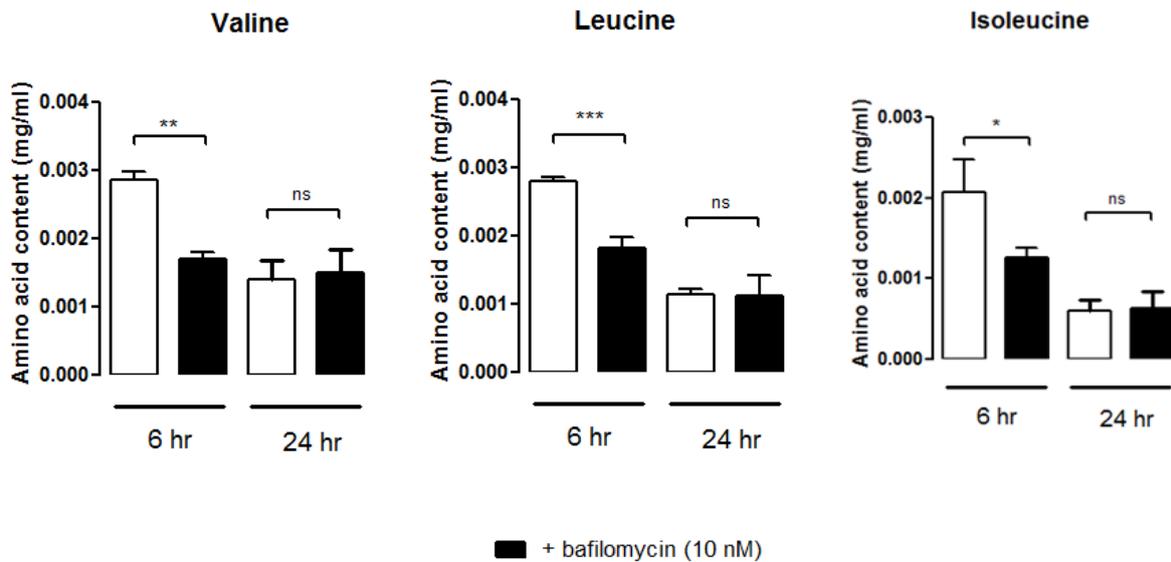
Fig. 3.15 Bafilomycin (10 nM) significantly lowers the total branched chain amino acid content in MCF12A cells after 6 but not 24 hours of amino acid starvation. Amino acid concentrations were measured at 6 and 24 hours of complete amino acid deprivation from culture medium. Bafilomycin A1 (10 nM) was added to culture medium 6 hours prior to analysis. hr = hours. Each value is the mean ± SEM of at least three independent determinations. *, $P < 0.05$; **, $P < 0.01$; ***, $P < 0.001$. ns = no significance.

The presence of bafilomycin A1 (10 nM) also prevented the maintenance of cellular branched chain amino acid levels during 6 hours but not 24 hours of amino acid starvation in MCF12A cells (Fig 3.15).

151

4.8 Silencing the branched-chain alpha-keto acid dehydrogenase (BCKDH) enzyme complex results in an accumulation of the branched chain amino acids and a corresponding decrease in ATP content at 6 but not 24 hours of amino acid starvation in MDAMB231 cells

The branched-chain alpha-keto acid dehydrogenase (BCKDH) enzyme complex converts the branched chain amino acids into derivatives capable of entering the mitochondria. The BCKDH enzyme was silenced using siRNA towards BCKDH in this study. Validation experiments confirmed a prominent down-regulation of BCKDH expression in both cell lines (Fig 3.17), while addition of scrambled siRNA duplexes did not have any effect on expression of BCKDH or the cellular content of the branched chain amino acids (Fig 3.16).
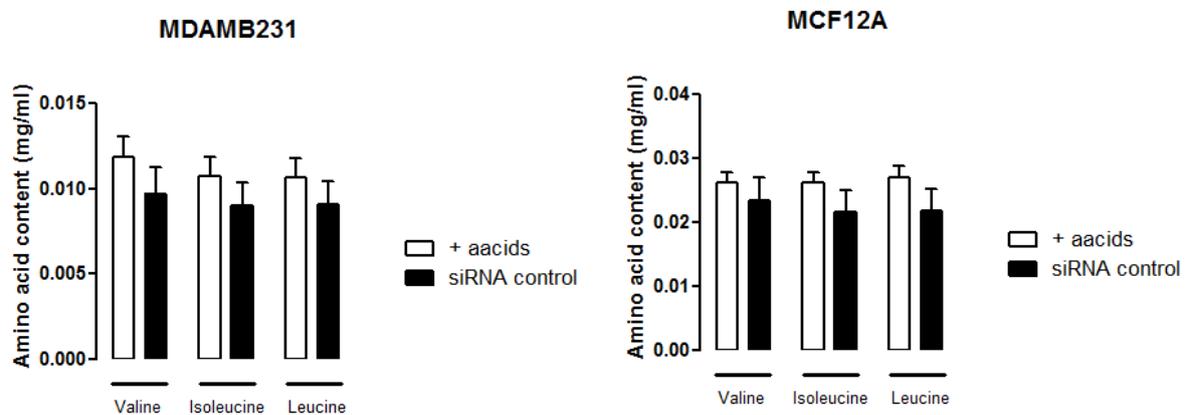
Fig. 3.16 Control siRNA does not alter branched chain amino acid content. Each value is the mean ± SEM of at least three independent determinations.
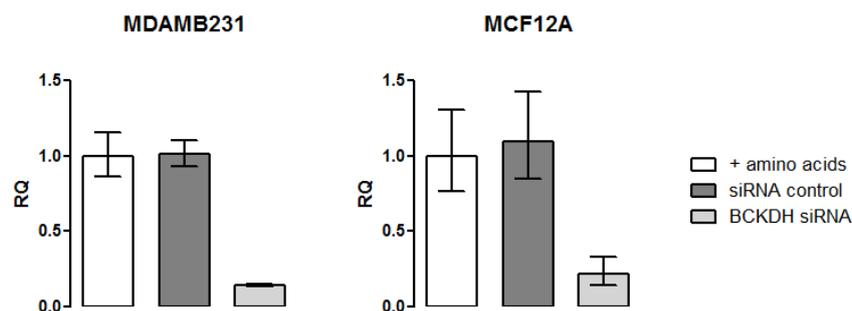
Fig. 3.17 Validation experiments confirmed a prominent down-regulation of BCKDH expression in both cell lines after transfection with BCKDH siRNA. Addition of a scrambled siRNA negative control did not have any effect on expression of BCKDH. Results represent quantification values of the amount of target BCKDH cDNA, normalized to an endogenous control (90 kDa), and relative to a calibrator (+ amino acids; RQ = 1.00). Error bars are representative of RQ min and RQ max values. BCKDH = branched chain keto acid dehydrogenase.

A.
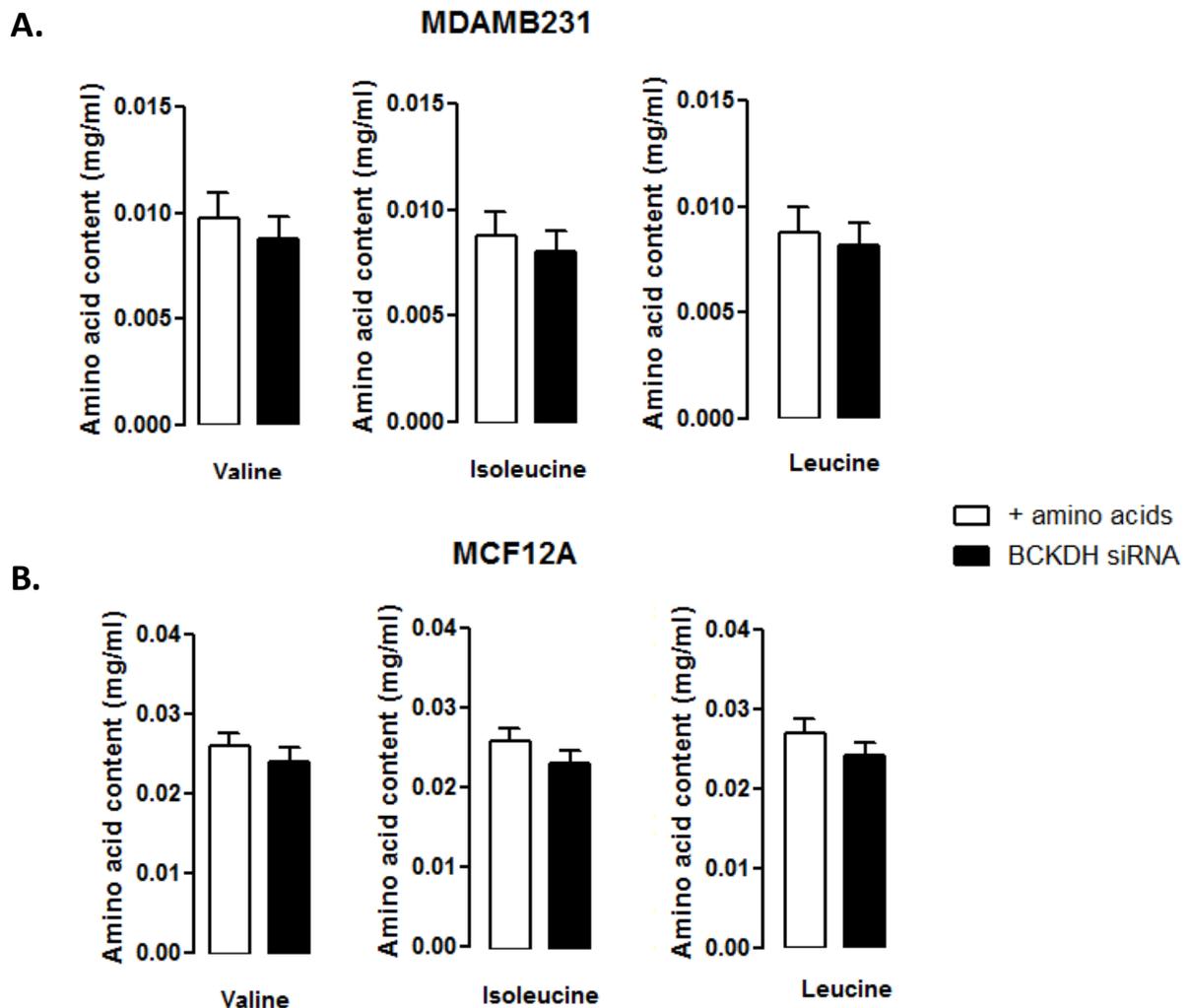
Fig. 3.18 BCKDH siRNA does not alter the branched chain amino acid content in MDAMB231 cells or MCF12A cells cultured in amino acid complete medium for 24 hours. Amino acid concentrations were measured after a 24 hour incubation in normal culture medium after having been transfected with BCKDH siRNA. BCKDH siRNA was transfected 48 hours prior to treatment as per the suggested manufacturer's protocol. No statistical differences were observed. BCKDH = branched chain keto acid dehydrogenase.

BCKDH siRNA was reverse transfected into MDAMB231 cells 48 hours prior to replacement of culture medium with fresh medium complete of amino acids. No change in the free amino acid content of any of the branched chain amino acids was observed during this incubation period (Fig 3.18).
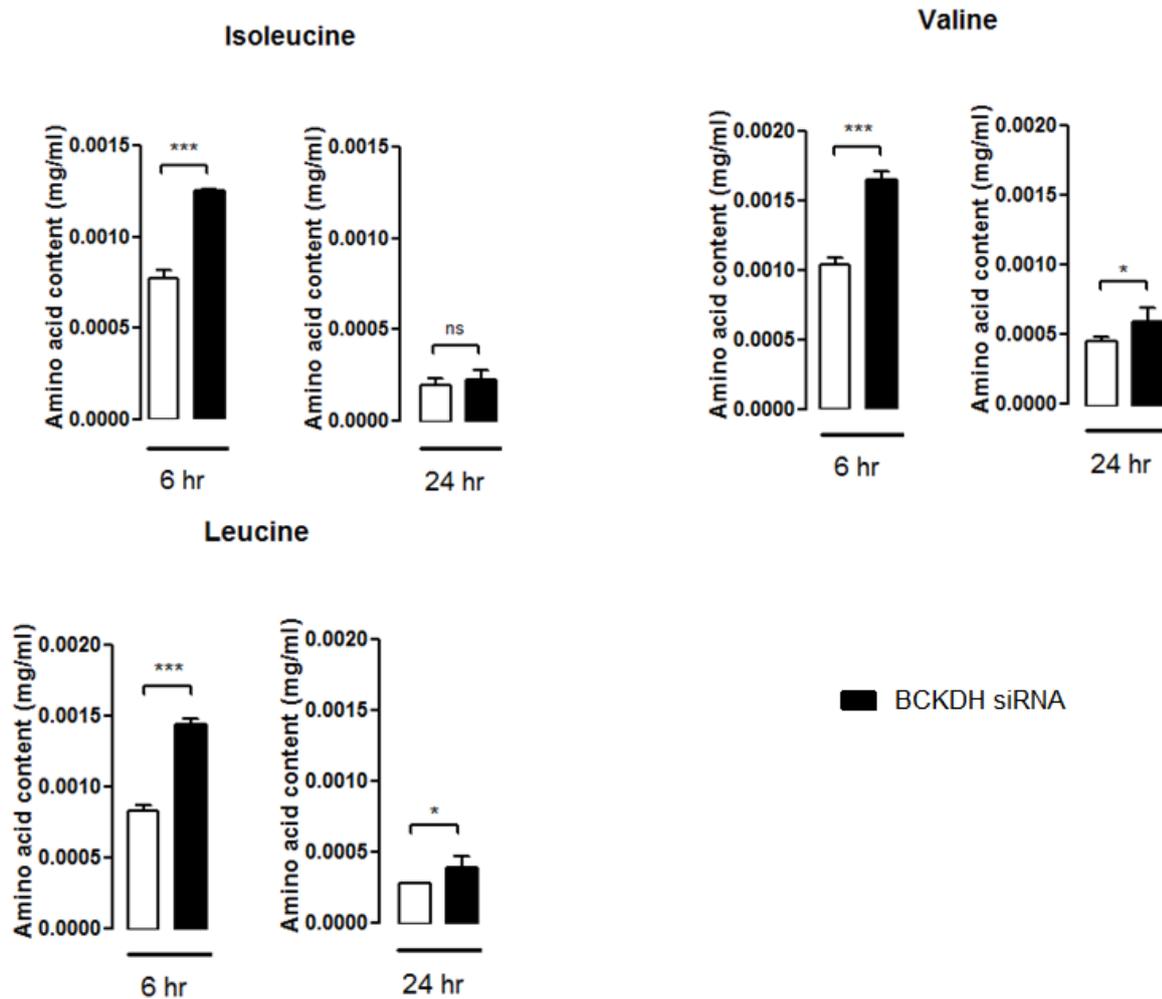
Fig. 3.19 BCKDH siRNA significantly increases the branched chain amino acid content in MDAMB231 cells at 6 hours of amino acid starvation. Amino acid concentrations were measured at 6 and 24 hours of complete amino acid deprivation from culture medium in the presence of BCKDH siRNA. BCKDH siRNA was transfected 48 hours prior to treatment as per the suggested manufacturer's protocol. hr = hours; BCKDH = branched chain keto acid dehydrogenase. Each value is the mean ± SEM of at least three independent determinations. *, $P < 0.05$; ***, $P < 0.001$. ns = no significance.

BCKDH siRNA was transfected into proliferating MDAMB231 cells 24 hours prior to omitting amino acids from the culture medium for 6 and 24 hours. The addition of BCKDH siRNA during amino acid starvation lead to a significant accumulation of the branched chain amino acids in MDAMB231 cells at 6 hours of amino acid starvation (Fig 3.19). An accumulation of valine and leucine, but not isoleucine was detected at 24 hours of starvation.
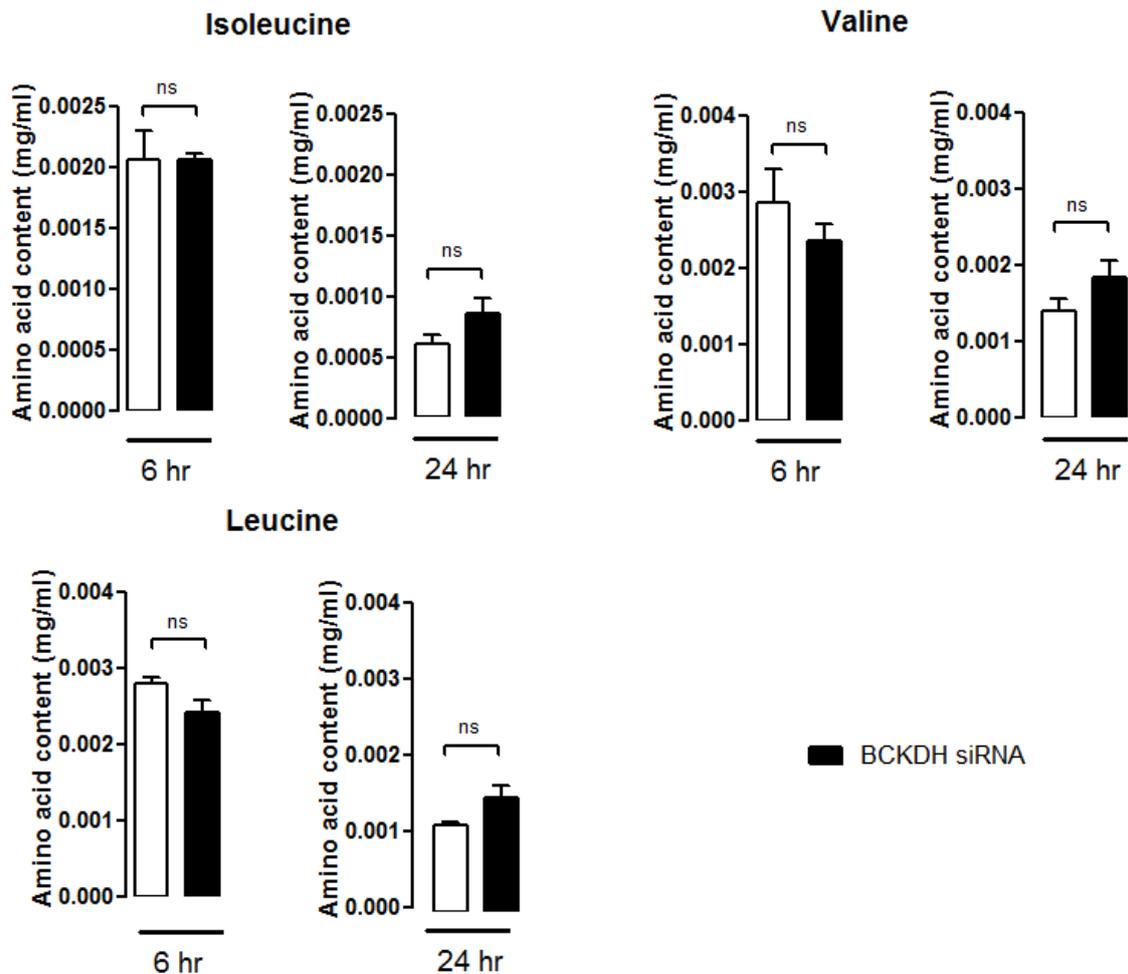
Fig. 3.20 BCKDH siRNA does not alter the branched chain amino acid content in MCF12A cells during amino acid starvation. Amino acid concentrations were measured at 6 and 24 hours of complete amino acid deprivation from culture medium in the presence of BCKDH siRNA. BCKDH siRNA was transfected 24 hours prior to treatment as per the suggested manufacturer's protocol. hr = hours; BCKDH = branched chain keto acid dehydrogenase. Each value is the mean ± SEM of at least three independent determinations. ns = no significance.

A similar increase of branched chain amino acid accumulation is not observed in MCF12A cells following silencing of BCKDH (Fig 3.20). Interestingly, MCF12A cells appear to show a trend towards increased accumulation of branched chain amino acids at 24 hours of starvation in the presence of BCKDH siRNA.
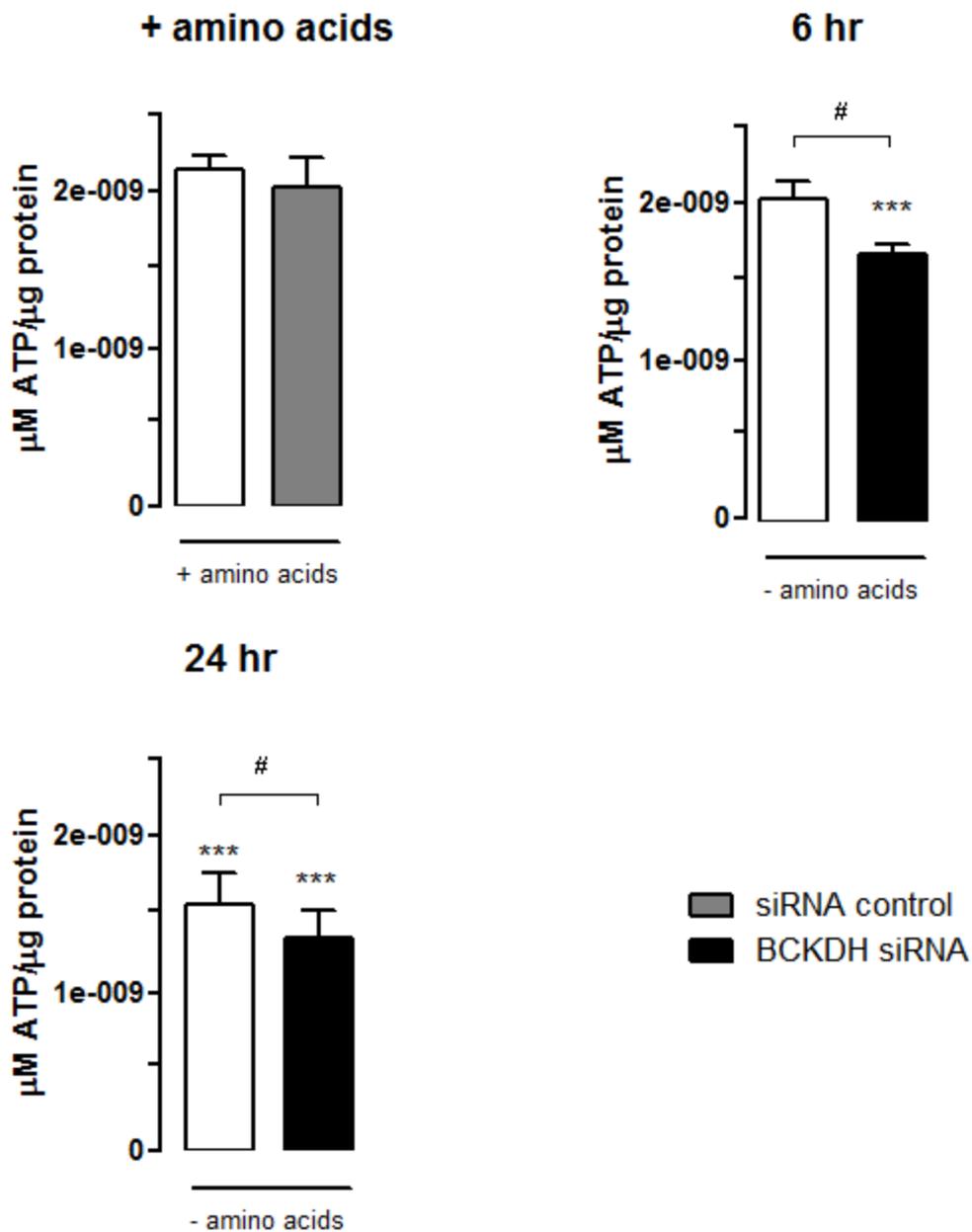
Fig. 3.21 BCKDH siRNA lowers the ATP content in MDAMB231 cells at 6 and 24 hours of amino acid depletion. ATP levels are observed to be significantly lower at 6 and 24 hours of amino acid deprivation if BCKDH siRNA is present. ATP levels were measured after 0, 6 and 24 hours of incubation in total amino acid deprived culture medium. BCKDH siRNA was transfected 48 hours prior to treatment as per the suggested manufacturer's protocol. hr = hours; BCKDH = branched chain keto acid dehydrogenase. Each value is the mean ± SEM of at least three independent determinations. ***, $P < 0.001$ vs. + amino acids. #, $P < 0.01$. ns = no significance.

BCKDH siRNA lowered the ATP content in MDAMB231 cells at 6 and 24 hours of amino acid depletion (Fig 3.21).

156
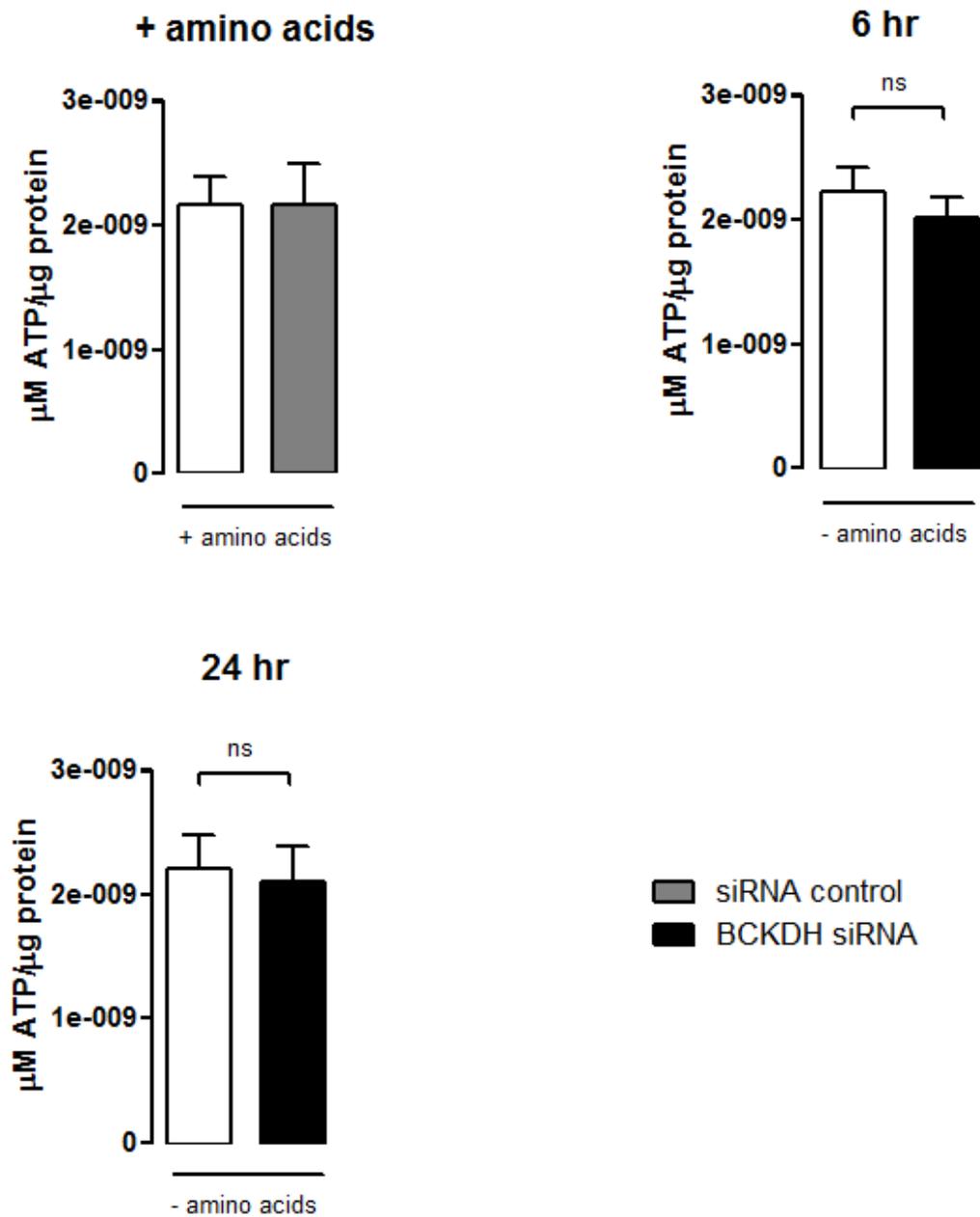
Fig. 3.22 BCKDH siRNA does not lower the ATP content in MCF12A cells at 6 or 24 hours of amino acid depletion. ATP levels are observed to remain constant at 6 and 24 hours of amino acid deprivation if BCKDH siRNA is present. ATP levels were measured after 0, 6 and 24 hours of incubation in total amino acid deprived culture medium. BCKDH siRNA was transfected 48 hours prior to treatment as per the suggested manufacturer's protocol. hr = hours; BCKDH = branched chain keto acid dehydrogenase. Each value is the mean ± SEM of at least three independent determinations. ns = no significance.

BCKDH siRNA did not lower the ATP content in MCF12A cells at 6 or 24 hours of amino acid depletion (Fig 3.22).

157
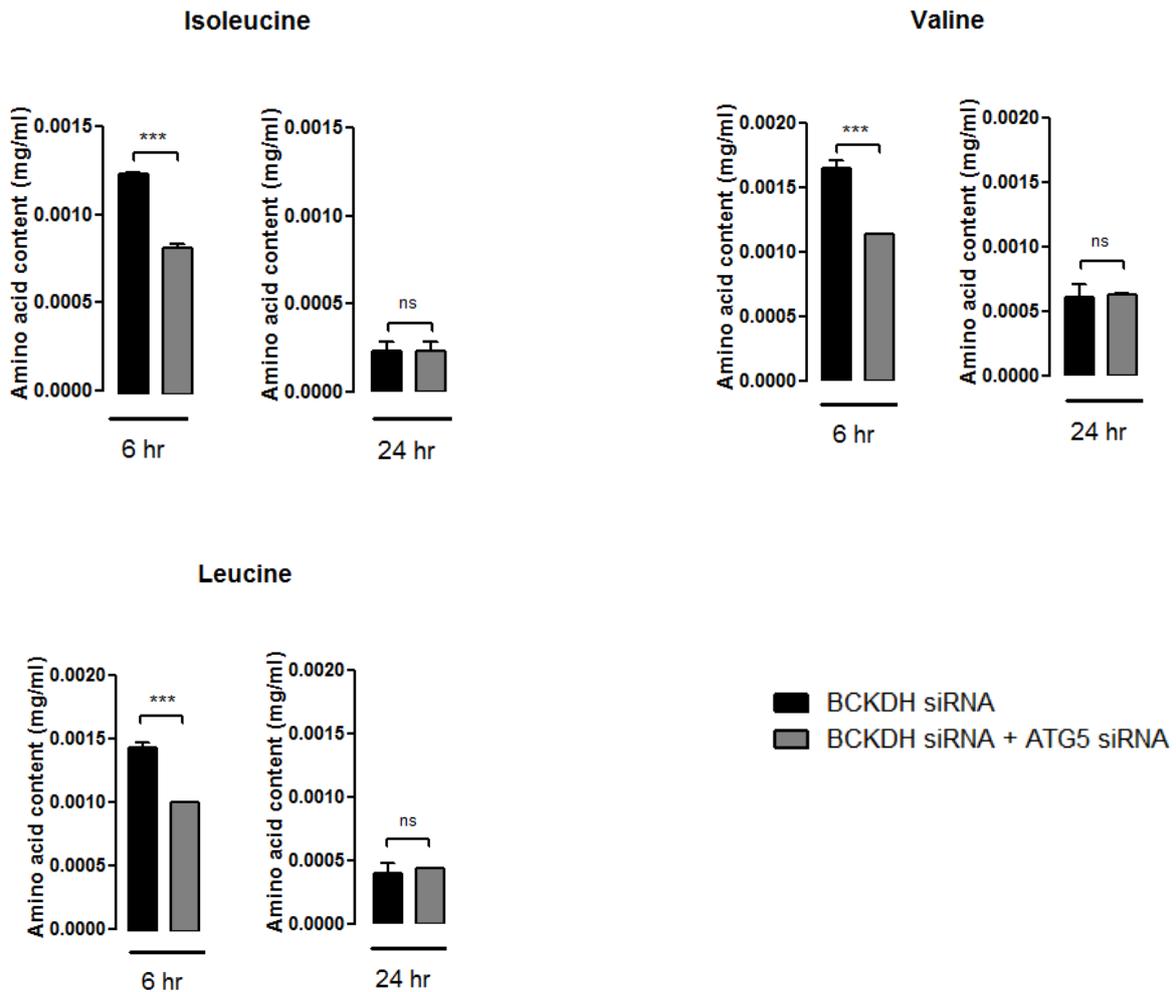
Fig. 3.23 Autophagy inhibition with ATG5 siRNA significantly decreases the branch chain amino acid content in MDAMB231 cells at 6 but not 24 hours of amino acid starvation in the presence of BCKDH siRNA. Amino acid concentrations were measured at 6 and 24 hours of complete amino acid deprivation from culture medium in the presence of BCKDH siRNA and ATG5 siRNA. BCKDH siRNA and ATG5 siRNA was transfected 48 hours prior to treatment as per the suggested manufacturer's protocols. hr = hours; BCKDH = branched chain keto acid dehydrogenase. Each value is the mean ± SEM of at least three independent determinations. ***, $P < 0.001$. ns = no significance.

If autophagy was blocked using siRNA towards ATG5 in the presence of BCKDH siRNA during amino acid starvation then branched chain amino acid content decreased further in MDAMB231 cells (Fig 3.23). This indicates that autophagy is at least partly responsible for generation of the branched chain amino acids during amino acid starvation.
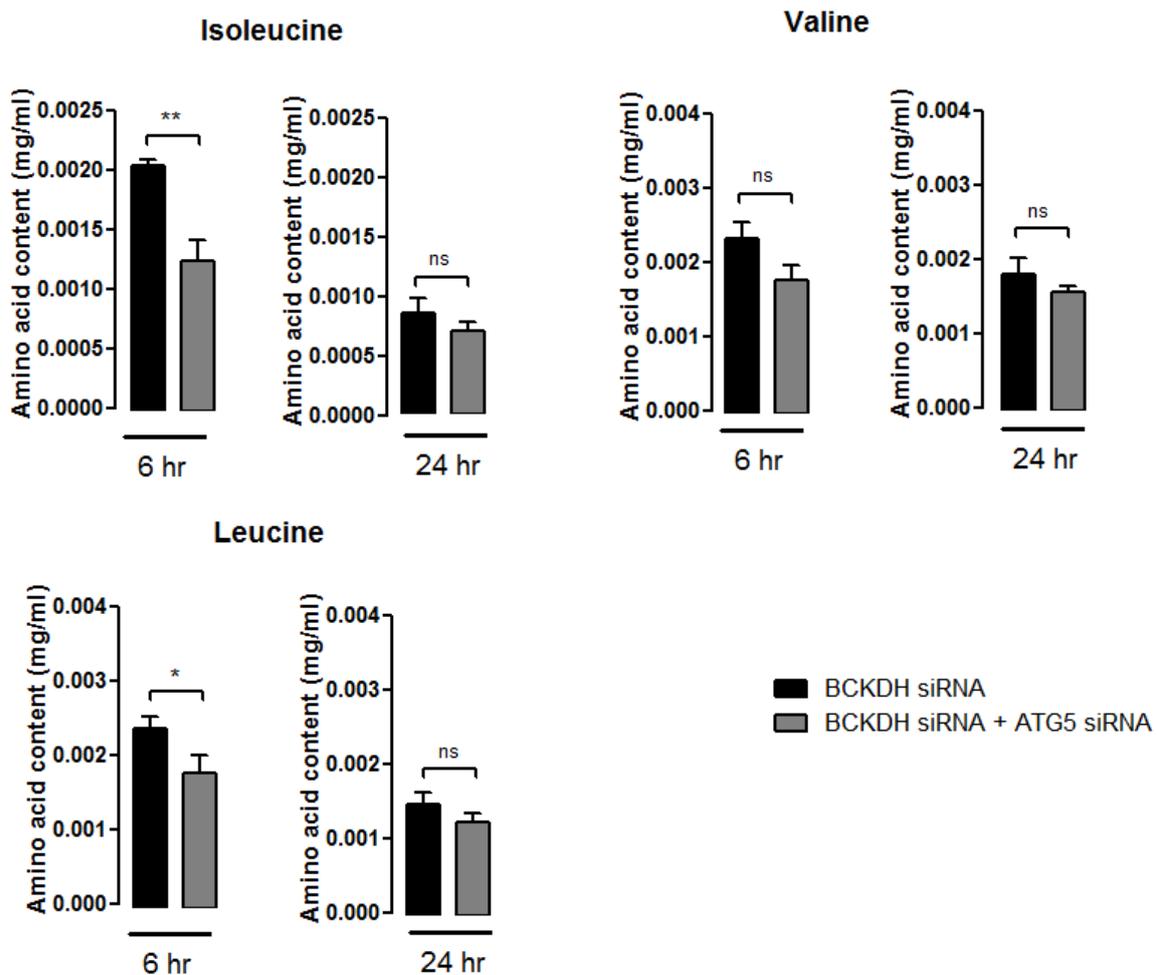
Fig. 3.24 Autophagy inhibition with ATG5 siRNA does not alter the branched chain amino acid content in MCF12A during amino acid starvation in the presence of BCKDH siRNA. Amino acid concentrations were measured at 6 and 24 hours of complete amino acid deprivation from culture medium in the presence of BCKDH siRNA and ATG5 siRNA. BCKDH siRNA and ATG5 siRNA was transfected 48 hours prior to treatment as per the suggested manufacturer's protocols. hr = hours; BCKDH = branched chain keto acid dehydrogenase. Each value is the mean ± SEM of at least three independent determinations. *, $P < 0.05$; **, $P < 0.01$. ns = no significance.

Branched chain amino acid content decreased in MCF12A cells if autophagy was blocked using siRNA towards ATG5 in the presence of BCKDH siRNA during amino acid starvation (Fig 3.24). Also, there was a strong trend towards a decrease in valine levels. Branched chain amino acid levels were significantly lower in cells treated with ATG5 siRNA than in cells where only control siRNA was added (data not shown).

4.9 Maintenance of free fatty acid levels at 6 hours of amino acid depletion is prevented by bafilomycin A1 (10 nM) and ATG5 siRNA
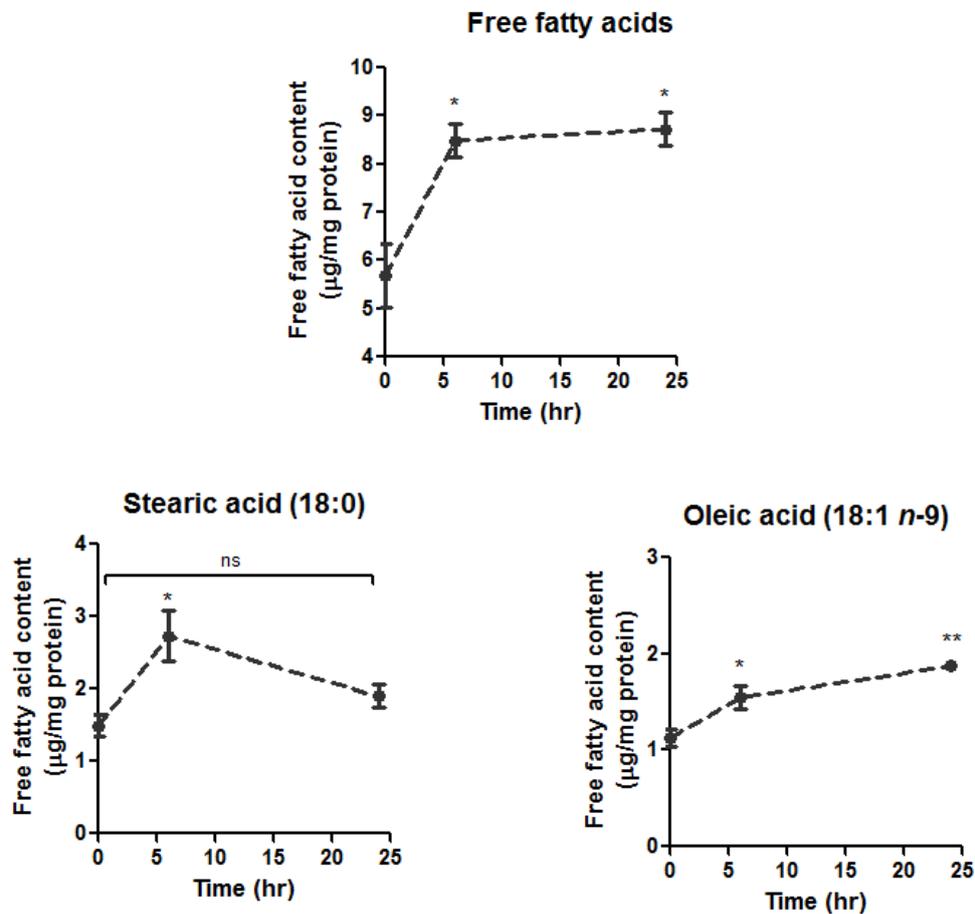
Fig. 3.25 The free fatty acid content of MDAMB231 cells increases during amino acid starvation. Total free fatty acid content is significantly higher after 6 hours and after 24 hours of amino acid deprivation. Stearic acid is significantly higher at 6 hours but not at 24 hours of amino acid starvation. Oleic acid increases during 24 hours of amino acid deprivation. Fatty acids were separated using GLC. hr = hours. Each value is the mean ± SEM of at least three independent determinations. *, $P < 0.05$; **, $P < 0.01$. vs. 0 hr. ns = no significance 0 hr vs. 24 hr.

The free fatty acid content of MDAMB231 cells was higher if they were incubated for 6 hours in amino acid free medium (Fig 3.25). This elevated level was maintained at 24 hours of amino acid starvation. The quantity of the most abundant saturated fatty acid, stearic acid, was higher in MDAMB231 cells after 6 hours, but not after 24 hours in amino acid free

medium. The quantity of the most abundant unsaturated fatty acid, oleic acid, was increased after 6 hours and 24 hours of amino acid starvation.
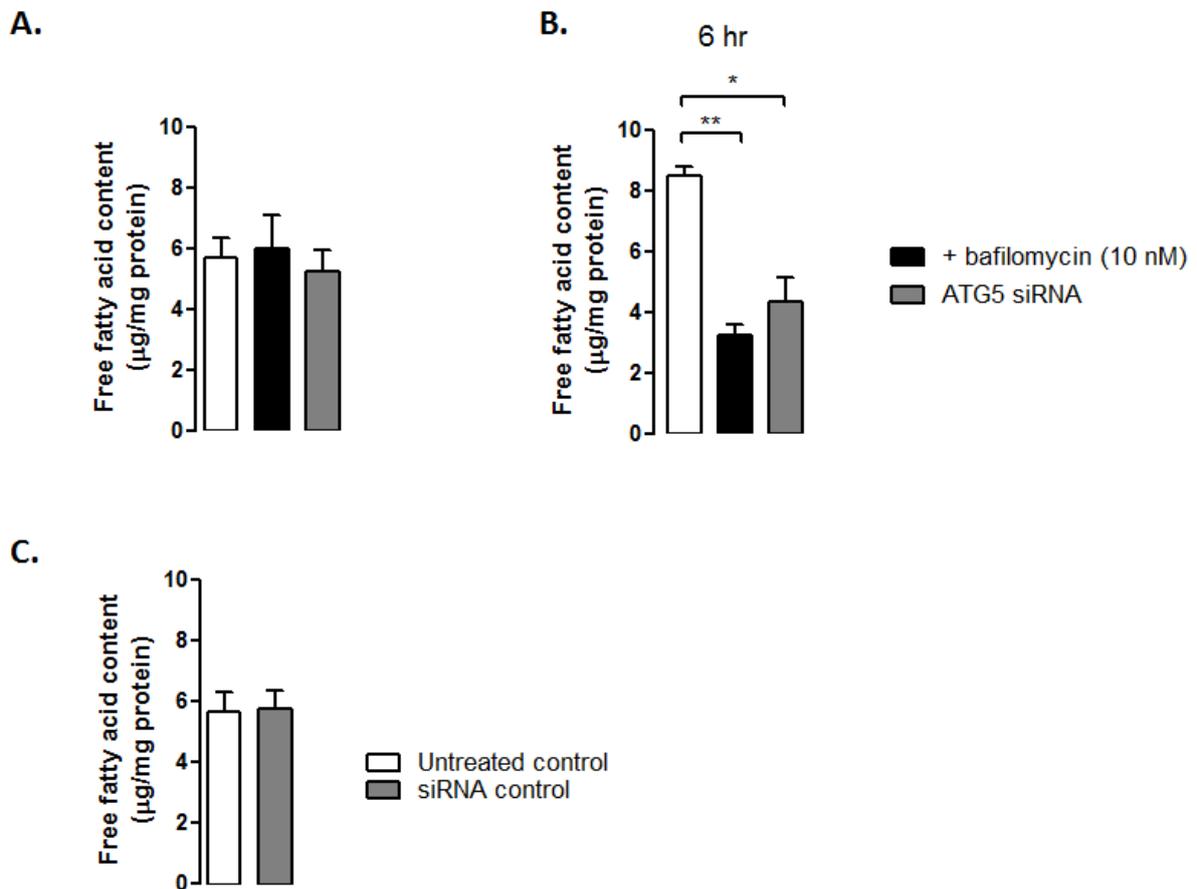
Fig. 3.26 Bafilomycin A1 (10 nM) and autophagy inhibition with ATG5 siRNA prevent an increase in free fatty acid content in MDAMB231 cells during amino acid deprivation. Neither bafilomycin A1 (10 nM) nor ATG5 siRNA altered free fatty acid levels in cells incubated in amino acid complete culture medium. Incubation with scrambled siRNA lead to no change in free fatty acid content. ATG5 siRNA was transfected 48 hours prior to treatment as per the suggested manufacturer's protocol. hr = hours. Each value is the mean ± SEM of at least three independent determinations. *, $P < 0.05$; **, $P < 0.01$.

Neither bafilomycin A1 (10 nM), nor autophagy inhibition with ATG5 siRNA altered the fatty acid content of MDAMB231 cells incubated in amino acid complete medium (Fig 3.26a). On the other hand, both bafilomycin A1 (10 nM) and ATG5 siRNA prevented an increase in fatty acid levels in MDAMB231 cells during 6 hours of amino acid starvation (Fig 3.26b). Scrambled siRNA did not change the fatty acid content of these cells (Fig 3.26c).

161

Total phospholipid (TPL) fatty acid content
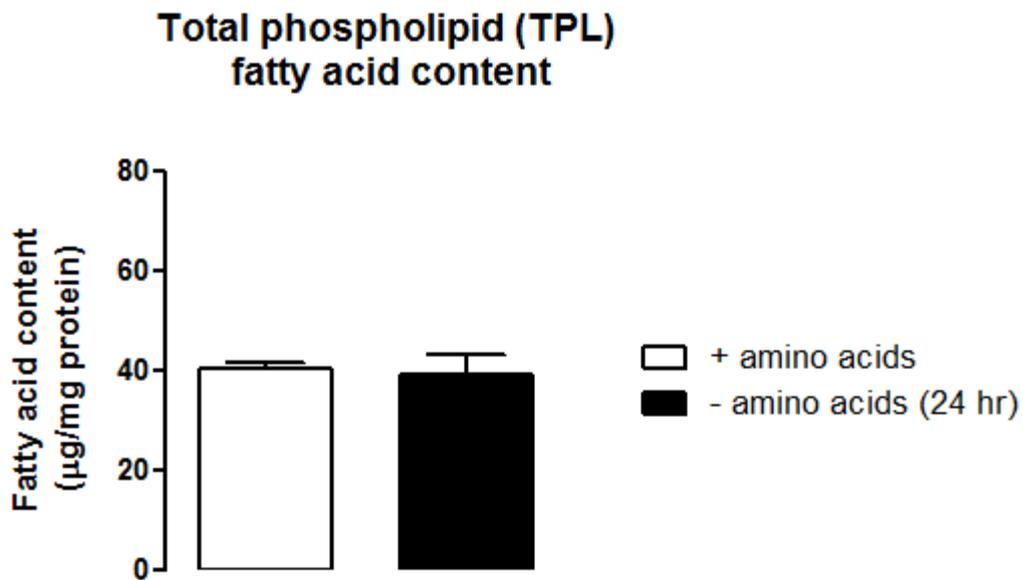
Fig. 3.27 Amino acid starvation does not change the total phospholipid (TPL) fatty acid content of MDAMB231 cells after 24 hours of amino acid starvation. Each value is the mean ± SEM of at least three independent determinations. hr =hours.

The total phospholipid fatty acid content of MDAMB231 cells is the same in cells incubated in culture medium with amino acids and in cells incubated in culture medium without amino acids for 24 hours (Fig 3.27).
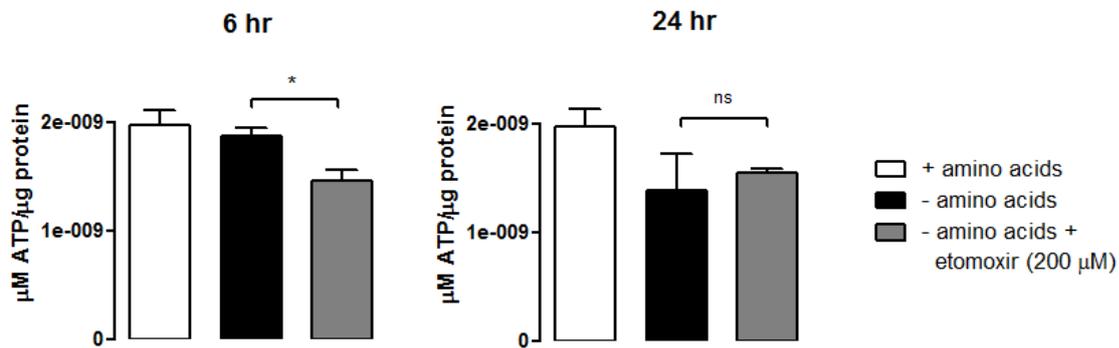
Fig. 3.28 Etomoxir lowers the ATP content in MDAMB231 cells at 6 but not 24 hours of amino acid depletion. ATP levels are observed to be significantly lower at 6 but not at 24 hours of amino acid deprivation if etomoxir (200 µM) is present. ATP levels were measured after 0, 6 and 24 hours of incubation in total amino acid deprived culture medium. Etomoxir (200 µM) was present during treatment. hr = hours. Each value is the mean ± SEM of at least three independent determinations. *, $P < 0.05$. ns = no significance.

The fatty acid β-oxidation inhibitor etomoxir (200 µM) lowers ATP content in MDAMB231 cells incubated in amino acid free medium for 6 hours (Fig 3.28). A similar decrease in ATP content is not observed if cells were incubated in amino acid free medium for 24 hours in the presence of etomoxir (200 µM).
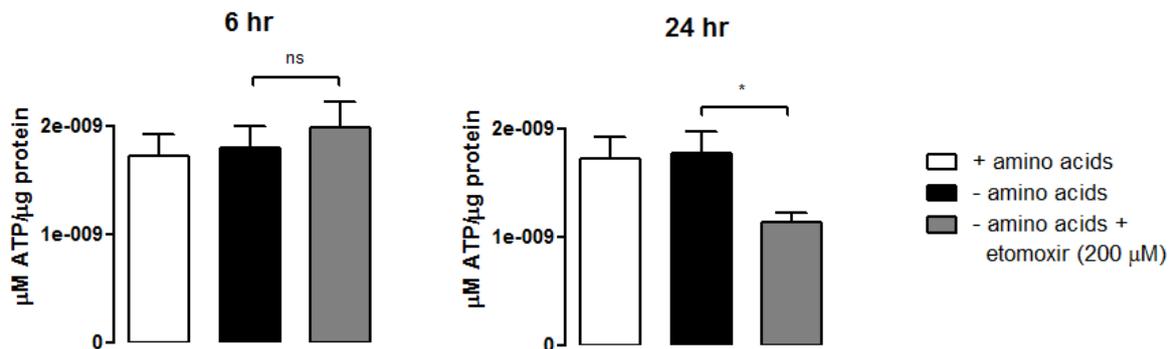
Fig. 3.29 Etomoxir lowers the ATP content in MCF12A cells at 24 but not 6 hours of amino acid depletion. ATP levels are observed to be significantly lower at 24 but not at 6 hours of amino acid deprivation if etomoxir (200 µM) is present. ATP levels were measured after 0, 6 and 24 hours of incubation in total amino acid deprived culture medium. Etomoxir (200 µM) was present during treatment. hr = hours. Each value is the mean ± SEM of at least three independent determinations. *, $P < 0.05$. ns =no significance.

The fatty acid β-oxidation inhibitor etomoxir (200 µM) lowers ATP content in MCF12A cells incubated in amino acid free medium for 24 hours (Fig 3.29). A similar decrease in ATP content is not observed if cells were incubated in amino acid free medium for 6 hours in the presence of etomoxir (200 µM).

5   Discussion

Established tumours are known to develop regions of transient nutrient limitation and ischemia, and it is believed that autophagy has a potentiating role in these microenvironments, generally attributed to its functional capacity to generate constituents for continued biosynthesis and energy generation (Degenhardt et al., 2006). Additionally, autophagy within neoplasms might also be able to confer protection during chemotherapy (Yang and Chen, 2011). The protective role of autophagy within these tumours, due to its homeostatic function within regions with limited access to blood supply, is thought to prevent so-called metabolic catastrophe (Jin and White, 2008). However, data for direct measures of amino acids in nutrient starved cancer cells are currently completely absent. Furthermore, direct assessment of ATP levels are almost never published, particularly in association with cancer studies. Therefore, assessment of amino acid levels during short term starvation and correlation with ATP levels under these conditions is a vital next step if therapeutic interventions are to be designed on the basis that autophagy increases survival through generation of substrates for energy production.

Many of the prominent reviews describing autophagy processes in detail highlight the point that the degradation of cytoplasmic material through increased activation of the autophagosomal-lysosomal system increases the availability of amino acids, which are then accessible for use in the generation of energy and to buffer the systemic amino acid pool (Mizushima, 2007, Klionsky, 2007, Levine and Kroemer, 2008). However, little evidence linking these claims is presented. Although a few studies have assessed some of these parameters independently, the generation of amino acids by autophagy is never directly correlated with their utility. Moreover, even though autophagy is thought to be vital for the generation of these substrates in harsh cancer microenvironments, even less investigation into

165

nutrient generation in the cancer setting has been undertaken as yet. Furthermore, the drive to use low protein diets and autophagy inhibition in patients receiving cancer therapy (information from clinicaltrials.gov) necessitates increased research.

5.1   Autophagy regulation of cellular amino acid levels in MDAMB231 cells

Previous experiments demonstrated that a breast cancer cell line with high basal autophagy (MDAMB231) is able to respond to an acute bout of nutrient deprivation by further increasing autophagy activity (detailed in chapter 2). The current study was undertaken in order to provide some mechanistic support to explain how autophagy is accomplishing this protective feat. It is often assumed that by generating substrates from the degradation of cytoplasmic material, autophagy is able to buffer any nutrient losses. However, support for this idea is rarely offered. Our model of dynamic autophagy assessment in cell lines with high and low basal autophagy provides an opportunity to assess this hypothesis. As only amino acids have been eliminated from the cells in this model, assessment of the amino acid content and the consequences to energy production during amino acid starvation would provide great insight into the mechanism whereby autophagy is able to aid in survival during a starvation event.

Experimental data, using a model of complete amino acid starvation, provides evidence of a robust surge of increased amino acids at 6 hours of amino acid deprivation in MDAMB231 cells (Fig 3.1). A significant increase in the total and essential amino acid content of these cells was observed between 2 and 6 hours of complete amino acid starvation. Thereafter, cellular free amino acid content decreased and remained significantly low between 12 and 24 hours. Presumably, the amino acids generated in this way were utilized for functions within

166

the cells. Analysis of the supernatant medium extracted from these cells at the end of the treatment period indicated that there were no amino acids present in the culture medium (data not shown). This implies that the amino acids generated during amino acid starvation did not diffuse out of these cells into the incubation medium and must have been used within the cells for some purpose. Although a non-tumourogenic cell line (MCF12A) displayed a similar significant increase in amino acids at 6 hours following starvation, these levels remained relatively high compared to those in the cancer cell line (Fig 3.2). This demonstrates that these cells are able to maintain amino acid levels during starvation over this period, possibly a reflection of their slower rate of proliferation (and relatively inferior requirement for free amino acids) compared to MDAMB231 cells. Interestingly, the capacity of MDAMB231 cells and MCF12A cells to maintain amino acid levels at 6 and 24 hours respectively reflects their tolerance to amino acid deprivation and their ability to mitigate cell death during these conditions (chapter 1). Further investigation revealed that a bafilomycin-sensitive mechanism is responsible for the buffering of amino acid levels at 6 hours of amino acid deprivation in MDAMB231 cells (Fig 3.5). Remarkably, bafilomycin A1 (10 nM) during amino acid starvation completely abolished the transient surge in free intracellular total and essential amino acid levels at 6 hours in MDAMB231 cells. A similar bafilomycin-sensitive decrease in amino acid content was also noted in MCF12A cells at 6 hours (Fig 3.6). Notably, a significant decrease in total cellular amino content of MCF12A cells was observed at 24 hours as well. Taken together, it is clear that the capacity of these cell lines to successfully maintain amino acid levels is directly related to their respective tolerances to a starvation event of this type, which can be effectively blunted with bafilomycin A1 (described in chapter 1 and chapter 2). As bafilomycin A1 inhibits the fusion of autophagosomes with lysosomes (and thereby inhibits degradation of proteins and generation of amino acids by autophagy), this is strong support for the hypothesis that autophagy is responsible for the generation of amino acids during these conditions.

167

Much indirect evidence suggests that autophagy is an intracellular system of amino acid generation, although amino acids have also been repeatedly demonstrated to inhibit autophagy (Mortimore and Schworer, 1977). Liver autophagy has recently been shown to contribute to the maintenance of amino acid levels (Ezaki et al., 2011), but as the amino acid concentrations in blood are mostly unchanged during starvation (Kuma and Mizushima, 2010), few studies have thought to directly measure amino acid changes and relate them to autophagy. The transient amino acid surge observed in this study has not been demonstrated elsewhere in the cancer context, but similar transient increases have infrequently been described in the literature before. During nitrogen starvation, yeast were found to transiently generate amino acids in a similar way, but autophagy defective cells treated in a comparable manner did not display a similar spike in amino acid content (Onodera and Ohsumi, 2005). Also, starved rat kidney cells in culture also show a rapid short lived increase in autophagy (Yu et al., 2010). In the seminal *in vivo* study describing the role of autophagy during the early neonatal period it was shown that, after birth, a transient increase in autophagy peaks after 3-6 hours before subsiding (Kuma et al., 2004), and is vital for the maintenance of plasma and tissue amino acid concentrations during this period.

Recently it has been proposed that cancers with high basal autophagy levels may have evolved to require autophagy for continued progression. In particular, cancers with mutations in H-*ras* or K-*ras* may need autophagy for tumour survival (Guo et al., 2011), and data from recent studies suggests that pancreatic (Yang et al., 2011) and other Ras-driven tumours (Lock et al., 2011) require autophagy for sustained growth. In fact, it appears as though these cancers are partly reliant on a system of oxidative phosphorylation for energy production. Indeed, inhibition of autophagy in these cancers leads to a decrease in ATP generation (Yang et al., 2011). This so-called autophagy-addiction has been suggested to be a property typical of these Ras-driven tumours. Although genetic *ras* mutations are infrequent in breast cancer,

168

Ras was shown to be highly and abnormally activated in over 50% of tested cancers in one study (von Lintig et al., 2000), owing to the high prevalence of mutations elsewhere in this pathway. MDAMB231 cells are known to have high basal autophagy and high *ras* activation (Ogata et al., 2001), and therefore may also rely on autophagy for the generation of substrates for energy production.

5.2   Autophagy regulation of ATP levels in MDAMB231 cells

Bioenergetic activities are regulated by the TCA cycle in the mitochondria. Oxidizable substrates are provided through the electron transport chain, reducing molecular oxygen to water and fuelling oxidative phosphorylation for ATP production. Although generally considered to be poor fuel substrates, amino acids can be consumed to generate energy in this way. Although infrequently demonstrated experimentally, there is some precedent in the literature, and amino acid starvation of yeast leads to the rapid depression of ATP levels after just 3 hours. Also, extreme decreases in ATP levels of growth factor deprived cells after 5 hours of incubation with 3-methyladenine can be mostly rescued by the administration of methylpyruvate (Lum et al., 2005). As bafilomycin A1 (10 nM) is only administered 6 hours prior to analysis in the current study, it allows for delineation of autophagy influence at specific times of interest in this model.

Interestingly, the ATP content in MDAMB231 cells mirrored the changes in the capacity of this cell line to maintain intracellular amino acid levels (Fig 3.3). Furthermore, the ability of MDAMB231 cells to maintain ATP levels during the first 6 hours of amino acid starvation was abolished in the presence of bafilomycin A1 (10 nM) (Fig 3.7). This evidence suggests that either amino acids generated in a bafilomycin-sensitive manner (such as autophagy) or

169

another corresponding mechanism associated with this amino acid generation might be important for the maintenance of ATP in this cell line. In order to investigate if the decreases in ATP observed when bafilomycin A1 was added to culture medium was due to an autophagy related mechanism, MDAMB231 and MCF12A cells were transfected with ATG5 siRNA 48 hours prior to incubation in amino acid free medium. Indeed, the ATP levels of cells in either the normal or amino acid free medium were observed to be significantly lower if the cells had been transfected with ATG5 siRNA (Fig 3.9). Furthermore, ATP levels were significantly diminished in both cell lines when they were incubated in the absence of amino acids compared to when they were incubated in the presence of amino acids (Fig 3.9). Collectively, this suggests that the maintenance of intracellular amino acids by autophagy (in a process inhibitable by bafilomycin A1) is important for the preservation of ATP levels in these cell lines, and that MDAMB231 cells are particularly reliant on autophagy derived amino acids for homeostasis during the first 6 hours of amino acid deprivation. At this point it is not clear how a decrease in amino acid levels leads to a decrease in cellular ATP content, but it is evident that the buffering capacity of autophagy is able to prevent this decline in ATP in both cell lines.

Cancer is widely believed to rely on glycolysis for energy production. Although this observation remains true for some cancer types, it now appears that many cancers rely on both glycolysis and oxidative phosphorylation for energy production. Moreover, in many other cancers, oxidative phosphorylation may be the predominant and preferred form of energy generation. A particular strength of the model used in this study is that it does not limit cellular access to glucose. Therefore, any changes to energy levels following amino acid depletion could be correlated with glucose uptake in order to assess if a dearth in available amino acids impacts on the ability of these cells to take in glucose. Interestingly, the non-malignant epithelial cell line, MCF12A, has measurable levels of GLUT 1 and HK 1, which

170

are considerably higher than other non-cancer cell lines; and these cells are able to take up significant amounts of a 2-deoxy-glucose analogue from a glucose free medium (Millon et al., 2011). Although normal mammary epithelial cells rarely over-express GLUT 1 (Bos et al., 2002) it is likely that GLUT 1 expression occurred during immortalization of these cells. For the purposes of this study it allowed direct measurement of 2-deoxy-glucose uptake and comparison with another GLUT 1 over-expressing cell line, MDAMB231 (Millon et al., 2011). Experimental evidence presented here demonstrates that MDAMB231 cells have high glucose uptake at baseline compared to the non-cancer line, and that starvation leads to significantly increased glucose uptake after 24 hours, in the cancer cell line only (Fig 3.11). This indicates that molecular changes within these cells have allowed them to adapt to metabolic stress by increasing glucose uptake, a phenomenon that has been demonstrated in these cells previously (Li et al., 2009). However, despite increases in glucose uptake decreases in ATP levels were still observed. In fact, even though glucose uptake was shown to increase slightly, ATP levels dropped significantly after 24 hours of amino acid starvation.

5.3   Branched chain amino acids, and possibly free fatty acids, are potential sources for ATP generation in MDAMB231 cells

The three branched chain amino acids (leucine, isoleucine, and valine) are among the essential amino acids for humans. These amino acids have been postulated as a source of oxidizable substrates for use in energy production, and activity of the branched-chain α-ketoacid dehydrogenase complex (BCKDH) has been shown to be up-regulated during starvation (Harris et al., 1989). Still, no discernable increase in the expression levels of BCKDH were found during the 24 hour amino acid starvation of MDAMB231 cells in this study (data not shown). Activation of the BCKDH complex catalyzes the second-step in the reaction of the

BCAA catabolic pathway and is essential for branched chain amino acid catabolism in the mitochondria. Also, the preferential reduction of BCAA in neonates with Atg5−/− and Atg7 −/− is an indication of enhanced consumption of these amino acids as an energy source (Kuma et al., 2004). As MDAMB231 cells do not appear to have a diminished capacity for glucose uptake during amino acid starvation, and a surge in the cellular free branched chain amino acids levels is obvious during short periods of amino acid deprivation, further investigation into whether this particular subset of amino acids are partly responsible for ATP maintenance was merited.

The addition of BCKDH siRNA during amino acid starvation lead to a significant accumulation of the branched chain amino acids in MDAMB231 cells at 6 hours of amino acid starvation but no corresponding accumulation in MCF12A cells (Fig 3.19 and Fig 3.20). As no accumulation is observed if BCKDH translation is blocked in cells cultured in amino acid complete conditions, it is plausible that a significant amount of the branched chain amino acids generated at 6 hours during amino acid starvation are being converted into substrates useable by the mitochondria, potentially for energy production in these cells. Furthermore, the fact that the inhibition of BCKDH expression significantly decreases ATP content in these cells (Fig 3.21), but not in MCF12A cells (Fig 3.22), during amino acid starvation adds credence to the assertion that branched chain amino acids generated during amino acid starvation are being used as fuel substrates for homeostasis maintenance. Importantly, if autophagy is simultaneously inhibited in MDAMB231 cells treated with BCKDH siRNA, then the accumulation of branched chain amino acids decreases (Fig 3.23), indicating that autophagy is an important process responsible for the generation of these amino acids for use as fuel substrates. Also, as branched chain amino acids are not a major fuel source during basal, amino acid replete, conditions (Fig 3.18), this evidence signifies that these cells may

have shifted their preference for substrate utilization in energy generation. More evidence is required to assess the plausibility of this claim.

Proteins are not the only constituents of the cytoplasm that become degraded during autophagy. Although only scant evidence is currently available, it now appears that autophagy has an important role in the degradation of intracellular lipids and in the regulation of lipid metabolism. Since numerous organelles (including mitochondria and peroxisomes) have been observed in autophagosomes and autolysosomes, degradation of their membrane phospholipids could contribute to energy generation in times of need. As evidence within this study does imply a change in substrate preference during amino acid deprivation, the fatty acid content within these cells was analysed during amino acid starvation. Indeed, the free fatty acid content of MDAMB231 cells was higher if they were incubated for 6 hours in amino acid free medium (Fig 3.25), and remained elevated at 24 hours of amino acid starvation. Importantly, the quantity of the most abundant saturated fatty acid, stearic acid, was higher in MDAMB231 cells after 6 hours, but not after 24 hours in amino acid free medium, this apparent decrease indicating its utilization within the cell. As bafilomycin (10 nM) and ATG5 siRNA were able to prevent the increase in free fatty acids at 6 hours of amino acid starvation, it is likely that it is driven by a process mediated through autophagy. Also, inhibition of β-oxidation using etomoxir (200 µM) lowers ATP content in MDAMB231 cells at 6 hours (Fig 3.28) and in MCF12A at 24 hours (Fig 3.29). This change correlates directly with previous findings that show autophagy to be important for tolerance of amino acid deprivation when these cell lines are deprived of amino acids for those time periods.

5.4   Conclusions

Collectively, this study provides very compelling evidence that MDAMB231 cells are able to transiently degrade cytoplasmic contents in order to tolerate a short term reduction in amino acids. Additionally, a potential mechanism is provided here, where preferential utilization of autophagy-produced fuel substrates, can buffer against decreases in ATP levels during this short period of amino acid deprivation.

The need for ATP does not always remain constant. Demand for substrates (assessed though demand for the universal free energy transmitter (ATP) of the cell) must be balanced with supply, and the increase in autophagy activity should not be separated from the processes that utilize its products. Currently, ignorance of the energy requirements of cancer cells and the possible role of autophagy necessitates continued research into this important area of oncology.

5.5   Limitations and future recommendations

Although evidence in the present study convincingly implicates autophagy, and the associated generation of amino acids, in tolerance to amino acid deprivation (partly through maintenance of ATP levels), other mechanisms for amino acid maintenance do exist. The addition of proteosome inhibitors and further assessment of the role of the proteosome in the maintenance of amino acids is important. Furthermore, this study is not able to delineate whether MDAMB231 cells have an altered substrate preference during amino acid starvation. Future assessment of oxygen consumption and the role (and relative weight) that various substrates have with regard to ATP generation is recommended.

6   References

AZNAVOORIAN, S., STRACKE, M. L., KRUTZSCH, H., SCHIFFMANN, E. & LIOTTA, L. A. 1990. Signal transduction for chemotaxis and haptotaxis by matrix molecules in tumor cells. *J Cell Biol,* 110**,** 1427-38.

BOS, R., VAN DER HOEVEN, J. J., VAN DER WALL, E., VAN DER GROEP, P., VAN DIEST, P. J., COMANS, E. F., JOSHI, U., SEMENZA, G. L., HOEKSTRA, O. S., LAMMERTSMA, A. A. & MOLTHOFF, C. F. 2002. Biologic correlates of (18)fluorodeoxyglucose uptake in human breast cancer measured by positron emission tomography. *J Clin Oncol,* 20**,** 379-87.

BROWN, J. M. 2000. Exploiting the hypoxic cancer cell: mechanisms and therapeutic strategies. *Mol Med Today,* 6**,** 157-62.

BRUGAROLAS, J., LEI, K., HURLEY, R. L., MANNING, B. D., REILING, J. H., HAFEN, E., WITTERS, L. A., ELLISEN, L. W. & KAELIN, W. G., JR. 2004. Regulation of mTOR function in response to hypoxia by REDD1 and the TSC1/TSC2 tumor suppressor complex. *Genes Dev,* 18**,** 2893-904.

CHENG, Y., LI, H., REN, X., NIU, T., HAIT, W. N. & YANG, J. 2010. Cytoprotective effect of the elongation factor-2 kinase-mediated autophagy in breast cancer cells subjected to growth factor inhibition. *PLoS One,* 5**,** e9715.

DA POIAN, A. T., EL-BACHA, T. & LUZ, M. R. 2010. Nutrient Utilization in Humans: Metabolism Pathways. . *Nature Education* 3(9):11.

DEGENHARDT, K., MATHEW, R., BEAUDOIN, B., BRAY, K., ANDERSON, D., CHEN, G., MUKHERJEE, C., SHI, Y., GELINAS, C., FAN, Y., NELSON, D. A., JIN, S. & WHITE, E. 2006. Autophagy promotes tumor cell survival and restricts necrosis, inflammation, and tumorigenesis. *Cancer Cell,* 10**,** 51-64.

DEGENHARDT, K. & WHITE, E. 2006. A mouse model system to genetically dissect the molecular mechanisms regulating tumorigenesis. *Clin Cancer Res,* 12**,** 5298-304.

EZAKI, J., MATSUMOTO, N., TAKEDA-EZAKI, M., KOMATSU, M., TAKAHASHI, K., HIRAOKA, Y., TAKA, H., FUJIMURA, T., TAKEHANA, K., YOSHIDA, M., IWATA, J., TANIDA, I., FURUYA, N., ZHENG, D. M., TADA, N., TANAKA, K., KOMINAMI, E. & UENO, T. 2011. Liver autophagy contributes to the maintenance of blood glucose and amino acid levels. *Autophagy,* 7**,** 727-36.

FINN, P. F. & DICE, J. F. 2006. Proteolytic and lipolytic responses to starvation. *Nutrition,* 22**,** 830-44.

FOLKMAN, J. 1971. Tumor angiogenesis: therapeutic implications. *N Engl J Med,* 285**,** 1182-6.

FORSYTHE, J. A., JIANG, B. H., IYER, N. V., AGANI, F., LEUNG, S. W., KOOS, R. D. & SEMENZA, G. L. 1996. Activation of vascular endothelial growth factor gene transcription by hypoxia-inducible factor 1. *Mol Cell Biol,* 16**,** 4604-13.

FREZZA, C., ZHENG, L., TENNANT, D. A., PAPKOVSKY, D. B., HEDLEY, B. A., KALNA, G., WATSON, D. G. & GOTTLIEB, E. 2011. Metabolic profiling of hypoxic cells revealed a catabolic signature required for cell survival. *PLoS One,* 6**,** e24411.

FRIBERG, S. & MATTSON, S. 1997. On the growth rates of human malignant tumors: implications for medical decision making. *J Surg Oncol,* 65**,** 284-97.

GILLIES, R. J., ROBEY, I. & GATENBY, R. A. 2008. Causes and consequences of increased glucose metabolism of cancers. *J Nucl Med,* 49 Suppl 2**,** 24S-42S.

GU, J., YAMAMOTO, H., OGAWA, M., NGAN, C. Y., DANNO, K., HEMMI, H., KYO, N., TAKEMASA, I., IKEDA, M., SEKIMOTO, M. & MONDEN, M. 2006. Hypoxia-induced up-regulation of angiopoietin-2 in colorectal cancer. *Oncol Rep,* 15**,** 779-83.

GUO, J. Y., CHEN, H. Y., MATHEW, R., FAN, J., STROHECKER, A. M., KARSLI-UZUNBAS, G., KAMPHORST, J. J., CHEN, G., LEMONS, J. M., KARANTZA, V., COLLER, H. A., DIPAOLA, R. S., GELINAS, C., RABINOWITZ, J. D. & WHITE, E. 2011. Activated Ras requires autophagy to maintain oxidative metabolism and tumorigenesis. *Genes Dev,* 25**,** 460-70.

GUPPY, M., LEEDMAN, P., ZU, X. & RUSSELL, V. 2002. Contribution by different fuels and metabolic pathways to the total ATP turnover of proliferating MCF-7 breast cancer cells. *Biochem J,* 364**,** 309-15.

HAN, X., LIU, J. X. & LI, X. Z. 2011. Salvianolic acid B inhibits autophagy and protects starving cardiac myocytes. *Acta Pharmacol Sin,* 32**,** 38-44.

HANAHAN, D. & WEINBERG, R. A. 2011. Hallmarks of cancer: the next generation. *Cell,* 144**,** 646-74.

HARDIE, D. G. 2007. AMP-activated/SNF1 protein kinases: conserved guardians of cellular energy. *Nat Rev Mol Cell Biol,* 8**,** 774-85.

HARRIS, R. A., GOODWIN, G. W., PAXTON, R., DEXTER, P., POWELL, S. M., ZHANG, B., HAN, A., SHIMOMURA, Y. & GIBSON, R. 1989. Nutritional and hormonal regulation of the activity state of hepatic branched-chain alpha-keto acid dehydrogenase complex. *Ann N Y Acad Sci,* 573**,** 306-13.

HEGEN, A., KOIDL, S., WEINDEL, K., MARME, D., AUGUSTIN, H. G. & FIEDLER, U. 2004. Expression of angiopoietin-2 in endothelial cells is controlled by positive and negative regulatory promoter elements. *Arterioscler Thromb Vasc Biol,* 24**,** 1803-9.

HSU, P. P. & SABATINI, D. M. 2008. Cancer cell metabolism: Warburg and beyond. *Cell,* 134**,** 703-7.

INOKI, K., ZHU, T. & GUAN, K. L. 2003. TSC2 mediates cellular energy response to control cell growth and survival. *Cell,* 115**,** 577-90.

IZUISHI, K., KATO, K., OGURA, T., KINOSHITA, T. & ESUMI, H. 2000. Remarkable tolerance of tumor cells to nutrient deprivation: possible new biochemical target for cancer therapy. *Cancer Res,* 60**,** 6201-7.

JIN, S. & WHITE, E. 2008. Tumor suppression by autophagy through the management of metabolic stress. *Autophagy,* 4**,** 563-6.

KALLINOWSKI, F., SCHLENGER, K. H., KLOES, M., STOHRER, M. & VAUPEL, P. 1989. Tumor blood flow: the principal modulator of oxidative and glycolytic metabolism, and of the metabolic micromilieu of human tumor xenografts in vivo. *Int J Cancer,* 44**,** 266-72.

KANAMORI, H., TAKEMURA, G., MARUYAMA, R., GOTO, K., TSUJIMOTO, A., OGINO, A., LI, L., KAWAMURA, I., TAKEYAMA, T., KAWAGUCHI, T., NAGASHIMA, K., FUJIWARA, T., FUJIWARA, H., SEISHIMA, M. & MINATOGUCHI, S. 2009. Functional significance and morphological characterization of starvation-induced autophagy in the adult heart. *Am J Pathol,* 174**,** 1705-14.

KARANTZA-WADSWORTH, V., PATEL, S., KRAVCHUK, O., CHEN, G., MATHEW, R., JIN, S. & WHITE, E. 2007. Autophagy mitigates metabolic stress and genome damage in mammary tumorigenesis. *Genes Dev,* 21**,** 1621-35.

KATAYAMA, M., KAWAGUCHI, T., BERGER, M. S. & PIEPER, R. O. 2007. DNA damaging agent-induced autophagy produces a cytoprotective adenosine triphosphate surge in malignant glioma cells. *Cell Death Differ,* 14**,** 548-58.

KERBEL, R. S. 2000. Tumor angiogenesis: past, present and the near future. *Carcinogenesis,* 21**,** 505-15.

KLIONSKY, D. J. 2007. Autophagy: from phenomenology to molecular understanding in less than a decade. *Nat Rev Mol Cell Biol,* 8**,** 931-7.

KOMATSU, M., WAGURI, S., UENO, T., IWATA, J., MURATA, S., TANIDA, I., EZAKI, J., MIZUSHIMA, N., OHSUMI, Y., UCHIYAMA, Y., KOMINAMI, E., TANAKA,

K. & CHIBA, T. 2005. Impairment of starvation-induced and constitutive autophagy in Atg7-deficient mice. *J Cell Biol,* 169**,** 425-34.

KOTOULAS, O. B., KALAMIDAS, S. A. & KONDOMERKOS, D. J. 2006. Glycogen autophagy in glucose homeostasis. *Pathol Res Pract,* 202**,** 631-8.

KUMA, A., HATANO, M., MATSUI, M., YAMAMOTO, A., NAKAYA, H., YOSHIMORI, T., OHSUMI, Y., TOKUHISA, T. & MIZUSHIMA, N. 2004. The role of autophagy during the early neonatal starvation period. *Nature,* 432**,** 1032-6.

KUMA, A. & MIZUSHIMA, N. 2010. Physiological role of autophagy as an intracellular recycling system: with an emphasis on nutrient metabolism. *Semin Cell Dev Biol,* 21**,** 683-90.

LEVINE, B. & KROEMER, G. 2008. Autophagy in the pathogenesis of disease. *Cell,* 132**,** 27-42.

LI, Y., WANG, H., OOSTERWIJK, E., TU, C., SHIVERICK, K. T., SILVERMAN, D. N. & FROST, S. C. 2009. Expression and activity of carbonic anhydrase IX is associated with metabolic dysfunction in MDA-MB-231 breast cancer cells. *Cancer Invest,* 27**,** 613-23.

LIANG, J., SHAO, S. H., XU, Z. X., HENNESSY, B., DING, Z., LARREA, M., KONDO, S., DUMONT, D. J., GUTTERMAN, J. U., WALKER, C. L., SLINGERLAND, J. M. & MILLS, G. B. 2007. The energy sensing LKB1-AMPK pathway regulates p27(kip1) phosphorylation mediating the decision to enter autophagy or apoptosis. *Nat Cell Biol,* 9**,** 218-24.

LOCK, R., ROY, S., KENIFIC, C. M., SU, J. S., SALAS, E., RONEN, S. M. & DEBNATH, J. 2011. Autophagy facilitates glycolysis during Ras-mediated oncogenic transformation. *Mol Biol Cell,* 22**,** 165-78.

LU, Z., LUO, R. Z., LU, Y., ZHANG, X., YU, Q., KHARE, S., KONDO, S., KONDO, Y., YU, Y., MILLS, G. B., LIAO, W. S. & BAST, R. C., JR. 2008. The tumor suppressor gene ARHI regulates autophagy and tumor dormancy in human ovarian cancer cells. *J Clin Invest,* 118**,** 3917-29.

LUM, J. J., BAUER, D. E., KONG, M., HARRIS, M. H., LI, C., LINDSTEN, T. & THOMPSON, C. B. 2005. Growth factor regulation of autophagy and cell survival in the absence of apoptosis. *Cell,* 120**,** 237-48.

MARUYAMA, R., GOTO, K., TAKEMURA, G., ONO, K., NAGAO, K., HORIE, T., TSUJIMOTO, A., KANAMORI, H., MIYATA, S., USHIKOSHI, H., NAGASHIMA, K., MINATOGUCHI, S., FUJIWARA, T. & FUJIWARA, H. 2008. Morphological and biochemical characterization of basal and starvation-induced autophagy in isolated adult rat cardiomyocytes. *Am J Physiol Heart Circ Physiol,* 295**,** H1599-607.

MATHEW, R., KARANTZA-WADSWORTH, V. & WHITE, E. 2007a. Role of autophagy in cancer. *Nat Rev Cancer,* 7**,** 961-7.

MATHEW, R., KONGARA, S., BEAUDOIN, B., KARP, C. M., BRAY, K., DEGENHARDT, K., CHEN, G., JIN, S. & WHITE, E. 2007b. Autophagy suppresses tumor progression by limiting chromosomal instability. *Genes Dev,* 21**,** 1367-81.

MATSUI, Y., TAKAGI, H., QU, X., ABDELLATIF, M., SAKODA, H., ASANO, T., LEVINE, B. & SADOSHIMA, J. 2007. Distinct roles of autophagy in the heart during ischemia and reperfusion: roles of AMP-activated protein kinase and Beclin 1 in mediating autophagy. *Circ Res,* 100**,** 914-22.

MILLON, S. R., OSTRANDER, J. H., BROWN, J. Q., RAHEJA, A., SEEWALDT, V. L. & RAMANUJAM, N. 2011. Uptake of 2-NBDG as a method to monitor therapy response in breast cancer cell lines. *Breast Cancer Res Treat,* 126**,** 55-62.

MIZUSHIMA, N. 2007. Autophagy: process and function. *Genes Dev,* 21**,** 2861-73.

MORTIMORE, G. E. & POSO, A. R. 1987. Intracellular protein catabolism and its control during nutrient deprivation and supply. *Annu Rev Nutr,* 7**,** 539-64.

MORTIMORE, G. E. & SCHWORER, C. M. 1977. Induction of autophagy by amino-acid deprivation in perfused rat liver. *Nature,* 270**,** 174-6.

NELSON, D. A., TAN, T. T., RABSON, A. B., ANDERSON, D., DEGENHARDT, K. & WHITE, E. 2004. Hypoxia and defective apoptosis drive genomic instability and tumorigenesis. *Genes Dev,* 18**,** 2095-107.

OGATA, H., SATO, H., TAKATSUKA, J. & DE LUCA, L. M. 2001. Human breast cancer MDA-MB-231 cells fail to express the neurofibromin protein, lack its type I mRNA isoform and show accumulation of P-MAPK and activated Ras. *Cancer Lett,* 172**,** 159-64.

ONODERA, J. & OHSUMI, Y. 2005. Autophagy is required for maintenance of amino acid levels and protein synthesis under nitrogen starvation. *J Biol Chem,* 280**,** 31582-6.

OWEN, O. E., KALHAN, S. C. & HANSON, R. W. 2002. The key role of anaplerosis and cataplerosis for citric acid cycle function. *J Biol Chem,* 277**,** 30409-12.

PAUWELS, E. K., STURM, E. J., BOMBARDIERI, E., CLETON, F. J. & STOKKEL, M. P. 2000. Positron-emission tomography with [18F]fluorodeoxyglucose. Part I. Biochemical uptake mechanism and its implication for clinical studies. *J Cancer Res Clin Oncol,* 126**,** 549-59.

POUYSSEGUR, J., DAYAN, F. & MAZURE, N. M. 2006. Hypoxia signalling in cancer and approaches to enforce tumour regression. *Nature,* 441**,** 437-43.

QU, X., ZOU, Z., SUN, Q., LUBY-PHELPS, K., CHENG, P., HOGAN, R. N., GILPIN, C. & LEVINE, B. 2007. Autophagy gene-dependent clearance of apoptotic cells during embryonic development. *Cell,* 128**,** 931-46.

RACKER, E. 1974. History of the Pasteur effect and its pathobiology. *Mol Cell Biochem,* 5**,** 17-23.

REITZER, L. J., WICE, B. M. & KENNELL, D. 1979. Evidence that glutamine, not sugar, is the major energy source for cultured HeLa cells. *J Biol Chem,* 254**,** 2669-76.

REW, D. A. & WILSON, G. D. 2000. Cell production rates in human tissues and tumours and their significance. Part II: clinical data. *Eur J Surg Oncol,* 26**,** 405-17.

RODRIGUEZ-ENRIQUEZ, S., VITAL-GONZALEZ, P. A., FLORES-RODRIGUEZ, F. L., MARIN-HERNANDEZ, A., RUIZ-AZUARA, L. & MORENO-SANCHEZ, R. 2006. Control of cellular proliferation by modulation of oxidative phosphorylation in human and rodent fast-growing tumor cells. *Toxicol Appl Pharmacol,* 215**,** 208-17.

SEMENZA, G. L. 2008. Tumor metabolism: cancer cells give and take lactate. *J Clin Invest,* 118**,** 3835-7.

SHIBATA, M., YOSHIMURA, K., FURUYA, N., KOIKE, M., UENO, T., KOMATSU, M., ARAI, H., TANAKA, K., KOMINAMI, E. & UCHIYAMA, Y. 2009. The MAP1-LC3 conjugation system is involved in lipid droplet formation. *Biochem Biophys Res Commun,* 382**,** 419-23.

SINGH, R., KAUSHIK, S., WANG, Y., XIANG, Y., NOVAK, I., KOMATSU, M., TANAKA, K., CUERVO, A. M. & CZAJA, M. J. 2009. Autophagy regulates lipid metabolism. *Nature,* 458**,** 1131-5.

TOKUNAGA, C., YOSHINO, K. & YONEZAWA, K. 2004. mTOR integrates amino acid- and energy-sensing pathways. *Biochem Biophys Res Commun,* 313**,** 443-6.

TREDAN, O., GALMARINI, C. M., PATEL, K. & TANNOCK, I. F. 2007. Drug resistance and the solid tumor microenvironment. *J Natl Cancer Inst,* 99**,** 1441-54.

TSUKADA, M. & OHSUMI, Y. 1993. Isolation and characterization of autophagy-defective mutants of Saccharomyces cerevisiae. *FEBS Lett,* 333**,** 169-74.

TSUKAMOTO, S., KUMA, A., MURAKAMI, M., KISHI, C., YAMAMOTO, A. & MIZUSHIMA, N. 2008. Autophagy is essential for preimplantation development of mouse embryos. *Science,* 321**,** 117-20.

VAUPEL, P., KALLINOWSKI, F. & OKUNIEFF, P. 1989. Blood flow, oxygen and nutrient supply, and metabolic microenvironment of human tumors: a review. *Cancer Res,* 49**,** 6449-65.

VON LINTIG, F. C., DREILINGER, A. D., VARKI, N. M., WALLACE, A. M., CASTEEL, D. E. & BOSS, G. R. 2000. Ras activation in human breast cancer. *Breast Cancer Res Treat,* 62**,** 51-62.

WARBURG, O. 1956. On the origin of cancer cells. *Science,* 123**,** 309-14.

YANG, S., WANG, X., CONTINO, G., LIESA, M., SAHIN, E., YING, H., BAUSE, A., LI, Y., STOMMEL, J. M., DELL'ANTONIO, G., MAUTNER, J., TONON, G., HAIGIS, M., SHIRIHAI, O. S., DOGLIONI, C., BARDEESY, N. & KIMMELMAN, A. C. 2011. Pancreatic cancers require autophagy for tumor growth. *Genes Dev,* 25**,** 717-29.

YIN, X. M., DING, W. X. & GAO, W. 2008. Autophagy in the liver. *Hepatology,* 47**,** 1773-85.

YU, L., MCPHEE, C. K., ZHENG, L., MARDONES, G. A., RONG, Y., PENG, J., MI, N., ZHAO, Y., LIU, Z., WAN, F., HAILEY, D. W., OORSCHOT, V., KLUMPERMAN, J., BAEHRECKE, E. H. & LENARDO, M. J. 2010. Termination of autophagy and reformation of lysosomes regulated by mTOR. *Nature,* 465**,** 942-6.

ZONG, W. X. & THOMPSON, C. B. 2006. Necrotic death as a cell fate. *Genes Dev,* 20**,** 1-15.

ZU, X. L. & GUPPY, M. 2004. Cancer metabolism: facts, fantasy, and fiction. *Biochem Biophys Res Commun,* 313**,** 459-65.

4 _____

Changes in lysosomal acidity due to amino acid starvation are associated with susceptibility to doxorubicin mediated cell death in MDAMB231 cells and tolerance to doxorubicin in MCF12A cells

Autophagy appears to have conflicting roles in response to cancer therapy. Even so, many clinical trials are beginning to assess the effectiveness of compounds known to regulate autophagy, in patients receiving anticancer therapy. Furthermore, short term starvation has shown promise in alleviating some of the symptoms associated with chemotherapy, posing questions regarding the role of autophagy in these circumstances. Short term, complete amino acid deprivation elicits dynamic alterations to the acidic compartmentalization of the tumourogenic cancer cell line MDAMB231 (chapter 2). We demonstrate in this chapter that decreased lysosomal acidity associated with amino acid starvation in MDAMB231 cells treated with doxorubicin correlates with decreased cell survival, whereas sustained elevation of autophagy in MCF12A cells during similar treatment is associated with a relative protection from cell death.

1   Introduction

Solid tumours make up the majority of all human cancers. Once solid neoplasms become established they can partially adapt to local microenvironmental shortages in nutrient supply by increasing autophagy (Mathew et al., 2007a). Even though autophagy is considered to be an important mechanism whereby cancer cells are able to survive stressful environmental conditions, it has been given roles in tumour suppression (Aita et al., 1999) and the promotion of tumour progression and survival (Degenhardt et al., 2006) depending on context. It is now also known that many anti-cancer agents and therapies increase autophagy levels in treated cancer cells at certain doses (Wu et al., 2006, Park et al., 2008). Transient, rapid and unpredictable alterations in autophagy flux could modify the way that tumours respond to

180

chemotherapy and supposedly interfere with or even augment therapy outcomes in unexpected ways. In fact, reports vary as to whether increases in autophagy are protective (Park et al., 2008) or detrimental (Garcia-Escudero and Gargini, 2008) to cancer cells undergoing these treatments.

Autophagy has recently become a popular target for opposing chemotherapy resistance, and measurement of autophagy and its associated markers are now also being considered for their prognostic relevance and value (Giatromanolaki et al., 2010, Ma et al., 2011). Furthermore, many patients with increased solid tumour autophagy have presented with increased resistance to chemotherapy. On the other hand, cancer variants with known autophagy deficiencies could be susceptible to agents that are able to effectively augment autophagy (Turcotte et al., 2008). Divergent responses and outcomes demand that the basic underlying systems controlling autophagy in these situations be resolved if therapeutic modulation of this process is to be successfully implemented in cancer patients already receiving conventional treatments.

1.2   Clinical autophagy detection

If autophagy is to be used effectively in a clinical environment, then improved methods of detection for the autophagy status of tumour cells, and the influence of autophagy modulating agents on these autophagic levels, are needed. Currently, methods for the *in vivo* assessment of autophagy are lacking but, most recently, plasma levels of clusterin protein were demonstrated to decrease during autophagy induction *in vivo* (Powolny et al., 2011), implying the prospect for its use as a biomarker for autophagy. Furthermore, it is believed that autophagy can be used as a potential prognostic marker in certain cancer cells (Pirtoli et al., 2009). For example, cytoplasmic Beclin1 levels have been found to correlate with survival in

gliomas (Pirtoli et al., 2009), while morphological changes associated with increased autophagy predicted survival and invasiveness in melanomas (Ma et al., 2011). Interestingly, there has been a suggestion that increased autophagy levels could serve as a marker to indicate whether some cancers will be sensitive to chemotherapy or not (Nicotra et al., 2010), but evidence remains inconclusive at present (Won et al., 2010). It is crucial that oncologists develop methods to determine which cancers are capable of autophagy induction and whether any increases in autophagy would confer survival advantages or bring about changes in the capacity of these cells for drug resistance.

1.3   Role of autophagy in drug resistance

Cancers are able to develop resistance to drugs in a multitude of ways. Specialized transporters on cell membranes can accelerate the efflux of certain chemotherapy compounds (Krishna and Mayer, 2000), drugs can be inactivated (Giaccone and Pinedo, 1996) and programmed cell death pathways evaded (Adams and Cory, 2007). It is well established that many cancers possess mutations in key regulators of their apoptosis machinery, and in this way are able to avoid programmed cell death in the face of metabolic or other stresses (Mathew et al., 2007a). Autophagy is important for the maintenance of homeostasis and the initiation of autophagy in these circumstances has been demonstrated to either protect cancer cells from death or lead to it through so-called autophagic cell death (type-II programmed cell death) (Kondo and Kondo, 2006). Cancers such as malignant gliomas possessing the active variant of the Bcl2 gene are resistant to many chemotherapeutic interventions (Kondo et al., 1995), and these malignancies are known to activate autophagy, but not apoptosis, in response to chemotherapy or radiation treatment. Furthermore, HeLa cells over-expressing the anti-apoptotic BCL-XL also display increased autophagy in response to anti-cancer treatments

182

(Shao et al., 2004). Targeting autophagy in circumstances when apoptosis is defective could result in increased efficacy of some drugs.

Autophagy is often observed as a response to chemotherapy (Yang and Chen, 2011). The therapeutic efficacy of several antineoplastic treatments is increased if autophagy is inhibited, which is reliable indication that it is functioning as a mechanism of cytotoxic resistance to these therapies. Evidence in support of this has shown that the inhibition of autophagy sensitized tamoxifen-resistant breast cancer cells (Qadir et al., 2008), lymphomas (Amaravadi et al., 2007) and other mammalian cells (Boya et al., 2005) to apoptosis.

Autophagy is able to reduce the effectiveness of some chemotherapeutics and its regulation could provide a useful anticancer tool. Unfortunately, too little is understood about its role during treatment and there is some support that increasing autophagy could even aid in enhancing treatment efficacy through initiation of autophagy-mediated cell death. A better understanding of the mechanisms underlying autophagy regulation and its consequences is needed.

1.4   Diet, autophagy and cancer treatment

Dietary habits have long been implicated in cancer risk and tumour progression (Popkin, 2007), and one of the most potent stimulators of autophagy is cellular nutritional status. Several dietary factors are known to promote autophagy induction. One of the most effective of these is restriction of dietary calorie intake, which is thought to be one of the most promising strategies by which to extend lifespan (Heilbronn and Ravussin, 2005) and is believed to be an effective tumour suppression mechanism (Kritchevsky, 2003). Dietary restriction leads to reduced glucose and growth hormone levels, and a consequential

autophagy activation (governed by the mTOR pathway) has been implicated in a protective role in decreasing cancer formation and onset (Sell, 2003). Many additional bioactive compounds are also known to increase autophagy levels in cancer as well. For example, curcumin, resveratrol, tocotrienols, vitamin C and vitamin D_3 increased autophagy in brain (Aoki et al., 2007), ovarian and lung (Opipari et al., 2004, Ohshiro et al., 2007), pancreatic (Rickmann et al., 2007), glial and lung (Martin et al., 2002, Ohtani et al., 2007) and head and neck cancers (Tavera-Mendoza et al., 2006) respectively. Even though autophagy is increased in these and other instances, it is difficult to identify the consequences of autophagy augmentation in many of these cases. Further research is needed to clarify the function and role of autophagy in these circumstances before use of these compounds can be sanctioned for clinical use.

Interestingly, a clinical study using a low protein diet to „reactivate‟ autophagy is set to begin phase II trials shortly (table 4.1). Plans are to use a low-protein diet or treatment with the mitochondrial PTP inhibitor cyclosporine A in patients with Bethlem Myopathy or Ullrich Congenital Muscular Dystrophy. Patients will receive a diet with 0.6-0.8 grams of protein/kilogram body weight/day for one year and autophagy specifically monitored over that period (information from clinicaltrial.gov).

Remarkably, the recent application of short term starvation protocols in patients receiving high doses of chemotherapy has proven to have great success in reducing side effects in these patients (Safdie et al., 2009). Although the feasibility and effect of fasting remain unknown, patients diagnosed with a variety of cancers, and undergoing high dose chemotherapy, voluntarily fasted in a protocol of Differential Stress Resistance (DSR) and all enjoyed a decrease of many of the negative symptoms normally associate with the treatments they were receiving. In a cell culture and a neuroblastoma mouse xenograft model, normal cells placed

on a similar starvation protocol were shown to benefit from differential protection compared to cancer cells during high dose chemotherapy regimens (Raffaghello et al., 2008). Mice starved for 48 hours had reduced chemotoxicity following high dose treatment whereas mice fed on *ad libertum* diets were 50% more likely to die while cancer cell death was not compromised by the starvation protocol. The underlying mechanisms responsible for this differential protection of non-cancer cells are not yet known, although reduction of certain growth hormones and up-regulation of stress resistance proteins is believed to play a role (Spindler and Dhahbi, 2007). As many cancers have mutations in key pathways that regulate cellular growth, alterations in the levels of circulating growth factors could impact non-cancer cells to a greater degree. Indeed, extremely low levels of circulating IGF-1 have been associated with chemotherapy resistance in a mouse model (Safdie et al., 2009), and lower IGF-1 levels during dietary restriction correlates with a dramatic reduction in the progression of some cancers (Dunn et al., 1997). However, it is important to note that nutrient starvation protocols are largely untested and there is no evidence of consistency across cancers or even among similar cancer variants. For instance, although nutrient deprivation protected primary glioma cells to chemotherapy in one study (Kim, 2010), other glioma and neuroblastoma cells were not protected following similar treatment. The tolerance of different cell types to different forms of nutrient deprivation still needs extensive investigation.

1.5   Autophagy inhibition in cancer treatment

Based on the premise that autophagy leads to tumour survival in apoptosis deficient cancer cells, it is believed that targeted and specific inhibition of autophagy could be a promising therapeutic avenue. Several *in vitro* studies have illustrated the potential of class-III PI3K inhibitors such as 3-methyladenine, which prevent the formation of autophagosomes, in cancer therapy (Kanzawa et al., 2004). However, while starvation of a cervical cancer cell line

did result in apoptosis in the presence of this inhibitor (Boya et al., 2005), 3-methyladinine prevented tamoxifen induced apoptosis in breast cancer cells elsewhere (Bursch et al., 1996). Agents such as bafilomycin A1, hydroxychloroquine and monensin (all of which prevent lysosomal fusion with autophagosomes) trigger apoptosis during nutrient depletion of HeLa cells (Boya et al., 2005). Also, bafilomycin A1 is able to impede the protective effect of autophagy in several cancer lines undergoing radiation therapy (Paglin et al., 2001).

Several clinical trials, now active or in the recruiting stages, are assessing combination treatment of chemotherapy drugs with modulators of autophagy (table 4.1). The anti-malarial compound chloroquine has been in use since the 1940's but decreased usage has been reported in many countries on account of drug resistance (Savarino et al., 2006). Chloroquine can behave as an autophagy inhibitor due to its capacity to alkalinize lysosomes through proton quenching, and recent studies in mice have demonstrated that chloroquine administration can suppress cancer formation (Maclean et al., 2008) and diminish tumour cell survival (Amaravadi et al., 2007). Drugs such as choloquine and hydrochloroquine are especially attractive adjuvant compounds due to the fact that they have been proven safe for human use over many decades. One small clinical trial utilizing chloroquine in conjunction with standard chemotherapy in glioblastoma patients demonstrated increased survival in the chloroquine treated patients (Sotelo et al., 2006). Choloroquine behaved in a similar manner to another autophagy inhibitor, 3-methyladenine, when it reduced prostate cancer growth *in vitro* and *in vivo* following its administration in conjunction with an anti-cancer treatment (Wu et al., 2010). The autophagy inhibiting property of chloroquine was again implicated in imanitib associated cell death in a chronic myeloid leukaemia model (Bellodi et al., 2009). Another new and promising autophagy inhibitor is lucanthone. This molecule prevents autophagy mediated degradation and induces apoptosis in breast cancer models (Carew et al., 2010). The use of autophagy inhibition in combination with proteosome inhibition is also

under investigation in a clinical setting (table 4.1). Autophagy is functionally linked to the ubiquitin-proteosome system and inhibition of both pathways simultaneously could prove to be even more lethal. Bortezomib is one such proteosome inhibitor that has proven to be effective in treating multiple myeloma (Roccaro et al., 2006), and it is set to continue into phase II trials in combination with hydroxychloroquine in the near future.

Table 4.1 Selection of current clinical trials assessing interventions associated with autophagy alone or as adjuvant to traditional chemotherapy. Information from clinicaltrials.gov (as of October 2011).

Status	Study	Condition	Intervention	Phase
Recruiting	Autophagy Inhibition Using Hydrochloroquine in Breast Cancer Patients	Breast Cancer	Hydrochloroquine	II
Not yet recruiting	Low Protein Diet in Patients With Collagen VI Related Myopathies	Bethlem Myopathy; Ullrich Congenital Muscular Dystrophy	Low protein diet	II
Active, not recruiting	Hydroxychloroquine + Carboplatin, Paclitaxel and Bevacizumb in Non-Small Cell Lung Cancer (NSCLC)	Non-small Cell Lung Cancer	Paclitaxel Carboplatin; Hydroxychloroquine; Bevacizumab	I/II
Recruiting	Hydroxychloroquine in Patients With Stage III or Stage IV Melanoma That Can Be Removed by Surgery	Melanoma (Skin)	Hydroxychloroquine	0
Recruiting	Chloroquine as an Anti-Autophagy Drug in Small Cell Lung Cancer (SCLC) Patients	Small Cell Lung Cancer	Chloroquine, A-CQ 100	I/II
Recruiting	FOLFOX/Bevacizumab/Hydroxychloroquine (HCQ) in Colorectal Cancer	Rectal Cancer; Colon Cancer; Metastasis; Adenocarcinoma	Hydroxychloroquine; Oxaliplatin	I/II
Recruiting	Study of Hydroxychloroquine Before Surgery in Patients With Primary Renal Cell Carcinoma	Renal Cell Carcinoma	Hydroxychloroquine	I
Recruiting	Characterization of the Mechanisms of Resistance to Azacitidine	Myelodysplastic Syndromes or Acute Myeloid Leukemia With Multilineage Dysplasia	?	?
Recruiting	Study of the Efficacy of Chloroquine in the Treatment of Ductal Carcinoma in Situ (The PINC Trial)	Carcinoma, Intraductal, Noninfiltrating; DCIS; Ductal Carcinoma In Situ	Chloroquine	I/II
Recruiting	Hydroxychloroquine and Temsirolimus in Treating Patients With Metastatic Solid Tumors That Have Not Responded to Treatment	Unspecified Adult Solid Tumor, Protocol Specific	Hydroxychloroquine; temsirolimus	I
Recruiting	Hydroxychloroquine, Capecitabine, Oxaliplatin, and Bevacizumab in Treating Patients With Metastatic Colorectal Cancer	Colorectal Cancer	Bevacizumab; XELOX regimen; Hydroxychloroquine	II
Recruiting	Sirolimus or Vorinostat and Hydroxychloroquine in Advanced Cancer	Advanced Cancers	Drug: Hydroxychloroquine; Sirolimus; Vorinostat	I
Recruiting	Hydroxychloroquine + Vorinostat in Advanced Solid Tumors	Advanced Solid Tumor	Hydroxychloroquine; Vorinostat (Suberoylanilide Hydroxamic Acid)	I
Not yet recruiting	Topical Vitamin D3, Diclofenac or a Combination of Both to Treat Basal Cell Carcinoma	Basal Cell Carcinoma	Diclofenac; Diclofenac + Calcitriol; Calcitriol	III
Recruiting	A Study to Evaluate the Use of Chloroquine in Combination With VELCADE and Cyclophosphamide in Patients With Relapsed and Refractory Multiple Myeloma	Multiple Myeloma	Cyclophosphamide; Velcade; Chloroquine	II
Recruiting	Ritonavir and Its Effects on Biomarkers in Women Undergoing Surgery for Newly Diagnosed Breast Cancer	Breast Cancer	Ritonavir; Procedure: therapeutic conventional surgery	I/II
Unknown	Hydroxychloroquine and Bortezomib in Treating Patients With Relapsed or Refractory Multiple Myeloma	Multiple Myeloma and Plasma Cell Neoplasm	Bortezomib; Hydroxychloroquine	I/II
Recruiting	Treatment With Dasatinib in Patients With Acral Lentiginous, Mucosal, or Chronic Sun-damaged Melanoma	Melanoma	Dasatinib	II
Recruiting	Study of Pre-surgery Gemcitabine + Hydroxychloroquine (GcHc) in Stage IIb or III Adenocarcinoma of the Pancreas	Pancreatic Cancer	Hydroxychloroquine; Gemcitabine	I/II
Recruiting	Nelfinavir Mesylate and Bortezomib in Treating Patients With Relapsed or Progressive Advanced Hematologic Cancer	Leukemia; Lymphoma; Mature T-cell and Nk-cell Neoplasms; Multiple Myeloma and Plasma Cell Neoplasm	Bortezomib; nelfinavir mesylate	I

1.6   Autophagy promotion during cancer therapy

Many cancer treatments are known to cause increased autophagy (Yang and Chen, 2011). Although it has been suggested that overactive autophagy can itself be a cell death response, contemporary thought is that autophagy functions primarily as a survival mechanism and that cells die "with" rather than "by" autophagy albeit in rare circumstances (Levine and Kroemer, 2008). However, some cells do appear to undergo cell death by autophagy, with no sign of apoptosis initiation. For example, a pancreatic cancer cell line showed what has been termed an autophagy dependent cell death, that can be abolished with 3-methyladenine (Pardo et al., 2010). An autophagy induced cell death has also been reported in many instances for cancer cells undergoing radiation treatment (Paglin et al., 2001).

Pharmacological agents inhibiting PI3K or Akt can activate autophagy and cell death when used in combination with anti-cancer treatment (Fujiwara et al., 2007). Inhibition of mTOR can also lead to increased cancer cytotoxicity during chemotherapy or radiation treatment (Yao et al., 2010), but these effects have not been linked to autophagy directly, as yet. Even though many of these findings contradict studies using autophagy inhibition as a means to enhance death of cancer cells treated with cytotoxic agents, clinical trials using rapamycin to inhibit mTOR activity are still going ahead (table 4.1).

1.6.1 A role for autophagy in enhancing radiation treatment efficacy

Strategies to increase apoptosis in cancer cells and thereby boost radiation treatment are well sought after and finding measures that complement radiation therapy and amplify apoptosis is a major focus of cancer research. Cancer cells often respond to radiation therapy by inducing autophagy, possibly as an alternative cell death mechanism to apoptosis resistant cells (Paglin

et al., 2001). Inhibiting pro-apoptotic proteins can lead to the induction of autophagy and sensitize cancer cells to radiation treatment. siRNA against Bak/Bax increased autophagy in breast and lung cancer models and sensitized these cells to radiation therapy to a degree determined by the level of autophagy. This sensitization was augmented by the presence of the mTOR inhibitor, Rad001 (Kim et al., 2006b). Inhibition of the mTOR pathway by rapamycin has also been demonstrated to delay tumour growth in soft tissue sarcoma treated with radiation (Murphy et al., 2009). Impairment of apoptosis and an associated increase in autophagy is also thought to be responsible for the enhanced tumour cytotoxicity following radiation treatment in another breast and lung xenograft model (Moretti et al., 2009). Furthermore, induction of autophagy during caspase inhibition enhanced the anti-cancer effects of radiation treatment, in a lung *in vitro* and a mouse cancer xenograft model (Kim et al., 2008).

1.7   Can autophagy defy chemotherapy through drug sequestration?

As our understanding of autophagy broadens, it is becoming clear that the dynamics of this ancient and essential homeostatic mechanism are more complex than first realised. Autophagy has now been implicated in host defence and inflammation following exposure to toxic substances (Levine et al., 2011). Initially, considered as a regulated system of bulk degradation, it is now obvious that autophagy can engulf targets located within the cytoplasm of cells in a selective manner (Yu et al., 2008).

Autophagy is thought to confer resistance onto apoptosis deficient tumour cells receiving anti-cancer therapy by delaying the onset of cellular death in the form of necrosis, resulting from metabolic catastrophe (Mathew et al., 2007a). Although autophagy is viewed as a mechanism to maintain cellular energy homeostasis, its activity is frequently demonstrated to be increased

189

in response to stress. An intriguing alternative hypothesis is that autophagy could act in a complementary manner and ingest drugs that have entered the cell and thereby prevent cancer killing effects by obstructing the access of these agents to the site of their anti-cancer activity. In support of this assertion, the inhibition of autophagy was shown to cause increased cell death of Caco-2 cells following exposure to toxins released by the bacterium Vibrio cholera, where the engulfment and sequestration in lysosomal compartments was proposed as the predominant mechanism of defensive action (Gutierrez et al., 2007). Most recently, HMGB1 (high mobility group box 1) release following chemotherapy induced damage to leukaemia cells caused a protective autophagy response (Liu et al., 2011a), and it has been proposed that the release of damage-associated molecular pattern molecules (DAMPs) during chemotherapy can increase autophagy to grant a defensive reaction (Liu et al., 2011b). In this way, damage caused by cytotoxic agents could directly result in an increased autophagy response.

Alkaline chemotherapy drugs such as the anthracyclines are known to become sequestered and deactivated in the acidic compartments of lysosomes (Hurwitz et al., 1997). Vacuolar ATPases are over-expressed in many multi-drug resistant cancer cells and are associated with the increased sequestration of chemotherapy drugs within these lysosomes (Ma and Center, 1992). Targeting this mechanism of drug sequestration has been proposed as a potential anti-tumour target (Lee and Tannock, 2006). Pharmacologic and genetic inhibition of vacuolar ATPase activity or expression can also reverse resistance to some chemotherapy agents (Herlevsen et al., 2007). Also, agents that increase lysosomal pH, such as the vacuolar ATPase inhibitor bafilomycin A1, are known to inhibit autophagy by preventing fusion of autophagosomes with lysosomes (Klionsky et al., 2008). As autophagy results in bulk cytoplasmic engulfment and delivery of cytoplasmic cargo to acidic lysosomes, and basic cancer drugs that are inhibited upon entering lysosomes will be present within cytoplasmic regions of treated cells, then it stands to reason that increased autophagy could play a role in

the protection of cells from cancer agents in this way. Recent literature has shown how autophagy can become increased in response to chemotherapy induced damage, but, to date, no evidence for the engulfment and delivery of anticancer agents to lysosomes has been described.

1.8   Doxorubicin

The anthracyclines, doxorubicin and epirubicin, were first introduced in the 1960s, and they remain some of the most effective anticancer agents available and are important elements in many breast cancer chemotherapeutic treatment regimens to this day (O'Shaughnessy et al., 2002). Unfortunately, anthracyclines are also cytotoxic and affect a wide variety of systems, often leading to a reduction in the quality of life of many patients, and even death in some cases (Barrett-Lee et al., 2009). Utility of anthracyclines such as doxorubicin is limited as the cardiotoxicity of this drug class is cumulative and dose-limiting. Doxorubicin is more cardiotoxic than epirubicin and progressive myocardial damage is one possible result of its cumulative and dose related effects (Swain et al., 2003). As doxorubicin is a valuable tool in the treatment of breast cancer, strategies to reduce doses, increase efficacy and protect non-cancer cells from off-target cytotoxicity are desperately required.

2 Hypothesis and experimental aims

2.1 Hypothesis

Amino acid starvation will increase the sensitivity of MDAMB231cells, but not MCF12A cells, to doxorubicin (1 µM).

2.2 Experimental aims

1. Establish the relative sensitivity of MDAMB231 cells and MCF12A cells to doxorubicin (1 µM).

2. Establish whether autophagy increases during doxorubicin (1 µM) treatment in these cell lines.

3. Determine whether bafilomycin A1 (10 nM) alters the sensitivity of these cell lines to doxorubicin (1 µM).

4. Determine whether amino acid starvation in conjunction with doxorubicin (1 µM) treatment alters sensitivity of these cell lines to treatment and whether this is associated with similar changes in lysosomal acidity.

5. Assess how MCF7 cells respond to similar treatments.

3   Methods and materials

The materials and methods describing the following procedures utilized in this study can be found in previous chapters: Cell culture, caspase 3/7 activity assay, trypan blue assay, LC3 and beclin 1 western blotting, ATG5 siRNA transfection and cell cycle analysis.

3.1   Hoechst nuclear staining (analysis of pyknosis and karyorrhexis)

Differentiation between normal nuclear morphology and the nuclear condensation and fragmentation that is characteristic of apoptosis can be achieved by using the DNA intercalating dye, Hoechst. MDAMB231, MCF12A and MCF7 cells were cultured and maintained as described previously. 60 000 MCF12A cells or 45 000 MDAMB231 or MCF7 cells were plated into 35 mm culture dishes containing previously sterilised coverslips, 48 hours prior to treatment. After treatments, the cover slips were removed, placed over glass slides, and washed with 100 µL of ice cold PBS (phosphate buffer solution). They were then treated with 500 µL of ice cold acetone: methanol (1:1) and incubated at 4°C for 10 minutes. The fixative was then removed and cover slips again washed with 100 µL ice cold PBS. 100 µl of Hoechst (Hoechst 33342, Sigma Chemical Co., St Louis, MO, USA) in a 1:200 dilution (50 µg/ml) in sterile PBS was added directly onto cover slips and incubated in the dark for 10 minutes. Coverslips were then washed 5x with 100 µL of PBS at room temperature before being mounted on permanent slides. They were then viewed immediately using a Nikon E-400 fluorescence microscope (Nikon Microscopes, Kobe, Japan). Images were acquired using a Nikon DM X 1200 colour digital camera (Nikon Microscopes, Kobe, Japan) using ACT-I software (Nikon Microscopes, Kobe, Japan) to process the images. Three independent experiments were conducted and four representative regions of each condition were acquired per experiment. At least 200 cells were analysed per region. For each image the number of

condensed/fragmented nuclei was counted and expressed as a percentage of total number of nuclei counted. In this manner the percentage apoptosis was determined for each experimental condition.

3.2   Doxorubcin and LAMP-2A fluorescence imaging

15 000 MCF12A cells and 10 000 MDAMB231 cells were seeded per well into 8-well Nunc™ chambered plates (Nalge Nunc, Rochester, NY, USA). Cell monolayers were washed three times with sterile 0.1 M PBS before being fixed and permeabilised with an ice-cold 1:1 methanol/acetone mixture for 10 minutes at 4ºC. After being left to air dry for 20 minutes in the dark, cells were, once more, washed three times in sterile PBS. The following steps were conducted in a dark, humidified environment at room temperature. Non-specific binding was blocked by incubating in 5% donkey serum for 20 minutes. Cells were then incubated with anti-LAMP-2A primary antibody (Cell Signalling, MA, USA) for 90 minutes. Cells were then rinsed three times with sterile PBS and incubated with a FITC bound secondary antibody for 30 minutes. Immediately thereafter, cells were washed three times in sterile PBS and enough Hoechst 3342 (10 mg/ml in a 1:200 dilution) was then added to cover the entire cell monolayer. This was left to incubate for 10 minutes at 4ºC. Finally, cells were washed five times in sterile PBS and images were immediately acquired with an Olympus CellˆR fluorescence 1 X 81 inverted microscope (Olympus Biosystems, Germany) using an F-view II camera (Olympus Biosystems, Germany) for image acquisition and CellˆR software, (Olympus Biosystems, Germany) for processing images.

3.3   Drug preparation

Doxorubicin hydrochloride (D1515, Sigma Chemical Co., St Louis, MO, USA) was prepared in amino acid free medium in ready to use aliquots to avoid freeze thaw cycles, and was stored at -20°C. Bafilomycin A1 from *Streptomyces griseus* (B1793, Sigma Chemical Co., St Louis, MO, USA) was dissolved in DMSO in ready to use aliquots to avoid freeze thaw cycles, and was stored at -20°C.

3.4   Lysotracker™ (flow cytometry)

Lysotracker™ was used in conjunction with flow cytometry as described previously (chapter 2). However, all treated samples were split 1:1 and only one half stained with the lysotracker™ dye. Values obtained for the unstained samples were then subtracted from those obtained for the stained samples.

3.5   Statistical analysis

All values are presented as the mean ± standard error of the mean (SEM). Differences between time points and treatment groups were analysed using one or two analysis of variance (ANOVA). Significant changes were further assessed by means of the Bonferroni *post hoc* analysis where appropriate. All statistical analyses were performed using Graphpad Prism version 5.01 (Graphpad Software, Inc, CA, USA). The minimum level of significance accepted was $p < 0.05$.

4   Results

4.1   MDAMB231 cells are more resistant to a 24 hour treatment of doxorubicin (1 µM) than MCF12A cells
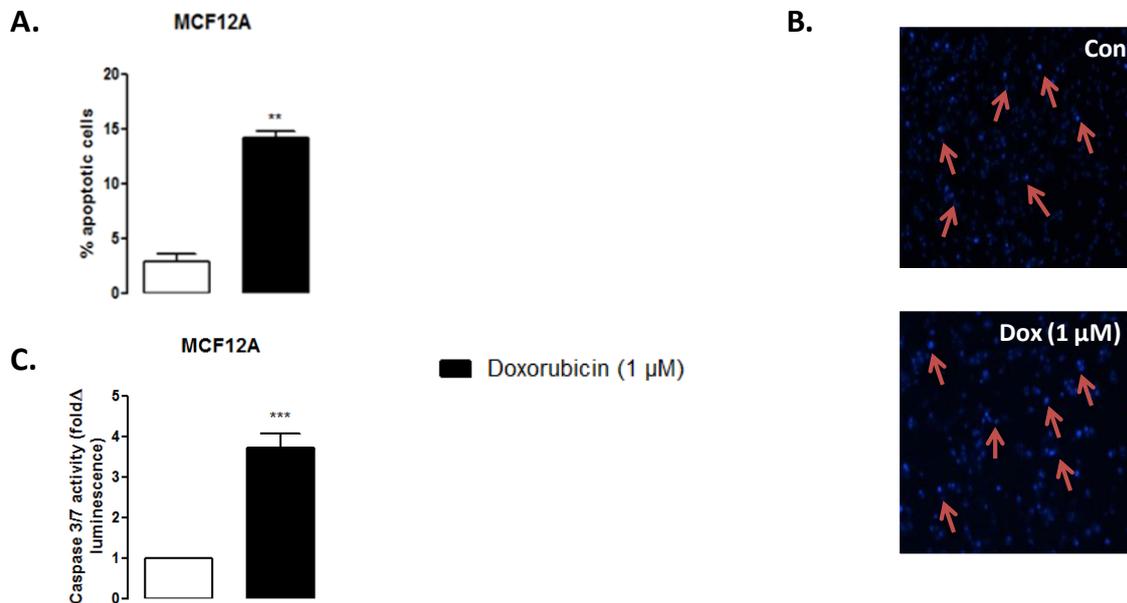
Fig. 4.1 Doxorubicin (1 µM) treatment increases apoptosis in MCF12A cells. A) Bar graph indicating the percentage of nuclei presenting with morphological changes characteristic of apoptosis. B) MCF12A cells stained with Hoescht. Red arrows demonstrating apoptotic nuclear features. C) MCF12A cells display significantly increased caspase 3/7 activity following treatment with doxorubicin (1 µM). Results represent the fold change in luminescence in cultures incubated with doxorubicin (1 µM) versus untreated cells. Caspase 3/7 activity was taken to be proportionate to produced luminescence intensity. Images were obtained using a 10x magnification. Cells were incubated in doxorubicin (1 µM) for 24 hours. Con = untreated control; dox = doxorubicin. Each value is the mean ± SEM of at least three independent determinations. **, $P < 0.01$; ***, $P < 0.001$.

Doxorubicin (1 µM) treatment significantly increased apoptosis in MCF12A cells (Fig 4.1). Approximately 15% percent of MCF12A nuclei presented with morphological changes to their nuclei that are characteristic of apoptosis, following treatment with doxorubicin (1 µM) and staining with Hoechst (Fig 4.1a and Fig 4.1b). MCF12A cells also displayed significantly increased caspase 3/7 activity following treatment with doxorubicin (1 µM) for 24 hours (Fig 4.1c).

196

A.

B.

C.
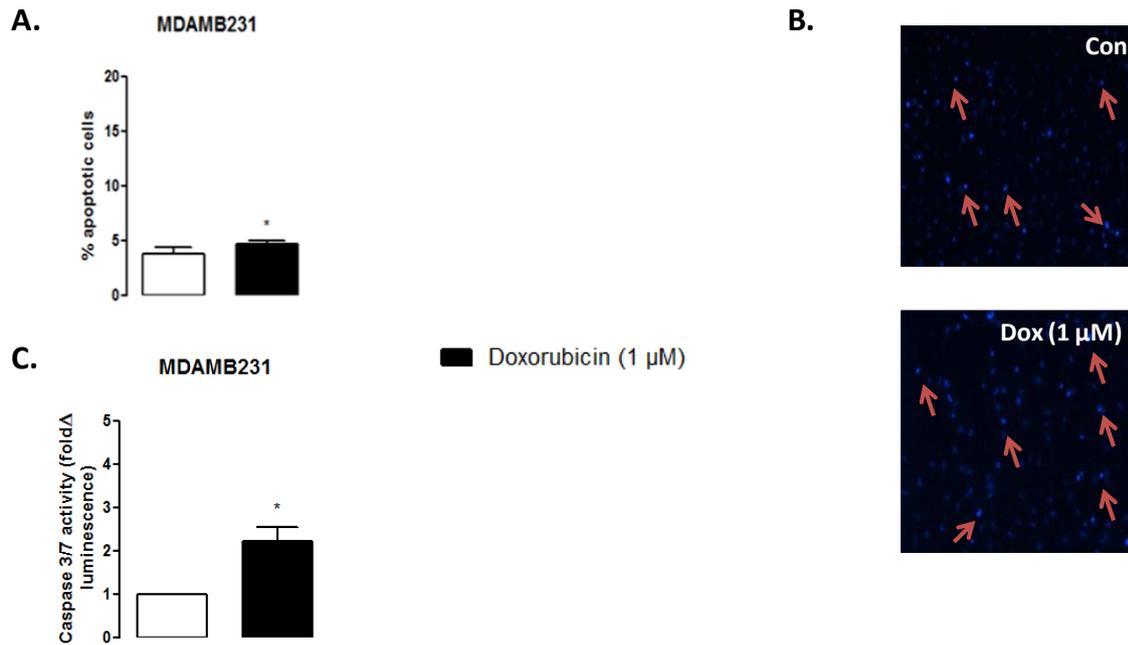
Doxorubicin (1 µM)

Fig. 4.2 MDAMB231 cells display a resistance to apoptosis following treatment with doxorubicin (1 µM). A) Bar graph indicating the percentage of nuclei presenting with morphological changes characteristic of apoptosis. B) MDAMB231cells stained with Hoescht. Red arrows demonstrating apoptotic nuclear features. C) MDAMB231cells display significantly increased caspase 3/7 activity following treatment with doxorubicin (1 µM). Results represent the fold change in luminescence in cultures incubated with doxorubicin (1 µM) versus untreated cells. Caspase 3/7 activity was taken to be proportionate to produced luminescence intensity. Images were obtained using a 10x magnification. Cells were incubated in doxorubicin (1 µM) for 24 hours. Con = untreated control; dox = doxorubicin. Each value is the mean ± SEM of at least three independent determinations. *, $P < 0.05$.

MDAMB231 cells display a relative resistance to apoptosis following treatment with doxorubicin (1 µM), when compared to the non-tumourogenic MCF12A cell line. A very small, but statistically significant percentage of MDAMB231 nuclei presented with morphological changes that are characteristic of apoptosis, following treatment with doxorubicin (1 µM) and staining with Hoechst (Fig 4.2a and Fig 4.2b). MDAMB231cells also displayed a more pronounced (and significant) increase in caspase 3/7 activity following treatment with doxorubicin (1 µM) (Fig 4.2c).

197

4.2 Depleting culture medium of amino acids during 24 hours of doxorubicin (1 μM) treatment protects MCF12A cells but not MDAMB231 cells from a loss of cellular membrane integrity
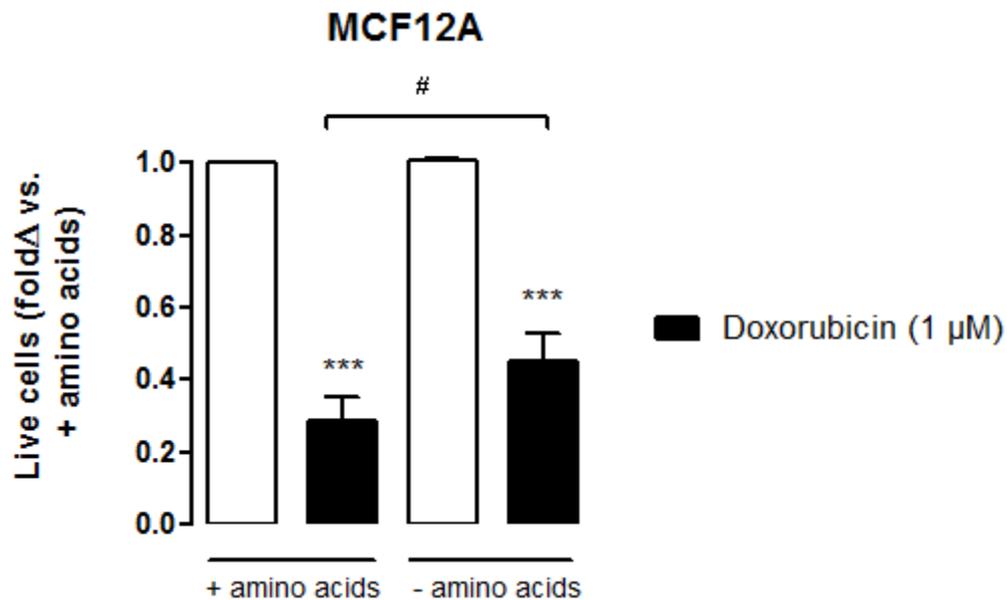
Fig. 4.3 Amino acid starvation decreases the percentage of trypan blue positive MCF12A cells following treatment with doxorubicin (1 μM). Live cells are defined as those that exclude trypan blue dye. Results represent the fold change of live cells versus untreated cells cultured in medium containing amino acids. Significance markers depict comparisons versus untreated cells cultured in the presence of amino acids unless indicated otherwise. Cells were incubated in doxorubicin (1 μM) for 24 hours. Each value is the mean ± SEM of at least three independent determinations. ***, $P < 0.001$ vs. untreated control. #, $P < 0.05$.

The trypan blue vital stain is able to traverse only those cell membranes with compromised integrity, and therefore functions as a marker of necrotic and late stage apoptotic cell death and can be used as an indicator of actual cellular impairment following an intervention. MCF12A cells are extremely susceptible to doxorubicin (1 μM) cytotoxicity. Approximately 80% of these cells become trypan blue positive after a 24 hour incubation in 1 μM doxorubicin (Fig 4.3). Treatment with doxorubicin (1 μM) in culture medium completely depleted of amino acids resulted in significantly less MCF12A cells becoming trypan blue positive.
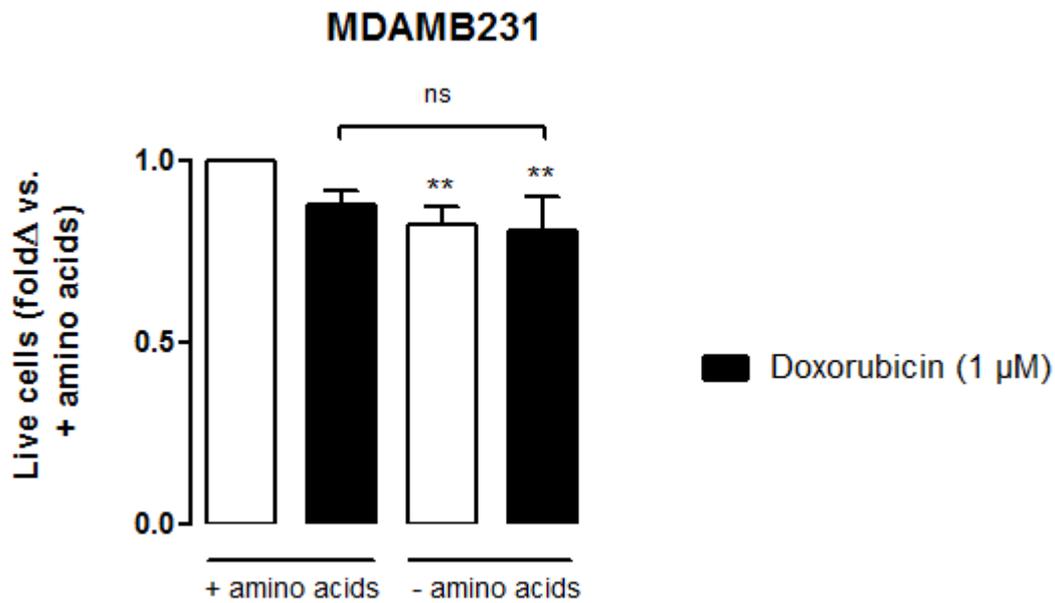
MDAMB231

Fig. 4.4 Amino acid starvation does not alter the percentage of trypan blue positive MDAMB231 cells following treatment with doxorubicin (1 μM). Live cells are defined as those that exclude trypan blue dye. Results represent the fold change of live cells versus untreated cells cultured in medium containing amino acids. Significance markers depict comparisons versus untreated cells cultured in the presence of amino acids unless indicated otherwise. Cells were incubated in doxorubicin (1 μM) for 24 hours. Each value is the mean ± SEM of at least three independent determinations. **, $P < 0.01$ vs. + amino acids. ns = no significance.

MDAMB231 cells appeared to be comparatively resistant to doxorubicin (1 μM) induced membrane impairment, and amino acid starvation did not change the percentage of trypan blue positive MDAMB231 cells following treatment with doxorubicin (1 μM) (Fig 4.4).

4.3   A 24 hour treatment with doxorubicin (1 µM) increases LC3 II levels in MCF12A and MDAMB231 cells
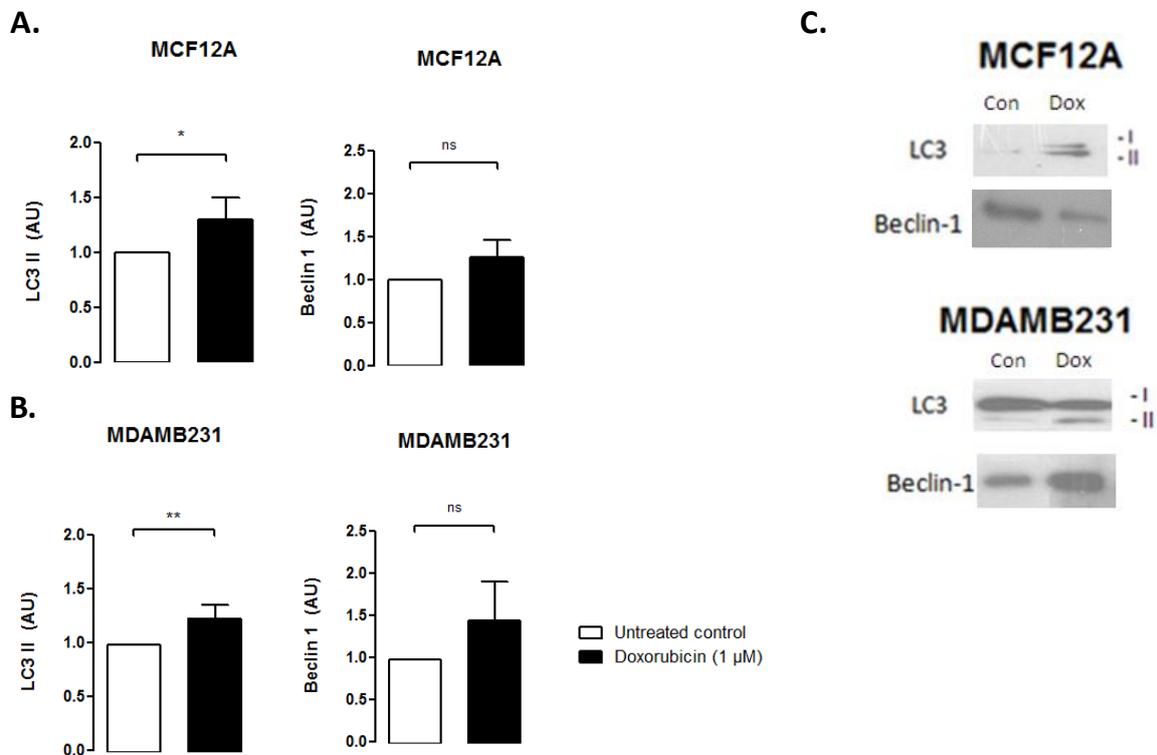
Fig. 4.5 Doxorubicin (1 µM) increases protein levels of LC3 II in both MCF12A cells and MDAMB231cells. Bar graphs show densitometric representation of LC3-II and Beclin 1 protein levels in A) MCF12A cells and B) MDAMB231 cells. C) Representative western blots of LC3 II and beclin 1. No significant changes to Beclin 1 levels were detected. Cells were incubated in doxorubicin (1 µM) for 24 hours, and then cell lysates were western blotted with antibodies against LC3 and beclin 1. AU = Arbitrary Units. Each value is the mean ± SEM of at least three independent determinations. *, $P < 0.05$; **, $P < 0.01$. ns = no significance.

Both MCF12A and MDAMB231 cells responded to the presence of doxorubcin (1 µM) by increasing LC3 II protein levels (Fig 4.5). Levels of the autophagy protein beclin 1 did not change during these experiments.

4.4 Autophagy inhibition increases caspase 3/7 activity in MDAMB231 cells but not MCF12A cells treated with doxorubicin (1 µM)
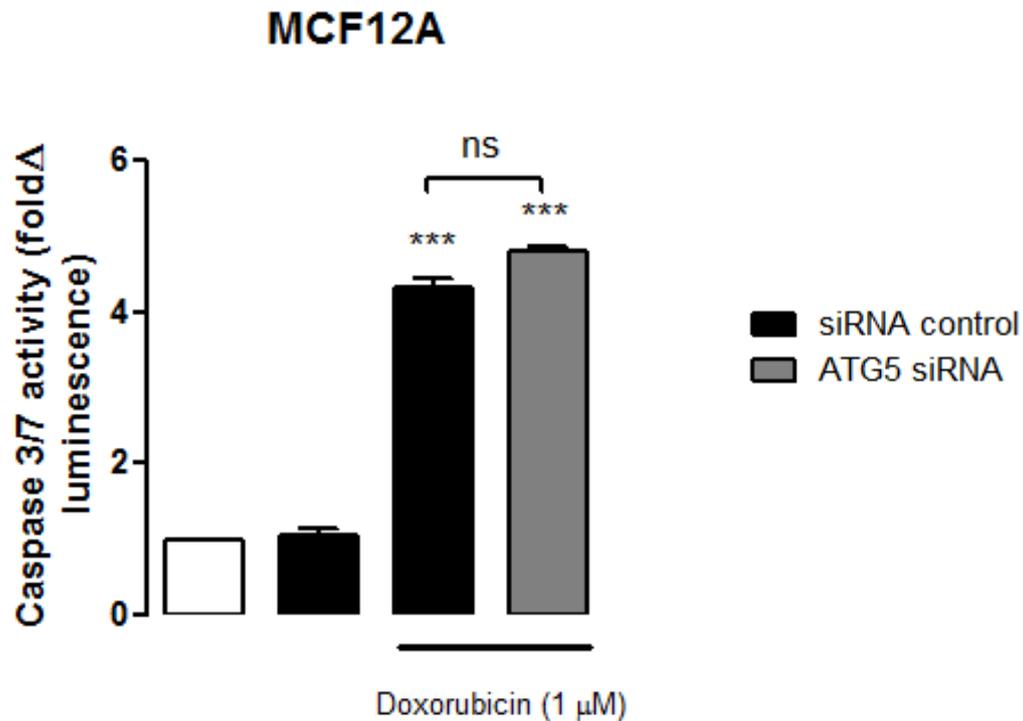
Fig. 4.6 Inhibition of autophagy in MCF12A cells with ATG5 siRNA before treating with doxorubicin (1 µM) does not alter caspase 3/7 activity. ATG5 siRNA or siRNA controls were transfected into MCF12A cells 24 hours prior to treatment. Results represent the fold change in luminescence in cultures incubated with doxorubicin (1 µM) versus untreated cells. Caspase 3/7 activity was taken to be proportionate to produced luminescence intensity. Significance markers depict comparisons versus untreated cells cultured in the presence of amino acids unless indicated otherwise. Cells were incubated in doxorubicin (1 µM) for 24 hours. Each value is the mean ± SEM of at least three independent determinations. ***, $P < 0.001$ vs. untreated control. ns = no significance.

Inhibition of autophagy using ATG5 siRNA did not alter the level of caspase 3/7 activity in MCF12A cells treated with doxorubicin (1 µM) (Fig 4.6).
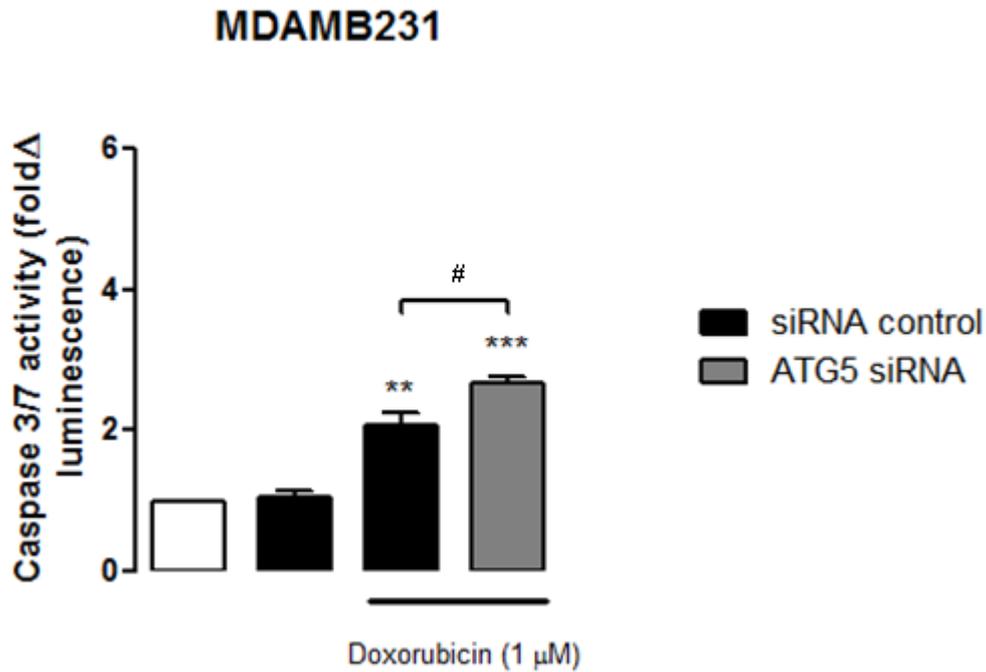
MDAMB231

Fig. 4.7 Inhibition of autophagy in MDAMB231cells with ATG5 siRNA before treating with doxorubicin (1 µM) increases caspase 3/7 activity. ATG5 siRNA or siRNA controls were transfected into MDAMB231cells 24 hours prior to treatment. Results represent the fold change in luminescence in cultures incubated with doxorubicin (1 µM) versus untreated cells. Caspase 3/7 activity was taken to be proportionate to produced luminescence intensity. Significance markers depict comparisons versus untreated cells cultured in the presence of amino acids unless indicated otherwise. Cells were incubated in doxorubicin (1 µM) for 24 hours. Each value is the mean ± SEM of at least three independent determinations.**, $P < 0.01$; ***, $P < 0.001$ vs. untreated control. #, $P < 0.05$.

Inhibition of autophagy in MDAMB231 cells with ATG5 siRNA lead to a significant increase in measurable caspase 3/7 activity when these cells were treated with doxorubicin (1 µM) (Fig 4.7).

4.5   Bafilomycin (10 nM) increases caspase 3/7 activity in MDAMB231 cells and MCF12A cells treated with doxorubicin (1 μM)
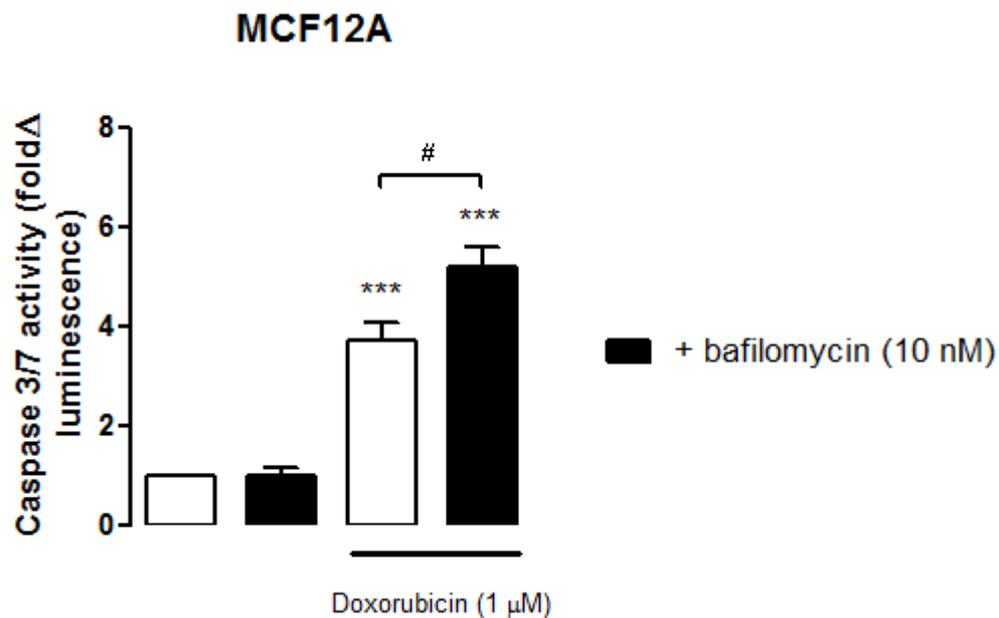
Fig. 4.8 MCF12A cells incubated with bafilomycin A1 (10 nM) during treatment with doxorubicin (1 μM) display increased caspase 3/7 activity. MCF12A cells were incubated with bafilomycin A1 (10 nM) 6 hours prior to analysis. Results represent the fold change in luminescence in cultures incubated with doxorubicin (1 μM) versus untreated cells. Caspase 3/7 activity was taken to be proportionate to produced luminescence intensity. Significance markers depict comparisons versus untreated cells cultured in the presence of amino acids unless indicated otherwise. Cells were incubated in doxorubicin (1 μM) for 24 hours. Bafilomycin A1 (10 nM) was added to culture medium 6 hours prior to analysis. Each value is the mean ± SEM of at least three independent determinations. ***, $P < 0.001$ vs. untreated control. #, $P < 0.05$.

Treating MCF12A cells with 10 nM of bafilomycin 6 hours prior to analysis greatly increased

caspase 3/7 activity when these cells were treated with doxorubicin (1 μM) (Fig 4.8).
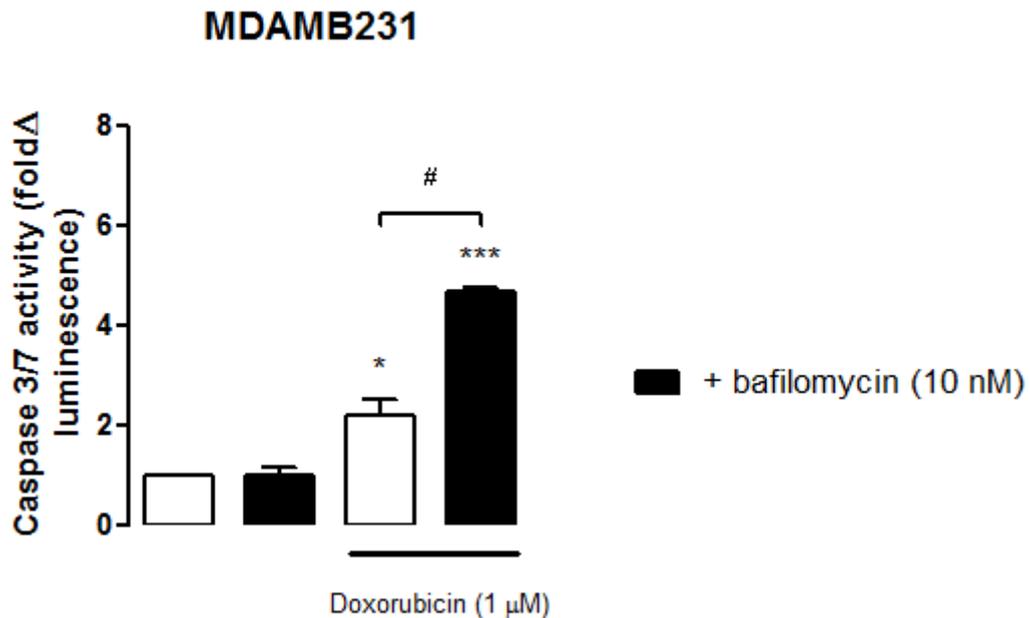
MDAMB231

Fig. 4.9 MDAMB231cells incubated with bafilomycin A1 during treatment with doxorubicin (1 µM) display significantly increased caspase 3/7 activity. MDAMB231cells were incubated with bafilomycin A1 (10 nM) 6 hours prior to analysis. Results represent the fold change in luminescence in cultures incubated with doxorubicin (1 µM) versus untreated cells. Caspase 3/7 activity was taken to be proportionate to produced luminescence intensity. Cells were incubated in doxorubicin (1 µM) for 24 hours. Bafilomycin A1 (10 nM) was added to culture medium 6 hours prior to analysis. Significance markers depict comparisons versus cells cultured 6 hours of amino acid deprived medium unless indicated otherwise. Each value is the mean ± SEM of at least three independent determinations. *, $P < 0.05$; ***, $P < 0.001$. vs. untreated control. #, $P < 0.05$.

As in MCF12A cells, treating MDAMB231 cells with 10 nM of bafilomycin 6 hours prior to analysis greatly increased caspase 3/7 activity when these cells were treated with doxorubicin (1 µM) (Fig 4.9).

4.6 Bafilomycin (10 nM) increases detectable levels of intracellular doxorubicin in MDAMB231 cells and MCF12A cells treated with doxorubicin (1 µM)

LAMP-2A   Doxorubicin

Doxorubicin (1 µM)

Doxorubicin (1 µM) +
Bafilomycin (10 nM)
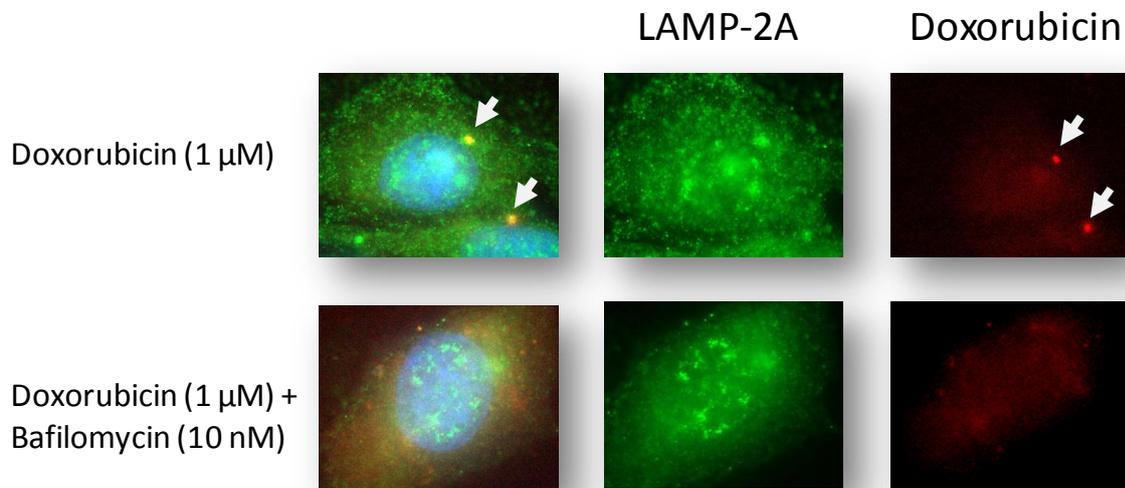
Fig. 4.10 Bafilomycin A1 (10 nM) treated MCF12A cells present with increased levels of intracellular doxorubicin during treatment. No specific pattern of LAMP-2A staining in MCF12A cells is noted during doxorubicin (1 µM) treatment with bafilomycin A1 (10 nM). However, small localized areas of intense doxorubcin (white arrows) were noted in doxorubicin treatments but were not present if cells were treated with bafilomycin. Cells were incubated in doxorubicin (1 µM) for 24 hours and bafilomycin A1 (10 nM) for 6 hours prior to staining. Images were obtained using a 40x magnification.

Cells were stained with the lysosomal associated membrane protein (LAMP-2A) during doxorubicin treatment (1 µM). Intracellular localization of doxorubicin was tracked by exploiting the autofluorescence of doxorubicin, a technique that has been utilized successfully in MDAMB231 and other cell lines (Li et al., 2010). MCF12A cells treated with doxorubicin (1 µM) displayed obvious intracellular red fluorescence associated with doxorubicin (Fig 4.10). Notably, small localized regions of intense red fluorescence were observed in most doxorubicin treated (1 µM) MCF12A cells (white arrows in above images) but were completely absent in cells that had also been supplemented with bafilomycin (10 nM).
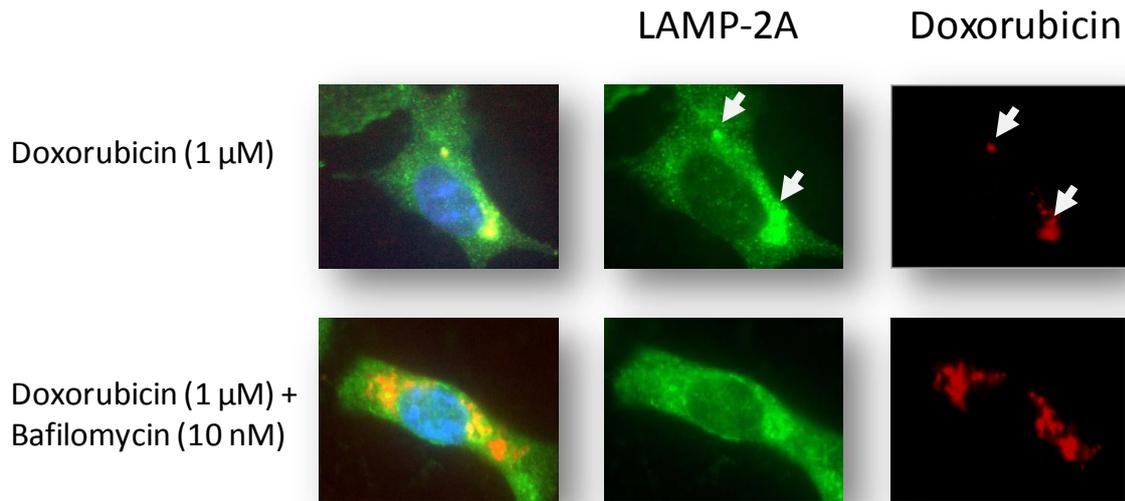
Fig. 4.11 MDAMB231 cells treated with bafilomycin A1 (10 nM) present with increased levels of intracellular doxorubicin during treatment. Furthermore, pooling of LAMP-2A at the perinuclear region in MDAMB231 cells treated with doxorubicin (1 μM) is lost following treatment with bafilomycin A1 (10 nM). Cells were incubated in doxorubicin (1 μM) for 24 hours and bafilomycin A1 (10 nM) for 6 hours prior to staining and imaging. Images were obtained using a 40x magnification.

MDAMB231 cells treated with doxorubicin (1 μM) displayed obvious and intense localized regions of intracellular red fluorescence associated with doxorubicin (Fig 4.11). This red fluorescence was associated with pooling of the LAMP-2A signal (white arrows in the above image) in doxorubicin (1 μM) treated MDAMB231 cells. Notably, LAMP-2A pooling disappeared if bafilomycin (10 nM) was added. Importantly, MDAMB231 cells treated with doxorubicin (1 μM) and bafilomycin (10 nM) had significantly more observable red fluorescence within the cytoplasmic regions of these cells. However, unlike MCF12A cells, there was no doxorubicin associated with nuclear regions of these cells.

206

4.7 Amino acid deprivation increases autophagy induction and autophagy flux in MCF12A cells and in MDAMB231 cells treated with doxorubicin (1 µM) respectively
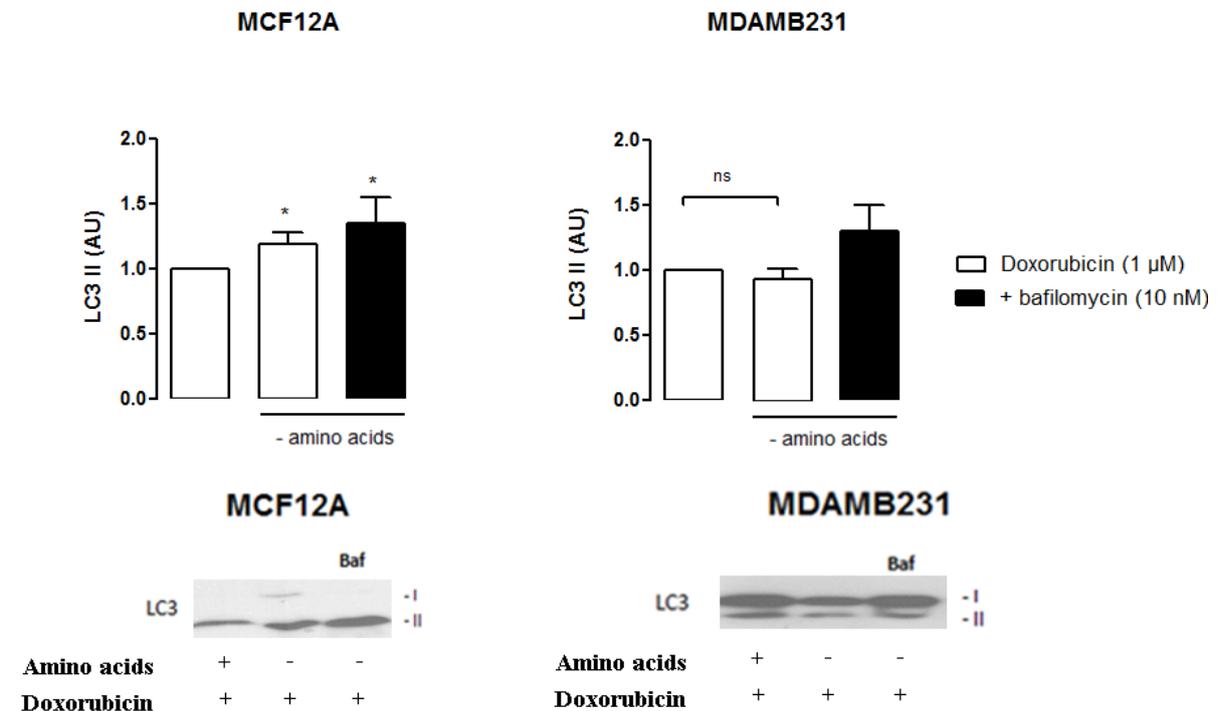
Fig. 4.12 Doxorubicin (1 µM) increases autophagy flux in MCF12A and MDAMB231cells during amino acid deprivation. Bar graphs show densitometric representations of LC3-II protein levels. Addition of the lysomotropic reagent bafilomycin A1 (10 nM) causes a further increased in detectable LC3 II in both cell lines. Bafilomycin A1 (10 nM) was added to culture medium 6 hours prior to cell harvesting. Cells were incubated in doxorubicin (1 µM) for 24 hours. Each value is the mean ± SEM of at least three independent determinations. *, $P < 0.05$ vs. + amino acids + doxorubicin . ns = no significance.

Doxorubicin (1 µM) treatment during amino acid deprivation resulted in increased induction of LC3 in MCF12A cells (Fig 4.12). Furthermore, decreased LC3 II protein levels following doxorubicin (1 µM) treatment during amino acid deprivation were shown to accumulate if bafilomycin (10 nM) was administered 6 hours prior to analysis. This indicates increased autophagy flux in MDAMB231 cells following doxorubicin (1 µM) treatment during amino acid starvation.

4.8   Amino acid deprivation during doxorubicin (1 µM) treatment causes lower levels of lysosomal acidity in MDAMB231 cells but not in MCF12A cells which correspond to increased and decreased caspase activity respectively
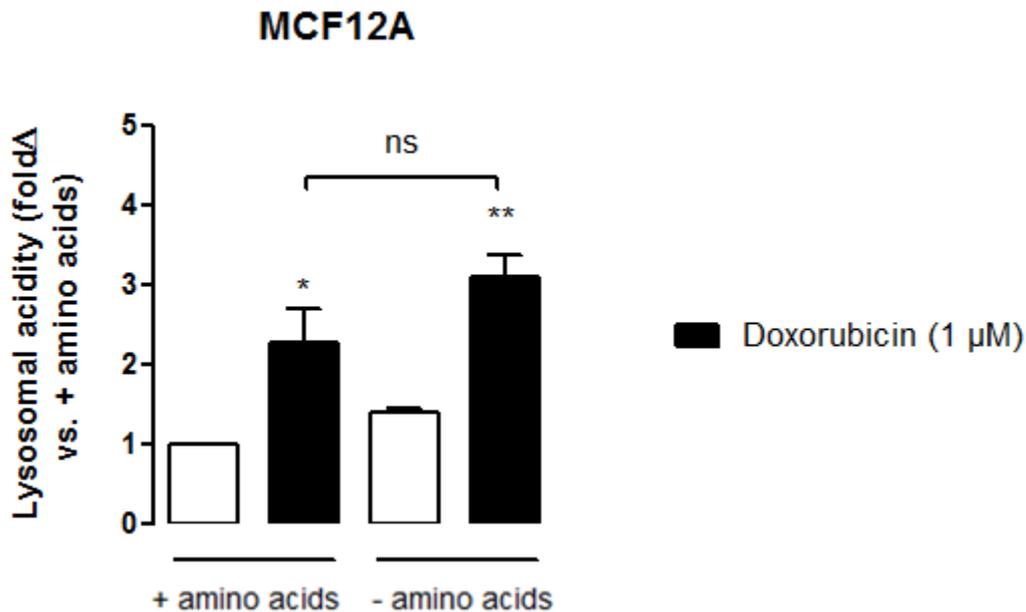
Fig. 4.13 An elevation in lysosomal acidity is observed in MCF12A cells during a 24 hour treatment with doxorubicin (1 µM). Treatment with doxorubicin (1 µM) in culture medium deprived of all amino acids also showed a trend towards a further increase in lysosomal acidity. Lysosomal acidity was monitored using a Lysotracker dye and flow cytometry and is plotted as fold change compared to cells cultured in amino acid complete medium. Significance markers depict comparisons versus untreated cells cultured in the presence of amino acids unless indicated otherwise. Cells were incubated in doxorubicin (1 µM) and/or in amino acid deprived medium for 24 hours where applicable. Each value is the mean ± SEM of at least three independent determinations. *, $P < 0.05$; **, $P < 0.01$ vs. Untreated controls. ns = no significance.

In concurrence with previous experimental data (described in chapter 2), amino acid deprivation during a 24 hour treatment with doxorubicin (1 µM) resulted in higher, albeit non-significant, lysosomal acidity levels in MCF12A cells (Fig 4.13).
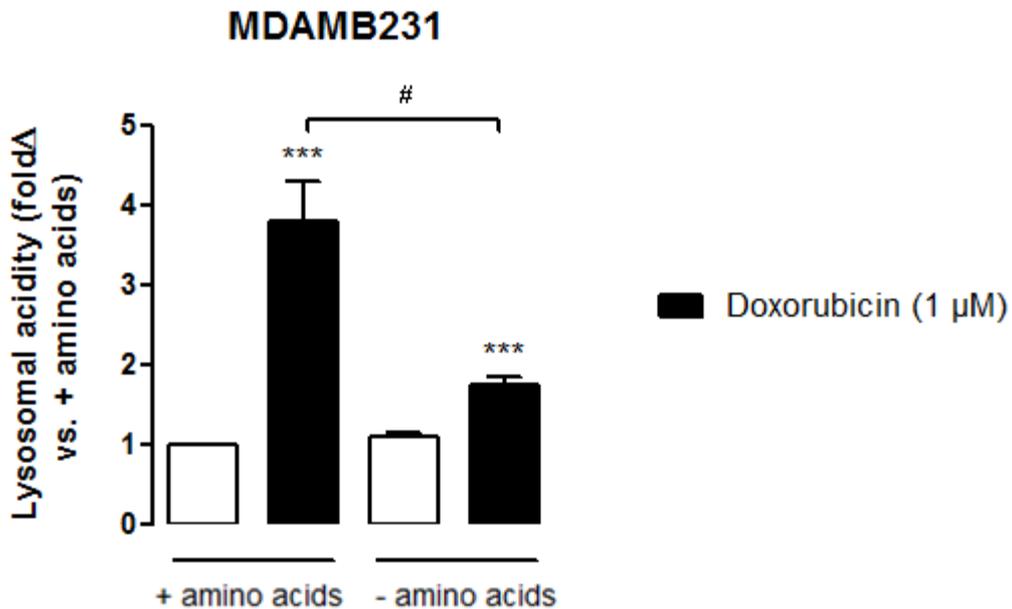
MDAMB231

Fig. 4.14 The elevation in lysosomal acidity observed in MDAMB231cells during a 24 hour treatment with doxorubicin (1 μM) is mostly abolished if amino acids are absent from culture medium. Treatment with doxorubicin (1 μM) in culture medium deprived of all amino acids causes a significant decrease in lysosomal acidity compared to treatments occurring in the presence of amino acids. Lysosomal acidity was monitored using a Lysotracker dye and flow cytometry and is plotted as fold change compared to cells cultured in amino acid complete medium. Significance markers depict comparisons versus untreated cells cultured in the presence of amino acids unless indicated otherwise. Cells were incubated in doxorubicin (1 μM) and/or in amino acid deprived medium for 24 hours where applicable. Each value is the mean ± SEM of at least three independent determinations. ***, $P < 0.001$ vs. untreated controls. #, $P < 0.001$.

In concurrence with previous experimental data (described in chapter 2), amino acid deprivation during a 24 hour treatment with doxorubicin (1 μM) resulted in significantly diminished lysosomal acidity levels, close to baseline, in MDABM231 cells (Fig 4.14).

MCF12A

Fig. 4.15 MCF12A cells treated with doxorubicin (1 μM) are partially protected from apoptosis initiation if amino acids are absent from culture medium during treatment. Results represent the fold change in luminescence in cultures incubated with doxorubicin (1 μM) versus untreated cells. Caspase 3/7 activity was taken to be proportionate to produced luminescence intensity. Significance markers depict comparisons versus untreated cells cultured in the presence of amino acids unless indicated otherwise. Cells were incubated in doxorubicin (1 μM) and/or in amino acid deprived medium for 24 hours where applicable. Each value is the mean ± SEM of at least three independent determinations.;***, $P < 0.001$ vs. untreated control. # $P < 0.01$.

Omission of amino acids from culture medium during treatment of MCF12A cells with doxorubicin (1 μM) resulted in decreased caspase 3/7 activity in these cells (Fig.4.15). This protection from increased caspase activation corresponds with the increased and sustained lysosomal acidity observed during amino acid starvation (described in chapter 2).
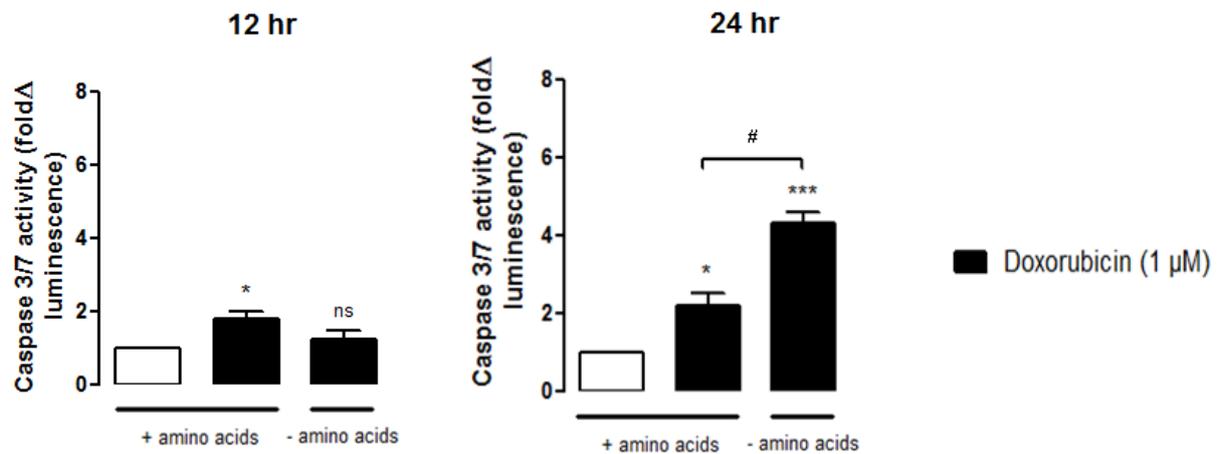
Fig. 4.16 Treatment of MDAMB231 cells with doxorubicin (1 µM) results in increased caspase 3/7 activity if amino acids are absent from culture medium for 24 hours but not 12 hours. Results represent the fold change in luminescence in cultures incubated with doxorubicin (1 µM) versus untreated cells. Caspase 3/7 activity was taken to be proportionate to produced luminescence intensity. Significance markers depict comparisons versus untreated cells cultured in the presence of amino acids unless indicated otherwise. Cells were incubated in doxorubicin (1 µM) and/or in amino acid deprived medium for 12 hours or 24 hours where applicable. hr = hours. Each value is the mean ± SEM of at least three independent determinations. *, $P < 0.05$; ***, $P < 0.001$; ns = no significance vs. untreated control. #, $P < 0.01$

Incubation of MDAMB231 cells in culture medium deprived of amino acids, during treatment with doxorubicin (1 µM), resulted in significantly increased caspase 3/7 activity at 24 hours, but not 12 hours after intervention (Fig 4.16). These findings are in accordance with dynamic changes in lysosomal acidity levels at these times during amino acid deprivation (described in chapter 2).

4.9 Amino acid deprivation during doxorubicin (1 µM) treatment exacerbates g2/m cell cycle arrest associated with doxorubicin toxicity in MDAMB231 cells
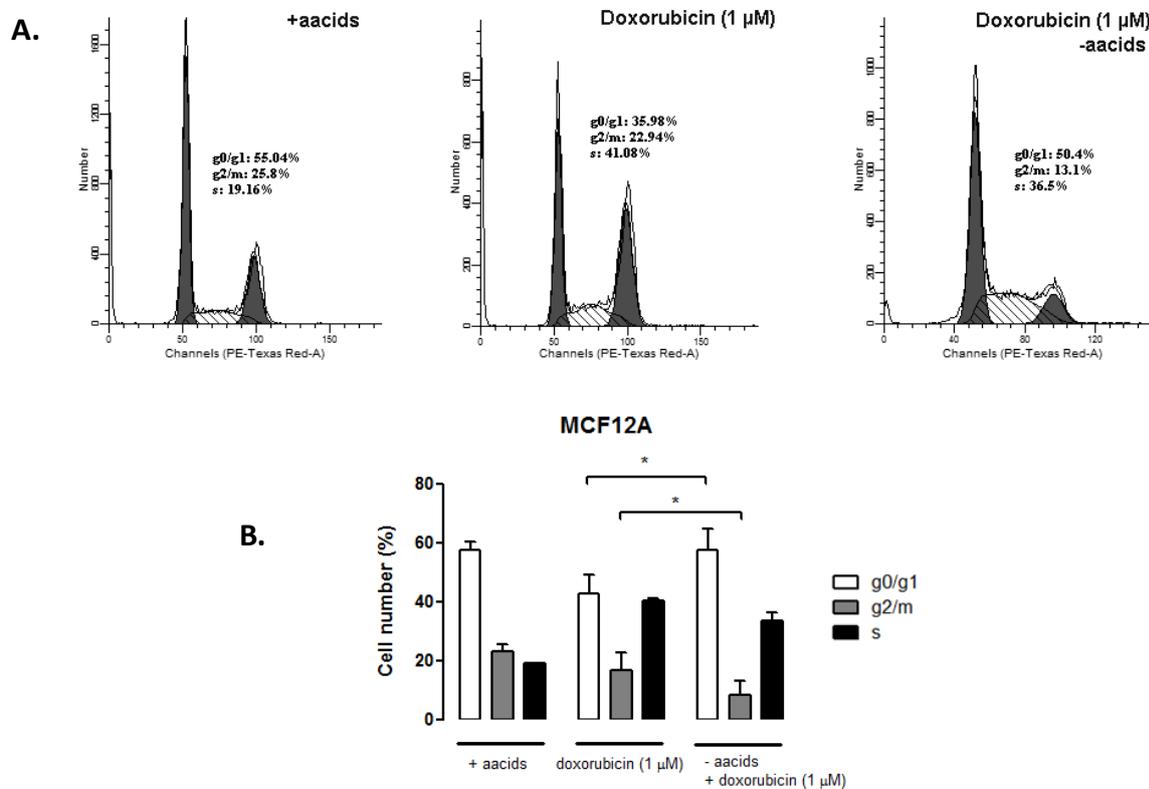
Fig. 4.17 Treatment of MCF12A cells with doxorubicin (1 µM) during 24 hours of amino acid deprivation partially prevents alterations to the cell cycle. Cell cycle progression was assessed using flow cytometry and addition of doxorubicin (1 µM) was observed to result in an increased g0/g1 phase and a decreased g2/m phase of the cell cycle if cells were deprived of amino acids during treatment. Cells were incubated in amino acid deprived medium and/or in doxorubicin (1 µM) for 24 hours where applicable. A. Typical DNA histograms and cell cycle phase percentages. B. Bar graphs representing the mean ± SEM of at least three independent determinations. hr = hours; aacids = amino acids. *, $P < 0.05$.

Doxorubicin (1 µM) treatment of MCF12A cells results in significant changes to the cell cycle profile in these cells. Deprivation of amino acids from culture medium during treatment of MCF12A cells with doxorubicin (1 µM) resulted in the percentage of cells in the g0/g1 phase being similar to those in untreated controls (Fig 4.17). However, the percentage of cells in g2/m phase decreased further if amino acids were absent.
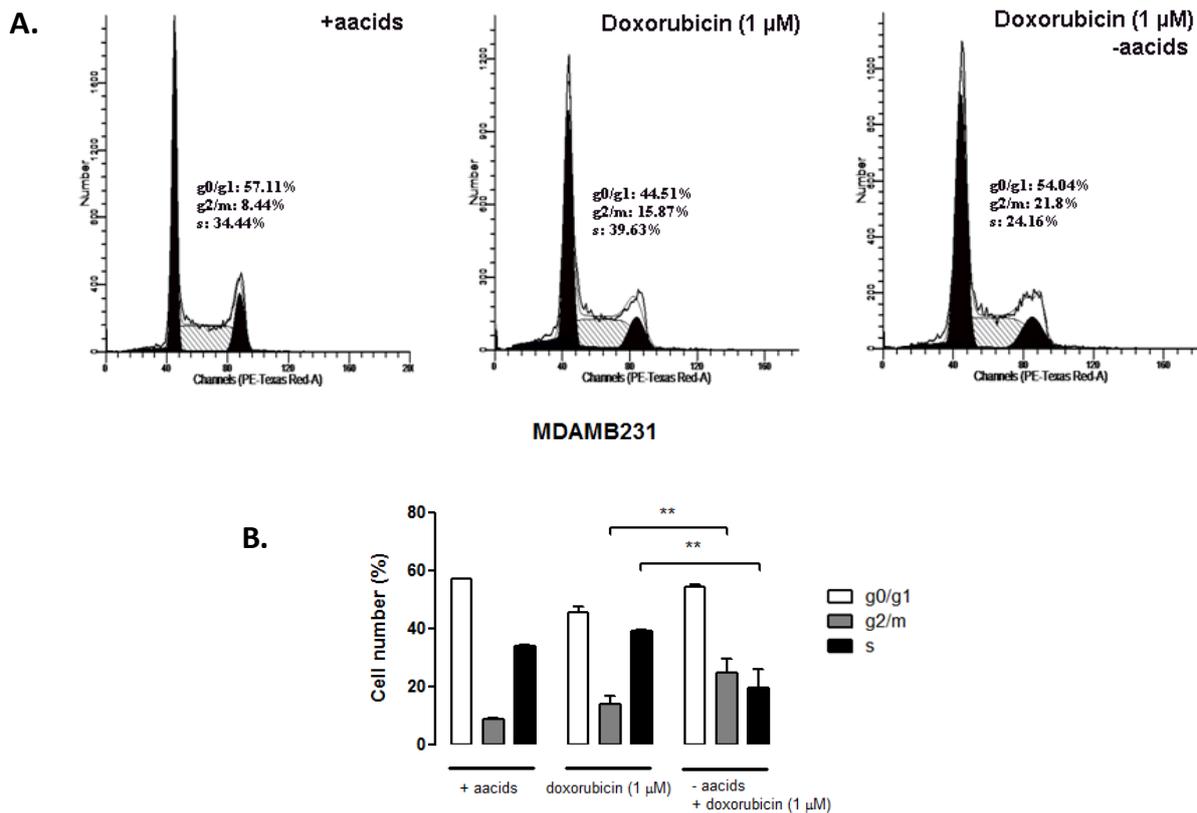
212

Fig. 4.18 Treatment of MDAMB231 cells with doxorubicin (1 μM) during 24 hours of amino acid deprivation leads to an increased g2/m phase and a decreased s phase. Cell cycle progression was assessed using flow cytometry, and the addition of doxorubicin (1 μM) was observed to result in significant alterations to g2/m and s phases of the cell cycle. Cells were incubated in amino acid deprived medium and/or in doxorubicin (1 μM) for 24 hours where applicable. A. Typical DNA histograms and cell cycle phase percentages. B. Bar graphs representing the mean ± SEM of at least three independent determinations. hr = hours; aacids = amino acids. **, $P < 0.01$.

Doxorubicin treatment is typically associated with an increased g2/m arrest in MDAMB231 cells (Lambert et al., 2008), a phenomenon that was also observed in our model (Fig 4.18). Treatment of MDAMB231 cells with doxorubicin (1 μM) in culture medium deprived of amino acids resulted in a further increase in the percentage of cells in the g2/m phase of the cell cycle.

213

4.10 Amino acid deprivation or autophagy inhibition with ATG5 siRNA during doxorubicin (1 µM) treatment results in increased levels of doxorubicin in the nuclear regions of MDAMB231 cells
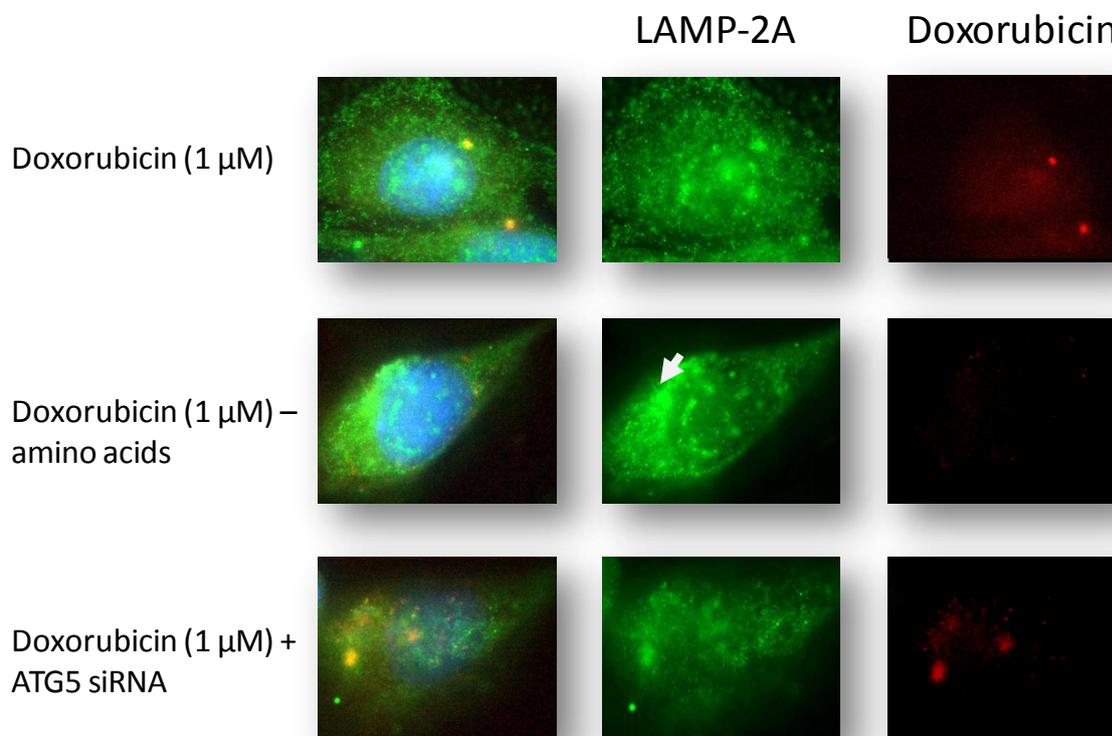
Fig. 4.19 MCF12A cells treated doxorubicin (1 µM) in the absence of amino acids show no signs of increased intracellular doxorubicin but appear to possess areas of increased LAMP-2A pooling. Pooling of LAMP-2A lost if MCF12A cells treated with doxorubicin are also transfected with ATG5 siRNA. Cells were incubated in doxorubicin (1 µM) for 24 hours and reverse transfected with ATG5 siRNA 48 hours prior to staining and imaging. Images were obtained using a 40x magnification.

Amino acid deprivation from culture medium during treatment of MCF12A cells with doxorubicin (1 µM) caused an apparent increase in LAMP-2A pooling in the perinuclear area of these cells (illustrated by the white arrow) (Fig 4.19). Furthermore, amino acid deprivation during treatment resulted in a prominent decrease in observable doxorubicin (red fluorescence). Inhibition of autophagy with ATG5 siRNA resulted in a dispersed pattern of LAMP-2A staining, but doxorubicin was still readily visible in these cells.
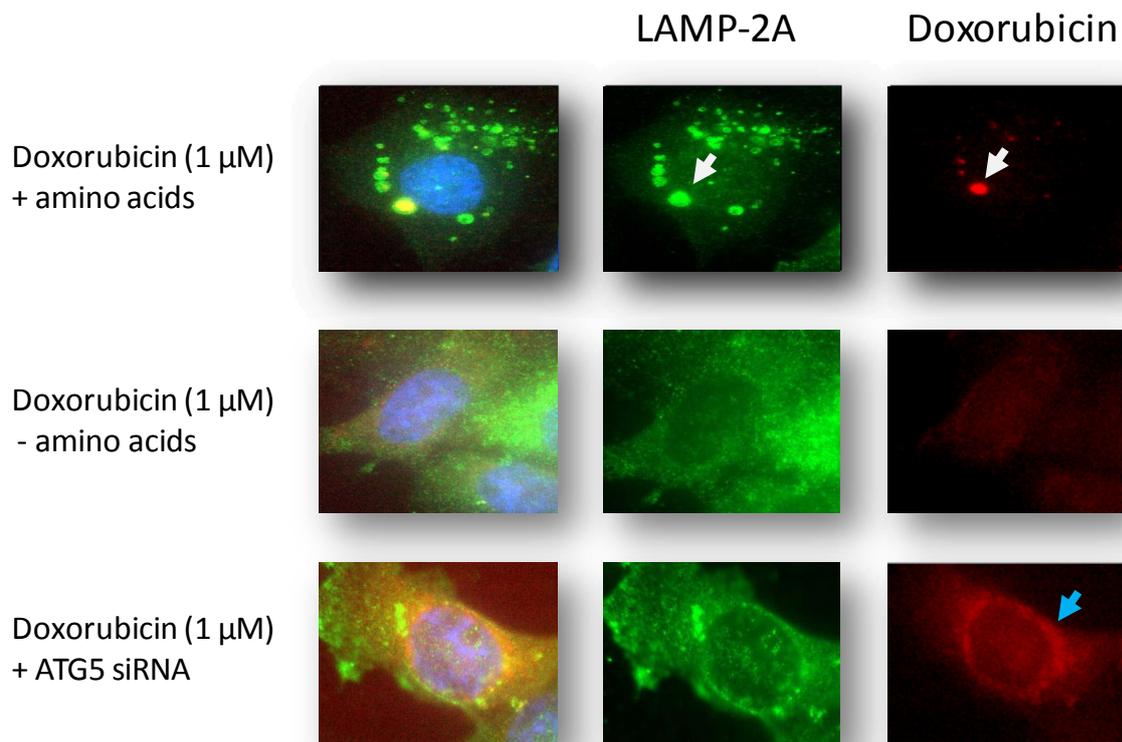
214

Fig. 4.20 MDAMB231 cells treated with doxorubicin (1 µM) in culture medium without amino acids or with ATG5 siRNA appear to contain high intracellular levels of doxorubicin. Furthermore, pooling of LAMP-2A at the perinuclear region in MDAMB231 cells treated with doxorubicin (1 µM) is lost if compared to cells treated in amino acid complete medium (white arrow). Cells were incubated in doxorubicin (1 µM) for 24 hours and and reverse transfected with ATG5 siRNA 48 hours prior to staining and imaging. Images were obtained using a 40x magnification.

MDAMB231 cells treated with doxorubicin (1 µM) displayed obvious cytoplasmic pooling of LAMP-2A and intense localized regions of intracellular red fluorescence associated with these regions (illustrated by the white arrow) (Fig 4.20). Amino acid deprivation during treatment resulted in a loss of LAMP-2A pooling and a more dispersed staining pattern for this marker. Furthermore, these cells displayed increased levels of nuclear doxorubicin (red fluorescence). Inhibition of autophagy with ATG5 siRNA resulted in a prominent increase in cellular doxorubicin, especially at the perinuclear zone (illustrated by the blue arrow).

4.11 Amino acid deprivation does not alter lysosomal acidity or apoptosis levels during doxorubicin (1 µM) treatment in beclin 1 haploinsufficient MCF7 cells
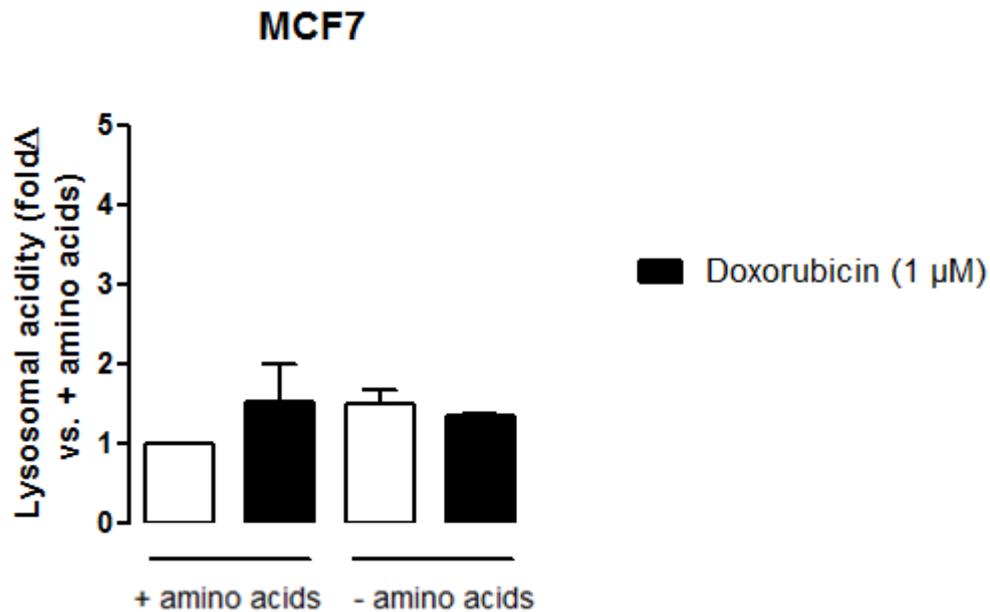
Fig. 4.21 No changes in lysosomal acidity are observed in MCF7 cells during a 24 hour treatment with doxorubicin (1 µM) with or without amino acids. Lysosomal acidity was monitored using a Lysotracker dye and flow cytometry and is plotted as fold change compared to cells cultured in amino acid complete medium. Cells were incubated in doxorubicin (1 µM) and/or in amino acid deprived medium for 24 hours where applicable.

MCF7 cells are autophagy incompetent due to a haploinsufficiency in the gene associated with the autophagy protein beclin 1. Doxorubicin (1 µM) treatment, either with or without amino acids, did not significantly alter lysosomal acidity in these cells (Fig 4.21).
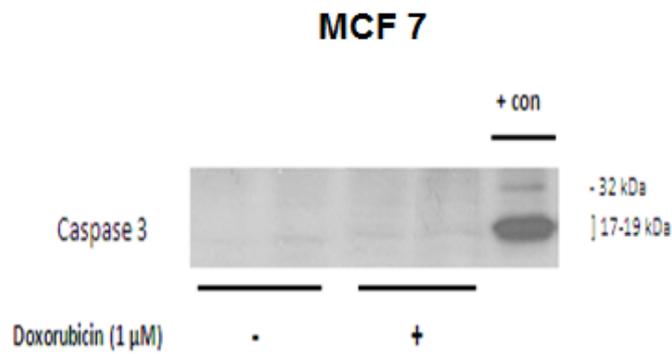
MCF 7

+ con

Caspase 3 .... -32 kDa] 17-19 kDa

Doxorubicin (1 µM)   -   +

Fig 4.22 MCF7 cells do not express caspase 3. Western blots confirm that MCF7 cells do not possess active caspase 3. + con = positive control (MDAMB231 cells incubated in phosphate buffered saline (PBS) for 24 hours.

A.

MCF 7

% apoptotic cells

■ Doxorubicin (1 µM)
□ Doxorubicin (1 µM) + Bafilomycin (10 mM)

+ amino acids   - amino acids

B.

Con   Dox (1 µM)

Dox (1 µM) - aacids   + baf (10 mM)
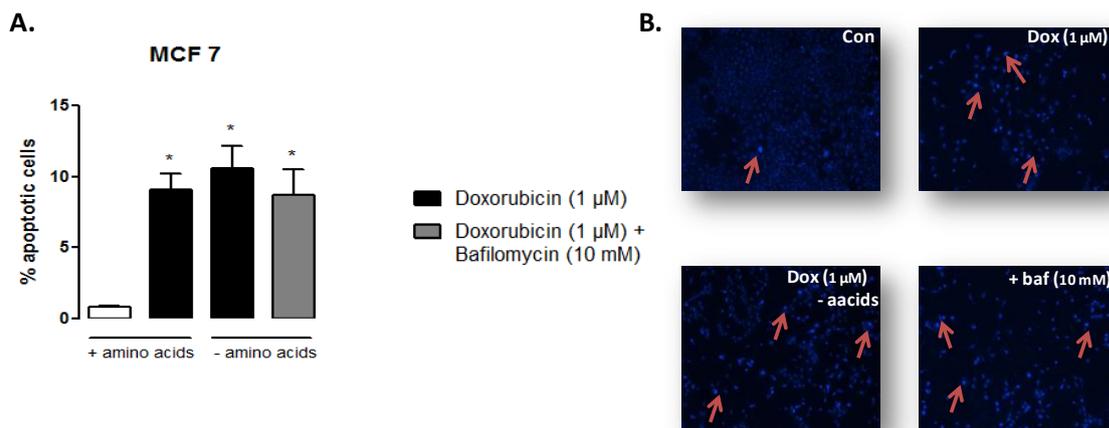
Fig. 4.23 Doxorubicin (1 µM) treatment increases apoptosis in MCF7 cells. A) Bar graph indicating the percentage of nuclei presenting with morphological changes characteristic of apoptosis, during various treatments B) MCF7 cells stained with Hoechst. Red arrows demonstrate apoptotic nuclear features. Images were obtained using a 10x magnification. Cells were incubated in doxorubicin (1 µM) for 24 hours. aacids = amino acids; dox = doxorubicin; baf= bafilomycin. Bafilomycin A1 (10 nM) was added to culture medium 6 hours prior to analysis. Each value is the mean ± SEM of at least three independent determinations. *, $P < 0.05$ vs. + amino acids.

Doxorubicin (1 µM) treatment of MCF7 cells resulted in increased apoptosis (Fig 4.23). However, doxorubicin (1 µM) treatment of these cells in culture medium deprived of amino acids, either with or without bafilomycin (10 nM), does not significantly alter apoptosis levels (Fig 4.23). Notably, MCF7 cells do not possess active caspase 3 (Fig 4.22).

5   Discussion

Many cancers are known to respond to certain chemotherapy or to radiation therapy by increasing autophagy activity. Although the consequences of autophagy activation in these circumstances are still debatable, it appears as though autophagy acts in its predominant role of survival mediator in many of these cases (Yang and Chen, 2011). Anthracyclins such as doxorubicin have also been shown to increase autophagy levels in cancer cells in some instances. At lower doses, doxorubicin elicits an autophagy response in breast cancer cells (Akar et al., 2008) as well as in sarcoma cell lines (Lambert et al., 2008). Additionally, increased levels of ATG2A mRNA have been observed following doxorubicin treatment (Levy and Thorburn, 2011), suggesting increased autophagy activation at the transcriptional level.

In a recent study, 2-deoxy-glucose preserved ATP content and contributed to the cytoprotection of rat cardiomyocytes treated with 1 µM doxorubicin (Chen et al., 2011). This glucose analogue increased markers of autophagy which was posited as a potential reason for protection from cytotoxicity. Conversely, activation of autophagy in cultured cardiomyocytes following doxorubicin (1 µM) treatment mediated its cardiotoxic effect (Kobayashi et al., 2010). Here, it was shown that autophagy inhibition resulted in decreased cell death and it was postulated that autophagy directly contributed to doxorubicin induced toxicity. These exemplify the conflicting nature of studies and reported findings relating autophagy to drug toxicity and illustrate the need for further research into this important topic.

Autophagy activity is increased in response to stress, where it functions as an important mechanism whereby damaged organelles and aggregated proteins are degraded in lysosomes. However, there is still no clear mechanism whereby induction of autophagy could lead to

218

tolerance against chemotherapy agents. Recently it has been shown that release of damage-associated molecular pattern molecules (DAMPs) during chemotherapy is related to autophagy mediated resistance to anticancer treatment in some contexts (Liu et al., 2011b), providing a mechanism where damage caused by drug treatment can directly result in increased autophagy. Elevation of high mobility group box 1 (HMGB1), released in response to chemotherapy induced cell damage, was also shown to increase drug resistance in leukaemia cells by increasing autophagy (Liu et al., 2011a). Bafilomycin A1 increased sensitivity of leukaemia cells to chemotherapy in the aforementioned study. Lysosomal fusion and throughput of autophagy depends on the low pH of lysosomal compartments (Klionsky et al., 2008). Increasing the lysosomal pH with pharmacological agents is an effective method of autophagy inhibition as disruption of the fusion event between autophagosomes and lysosomes prevents progression of autophagy. Some drug resistant cell lines are able to tolerate alkaline chemotherapy drugs such as the anthracyclines by sequestering and deactivating these agents in the acidic compartments of lysosomes (Hurwitz et al., 1997). Exposure of these compounds to environments of low pH renders them inactive and unable to access sites of chemotoxicity such as the nucleus.

In the previous chapters (chapter 2 and chapter 3), experimental data suggested that a metastatic adenocarcinoma cell line with high basal autophagy (MDAMB231) is susceptible to amino acid starvation and relies on autophagy for survival in these circumstances. However, during longer periods of amino acid starvation (24 hours), increased autophagy flux resulted in a particular and reproducible pattern of decreased lysosomal acidity in these cancer cells with high basal autophagy. Importantly, it was noted that lysosomal acidity levels underwent dynamic changes during amino acid starvation and returned to baseline levels following peak acidity between 6 and 12 hours of starvation while non-cancer cells displayed a sustained increase in lysosomal acidic compartmentalisation. Lysosomal acidity appears to

219

be important to autophagy continuance. Therefore, it was postulated that a protective increase in autophagy during drug treatment could be circumvented during amino acid starvation therapy, were drug induced autophagy to coincide with amino acid induced lysosomal acidity depression (even in conditions of high autophagy flux).

Data clearly indicates that a non-tumourogenic cell line (MCF12A) with low basal autophagy is less resistant to programmed cell death during treatment with a moderate dose of doxorubicin (1 µM) than a metastatic cell line with high basal autophagy (MDAMB231). MCF12A cells had a significantly increased appearance of morphological changes characteristic of apoptosis as well as significantly enhanced caspase 3/7 activity (Fig 4.1). On the other hand, MDAMB231 cells showed few signs of late stage apoptosis and a more modest increase in activation of caspase 3/7 (Fig 4.2). Interestingly, depletion of amino acids from the culture medium of MCF12A cells during doxorubicin treatment resulted in a significant protection from loss of membrane integrity (a sign of late stage cell damage), as assessed by the trypan blue assay (Fig 4.3). Previous experimental data revealed that amino acid starvation resulted in an enhanced autophagy response (chapter 2). It is suggested here that this increase in autophagy could be responsible, at least in part, for the tolerance to doxorubicin treatment seen here. On the other hand, MDAMB231 cells did not experience any protection if starved of amino acids during treatment.

Both MCF12A and MDAMB231 cells responded to the presence of doxorubicin (1 µM) by increasing LC3 II protein levels (Fig 4.5), indicating an autophagy response during treatment. Inhibition of autophagy with ATG5 siRNA lead to a significant increase in caspase 3/7 activity only in MDAMB231 cells (Fig 4.7), suggesting that autophagy has a protective role during chemotherapy of these cells. Importantly, the addition of bafilomycin (10 nM), 6 hours prior to analysis, greatly increased caspase 3/7 activity during doxorubicin treatment in both

cell lines, but had a particularly pronounced influence on the partially resistant cancer cell line. Agents such as bafilomycin A1, a specific inhibitor of vacuolar H+ATPase (V-ATPase) (Yoshimori et al., 1991), are now known to rapidly and reversibly inhibit fusion between autophagosomes and lysosomes, if administered for short time periods (Klionsky et al., 2008), through the mechanism of inhibiting lysosomal acidification (Yamamoto et al., 1998). Furthermore, many drug resistant cancer cells are thought to increase sequestration and deactivation of chemotherapy drugs within lysosomes (Hurwitz et al., 1997). The proposed mechanism is through increased uptake of these compounds into endosomes which eventually fuse with lysosomes to deliver these drugs into the acidic internal environments where they become deactivated (Lee and Tannock, 2006). Bafilomycin A1 and other agents that raise the pH of lysosomes can increase cytotoxcity by preventing fusion and delivery of drugs in this way. Therefore, the increased caspase activity observed here, following bafilomycin administration, suggests that doxorubicin is being delivered to and accumulating in lysosomes and is therefore unable to exert its cytotoxic effects on the cell. As autophagy inhibition also results in increased caspase activity here, it is possible that mass engulfment of cytoplasmic material (which includes doxorubicin) could facilitate delivery of this drug into lysosomal compartments in this cell line and thereby have a protective influence. As MDAMB231 cells have high basal autophagy levels, internalized doxorubicin could rapidly be delivered to lysosomes and deactivated, conferring a partial resistance.

These assertions are further strengthened by qualitative evidence gained from fluorescence microscopy of MDAMB231 cells receiving doxorubicin treatment. Intracellular localization of doxorubicin can be tracked by exploiting the autofluorescence of doxorubicin, a technique that has been utilized successfully in MDAMB231 and other cell lines in the past (Li et al., 2010). Treatment of MDAMB231 cells results in the clear accumulation of doxorubicin at perinuclear regions (Fig 4.11). Identification of the spatial location of lysosomes at the same

time, by fluorescently tagging the lysosomal associated membrane protein LAMP-2A, demonstrates lysosomal pooling in regions associated with doxorubicin accumulation in these cells. This implies that doxorubicin is located in association with lysosomes during these conditions. MCF12A cells show little pooling of doxorubicin after a 24 hour treatment and have no discernable pooling of LAMP-2A signal (Fig 4.10). Furthermore, the addition of bafilomycin A1 (10 nM), 6 hours prior to imaging, led to a vast and pronounced accumulation of doxorubicin within the cytoplasmic compartment of MDAMB231 cells. Intriguingly, pooling of LAMP-2A signal is mostly dissipated and little association between LAMP-2A and doxorubicin is evident after the addition of bafilomycin A1. Therefore, it appears as though doxorubicin is not associated with lysosomes when administered in the presence of vacuolar H+ATPase inhibitor bafilomycin A1. However, excessive pooling of the drug does suggest that it is accumulating somewhere. As bafilomycin A1 inhibits the fusion of autophagosomes and endosomes with lysosomes, it is possible that the observed accumulations of doxorubicin is due to increased cytoplasmic accumulation of autophagosomes and endosomes containing doxorubicin, but which are unable to fuse with lysosomes. Further investigation of this phenomenon is required.

Autophagy flux is clearly increased in MDAMB231 cells in response to doxorubicin (1 µM) treatment (Fig 4.12) as well as during a short term bout of amino acid starvation (chapter 2), and lysosomal acidity greatly increases as a consequence of this treatment in both MCF12A cells (Fig 4.13) and in MDAMB231 cells (Fig 4.14). Interestingly, when these cell lines were treated with the anticancer agent in culture medium deprived of amino acids, lysosomal acidity significantly decreased in MDAMB231 cells but remained elevated in MCF12A cells. These findings mirrored previous observations when these cell lines were exposed to conditions of amino acid starvation (chapter 2). Notably, alterations in lysosomal acidity were associated with corresponding changes in caspase 3/7 activity in both cell lines. MDAMB231

cells experienced significantly greater levels of caspase 3/7 activity during conditions of depressed lysosomal acidity while MCF12A cells were granted a relative protection from the cytotoxic impact of drug treatment (Fig 4.15 and Fig 4.16). Strikingly, if MDAMB231 cells were analysed after 12 hours of combined doxorubicin/amino acid starvation treatment, these increases in apoptosis activation were not evident. Importantly, at this time point of amino acid starvation lysosomal acidity was confirmed to be elevated compared to baseline (chapter 2), further supporting the premise of lysosomal acidity deprivation facilitated increases in caspase activity in this model.

If decreased lysosomal acidity levels during amino acid starvation prevent fusion of autophagosomes with lysosomes then the probability of drug access to sites of cytoxic action would be increased. This would result in the increased apoptosis activation demonstrated here. Doxorubicin treatment is associated with genotoxic stress and prolonged g2/m cell cycle arrest (Koutsilieris et al., 1999, Lambert et al., 2008), due to intercalation of this agent with DNA and activation of the g2/m DNA damage checkpoint. Therefore, decreased abundance of doxorubicin within lysosomes during amino acid deprivation would result in an exacerbated accumulation of cells in the g2/m phase of the cell cycle. Our experimental data indicates this to be precisely the case with an approximately 6% increase in the percentage of MDAMB231 cells in the g2/m phase of the cell cycle if doxorubicin treated cells are simultaneously starved of amino acids (Fig 4.18). Additionally, the relative protection of MCF12A cells can be attributed to increased autophagy levels and decreased access of doxorubicin to the nucleus, as amino acid starvation during drug treatment resulted in a return of the cell cycle profile similar to that of untreated cells (Fig 4.17). Also, qualitative experimental evidence shows that doxorubicin treatment during amino acid starvation causes decreased doxorubicin accumulation and decreased LAMP-2A pooling and an increased

doxorubicin signal in the nuclear regions of MDAMB231 cells (Fig 4.20), whereas the converse is observed in MCF12A cells during similar treatment (Fig 4.19).

Data presented here suggests that alterations in lysosomal acidity are the cause for increased apoptosis induction or protection in MDAMB231 cells and MCF12A cells respectively. However, the role for autophagy should not be overlooked. Inhibition of autophagy with ATG5 siRNA resulted in a prominent increase in levels of doxorubicin, in the nucleus and at the perinuclear zone (Fig 4.20), while MCF12A cells exposed to ATG5 siRNA prior to treatment showed signs of increased cytoplasmic doxorubicin accumulation (Fig 4.19). Interestingly, a cell line with decreased autophagy (MCF7), due to haploinsufficiency in the gene coding for beclin 1, displayed no alterations to lysosomal acidity during doxorubicin (1 µM) treatment, in the presence or absence of amino acids (Fig 4.21). While this cell line does not possess active caspase 3 (Fig 4.22), it did show signs of significantly increased apoptosis during doxorubicin (1 µM) treatment. These levels of apoptosis did not increase if treatment occurred in the absence of amino acids or the presence of bafilomycin A1 (10 nM) (Fig 4.23). Together, these results indicate that active autophagy machinery is required for the accumulation of doxorubicin within lysosomes and demonstrates an important role for autophagy in these possesses.

5.1   Conclusions

It is suggested here that cancers with high basal autophagy, such as the *ras*-mutant MDAMB231 cells, possess an inherent resistance to alkaline chemotherapy agents such as doxorubicin that can be overcome with the pharmacologically mediated elevation of lysosomal pH. Furthermore, experimental evidence presented here indicates that short term starvation during chemotherapy is a realistic avenue for adjuvant therapy but there is need for

future investigation. Non-cancer cells, with low basal autophagy, able to increase autophagy activity in response to short term starvation could potentially benefit from protection during anthracycline treatment. Recent evidence of differential protection of non-cancer cells in human (Safdie et al., 2009) and animal studies (Raffaghello et al., 2008) during chemotherapy and the recent clinical interest in autophagy modulation during therapy necessitate additional studies such as the one presented here. Finally, this study is the first to our knowledge that describes a mechanism whereby autophagy can lead to the inactivation of basic cancer drugs by delivering these agents to acidic lysosomal compartments.
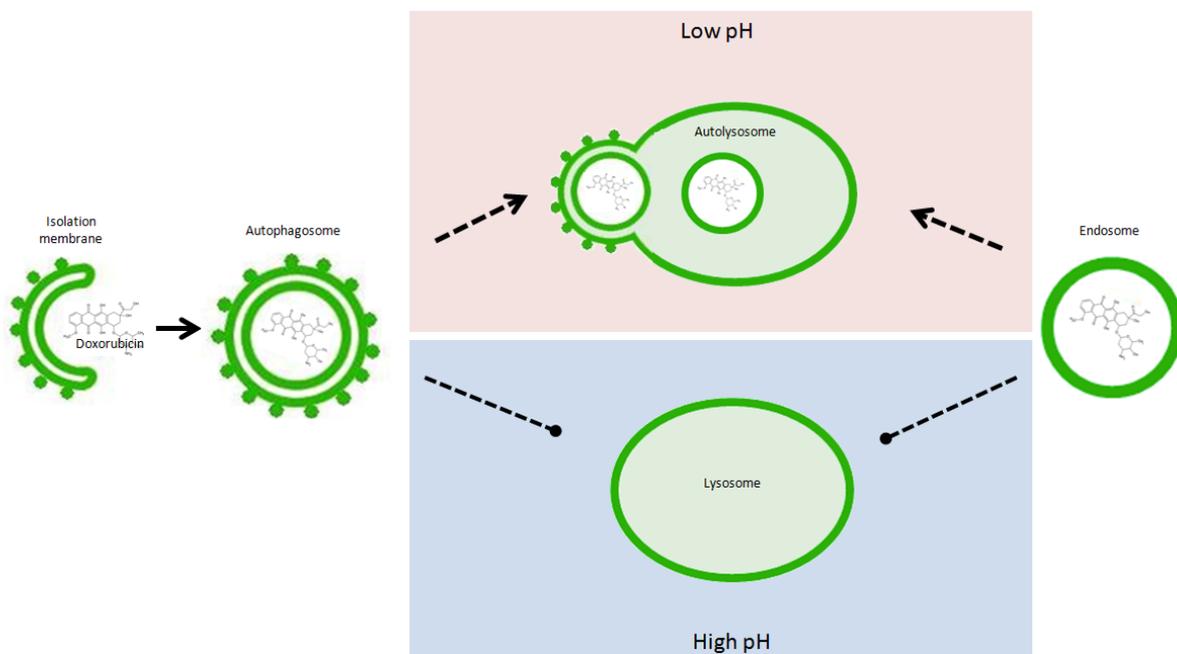
Image 4.1 Schematic depicting the delivery of doxorubicin by macroautophagy or endosomes to lysosomal compartments. It is proposed that bulk engulfment of cytoplasmic material (containingdoxorubicin) during treatment, and the subsequent delivery of the drug to lysosomes, can result in its protonation, sequestration and inactivation provided that lysosomes have low internal pH. Pharmacological (or other) modulation of lysosomal pH could result in decreased fusion and inactivation of the basic cancer drug, thereby decreasing its access to sites of cytotoxic action (such as DNA).

6 References

ADAMS, J. M. & CORY, S. 2007. Bcl-2-regulated apoptosis: mechanism and therapeutic potential. *Curr Opin Immunol,* 19**,** 488-96.

AITA, V. M., LIANG, X. H., MURTY, V. V., PINCUS, D. L., YU, W., CAYANIS, E., KALACHIKOV, S., GILLIAM, T. C. & LEVINE, B. 1999. Cloning and genomic organization of beclin 1, a candidate tumor suppressor gene on chromosome 17q21. *Genomics,* 59**,** 59-65.

AKAR, U., CHAVES-REYEZ, A., BARRIA, M., TARI, A., SANGUINO, A., KONDO, Y., KONDO, S., ARUN, B., LOPEZ-BERESTEIN, G. & OZPOLAT, B. 2008. Silencing of Bcl-2 expression by small interfering RNA induces autophagic cell death in MCF-7 breast cancer cells. *Autophagy,* 4**,** 669-79.

AMARAVADI, R. K., YU, D., LUM, J. J., BUI, T., CHRISTOPHOROU, M. A., EVAN, G. I., THOMAS-TIKHONENKO, A. & THOMPSON, C. B. 2007. Autophagy inhibition enhances therapy-induced apoptosis in a Myc-induced model of lymphoma. *J Clin Invest,* 117**,** 326-36.

AOKI, H., TAKADA, Y., KONDO, S., SAWAYA, R., AGGARWAL, B. B. & KONDO, Y. 2007. Evidence that curcumin suppresses the growth of malignant gliomas in vitro and in vivo through induction of autophagy: role of Akt and extracellular signal-regulated kinase signaling pathways. *Mol Pharmacol,* 72**,** 29-39.

BARRETT-LEE, P. J., DIXON, J. M., FARRELL, C., JONES, A., LEONARD, R., MURRAY, N., PALMIERI, C., PLUMMER, C. J., STANLEY, A. & VERRILL, M. W. 2009. Expert opinion on the use of anthracyclines in patients with advanced breast cancer at cardiac risk. *Ann Oncol,* 20**,** 816-27.

BELLODI, C., LIDONNICI, M. R., HAMILTON, A., HELGASON, G. V., SOLIERA, A. R., RONCHETTI, M., GALAVOTTI, S., YOUNG, K. W., SELMI, T., YACOBI, R., VAN ETTEN, R. A., DONATO, N., HUNTER, A., DINSDALE, D., TIRRO, E., VIGNERI, P., NICOTERA, P., DYER, M. J., HOLYOAKE, T., SALOMONI, P. & CALABRETTA, B. 2009. Targeting autophagy potentiates tyrosine kinase inhibitor-induced cell death in Philadelphia chromosome-positive cells, including primary CML stem cells. *J Clin Invest,* 119**,** 1109-23.

BOYA, P., GONZALEZ-POLO, R. A., CASARES, N., PERFETTINI, J. L., DESSEN, P., LAROCHETTE, N., METIVIER, D., MELEY, D., SOUQUERE, S., YOSHIMORI, T., PIERRON, G., CODOGNO, P. & KROEMER, G. 2005. Inhibition of macroautophagy triggers apoptosis. *Mol Cell Biol,* 25**,** 1025-40.

BURSCH, W., ELLINGER, A., KIENZL, H., TOROK, L., PANDEY, S., SIKORSKA, M., WALKER, R. & HERMANN, R. S. 1996. Active cell death induced by the anti-estrogens tamoxifen and ICI 164 384 in human mammary carcinoma cells (MCF-7) in culture: the role of autophagy. *Carcinogenesis,* 17**,** 1595-607.

CAREW, J. S., MEDINA, E. C., ESQUIVEL, J. A., 2ND, MAHALINGAM, D., SWORDS, R., KELLY, K., ZHANG, H., HUANG, P., MITA, A. C., MITA, M. M., GILES, F. J. & NAWROCKI, S. T. 2010. Autophagy inhibition enhances vorinostat-induced apoptosis via ubiquitinated protein accumulation. *J Cell Mol Med,* 14**,** 2448-59.

CHEN, K., XU, X., KOBAYASHI, S., TIMM, D., JEPPERSON, T. & LIANG, Q. 2011. Caloric restriction mimetic 2-deoxyglucose antagonizes doxorubicin-induced cardiomyocyte death by multiple mechanisms. *J Biol Chem,* 286**,** 21993-2006.

DEGENHARDT, K., MATHEW, R., BEAUDOIN, B., BRAY, K., ANDERSON, D., CHEN, G., MUKHERJEE, C., SHI, Y., GELINAS, C., FAN, Y., NELSON, D. A., JIN, S. & WHITE, E. 2006. Autophagy promotes tumor cell survival and restricts necrosis, inflammation, and tumorigenesis. *Cancer Cell,* 10**,** 51-64.

DUNN, S. E., KARI, F. W., FRENCH, J., LEININGER, J. R., TRAVLOS, G., WILSON, R. & BARRETT, J. C. 1997. Dietary restriction reduces insulin-like growth factor I levels, which modulates apoptosis, cell proliferation, and tumor progression in p53-deficient mice. *Cancer Res,* 57**,** 4667-72.

FUJIWARA, K., IWADO, E., MILLS, G. B., SAWAYA, R., KONDO, S. & KONDO, Y. 2007. Akt inhibitor shows anticancer and radiosensitizing effects in malignant glioma cells by inducing autophagy. *Int J Oncol,* 31**,** 753-60.

GARCIA-ESCUDERO, V. & GARGINI, R. 2008. Autophagy induction as an efficient strategy to eradicate tumors. *Autophagy,* 4**,** 923-5.

GIACCONE, G. & PINEDO, H. M. 1996. Drug Resistance. *Oncologist,* 1**,** 82-87.

GIATROMANOLAKI, A., KOUKOURAKIS, M. I., HARRIS, A. L., POLYCHRONIDIS, A., GATTER, K. C. & SIVRIDIS, E. 2010. Prognostic relevance of light chain 3 (LC3A) autophagy patterns in colorectal adenocarcinomas. *J Clin Pathol,* 63**,** 867-72.

GUTIERREZ, M. G., SAKA, H. A., CHINEN, I., ZOPPINO, F. C., YOSHIMORI, T., BOCCO, J. L. & COLOMBO, M. I. 2007. Protective role of autophagy against Vibrio cholerae cytolysin, a pore-forming toxin from V. cholerae. *Proc Natl Acad Sci U S A,* 104**,** 1829-34.

HEILBRONN, L. K. & RAVUSSIN, E. 2005. Calorie restriction extends life span--but which calories? *PLoS Med,* 2**,** e231.

HERLEVSEN, M., OXFORD, G., OWENS, C. R., CONAWAY, M. & THEODORESCU, D. 2007. Depletion of major vault protein increases doxorubicin sensitivity and nuclear accumulation and disrupts its sequestration in lysosomes. *Mol Cancer Ther,* 6**,** 1804-13.

HURWITZ, S. J., TERASHIMA, M., MIZUNUMA, N. & SLAPAK, C. A. 1997. Vesicular anthracycline accumulation in doxorubicin-selected U-937 cells: participation of lysosomes. *Blood,* 89**,** 3745-54.

KANZAWA, T., GERMANO, I. M., KOMATA, T., ITO, H., KONDO, Y. & KONDO, S. 2004. Role of autophagy in temozolomide-induced cytotoxicity for malignant glioma cells. *Cell Death Differ,* 11**,** 448-57.

KIM, K. W., HWANG, M., MORETTI, L., JABOIN, J. J., CHA, Y. I. & LU, B. 2008. Autophagy upregulation by inhibitors of caspase-3 and mTOR enhances radiotherapy in a mouse model of lung cancer. *Autophagy,* 4**,** 659-68.

KIM, K. W., MUTTER, R. W., CAO, C., ALBERT, J. M., FREEMAN, M., HALLAHAN, D. E. & LU, B. 2006. Autophagy for cancer therapy through inhibition of pro-apoptotic proteins and mammalian target of rapamycin signaling. *J Biol Chem,* 281**,** 36883-90.

KIM, Y. 2010. The effects of nutrient depleted microenvironments and delta-like 1 homologue (DLK1) on apoptosis in neuroblastoma. *Nutr Res Pract,* 4**,** 455-61.

KLIONSKY, D. J., ELAZAR, Z., SEGLEN, P. O. & RUBINSZTEIN, D. C. 2008. Does bafilomycin A1 block the fusion of autophagosomes with lysosomes? *Autophagy,* 4**,** 849-950.

KOBAYASHI, S., VOLDEN, P., TIMM, D., MAO, K., XU, X. & LIANG, Q. 2010. Transcription factor GATA4 inhibits doxorubicin-induced autophagy and cardiomyocyte death. *J Biol Chem,* 285**,** 793-804.

KONDO, S., BARNA, B. P., MORIMURA, T., TAKEUCHI, J., YUAN, J., AKBASAK, A. & BARNETT, G. H. 1995. Interleukin-1 beta-converting enzyme mediates cisplatin-induced apoptosis in malignant glioma cells. *Cancer Res,* 55**,** 6166-71.

KONDO, Y. & KONDO, S. 2006. Autophagy and cancer therapy. *Autophagy,* 2**,** 85-90.

KOUTSILIERIS, M., REYES-MORENO, C., CHOKI, I., SOURLA, A., DOILLON, C. & PAVLIDIS, N. 1999. Chemotherapy cytotoxicity of human MCF-7 and MDA-MB 231 breast cancer cells is altered by osteoblast-derived growth factors. *Mol Med,* 5**,** 86-97.

KRISHNA, R. & MAYER, L. D. 2000. Multidrug resistance (MDR) in cancer. Mechanisms, reversal using modulators of MDR and the role of MDR modulators in influencing the pharmacokinetics of anticancer drugs. *Eur J Pharm Sci,* 11**,** 265-83.

KRITCHEVSKY, D. 2003. Diet and cancer: what's next? *J Nutr,* 133**,** 3827S-3829S.

LAMBERT, L. A., QIAO, N., HUNT, K. K., LAMBERT, D. H., MILLS, G. B., MEIJER, L. & KEYOMARSI, K. 2008. Autophagy: a novel mechanism of synergistic cytotoxicity between doxorubicin and roscovitine in a sarcoma model. *Cancer Res,* 68**,** 7966-74.

LEE, C. M. & TANNOCK, I. F. 2006. Inhibition of endosomal sequestration of basic anticancer drugs: influence on cytotoxicity and tissue penetration. *Br J Cancer,* 94**,** 863-9.

LEVINE, B. & KROEMER, G. 2008. Autophagy in the pathogenesis of disease. *Cell,* 132**,** 27-42.

LEVINE, B., MIZUSHIMA, N. & VIRGIN, H. W. 2011. Autophagy in immunity and inflammation. *Nature,* 469**,** 323-35.

LEVY, J. M. & THORBURN, A. 2011. Targeting autophagy during cancer therapy to improve clinical outcomes. *Pharmacol Ther,* 131**,** 130-41.

LI, Y., ZOU, L., LI, Q., HAIBE-KAINS, B., TIAN, R., DESMEDT, C., SOTIRIOU, C., SZALLASI, Z., IGLEHART, J. D., RICHARDSON, A. L. & WANG, Z. C. 2010. Amplification of LAPTM4B and YWHAZ contributes to chemotherapy resistance and recurrence of breast cancer. *Nat Med,* 16**,** 214-8.

LIU, L., YANG, M., KANG, R., WANG, Z., ZHAO, Y., YU, Y., XIE, M., YIN, X., LIVESEY, K. M., LOTZE, M. T., TANG, D. & CAO, L. 2011a. HMGB1-induced autophagy promotes chemotherapy resistance in leukemia cells. *Leukemia,* 25**,** 23-31.

LIU, L., YANG, M., KANG, R., WANG, Z., ZHAO, Y., YU, Y., XIE, M., YIN, X., LIVESEY, K. M., LOZE, M. T., TANG, D. & CAO, L. 2011b. DAMP-mediated autophagy contributes to drug resistance. *Autophagy,* 7**,** 112-4.

MA, L. & CENTER, M. S. 1992. The gene encoding vacuolar H(+)-ATPase subunit C is overexpressed in multidrug-resistant HL60 cells. *Biochem Biophys Res Commun,* 182**,** 675-81.

MA, X. H., PIAO, S., WANG, D., MCAFEE, Q. W., NATHANSON, K. L., LUM, J. J., LI, L. Z. & AMARAVADI, R. K. 2011. Measurements of tumor cell autophagy predict invasiveness, resistance to chemotherapy, and survival in melanoma. *Clin Cancer Res,* 17**,** 3478-89.

MACLEAN, K. H., DORSEY, F. C., CLEVELAND, J. L. & KASTAN, M. B. 2008. Targeting lysosomal degradation induces p53-dependent cell death and prevents cancer in mouse models of lymphomagenesis. *J Clin Invest,* 118**,** 79-88.

MARTIN, A., JOSEPH, J. A. & CUERVO, A. M. 2002. Stimulatory effect of vitamin C on autophagy in glial cells. *J Neurochem,* 82**,** 538-49.

MATHEW, R., KARANTZA-WADSWORTH, V. & WHITE, E. 2007. Role of autophagy in cancer. *Nat Rev Cancer,* 7**,** 961-7.

MORETTI, L., KIM, K. W., JUNG, D. K., WILLEY, C. D. & LU, B. 2009. Radiosensitization of solid tumors by Z-VAD, a pan-caspase inhibitor. *Mol Cancer Ther,* 8**,** 1270-9.

MURPHY, J. D., SPALDING, A. C., SOMNAY, Y. R., MARKWART, S., RAY, M. E. & HAMSTRA, D. A. 2009. Inhibition of mTOR radiosensitizes soft tissue sarcoma and tumor vasculature. *Clin Cancer Res,* 15**,** 589-96.

NICOTRA, G., MERCALLI, F., PERACCHIO, C., CASTINO, R., FOLLO, C., VALENTE, G. & ISIDORO, C. 2010. Autophagy-active beclin-1 correlates with favourable clinical outcome in non-Hodgkin lymphomas. *Mod Pathol,* 23**,** 937-50.

O'SHAUGHNESSY, J., TWELVES, C. & AAPRO, M. 2002. Treatment for anthracycline-pretreated metastatic breast cancer. *Oncologist,* 7 Suppl 6**,** 4-12.

OHSHIRO, K., RAYALA, S. K., KONDO, S., GAUR, A., VADLAMUDI, R. K., EL-NAGGAR, A. K. & KUMAR, R. 2007. Identifying the estrogen receptor coactivator PELP1 in autophagosomes. *Cancer Res,* 67**,** 8164-71.

OHTANI, S., IWAMARU, A., DENG, W., UEDA, K., WU, G., JAYACHANDRAN, G., KONDO, S., ATKINSON, E. N., MINNA, J. D., ROTH, J. A. & JI, L. 2007. Tumor suppressor 101F6 and ascorbate synergistically and selectively inhibit non-small cell lung cancer growth by caspase-independent apoptosis and autophagy. *Cancer Res,* 67**,** 6293-303.

OPIPARI, A. W., JR., TAN, L., BOITANO, A. E., SORENSON, D. R., AURORA, A. & LIU, J. R. 2004. Resveratrol-induced autophagocytosis in ovarian cancer cells. *Cancer Res,* 64**,** 696-703.

PAGLIN, S., HOLLISTER, T., DELOHERY, T., HACKETT, N., MCMAHILL, M., SPHICAS, E., DOMINGO, D. & YAHALOM, J. 2001. A novel response of cancer cells to radiation involves autophagy and formation of acidic vesicles. *Cancer Res,* 61**,** 439-44.

PARDO, R., LO RE, A., ARCHANGE, C., ROPOLO, A., PAPADEMETRIO, D. L., GONZALEZ, C. D., ALVAREZ, E. M., IOVANNA, J. L. & VACCARO, M. I. 2010. Gemcitabine induces the VMP1-mediated autophagy pathway to promote apoptotic death in human pancreatic cancer cells. *Pancreatology,* 10**,** 19-26.

PARK, M. A., ZHANG, G., NORRIS, J., HYLEMON, P. B., FISHER, P. B., GRANT, S. & DENT, P. 2008. Regulation of autophagy by ceramide-CD95-PERK signaling. *Autophagy,* 4**,** 929-31.

PIRTOLI, L., CEVENINI, G., TINI, P., VANNINI, M., OLIVERI, G., MARSILI, S., MOURMOURAS, V., RUBINO, G. & MIRACCO, C. 2009. The prognostic role of Beclin 1 protein expression in high-grade gliomas. *Autophagy,* 5**,** 930-6.

POPKIN, B. M. 2007. Understanding global nutrition dynamics as a step towards controlling cancer incidence. *Nat Rev Cancer,* 7**,** 61-7.

POWOLNY, A. A., BOMMAREDDY, A., HAHM, E. R., NORMOLLE, D. P., BEUMER, J. H., NELSON, J. B. & SINGH, S. V. 2011. Chemopreventative potential of the cruciferous vegetable constituent phenethyl isothiocyanate in a mouse model of prostate cancer. *J Natl Cancer Inst,* 103**,** 571-84.

QADIR, M. A., KWOK, B., DRAGOWSKA, W. H., TO, K. H., LE, D., BALLY, M. B. & GORSKI, S. M. 2008. Macroautophagy inhibition sensitizes tamoxifen-resistant breast cancer cells and enhances mitochondrial depolarization. *Breast Cancer Res Treat,* 112**,** 389-403.

RAFFAGHELLO, L., LEE, C., SAFDIE, F. M., WEI, M., MADIA, F., BIANCHI, G. & LONGO, V. D. 2008. Starvation-dependent differential stress resistance protects normal but not cancer cells against high-dose chemotherapy. *Proc Natl Acad Sci U S A,* 105**,** 8215-20.

RICKMANN, M., VAQUERO, E. C., MALAGELADA, J. R. & MOLERO, X. 2007. Tocotrienols induce apoptosis and autophagy in rat pancreatic stellate cells through the mitochondrial death pathway. *Gastroenterology,* 132**,** 2518-32.

ROCCARO, A. M., HIDESHIMA, T., RICHARDSON, P. G., RUSSO, D., RIBATTI, D., VACCA, A., DAMMACCO, F. & ANDERSON, K. C. 2006. Bortezomib as an antitumor agent. *Curr Pharm Biotechnol,* 7**,** 441-8.

SAFDIE, F. M., DORFF, T., QUINN, D., FONTANA, L., WEI, M., LEE, C., COHEN, P. & LONGO, V. D. 2009. Fasting and cancer treatment in humans: A case series report. *Aging (Albany NY),* 1**,** 988-1007.

SAVARINO, A., LUCIA, M. B., GIORDANO, F. & CAUDA, R. 2006. Risks and benefits of chloroquine use in anticancer strategies. *Lancet Oncol,* 7**,** 792-3.

SELL, C. 2003. Caloric restriction and insulin-like growth factors in aging and cancer. *Horm Metab Res,* 35**,** 705-11.

SHAO, Y., GAO, Z., MARKS, P. A. & JIANG, X. 2004. Apoptotic and autophagic cell death induced by histone deacetylase inhibitors. *Proc Natl Acad Sci U S A,* 101**,** 18030-5.

SOTELO, J., BRICENO, E. & LOPEZ-GONZALEZ, M. A. 2006. Adding chloroquine to conventional treatment for glioblastoma multiforme: a randomized, double-blind, placebo-controlled trial. *Ann Intern Med,* 144**,** 337-43.

SPINDLER, S. R. & DHAHBI, J. M. 2007. Conserved and tissue-specific genic and physiologic responses to caloric restriction and altered IGFI signaling in mitotic and postmitotic tissues. *Annu Rev Nutr,* 27**,** 193-217.

SWAIN, S. M., WHALEY, F. S. & EWER, M. S. 2003. Congestive heart failure in patients treated with doxorubicin: a retrospective analysis of three trials. *Cancer,* 97**,** 2869-79.

TAVERA-MENDOZA, L., WANG, T. T., LALLEMANT, B., ZHANG, R., NAGAI, Y., BOURDEAU, V., RAMIREZ-CALDERON, M., DESBARATS, J., MADER, S. & WHITE, J. H. 2006. Convergence of vitamin D and retinoic acid signalling at a common hormone response element. *EMBO Rep,* 7**,** 180-5.

TURCOTTE, S., CHAN, D. A., SUTPHIN, P. D., HAY, M. P., DENNY, W. A. & GIACCIA, A. J. 2008. A molecule targeting VHL-deficient renal cell carcinoma that induces autophagy. *Cancer Cell,* 14**,** 90-102.

WON, K. Y., KIM, G. Y., KIM, Y. W., SONG, J. Y. & LIM, S. J. 2010. Clinicopathologic correlation of beclin-1 and bcl-2 expression in human breast cancer. *Hum Pathol,* 41**,** 107-12.

WU, H., YANG, J. M., JIN, S., ZHANG, H. & HAIT, W. N. 2006. Elongation factor-2 kinase regulates autophagy in human glioblastoma cells. *Cancer Res,* 66**,** 3015-23.

WU, Z., CHANG, P. C., YANG, J. C., CHU, C. Y., WANG, L. Y., CHEN, N. T., MA, A. H., DESAI, S. J., LO, S. H., EVANS, C. P., LAM, K. S. & KUNG, H. J. 2010. Autophagy Blockade Sensitizes Prostate Cancer Cells towards Src Family Kinase Inhibitors. *Genes Cancer,* 1**,** 40-9.

YAMAMOTO, A., TAGAWA, Y., YOSHIMORI, T., MORIYAMA, Y., MASAKI, R. & TASHIRO, Y. 1998. Bafilomycin A1 prevents maturation of autophagic vacuoles by inhibiting fusion between autophagosomes and lysosomes in rat hepatoma cell line, H-4-II-E cells. *Cell Struct Funct,* 23**,** 33-42.

YANG, P. M. & CHEN, C. C. 2011. Life or death? Autophagy in anticancer therapies with statins and histone deacetylase inhibitors. *Autophagy,* 7**,** 107-8.

YAO, J. C., LOMBARD-BOHAS, C., BAUDIN, E., KVOLS, L. K., ROUGIER, P., RUSZNIEWSKI, P., HOOSEN, S., ST PETER, J., HAAS, T., LEBWOHL, D., VAN CUTSEM, E., KULKE, M. H., HOBDAY, T. J., O'DORISIO, T. M., SHAH, M. H., CADIOT, G., LUPPI, G., POSEY, J. A. & WIEDENMANN, B. 2010. Daily oral everolimus activity in patients with metastatic pancreatic neuroendocrine tumors after failure of cytotoxic chemotherapy: a phase II trial. *J Clin Oncol,* 28**,** 69-76.

YOSHIMORI, T., YAMAMOTO, A., MORIYAMA, Y., FUTAI, M. & TASHIRO, Y. 1991. Bafilomycin A1, a specific inhibitor of vacuolar-type H(+)-ATPase, inhibits acidification and protein degradation in lysosomes of cultured cells. *J Biol Chem,* 266**,** 17707-12.

YU, L., STRANDBERG, L. & LENARDO, M. J. 2008. The selectivity of autophagy and its role in cell death and survival. *Autophagy,* 4**,** 567-73.

5 _____

Development of a novel *in vivo* mouse mammary cancer model to study autophagy in the non-cancer cell population of the tumour and apoptosis within the whole tumour

Solid tumours are heterogenous masses comprised of cancer cell and stromal elements that collectively make up the malignant neoplasm. Although generally thought of as a mass of cancer cells, much of the solid tumour is typically made up of a variety of cell subpopulations that are required for continued growth and invasion. This chapter describes the establishment of a novel mammary tumour model in GFP-LC3 transgenic mice in which the influence of protein deprivation (and theoretically other interventions) on autophagy in the non-cancer population of tumours was analysed. The impact of apoptosis after protein deprivation in this model was also assessed.

1   Introduction

Solid tumours are sometimes described as being organ-like and are now known to contain many different cell subpopulations. Neoplasms possess a heterogenous composition, and contain cancer and non-cancer cells of many varieties. In fact, invading non-cancer cells and stromal elements are vital for the continued survival of solid tumours (Mueller and Fusenig, 2004, Egeblad et al., 2008). Although Stephen Paget‟s well known metaphor of tumour cells behaving like plant seeds requiring favourable conditions and a microenvironment able to facilitate progression and growth is over 100 years old, the tumour microenvironment and the contribution of non-cancer cells within cancers has been largely ignored in the study of solid neoplasms (Mueller and Fusenig, 2004).

In addition to tumour cells, so-called non-cancer tumour cells such as fibroblasts, macrophages and other myeloid cells are all present within the tumour microenvironment (Egeblad et al., 2008). Together with interstitial fluid and other connective tissue elements such as elastin, fibrin and collagen, the relative amount of stroma to malignant cells can vary considerably between tumours (Dvorak et al., 1983). Additionally, neoangiogenesis and the development of blood vessels that are derived from native vascular stroma, throughout the tumour mass, are vital for continued progression of tumour growth (Johann et al., 2010, Tredan et al., 2007) where hematopoietic cells in the tumour stroma regulate tumour progression (Huynh et al., 2011). Moreover, prognosis and sensitivity to chemotherapeutics also depend on the makeup of the tumour microenvironment (Tredan et al., 2007).

All mammalian cells are believed to be able to induce autophagy in response to stress such as amino acid deprivation (Mizushima et al., 2004). Strategies aiming to induce cell death in cancer cells or protect non-cancer cells during treatments often overlook the impact of indirect effects on surrounding cell populations. It is vitally important that models are devised that take these aspects into account.

1.2 *In vivo* assessment of autophagy using GFP-LC3

Assessment of autophagy is complex and contains many pitfalls. The most common methods employ the use of fluorescence techniques or electron microscopy (Mizushima et al., 2010), but these techniques are laborious and require much experience if they are to be used accurately. LC3 is a mammalian homologue of yeast Atg8 and is a marker of autophagosomes. Frequent use of GFP (a green fluorescent protein that exhibits a green fluorescence when exposed to specfic wavelengths of light) fused LC3 to monitor incorporation of LC3 into autophagosomes, and thereby quantify autophagosome number and

232

by inference autophagy induction, is described in the literature (Mizushima et al., 2010). This method has been used most successfully to label autophagosomes *in vivo* in a number of organisms (Rusten et al., 2004, Melendez et al., 2003), including mammals (Mizushima et al., 2004). However, up to now models to describe autophagy in the cancer context *in vivo* are conspicuously absent.

2 Research problem and aims

2.1 Motivation

Findings in previous studies (presented in chapter 1 to 4) showed that while amino acid deprivation caused increased cell death in cancer cells, it also protected non-cancer cells from cell death. In order to apply the concepts outlined in those studies *in vivo*, and investigate if the findings revealed there would translate in the context of a living organism, it was neccessary that a novel animal model be established.

2.2 Research problem

Cancers are heterogenous masses that rely on non-cancer tumour cells and host tissue stroma to survive and grow. Most cancer cells are thought to induce autophagy as a protective mechanism in response to stress. Therefore, if increased autophagy in non-cancer cells within a solid neoplasm results in protection of these cells during treatment then, hypothetically, this could ultimately facilitate long term tumour progression and invasion. However, models capable of describing these events *in vivo* are currently lacking.

2.3 Aims

1. Determine if E0771 murine mammary adenocarcinoma cells can form tumours in a transgenic mouse that systematically expresses GFP fused to LC3 in most tissues.

2. Contingent to results obtained from aim 1, establish a protocol that details a method to reproducibly grow these tumours *in vivo*.

3. Establish a protocol and associated methods for excision and analysis of these tumours to determine if a GFP-LC3 signal derived from non-cancer cells is present within tumour tissue.

3   Methods, results and discussion

Previous experimental data has shown that amino acid deprivation from the culture medium of non-cancer mammary epithelial cells (MCF12A) resulted in a relative protection of these cells from cytotoxicity associated with chemotherapy whereas cytotoxicity appeared to be enhanced in cancer cells (MDAMB231) receiving similar treatments (described in chapter 4). As solid tumours rely on non-cancer cells for survival, protection of non-cancer cells, within tumours, from cytotoxicity during short term starvation could indirectly result in prolonged tumour cell survival during chemotherapy.

In this study a murine mammary adenocarcinoma cell line, originally isolated from an immunocompetent C57BL6 mouse, was utilized. This cell line is well established (Casey et al., 1951, Casey et al., 1952) and has a well characterized metastatic potential (Ewens et al., 2006). Furthermore, increased recent use of these cells (Young et al., 2010, Hiratsuka et al., 2011, McHowat et al., 2011, Sharma et al., 2008) and previous comparisons with MDAMB231 cells (Young et al., 2010, Li, 2009) made this cell line an attractive candidate for use in our model. E0771 cells are typically used in cell culture and in allografting mouse models in syngenic C57BL6 mice. However, these cells have also been used to establish mammary tumours in a transgenic knockout mouse model assessing calcium-independent phospholipase A2β deficiency during lung metastasis (McHowat et al., 2011). In order to establish a model where autophagy could be assessed in non-cancer cells within a tumour, transgenic mice systemically expressing GFP fused to LC3 (referred to as GFP-LC3 mice from here on) were used in conjunction with E0771 murine mammary adeoncarcinoma cells to generate tumours where the GFP signal could be related to autophagy status in the non-cancer cell population within tumours. GFP-LC3 mice were originally generated with the intention of being used to assess autophagosomes *in vivo* (Mizushima et al., 2004), and this

elegantly designed model has been used successfully to analyse autophagy induction *in vivo*. Using these mice, autophagy is monitored as GFP-LC3 becomes incorporated into autophagosomes. Currently, methods used to quantify and monitor autophagy are limited, time consuming and require vast amounts of expertise (Mizushima et al., 2010). Moreover, methods to assess autophagy specifically in the *in vivo* cancer setting are absent and assessing intratumour, non-cancer cell populations in the context of autophagy do not exist to date. Our aim was to establish such a model using GFP-LC3 mice. However, chemical induction of cancers can be difficult to characterize and xenografts of cancer cell lines usually require the use of immune compromised animals (Medina, 2007). As GFP-LC3 mice are crossed with C57BL/6N Crj mice, it was unclear if E0771 cells could be used to successfully establish tumours in these animals.

2.1   Sourcing and culture of E0771 mouse mammary cancer cells

Experiments were performed using the murine metastatic mammary adenocarcinoma cell line E0771. This cell line was generously provided by Fengzhi Li (Roswell Park Cancer Institute, Buffalo, New York, USA). During routine maintenance, cells were grown as monolayers in Glutamax-DMEM (Celtic Molecular Diagnostics, Cape Town, South Africa) supplemented with 10% foetal bovine serum (Sigma Chemical Co., St Louis, MO, USA) at 37°C in a humidified atmosphere of 95% air plus 5% CO_2 in T75 flasks (75cm^2 flasks, Greiner Bio One, Germany) until they reached 80% confluence. E0771 cells were then split 1:3. Splitting was accomplished by washing the cell monolayer with warm phosphate buffered saline (PBS) followed by incubation with 4 ml trypsin/EDTA (Sigma Chemical Co., St Louis, MO, USA) at 37°C, with occasional agitation, until cells loosened completely or for a maximum of four minutes. Experiments were performed using exponentially growing cells.

2.2   Tumour establishment and animal protocols

The protocols in this study were carried out according to the guidelines for the care and use of laboratory animals implemented at Stellenbosch University. Eight week-old female C57BL6 mice (Stellenbosch University animal facility) or GFP-LC3 mice (kindly donated by Noboru Mizushima, Department of Cell Biology, National Institute for Basic Biology, Okazaki, Japan) were used in this study. The mice were maintained on standard chow diet and tap water before beginning the experiment. Mice were inoculated subcutaneously on the left pad of the fourth mammary gland with 200 µl of 2.5×10^5 E0771 cells suspended in Hanks Balanced Salt Solution (Sigma Chemical Co., St Louis, MO, USA), using a 23-gauge needle (image 5.1). This protocol was adapted from Ewans et al. 2006.

A.

B.
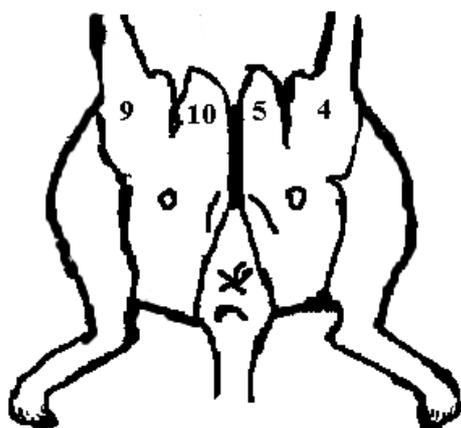
Image 5.1 200 µL cell suspensions (containing E0771 2.5 _$\times 10^5$ cells) were injected s.c. in the lower abdomen of each mouse, in or near the no. 4 mammary fat pad. A) Illustration depicting positions of mammary fat pads 9, 10, 5 and 4. B) s.c. injection of GFP-LC3 mouse with E0771 cell suspension. Protocol adapted from Ewans *et al.* 2006.
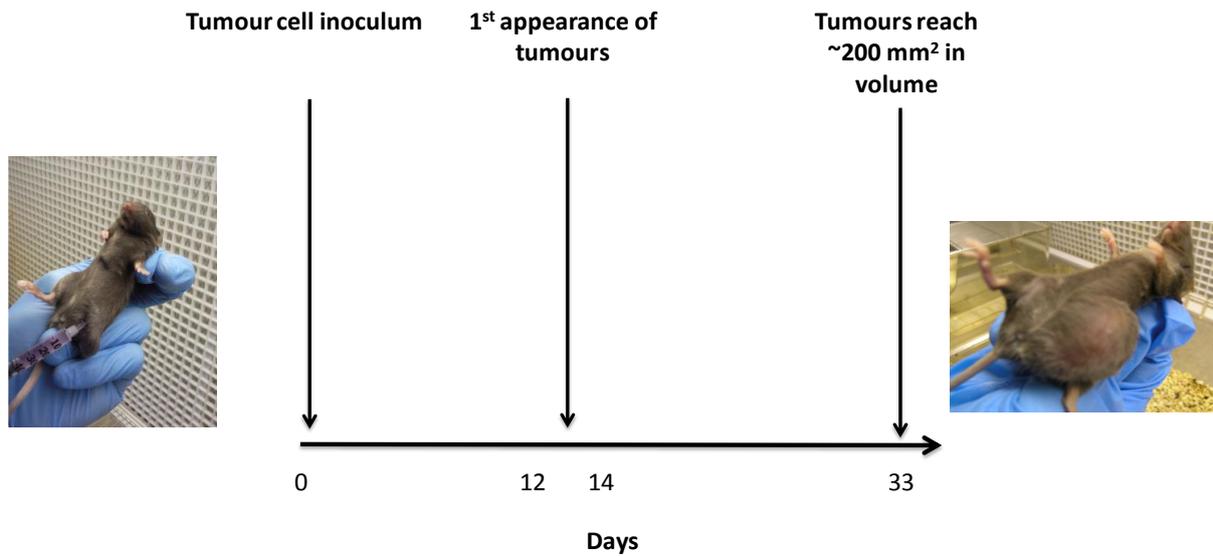
Tumour cell inoculum   **1st appearance of tumours**   **Tumours reach ~200 mm² in volume**

0   12   14   33

Days

Image 5.2 Diagrammatic depiction of experimental procedure and tumour developmental timeline.

Mice were injected with cell suspensions made up of E0771 cells on day 0 and small tumours were evident by days 12 to 14. Tumours grew to reach approximately 230 mm² in volume by day 33.

Image 5.3 Typical tumour of approximately 230 mm² in volume just prior to the initial intervention. Tumours in GFP-LC3 mice reached this volume about 33 days after injection with a E0771 cell suspension.
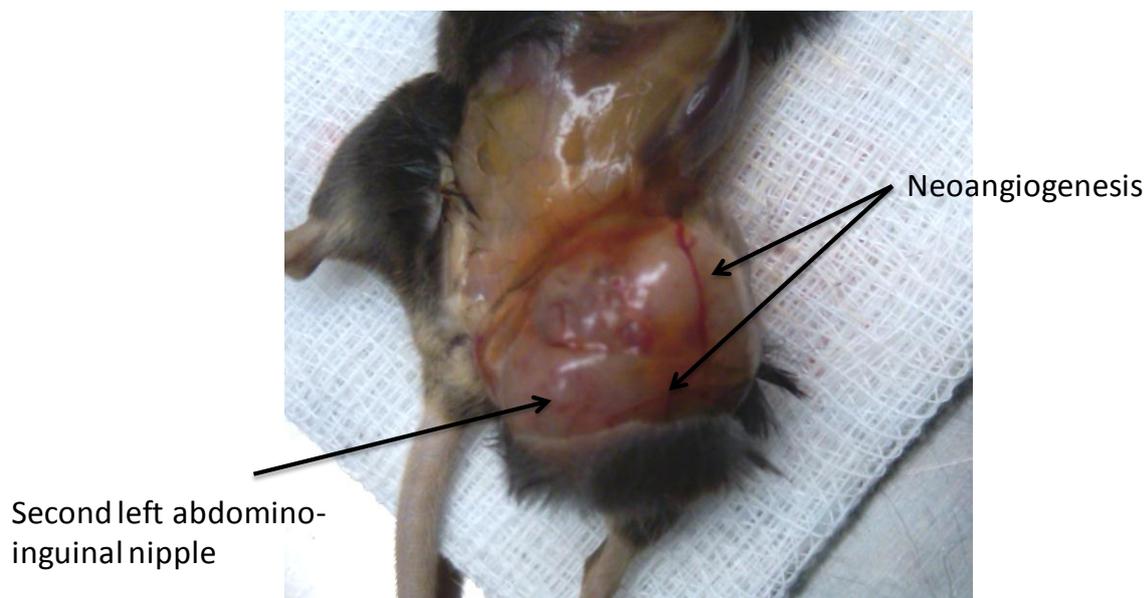
239

Image 5.4 Tumour in a GFP-LC3 mouse, 33 days after injection with a E0771 cell suspension, illustrating neovascularisation and the position of the second left abdomino-inguinal nipple.

Established tumours displayed evidence of extensive neovascularisation (image 5.4). Furthermore, the second left abdomino-inguinal nipple was always obviously located on the tumour surface upon excision.

2.3   E0771 cells are autophagy competent and show signs of increased autophagy flux during amino acid starvation

E0771 cells were grown to reach 60% confluence before being incubated in culture medium free of amino acids (Highveld Biological, South Africa) and supplemented with 10% foetal bovine serum (Sigma Chemical Co., St Louis, MO, USA) for a period of 24 hours. Cells were then scraped in RIPA buffer (appendix) on ice before being centrifuged at 4°C and 8000 rpm for 10 minutes. Resulting supernatants then had their protein content determined immediately using the Bradford protein determination method (Bradford, 1976). Following protein quantification, aliquots diluted in Laemmli sample buffer were prepared for all samples, each containing 40 µg of protein. Electrophoresis (SDS-PAGE) using 12% gels was followed by western blotting using antibodies against LC3 (Cell Signalling, MA, USA) and beclin 1 (Cell Signalling, MA, USA).

240

Fig. 5.1 Change in protein levels of the autophagy markers LC3 and beclin 1in E0771cells during a 6 hour period of amino acid starvation. Bar graphs show densitometric representation of A) Bar graph of LC3 II/LC3 I depicting lipidation of LC3I and autophagy flux. B) Representative western blots showing changes in LC3 II protein levels at 6 hours of complete amino acid deprivation. hr = hours; AU = Arbitrary Units. Values are expressed as mean ± SEM. *, $P < 0.05$.

E0771 cells have high levels of LC3 under baseline culture conditions. Depletion of amino acids from growth medium results in decreased LC3 I levels and apparent increased conversion to LC3 II after 6 hours (Fig 5.1). E0771 cells also have detectable levels of beclin 1. Together, these results indicate that E0771 cells are autophagy competent and are able to increase autophagy flux by increasing conversion of LC3 I to LC3 II during amino acid starvation in a pattern similar to MDAMB231 cells (chapter 2).

2.3   E0771 tumours established using this protocol grow extremely reproducibly and lead to increased total mouse weight after 30 days

Tumour size was monitored every two to three days by making measurements in two perpendicular dimensions parallel with the surface of the mice using digital calipers. The body weight of the mice was monitored twice weekly.
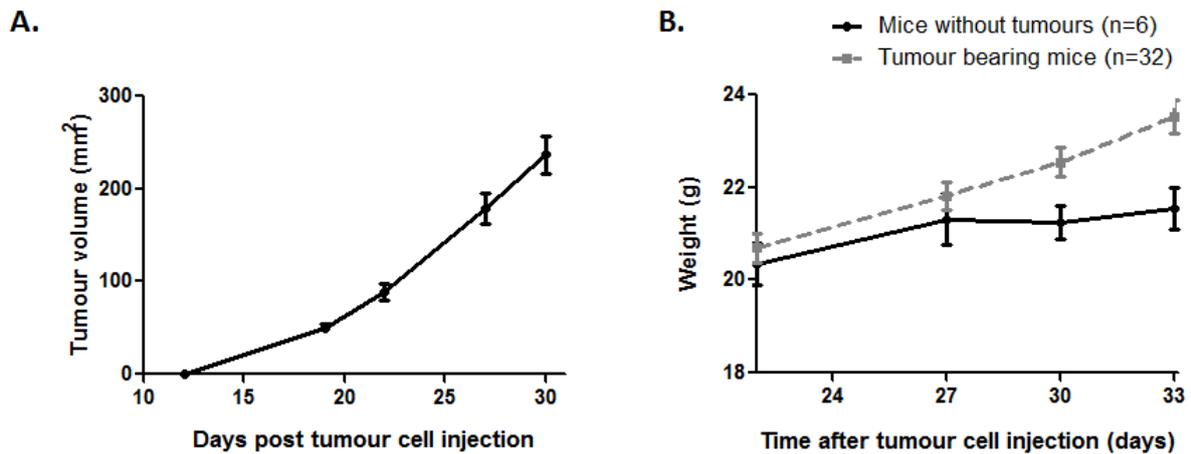
Fig. 5.2 Change in tumour volume. A) Change in tumour volume of GFP-LC3 mice injected with E0771 murine mammary cancer cells at day 0 (n=24). B) Total weight of mice after tumour cell of vehicle injections.

Tumours grown in GFP-LC3 mice using the protocol established in this study grow reproducibly. A pilot study showed that the gauge of the needle used to inject cell suspensions as well as the location of cell injection both influence reproducibility of tumour growth (data not shown). Data of tumour volumes from 24 mice demonstrated the small variance in tumour size at day 30 after the initial E0771 cell injection (Fig 5.2a). After day 30, the weight of tumour bearing animals was found to be greater than those without tumours (Fig 5.2b). This is presumed to be due to the increased tumour mass, as tumour bearing animals presented with less subcutaneous fat than those without tumours (data not shown).

2.4   E0771 tumours from GFP-LC3 mice have significantly greater GFP signal than those from C57BL6 mice

Tumours generated in GFP-LC3 mice and in C57BL6 mice are extremely dense (Fig 5.3a). Histological sections of the internal portions of these tumours show that cells are packed very close to one another, but still appear to have healthy nuclear features (Fig 5.3b).

A.

B.
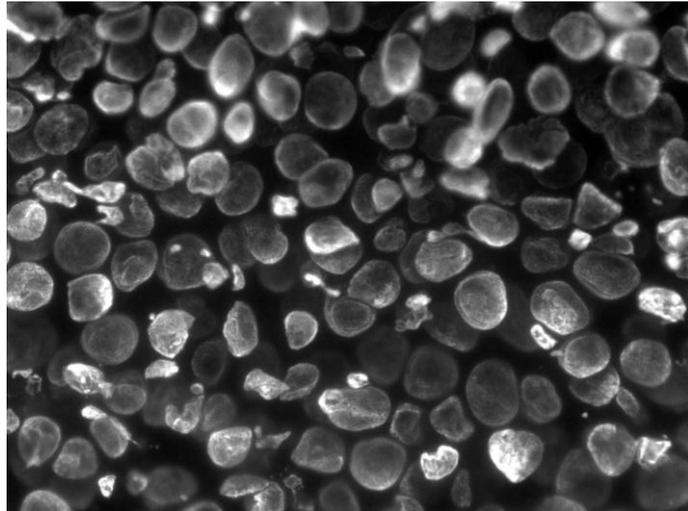
Fig. 5.3 Internal view of E0771 tumours in GFP-LC3 mice. A) cross section of excised tumour. B) Histological section of a central portion of a E0771 tumour, stained with Hoechst dye. Image was taken at 60x magnification using a DAPI filter. The section was prepared to be 8 μm in thickness.
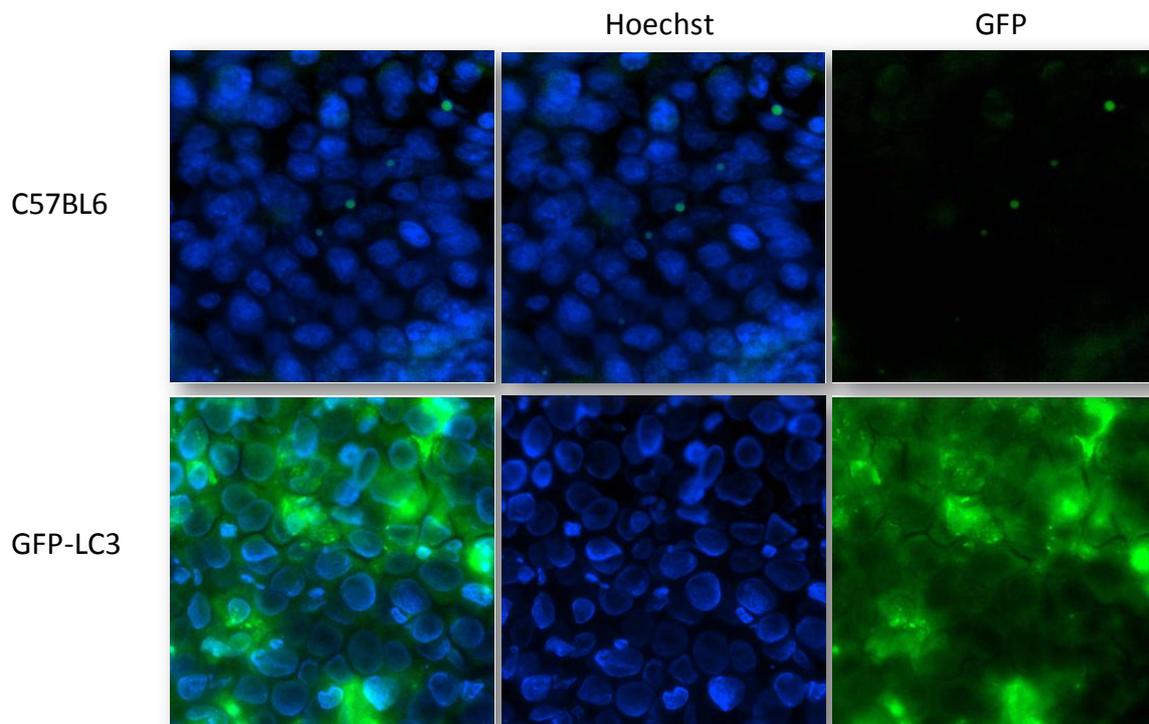
		Hoechst	GFP
C57BL6			
GFP-LC3			

Fig. 5.4 Histological sections of a central portion of a E0771 tumour from a C57BL6 mouse and a GFP-LC3 mouse depicting the basal level of GFP LC3 signal. Tumours from C57BL6 mice have considerably less GFP fluorescence than GFP-LC3 mouse. Images were taken at 60x magnification. Sections were prepared to be 8 μm in thickness.

243

After treatment, excised tumours were immediately snap-frozen in tissue freezing medium (Leica Microsystems) in liquid nitrogen and then stored at -80°C. 8 µm thick sections of tumours were cut from the central fraction of the tumour mass using a rotary microtome (Leica Microsystems CM1850, Nussloch, Germany). 100 µl of Hoechst (Hoechst 33342, Sigma Chemical Co., St Louis, MO, USA) in a 1:200 dilution (50 µg/ml) in sterile PBS was added directly onto the tissue sections and left to incubate for 10 minutes at 4°C. Thereafter, sections were washed in 100 µl of PBS and viewed under an Olympus CellˆR fluorescence 1 X 81 inverted microscope (Olympus Biosystems, Germany) using an F-view II camera (Olympus Biosystems, Germany) for image acquisition and CellˆR software (Olympus Biosystems, Germany) for processing images.

Sections of tumours excised from C57BL6 mice have significantly less visible GFP signal (Fig 5.4). As these mice do not possess GFP fused LC3, any green signal generated must be due to background autofluorescence. On the other hand, sections prepared from tumours from GFP-LC3 mice have pronounced GFP fluorescence (green). Some cells even display localized regions of green puncta under basal conditions (Fig 5.4). As E0771 cells do not possess GFP fused LC3, and tumours in C57Bl6 mice do not have much detectable GFP, any GFP signal must necessarily be derived from GFP-LC3 mice. This experiment serves as a qualitative illustration that autophagy competent mouse derived cells are present within E0771 tumours generated in this model. Furthermore, it is hypothesised that, during treatment, this LC3 signal could be used to quantify autophagy levels of non-cancer cells present within the tumour mass and associated microenvironment.

2.5 Basal GFP signal in E0771 tumours is detectable using flow cytometry in this model and is lower in C57BL6 mice than in GFP-LC3 mice

A.

B.
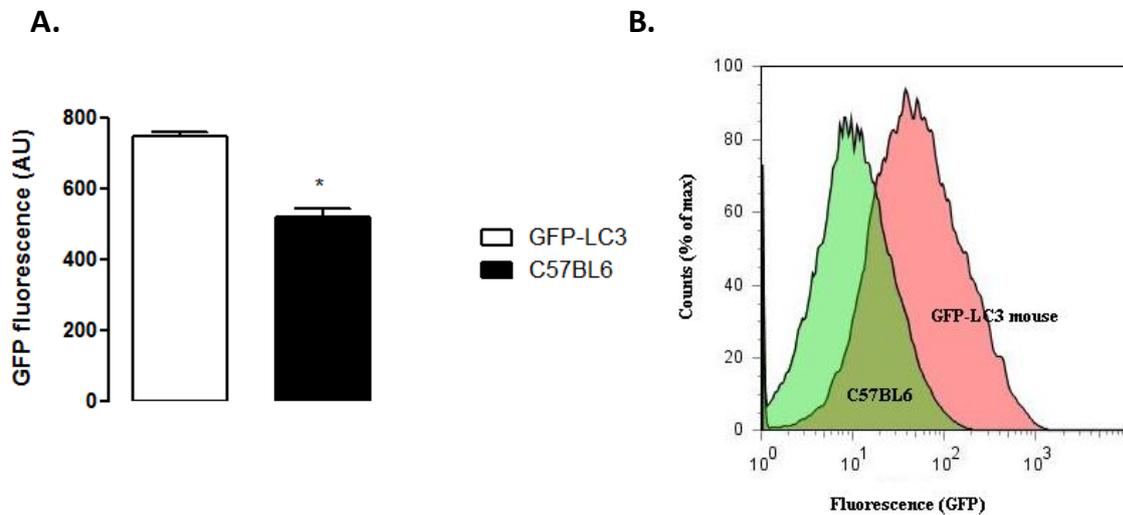
Fig. 5.5 Basal intratumour GFP signal is lower in C57BL6 mice than in GFP-LC3 mice. A) Bar graph depicting the difference in GFP fluorescence between untreated C57BL6 mice (n=2) and GFP-LC3 mice (n=3). B) Peak shift in fluorescence (GFP). Values are expressed as mean ± SEM. *, $P < 0.05$ vs. GFP-LC3.

Whole excised tumours were finely minced using sharp nose scissors and immersed in a collagenase (10 mg/ml) (Sigma Chemical Co., St Louis, MO, USA)/trypsin-EDTA (Sigma Chemical Co., St Louis, MO, USA) mixture and incubated with agitation for 1 hour in the dark at 37°C. The resulting suspension was then centrifuged at 950 g for 3 minutes. The pellet was then resuspended in PBS (with vortexing) and then centrifuged at 500 g for 10 minutes. The resulting suspension was then passed through a tea sieve and then a 100 μm cell strainer before being washed in PBS and centrifuged at 500 g for 3 minutes. Samples were again resuspended in PBS before being filtered through a 50 μm nylon mesh into 12x75 mm tubes. Sample GFP fluorescence was acquired using flow cytometry (BD FACSAria I) where 100 000 events were collected.

Basal intratumour GFP signal is significantly lower in untreated C57BL6 mice than in GFP-LC3 mice (Fig 5.5). This experiment serves to illustrate that the GFP signal is quantifiable using flow cytometry in our model and that this signal corresponds to qualitative evidence.

245

2.6   Protein deprivation results in a rapid autophagy response *in vivo* and a corresponding increase in intratumour GFP signal
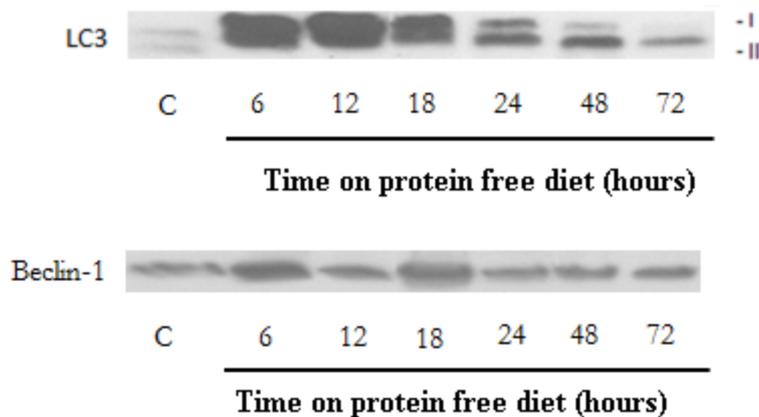
Fig. 5.6 Autophagy response in the gastrocnemius muscles of GFP-LC3 mice that have been placed on a protein free diet. GFP-LC3 mice had their normal diet replaced with pellets free of protein for 6, 12, 18, 24, 48 or 72 hours while control mice (C) were placed on an isocaloric diet which contained proteins. Blots are representative of a repeated experiment (n=2 for each group). Lysates prepared from whole right gastrocnemius muscles were western blotted using antibodies against LC3 and beclin 1.

Standard mouse chow was replaced with an open source protein free diet (Research Diets, Inc., NJ, USA) at the start of their night cycle for a period of 6, 12, 18, 24, 48 or 72 hours. Control animals were placed on isocaloric diets that contained protein (Research Diets, Inc., Nj, USA). After treatment, excised whole right gastrocnemius muscles were immediately snap-frozen in liquid nitrogen and then stored at -80°C. These samples were then homogenized in RIPA buffer (appendix) on ice before being centrifuged at 4°C and 8000 rpm for 10 minutes. Resulting lysates then had their protein content determined immediately using the Bradford protein determination method (Bradford, 1976). Following protein quantification, aliquots diluted in Laemmli sample buffer were prepared for all samples, each containing 40 μg of protein. Electrophoresis (SDS-PAGE) using 12% gels was followed by western blotting using antibodies against LC3 (Cell Signalling, MA, USA) and beclin 1 (Cell Signalling, MA, USA).

246

Surprisingly, a prominent increase in LC3 levels in the gastrocnemius muscles of these mice was noted already at 6 hours of protein depletion (Fig 5.6). A corresponding increase in beclin 1 levels was also seen after 6 hours. After 24 hours, an increase in conversion of LC3 I to LC3 II was evident, indicating an increased autophagy flux at this point. This increase in autophagy flux continued at 48 hours, but appeared diminished by 72 hours. Similar results were obtained from western blots of the hearts obtained from the same mice, prepared and analysed in the same manner (results not shown). This serves as a control to demonstrate that the protein free diet can rapidly increase LC3 accumulation in these mice.
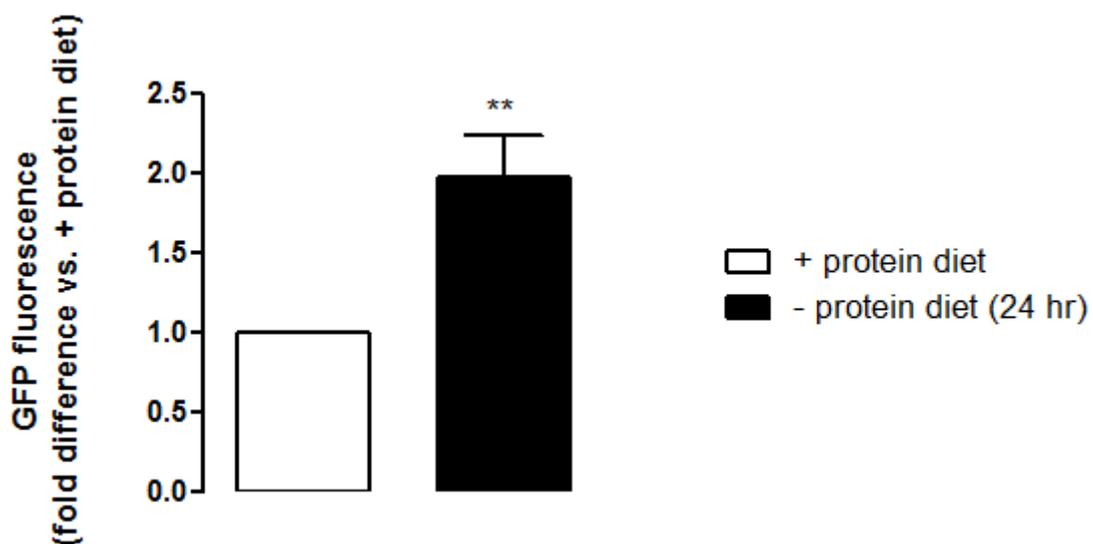
Fig. 5.7 Intratumour GFP fluorescence signal is significantly increased in GFP-LC3 mice that have been placed on a protein free diet for 24 hours. GFP-LC3 mice had their normal diet replaced for 24 hours with pellets free of protein while control mice were placed on an isocaloric diet containing proteins. n=5 for both groups. hr = hours. Values are expressed as mean ± SEM. **, $P < 0.01$ vs. + protein diet.

Flow cytometry is a rapid and well established technique for the quantitative measurement of fluorescence signals in cell populations. Flow cytometry and FACS can be used to monitor autophagy in cells containing GFP-LC3 by exploiting the fact that GFP is sensitive to acidic

247

environments, such as that of lysosomes (Martinet et al., 2006, Shvets et al., 2008). It is known that the GFP fluorescence disappears immediately on it entering the reduced pH environment of a lysosome. A reduction in GFP-LC3 therefore reflects delivery of this complex into lysosomes and the degree of autophagy flux (Shvets et al., 2008), while an increase in GFP-LC3 would reflect increased expression of this complex due to an increase in autophagy induction. GFP-LC3 mice placed on a protein free diet for 24 hours displayed a pronounced and significant increase in GFP signal as quantified using flow cytometry (Fig 5.7). This corresponds to the increase in LC3 levels seen in other tissues after 24 hours of protein starvation in this model. It is proposed here that this technique can be used to monitor and quantify autophagy in this model, and that when comparing treatment groups and the level of GFP fluorescence with flow cytometry a decrease in GFP signal would indicate an increase in autophagy flux.

These experiments illustrate that GFP-LC3 mice placed on a diet free of proteins have a rapid and pronounced increase in the level of autophagy protein markers *in vivo* and display a quantifiable increase in intratumour autophagy after 24 hours. It is believed that this is a viable model for the study of the effects of short term protein starvation *in vivo* and could be utilized as a model to assess the effects of short term starvation on the non-cancer cell population within tumours induced through this model. Furthermore, this technique may serve as an assay to quantify autophagy in non-cancer cells within the tumour microenvironment in response to other treatment stimuli that may induce an autophagy response.

2.7 Protein deprivation results in an increase in intratumour caspase cleavage in GFP-LC3 E0771 tumour bearing mice
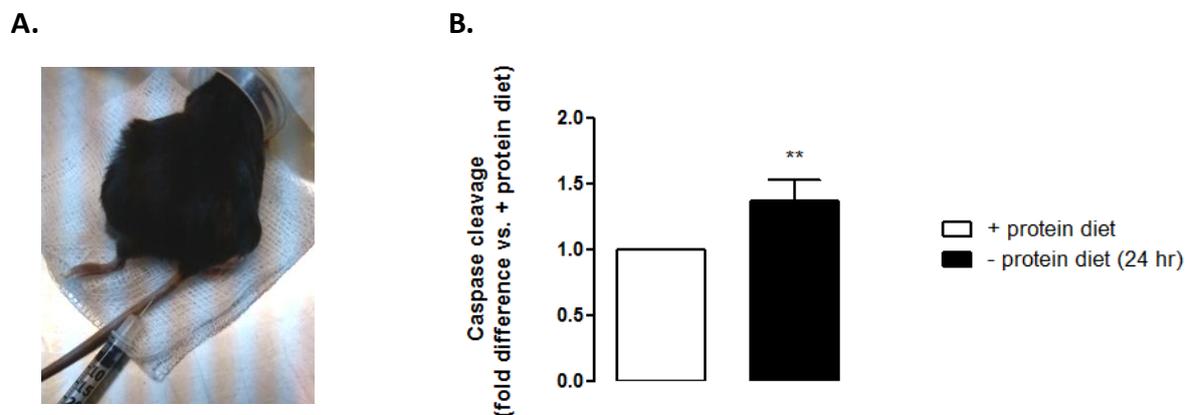
A.

B.

Fig. 5.8 Intratumour caspase cleavage is significantly increased in GFP-LC3 mice after being placed on a protein free diet for 24 hours. GFP-LC3 mice had their normal diet replaced for 24 hours with pellets free of protein while control mice were placed on an isocaloric diet containing proteins. A) i.v. injection of Flivo caspase dye. B) bar graph depicting an increase in caspase cleavage after being placed on a protein free diet for 24 hours. hr = hours. Values are expressed as mean ± SEM. n=5 for both groups.**, $P < 0.01$ vs. + protein diet.

FLIVO™ (FLuorescence in vIVO) *in vivo* apoptosis tracers (Immunochemistry Technologies LLC, MN, USA) have been validated and used to assess caspase activity in various *in vivo* cancer models (Tsai et al., 2007). Upon encountering active caspases, FLIVO forms irreversible covalent bonds with reactive cysteines on the large subunit of the caspase heterodimers, thus further inhibiting enzymatic activity and labelling the location of active caspases. Unbound FLIVO™ probes are removed from the circulation of the animal in about 1 hour. 100 µl of red SR FLIVO™ dye was prepared as per the manufacturer's protocol and injected i.v. into the tail vein of E0771 tumour bearing GFP-LC3 mice (Fig 5.8a) after appropriate treatments were completed. After 1 hour, whole tumours were excised and digested (described previously) and analysed using flow cytometry (BDFACSAria I). A significant increase in intratumour caspase activity was observed if GFP-LC3 mice were placed on a protein free diet for 24 hours (Fig 5.8b).

3   Closing remarks

This successful establishment of a novel tumour model, and the validation of techniques associated with assessment of autophagy and apoptosis within the tumour microenvironment, allows future studies investigating stimuli or treatments that may induce an autophagy or apoptosis response. This study outlines the protocols and the corresponding procedures necessary for the induction of reproducible, autophagy competent solid tumours in GFP-LC3 mice. Additionally, this model represents a unique opportunity for assessment of autophagy, during different treatment regimes or interventions, within the non-cancer cell population in solid tumours.

It is believed that this is a viable model for the investigation of short term protein starvation during chemotherapy *in vivo*, and that this model could be utilized to assess the effects of short term starvation on the non-cancer cell population within tumours.

4   References

BRADFORD, M. M. 1976. A rapid and sensitive method for the quantitation of microgram quantities of protein utilizing the principle of protein-dye binding. *Anal Biochem,* 72**,** 248-54.

CASEY, A. E., DRYSDALE, G. R., SHEAR, H. H. & GUNN, J. 1952. Second transplantations of E 0771 mouse carcinoma and of Brown-Pearce rabbit tumor. *Cancer Res,* 12**,** 807-13.

CASEY, A. E., LASTER, W. R., JR. & ROSS, G. L. 1951. Sustained enhanced growth of carcinoma EO771 in C57 black mice. *Proc Soc Exp Biol Med,* 77**,** 358-62.

DVORAK, H. F., SENGER, D. R. & DVORAK, A. M. 1983. Fibrin as a component of the tumor stroma: origins and biological significance. *Cancer Metastasis Rev,* 2**,** 41-73.

EGEBLAD, M., EWALD, A. J., ASKAUTRUD, H. A., TRUITT, M. L., WELM, B. E., BAINBRIDGE, E., PEETERS, G., KRUMMEL, M. F. & WERB, Z. 2008. Visualizing stromal cell dynamics in different tumor microenvironments by spinning disk confocal microscopy. *Dis Model Mech,* 1**,** 155-67; discussion 165.

EWENS, A., LUO, L., BERLETH, E., ALDERFER, J., WOLLMAN, R., HAFEEZ, B. B., KANTER, P., MIHICH, E. & EHRKE, M. J. 2006. Doxorubicin plus interleukin-2 chemoimmunotherapy against breast cancer in mice. *Cancer Res,* 66**,** 5419-26.

HIRATSUKA, S., GOEL, S., KAMOUN, W. S., MARU, Y., FUKUMURA, D., DUDA, D. G. & JAIN, R. K. 2011. Endothelial focal adhesion kinase mediates cancer cell homing to discrete regions of the lungs via E-selectin up-regulation. *Proc Natl Acad Sci U S A,* 108**,** 3725-30.

HUYNH, H., ZHENG, J., UMIKAWA, M., SILVANY, R., XIE, X. J., WU, C. J., HOLZENBERGER, M., WANG, Q. & ZHANG, C. C. 2011. Components of the hematopoietic compartments in tumor stroma and tumor-bearing mice. *PLoS One,* 6**,** e18054.

JOHANN, P. D., VAEGLER, M., GIESEKE, F., MANG, P., ARMEANU-EBINGER, S., KLUBA, T., HANDGRETINGER, R. & MULLER, I. 2010. Tumour stromal cells derived from paediatric malignancies display MSC-like properties and impair NK cell cytotoxicity. *BMC Cancer,* 10**,** 501.

LI, F. 2009. Every single cell clones from cancer cell lines growing tumors in vivo may not invalidate the cancer stem cell concept. *Mol Cells,* 27**,** 491-2.

MARTINET, W., DE MEYER, G. R., ANDRIES, L., HERMAN, A. G. & KOCKX, M. M. 2006. In situ detection of starvation-induced autophagy. *J Histochem Cytochem,* 54**,** 85-96.

MCHOWAT, J., GULLICKSON, G., HOOVER, R. G., SHARMA, J., TURK, J. & KORNBLUTH, J. 2011. Platelet-activating factor and metastasis: calcium-independent phospholipase A2beta deficiency protects against breast cancer metastasis to the lung. *Am J Physiol Cell Physiol,* 300**,** C825-32.

MEDINA, D. 2007. Chemical carcinogenesis of rat and mouse mammary glands. *Breast Dis,* 28**,** 63-8.

MELENDEZ, A., TALLOCZY, Z., SEAMAN, M., ESKELINEN, E. L., HALL, D. H. & LEVINE, B. 2003. Autophagy genes are essential for dauer development and life-span extension in C. elegans. *Science,* 301**,** 1387-91.

MIZUSHIMA, N., YAMAMOTO, A., MATSUI, M., YOSHIMORI, T. & OHSUMI, Y. 2004. In vivo analysis of autophagy in response to nutrient starvation using transgenic mice expressing a fluorescent autophagosome marker. *Mol Biol Cell,* 15**,** 1101-11.

MIZUSHIMA, N., YOSHIMORI, T. & LEVINE, B. 2010. Methods in mammalian autophagy research. *Cell,* 140**,** 313-26.

MUELLER, M. M. & FUSENIG, N. E. 2004. Friends or foes - bipolar effects of the tumour stroma in cancer. *Nat Rev Cancer,* 4**,** 839-49.

RUSTEN, T. E., LINDMO, K., JUHASZ, G., SASS, M., SEGLEN, P. O., BRECH, A. & STENMARK, H. 2004. Programmed autophagy in the Drosophila fat body is induced by ecdysone through regulation of the PI3K pathway. *Dev Cell,* 7**,** 179-92.

SHARMA, R., KACEVSKA, M., LONDON, R., CLARKE, S. J., LIDDLE, C. & ROBERTSON, G. 2008. Downregulation of drug transport and metabolism in mice bearing extra-hepatic malignancies. *Br J Cancer,* 98**,** 91-7.

SHVETS, E., FASS, E. & ELAZAR, Z. 2008. Utilizing flow cytometry to monitor autophagy in living mammalian cells. *Autophagy,* 4**,** 621-8.

TREDAN, O., GALMARINI, C. M., PATEL, K. & TANNOCK, I. F. 2007. Drug resistance and the solid tumor microenvironment. *J Natl Cancer Inst,* 99**,** 1441-54.

TSAI, Y. C., MENDOZA, A., MARIANO, J. M., ZHOU, M., KOSTOVA, Z., CHEN, B., VEENSTRA, T., HEWITT, S. M., HELMAN, L. J., KHANNA, C. & WEISSMAN, A. M. 2007. The ubiquitin ligase gp78 promotes sarcoma metastasis by targeting KAI1 for degradation. *Nat Med,* 13**,** 1504-9.

YOUNG, E., MIELE, L., TUCKER, K. B., HUANG, M., WELLS, J. & GU, J. W. 2010. SU11248, a selective tyrosine kinases inhibitor suppresses breast tumor angiogenesis and growth via targeting both tumor vasculature and breast cancer cells. *Cancer Biol Ther,* 10**,** 703-11.

6 ───────────────────────────────

Short term protein starvation results in increased tolerance to high dose chemotherapy but also increased autophagy flux and decreased apoptosis within tumours *in vivo*

Short term starvation of patients receiving chemotherapy is a promising new strategy that has been demonstrated to differentially protect non-cancer cells during treatment. Previous experimental data has shown that while a non-cancer cell line experienced protection if starved of amino acids during doxorubicin treatment, a cancer cell line with high basal autophagy activity had increased cell death (chapter 4). A recently established model with the capacity to assess the impact of protein starvation on autophagy in the host derived stromal subpopulation within mammary tumours (chapter 5) is used in this study. Evidence in this chapter shows that protein deprivation of mice receiving a high cumulative dose of doxorubicin treatment increases survival, whereas intratumour caspase activity decreases. Increased intratumour autophagy flux in the non-cancer cell population of these tumours is implicated in this protection.

1   Introduction

Recent application of short term starvation protocols in patients receiving high doses of chemotherapy has showed remarkable success in reducing side effects (Safdie et al., 2009). Furthermore, in a cell culture and a neuroblastoma mouse xenograft model, it was shown that non-cancer cells placed on a similar starvation protocol benefited from differential protection compared to cancer cells during high dose chemotherapy regimens as well (Raffaghello et al., 2008). Mice starved for 48 hours prior to chemotherapy in this study had reduced chemotoxicity following high dose treatment, whereas cancer cells and tumours did not benefit from a similar protection. In addition, many clinical trials are beginning to assess the effectiveness of compounds known to regulate autophagy, and a study using a low protein

diet to „reactivate‟ autophagy is set to begin phase II trials shortly (information from clinicaltrials.gov).

Previous experimental data has shown that amino acid deprivation from the culture medium of non-cancer mammary epithelial cells (MCF12A) results in a relative protection of these cells from cytotoxicity associated with chemotherapy (described in chapter 4), while cytotoxicity appears to be enhanced in cancer cells (MDAMB231) receiving similar treatments. However, cancers are extremely heterogenous by nature and much of their volume can be comprised of non-cancer cells that are vital for their continued growth and development (Mueller and Fusenig, 2004). As solid tumours rely on non-cancer cells for survival, any protection of these cells from cytotoxicity during short term starvation could indirectly result in prolonged tumour cell survival during chemotherapy. Also, the benefits of fasting in cellular protection from cytotoxicity may rely partly on altered circulating hormone levels (Lee and Longo, 2011), which necessitates further investigation using *in vivo* models. In fact, reduced circulating IGF-I levels have been implicated in the differential protection of normal cells and cancer cells in response to fasting and improved chemotherapeutic index during doxorubicin treatment (Lee et al., 2010).

2   Study aims

1. Use the previously developed tumour model (chapter 5) to assess survival in mice treated with a short regimen (3 days) of high dose of doxorubicin (10 mg/kg; 20 mg/kg cumulative) treatment.

2. Determine the effect of a short term exposure to a diet low in protein on survival in these animals.

3. Use the previously developed model to assess caspase activity in the tumours in these mice.

4. Use the previously developed model to assess autophagy in the non-cancer subpopulation in the tumours in these mice.

5. Assess survival, caspase activity and autophagy in tumour bearing mice treated with a moderate dose of doxorubicin (5 mg/kg; 20 mg/kg cumulative) treatment.

3 Materials and methods

The materials and methods describing the procedures utilized in this study are explained in detail in chapter 5 of this manuscript.

3.1 Experimental procedure
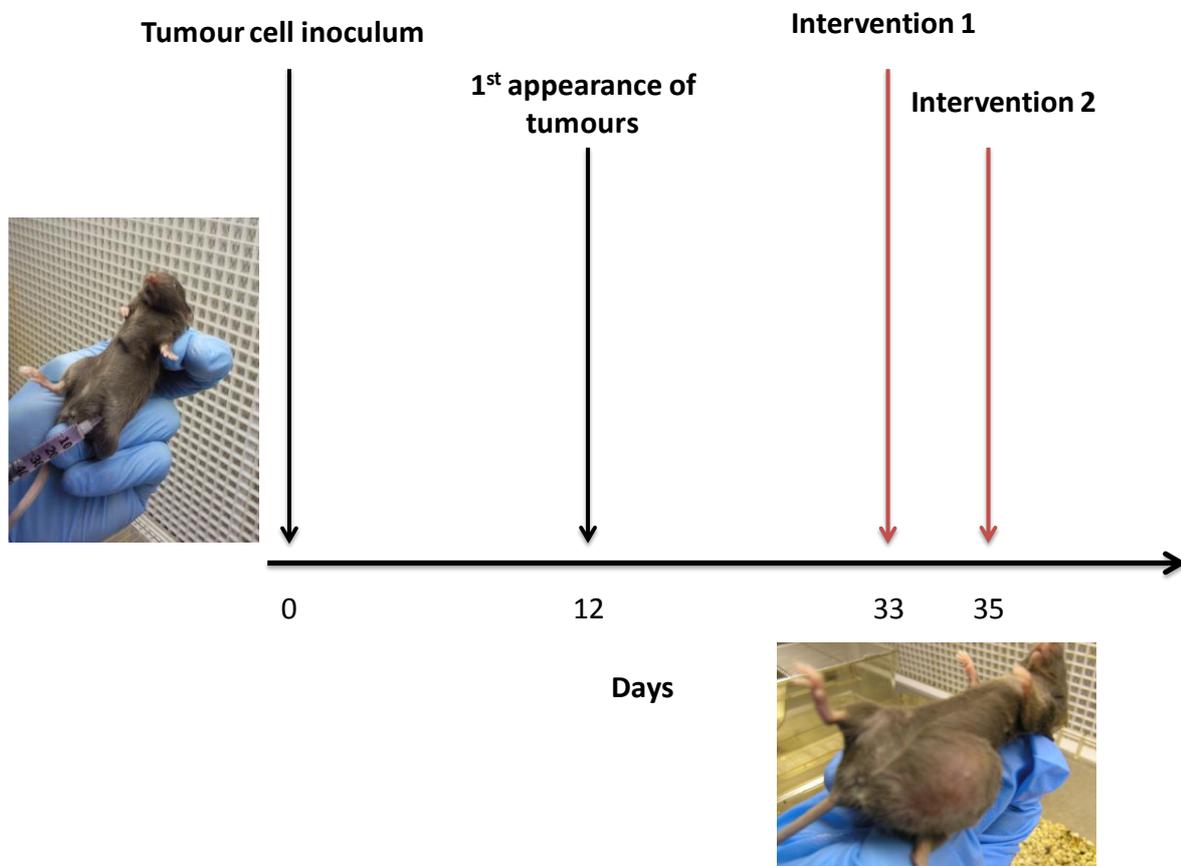
Image 6.1 Diagrammatic depiction of experimental procedure.

Further details describing deviations from and particulars of this experimental procedure are described in the results.

3.2   Drug preparation and administration

Doxorubicin hydrochloride (D1515, Sigma Chemical Co., St Louis, MO, USA) and Rapamycin from *Streptomyces hygroscopicus* (R0395, Sigma Chemical Co., St Louis, MO, USA) were prepared immediately prior to the injection procedure. Both agents were dissolved in Hanks Balanced Salt Solution (Sigma Chemical Co., St Louis, MO, USA), and mixed on a shaker to ensure that they were completely dissolved. Volumes were prepared to reflect the exact concentration required per kilogram (kg) of body weight for each mouse on the day of injection. Mice were restrained by the scruff method and 100 µl drug suspensions were injected i.p. into the right caudal thigh (avoiding the femur and sciatic nerve) of each mouse using a 23-gauge needle. Control mice were injected with the vehicle only.

3.3   Tumour measurement and animal weighing

Tumour size was monitored every two to three days by making measurements in two perpendicular dimensions parallel with the surface of the mice using digital callipers. The body weight of the mice was monitored twice weekly.

3.4   Statistical analysis

All values are presented as the mean ± standard error of the mean (SEM). Differences between time points and treatment groups were analysed using one or two analysis of variance (ANOVA). Significant changes were further assessed by means of the Bonferroni *post hoc* analysis where appropriate. All statistical analyses were performed using Graphpad Prism version 5.01 (Graphpad Software, Inc, CA, USA). The minimum level of significance accepted was $p < 0.05$.

4 Results

4.1 24 hour protein starvation during high dose doxorubicin (10 mg/kg) treatment results in increased survival of E0771 tumour bearing GFP-LC3 mice
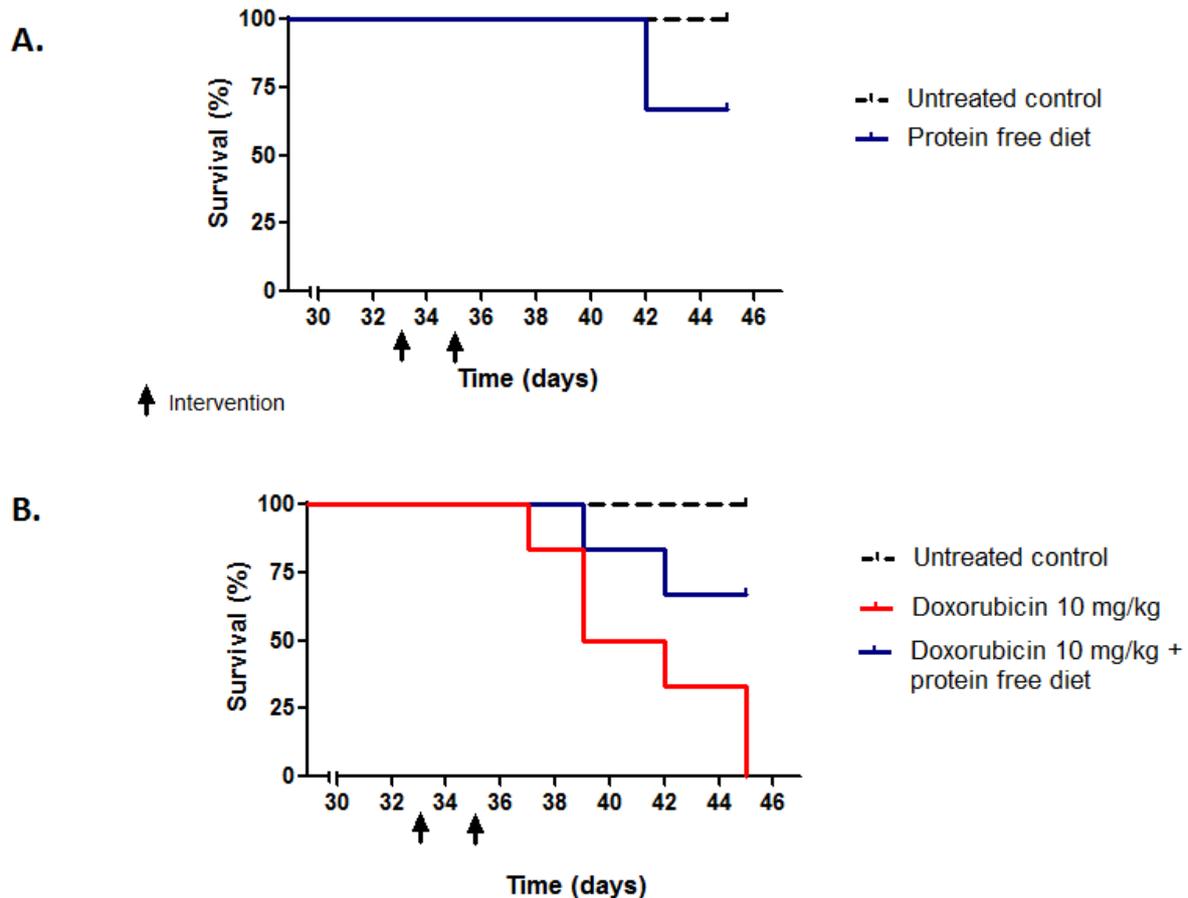
Fig. 6.1 24 hour protein starvation protects against high-dose chemotherapy *in vivo*. A) Tumour bearing GFP-LC3 mice had their normal diet replaced for 24 hours with pellets free of protein while control mice were placed on an isocaloric diet containing proteins. B) Tumour bearing mice were administered doxorubicin (10 mg/kg) i.p. twice over a period of three days and given diets either with or without protein. Time on the x-axis indicates the number of days after injection with E0771 cancer cells. Primary treatment interventions occurred on day 33. n=6 for all groups

GFP-LC3 mice with large tumours (>230 mm^2) derived from E0771 mammary adenocarcinoma cells were placed on a diet free of proteins for 24 hours for two days, either side of a day on a standard chow diet. Mice with large tumours and placed on this diet were more likely to have died twelve days after the initial intervention (Fig 6.1a). Mice with similar tumours and administered doxorubicin at a high dose (10 mg/kg) on two days, either side of a

258

day without treatment had all died by day 12 after the initial treatment (Fig 6.1b). However, if tumour bearing mice were placed on a diet free of protein, immediately after i.p. injection with a high dose of doxorubicin (10 mg/kg), then the survival of these mice was prolonged compared to those fed a standard diet. Furthermore, protein starved doxorubicin treated mice showed less signs of reduced mobility and ruffled hair compared to mice treated with doxorubicin but fed isocaloric protein complete diets (data not shown).

4.2   24 hour protein starvation during high dose doxorubicin (10 mg/kg) treatment does not influence changes in tumour volumes attributed to doxorubicin
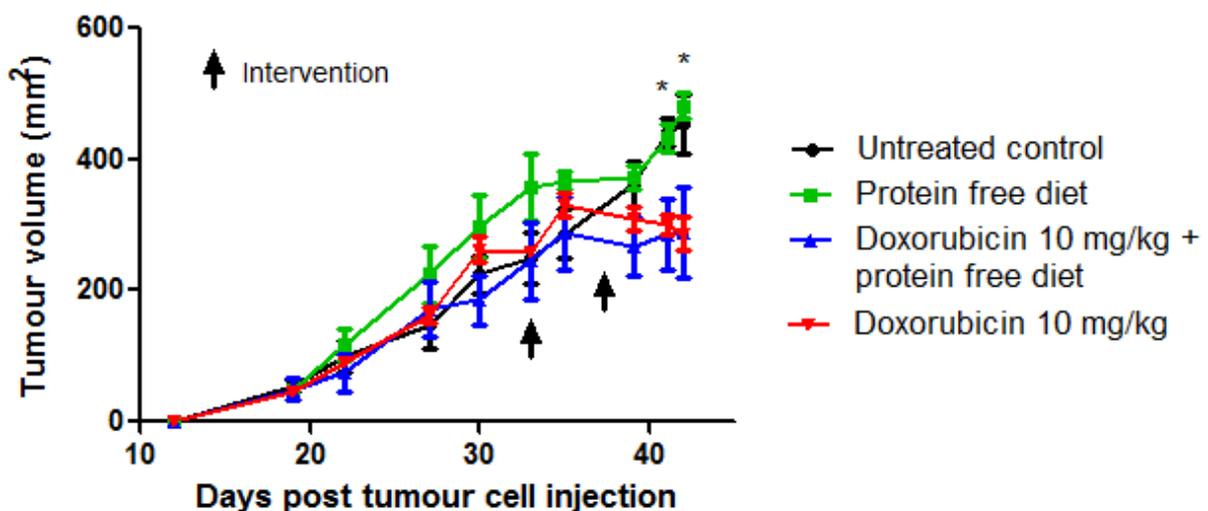
Fig. 6.2 Change in tumour volumes during doxorubicin (10 mg/kg) treatment either with or without proteins in the diet. All groups began with 6 animals. Values are expressed as mean ± SEM. *, $P < 0.05$ untreated control vs. Doxorubicin 10 mg/kg and vs. Doxorubicin 10mg/kg + protein free diet.

Growth rates of E0771 tumours in GFP-LC3 mice were very similar in size between groups, prior to the initial interventions (Fig 6.2).

A.
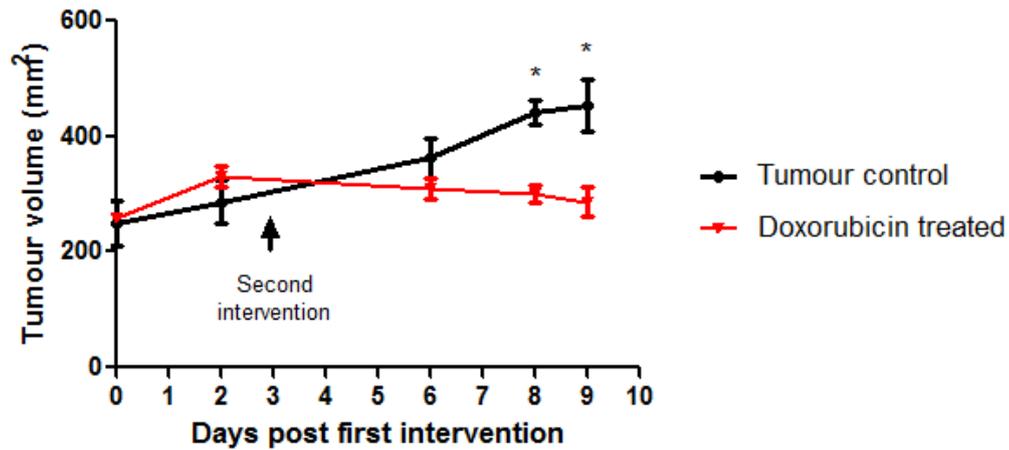
B.
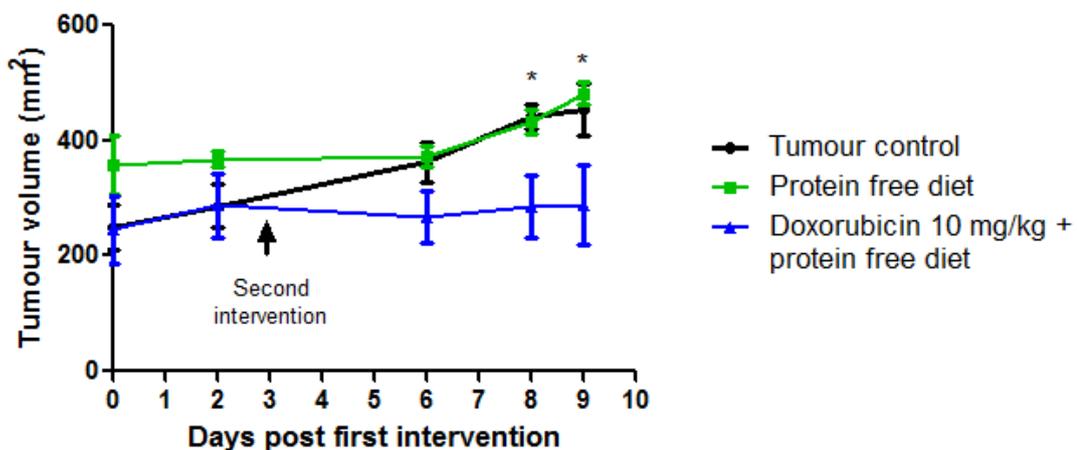
Fig. 6.3 Change in tumour volumes after treatment with doxorubicin (10 mg/kg) either with or without proteins in the diet. A) i.p. injection with doxorubicin (10 mg/kg) results in significantly smaller tumour volumes by day 8 after the initial injection with the drug. B) Treatment with doxorubicin (10 mg/kg) in mice placed on protein free diets results in similar reductions in tumour size. Values are expressed as mean ± SEM. Data is representative of the mean of at least 3 experimental animals. *, $P < 0.05$ untreated control vs. Doxorubicin 10 mg/kg and vs. Doxorubicin 10 mg/kg + protein free diet.

Administration of two high dose doxorubicin (10 mg/kg) treatments over three days in GFP-LC3 mice bearing large E0771 tumours (>230 mm^2) resulted in significant reductions in tumour size by day eight after the first intervention (Fig 6.3a). If tumour bearing mice were placed on diets free of protein during doxorubicin treatment (10 mg/kg), reductions in tumour size were shown to be similar to those treated with doxorubicin but fed protein complete diets (Fig 6.3b).

260

4.3   24 hour protein starvation during high dose doxorubicin (10 mg/kg) treatment results in significantly lower caspase activity within tumours

A.

B.

Fig. 6.4 Intratumour caspase cleavage is significantly lower if GFP-LC3 mice treated with doxorubicin (10 mg/kg) are placed on a protein free diet during treatment. GFP-LC3 mice had their normal diet replaced for 24 hours with pellets free of protein or were placed on an isocaloric diet containing proteins where applicable. FLIVO™ caspase dye was injected i.v. into the tail vein of all mice 1 hour prior to tumour excision. A) bar graph depicting changes in caspase cleavage during treatment. B) Peak shift in mean fluorescence (caspase cleavage). Values are expressed as mean ± SEM. *, $P < 0.05$ vs. + protein diet. *, $P < 0.05$; ns = no significance. n=3 for all groups.

Administration of two high dose doxorubicin (10 mg/kg) treatments over three days in GFP-LC3 mice bearing large E0771 induced tumours (>230 mm^2) resulted in a significant increase in caspase activity within whole excised tumours, using a FLIVO™ (FLuorescence in vIVO) *in vivo* apoptosis tracer (Immunochemistry Technologies LLC, MN, USA) and FACS flow cytometry (Fig 6.4). However, if mice were placed on a protein free diet for 24 hours at the start of their night cycle, beginning immediately after each doxorubicin injection, then caspase activity was observed to be significantly lower in excised tumours than in those mice treated but fed on protein complete diets.

261
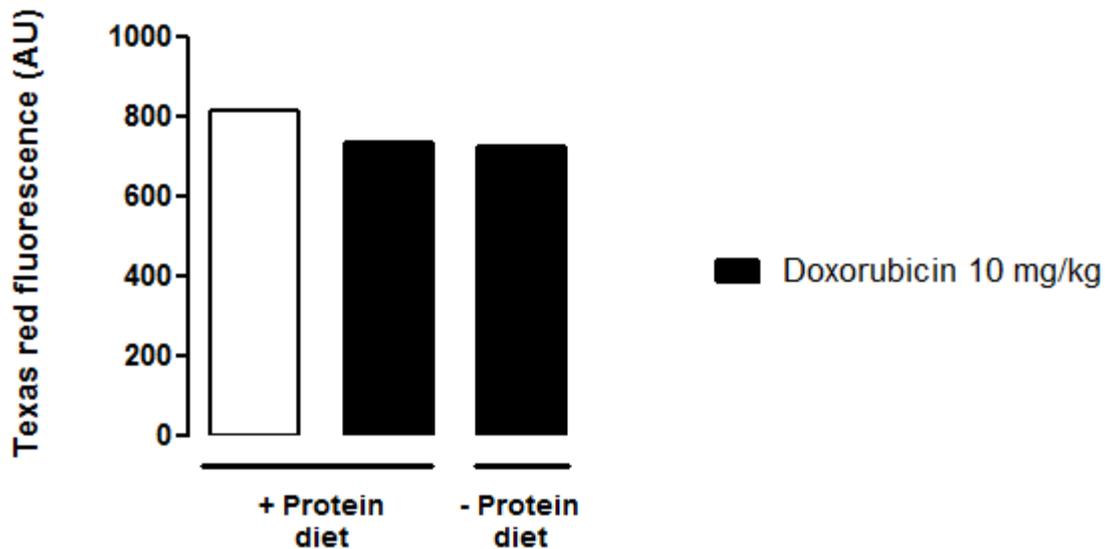
Fig. 6.5 Doxorubicin does not interfere with the signal generated from the FLIVO™ caspase dye. GFP-LC3 mice were treated in the same way as those used for analyses of caspase cleavage except they were not injected with the caspase dye. Background signal was not detectable on the channel used for analysis of caspase cleavage. n=1 for all groups. AU = Arbitrary Units.

In order to ensure that any background autofluorescence signal generated as a consequence of doxorubicin injections did not interfere with measurements, GFP-LC3 mice (treated in the same way as those used for caspase activity analyses) were not injected with the FLIVO™ tracer dye and analysed using flow cytometry. Excised whole tumours from GFP-LC3 mice treated with doxorubicin (10 mg/kg) and placed on either a protein free diet or a protein complete diet were not found to generate any detectable autofluorescence in our model (Fig 6.5).

4.4   24 hour protein starvation during high dose doxorubicin (10 mg/kg) treatment results in significantly increased intratumour autophagy flux in E0771 induced tumours in GFP-LC3 mice
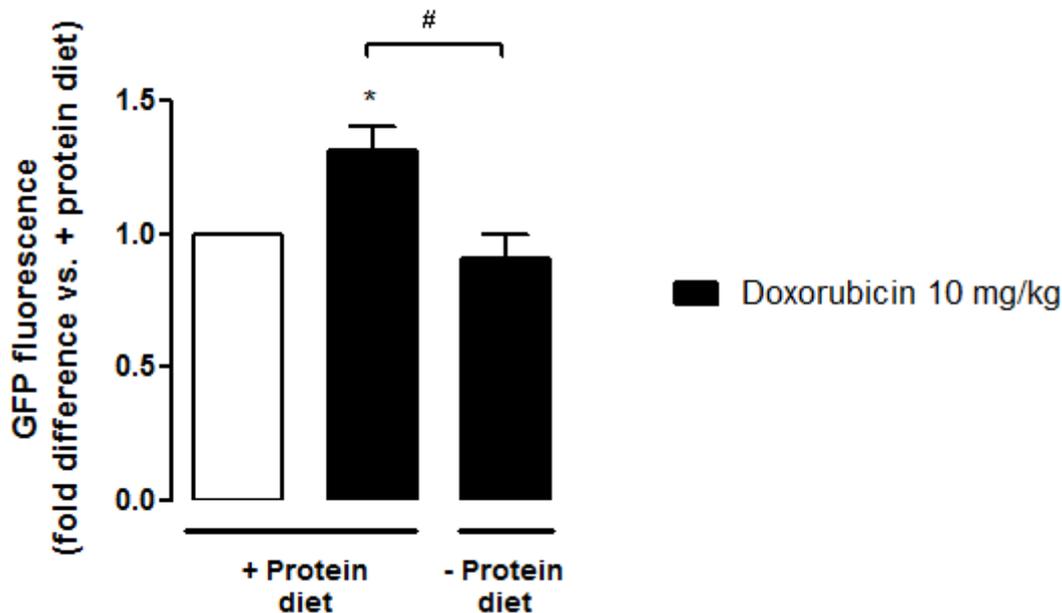
Fig. 6.6 Intratumour autophagy flux increases if GFP-LC3 mice treated with doxorubicin (10 mg/kg) are placed on a protein free diet during treatment. A decrease in GFP signal indicates increased autophagy flux. GFP-LC3 mice had their normal diet replaced for 24 hours with pellets free of protein or were placed on an isocaloric diet containing proteins where applicable. Bar graphs depict changes in GFP signal during treatment. Significance markers depict comparisons versus untreated mice fed on protein complete diets unless indicated otherwise. Values are expressed as mean ± SEM. *, $P < 0.05$ vs. + protein diet. #, $P < 0.05$. n=3 for all groups

Flow cytometry and FACS can be used to monitor autophagy in cells containing GFP-LC3 by exploiting the fact that GFP is sensitive to acidic environments, such as that of lysosmes (Martinet et al., 2006, Shvets et al., 2008), and GFP fluorescence disappears immediately on it entering the reduced pH environment of a lysosome. A reduction in GFP signal therefore reflects delivery of the GFP-LC3 complex into lysosomes and can be related to the degree of autophagy flux (Shvets et al., 2008). An increase in GFP signal indicates increased autophagy induction without high autophagy flux (chapter 5). Administration of two high dose doxorubicin (10 mg/kg) treatments over three days in GFP-LC3 mice bearing large E0771

induced tumours (>230 mm^2) resulted in a significant increase in GFP signal. This is inferred to indicate an increased autophagy induction and translation of the GFP-LC3 complex (Fig 6.6). However, if mice were placed on a protein free diet for 24 hours at the start of their night cycle, beginning immediately after each doxorubicin (10 mg/kg) injection, then a significant decrease in GFP signal indicates a significant increase in autophagy flux compared to mice treated but fed on protein complete diets. As only non-cancer cells contain the GFP-LC3 complex (chapter 5), significantly increased intratumour autophagy flux implies that there is an increased autophagy flux in non-cancer stromal cells within the E0771 induced tumours of treated GFP-LC3 mice fed protein free diets compared to those fed protein complete diets.

4.5 24 hour protein starvation during moderate dose doxorubicin (5 mg/kg) treatment prevents doxorubicin induced reductions in E0771 tumour volumes in GFP-LC3 mice
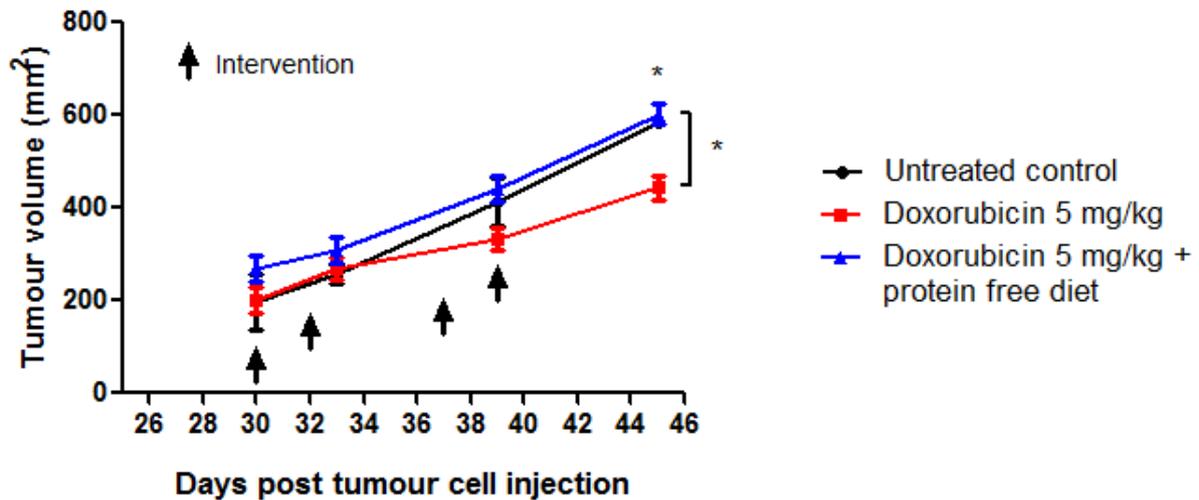
Fig. 6.7 Change in tumour volumes after treatment with doxorubicin (5 mg/kg) either with or without proteins in the diet. i.p. injection with doxorubicin (5 mg/kg) results in significantly smaller tumour volumes by day 15 after the initial injection with the anticancer drug. Treatment with doxorubicin (5 mg/kg) in mice placed on protein free diets does not result in similar reductions in tumour size. Values are expressed as mean ± SEM. n=5. *, $P < 0.05$ untreated control vs. Doxorubicin 5 mg/kg.

Administration of two treatment regimens one week apart of two moderate doses of doxorubicin (5 mg/kg) treatments over three days in GFP-LC3 mice bearing large E0771 tumours (~200 mm^2) resulted in significant reductions in tumour size by day 15 after the first intervention (Fig 6.7). Unlike in previous experiments, using higher doses of doxorubicin, no mice treated with these concentrations of doxorubicin (5 mg/kg) died during this treatment regime (data not shown). If tumour bearing mice were placed on diets free of protein during doxorubicin (5 mg/kg) treatment, then reductions in tumour size observed in mice treated with doxorubicin but fed protein complete diets were abolished and tumour sizes were similar to those of untreated control mice (Fig 6.7).

4.6   24 hour protein starvation during moderate dose doxorubicin (5 mg/kg) treatment results in significantly lower caspase activity within tumours

Fig. 6.8 Intratumour caspase cleavage is significantly lower if GFP-LC3 mice treated with doxorubicin (5 mg/kg) are placed on a protein free diet during treatment. GFP-LC3 mice had their normal diet replaced for 24 hours with pellets free of protein or were placed on an isocaloric diet containing proteins where applicable. FLIVO™ caspase dye was injected i.v. into the tail vein of all mice 1 hour prior to tumour excision. Significance markers depict comparisons versus untreated mice fed on protein complete diets unless indicated otherwise. Values are expressed as mean ± SEM. *, $P < 0.05$ vs. + protein diet. #, $P < 0.05$. n=3 for groups treated with doxorubicin and n=2 for control groups.

Administration of two treatment regimens one week apart of two moderate doses of doxorubicin (5 mg/kg) treatments over three days in GFP-LC3 mice bearing large E0771 tumours (~200 mm^2) resulted in a significant increase in caspase activity within whole excised tumours (Fig 6.8). However, if mice were placed on a protein free diet for 24 hours at the start of their night cycle, beginning immediately after each doxorubicin injection, then caspase activity was observed to be significantly lower in excised tumours than in those mice treated but fed on protein complete diets.

4.7 24 hour protein starvation during moderate dose doxorubicin (5 mg/kg) treatment results in significantly increased intratumour autophagy flux in E0771 induced tumours in GFP-LC3 mice
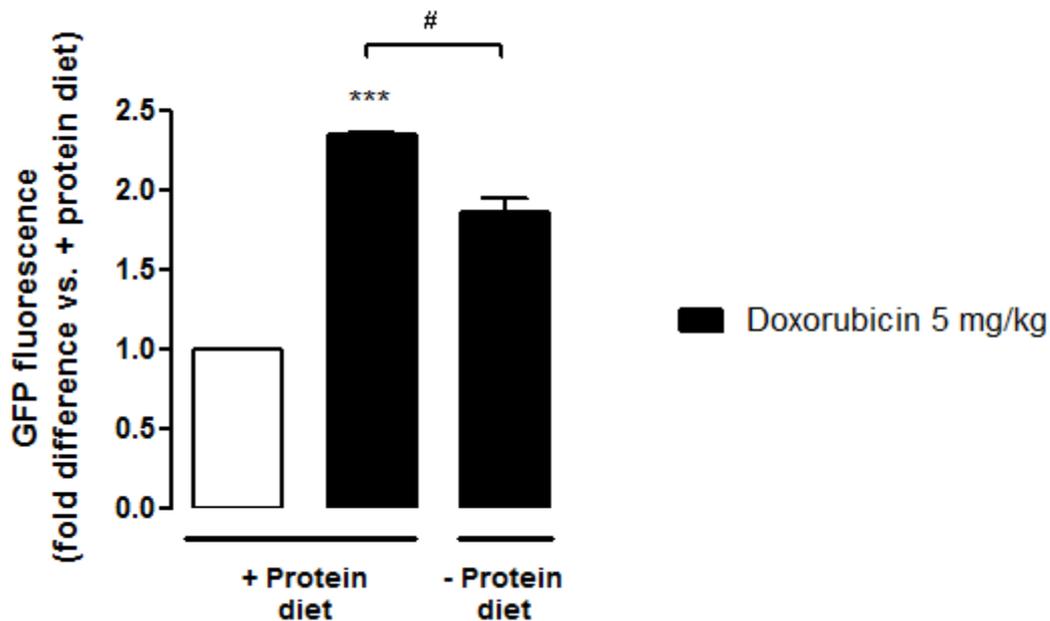
Fig. 6.9 Intratumour autophagy flux increases if GFP-LC3 mice treated with doxorubicin (5 mg/kg) are placed on a protein free diet during treatment. A decrease in GFP signal indicates increased autophagy flux. GFP-LC3 mice had their normal diet replaced for 24 hours with pellets free of protein or were placed on an isocaloric diet containing proteins where applicable. Significance markers depict comparisons versus untreated mice fed on protein complete diets unless indicated otherwise. Values are expressed as mean ± SEM. ***, $P < 0.001$ vs. + protein diet. #, $P < 0.05$ n=3 for groups treated with doxorubicin and n=2 for control groups.

Administration of two treatment regimens one week apart of two moderate doses of doxorubicin (5 mg/kg) treatments over three days in GFP-LC3 mice bearing large E0771 tumours (~200 mm^2) resulted in a significant increase in GFP signal. This is inferred to indicate an increased autophagy induction and translation of the GFP-LC3 complex (Fig 6.9). However, if mice were placed on a protein free diet for 24 hours at the start of their night cycle, beginning immediately after each doxorubicin (5 mg/kg) injection, then a significant decrease in GFP signal indicates a significant increase in autophagy flux compared to mice treated but fed on protein complete diets. As only non-cancer cells contain the GFP-LC3 complex (chapter 5), significantly increased intratumour autophagy flux implies that there is

267

an increased autophagy flux in non-cancer stromal cells within the E0771 induced tumours of treated GFP-LC3 mice fed protein free diets compared to those fed protein complete diets. However, the change in autophagy flux was noted to be smaller than is previous experiments using higher doses of doxorubicin.

4.8 Rapamycin (2 mg/kg) treatment during high dose doxorubicin (10 mg/kg) treatment does not influence changes in tumour volumes attributed to doxorubicin

A.
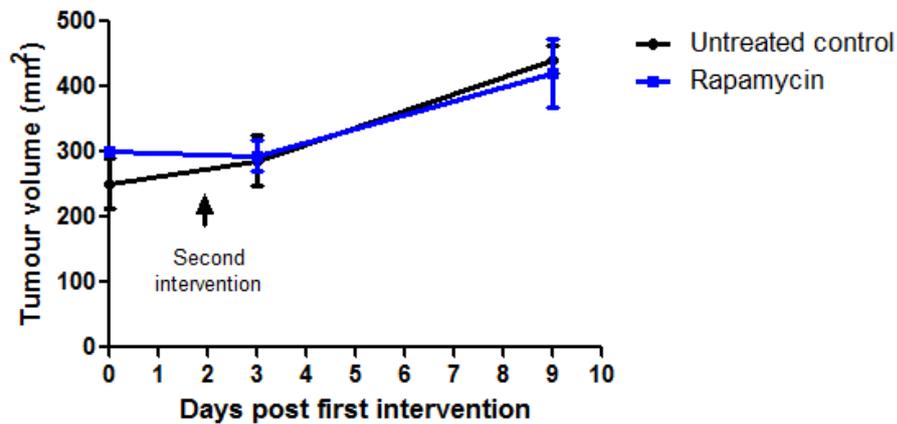
B.
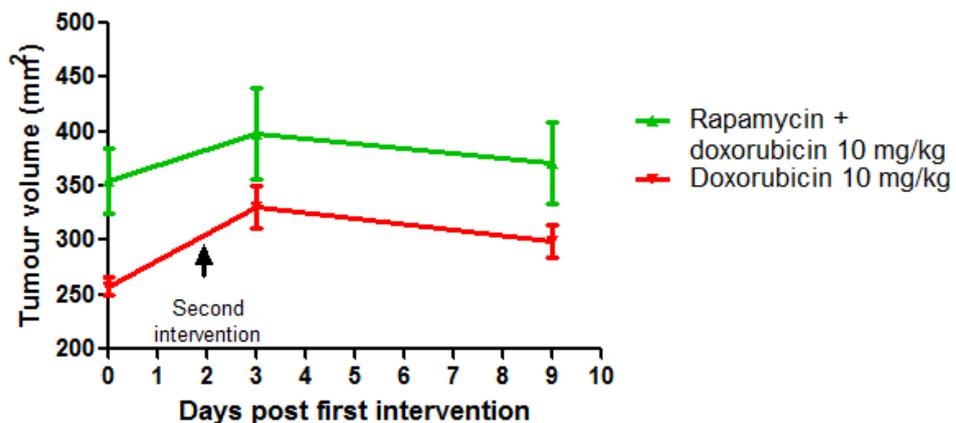
Fig. 6.10 Change in tumour volumes after treatment with doxorubicin (10 mg/kg) either with or without a rapamycin (2 mg/kg) injection. i.p. injection with rapamycin does not result in changes to tumour volumes after the initial injection with the drug. Treatment with doxorubicin (10 mg/kg) in mice also treated with rapamycin (2 mg/kg) results in a similar pattern of reductions in tumour sizes. Rapamycin treated animals were given one injection at day 0. Values are expressed as mean ± SEM. n=3 for all groups.

GFP-LC3 mice bearing large E0771 tumours (>230 mm^2) were administered two high dose doxorubicin (10 mg/kg) treatments over three days. If tumour bearing mice were injected with rapamycin (2 mg/kg) immediately prior to the first doxorubicin treatment (10 mg/kg), reductions in tumour size were shown to be similar to those treated with doxorubicin alone (Fig 6.3b). Rapamycin (2 mg/kg) alone had no influence on tumour volume (Fig 6.3a).

269

4.9 Rapamycin (2 mg/kg) treatment during high dose doxorubicin (10 mg/kg) treatment results in increased survival of E0771 tumour bearing GFP-LC3 mice
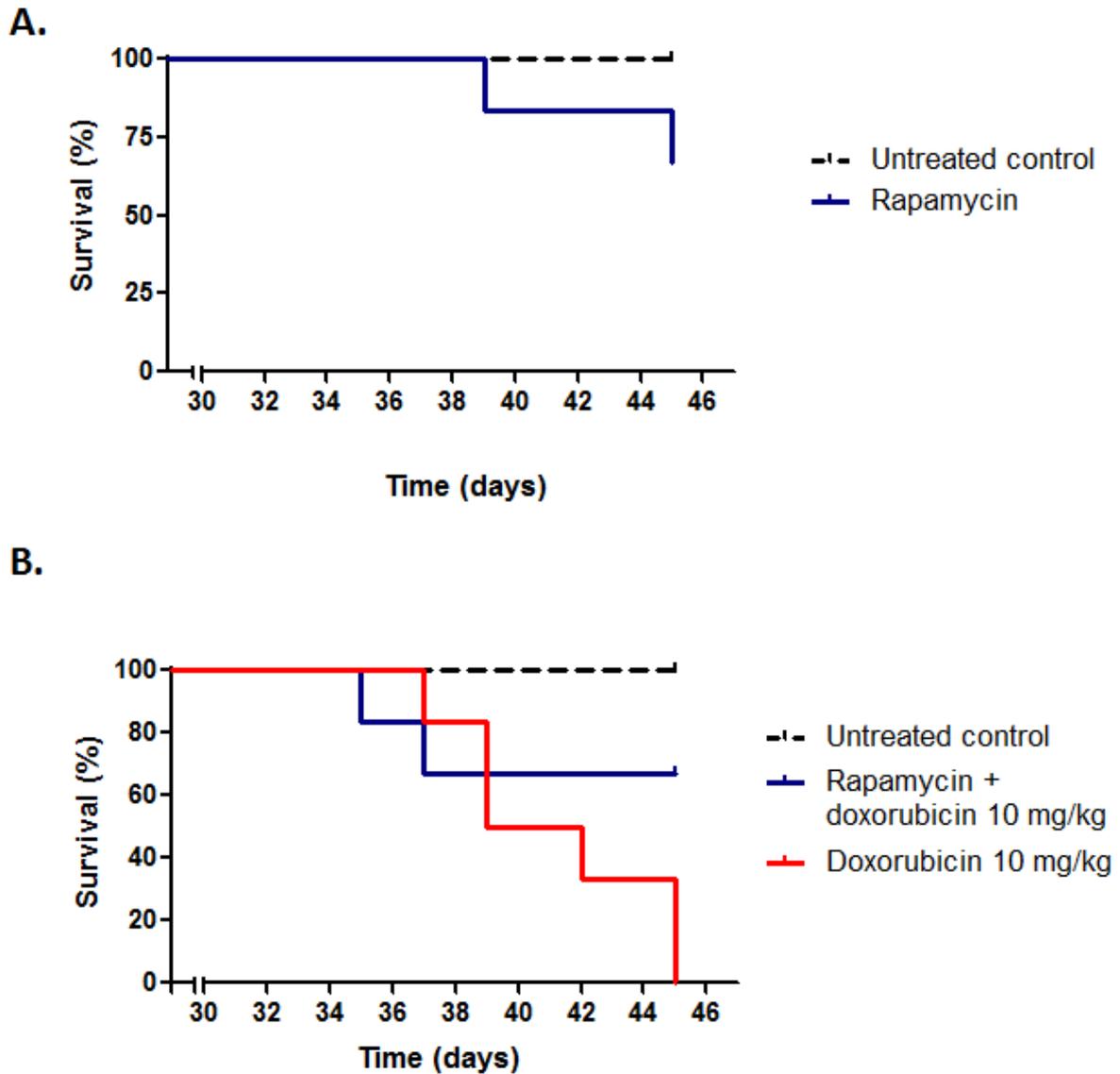
Fig. 6.11 Rapamycin protects against high-dose chemotherapy *in vivo*. A) Tumour bearing GFP-LC3 mice were treated with rapamycin (2 mg/kg) B) Mice were administered doxorubicin (10 mg/kg) i.p. twice over a period of three days and administered rapamycin (2 mg/kg) once on the same day as the doxorubicin injection. Values are expressed as mean ± SEM. N=6 for all groups

GFP-LC3 mice with large tumours (>230 mm^2) derived from E0771 mammary adenocarcinoma cells were injected i.p. with rapamycin (2 mg/kg) on day 33 after the initial injection of E0771 cell suspension. Mice with large tumours and injected with rapamycin

were more likely to have died twelve days after the initial intervention (Fig 6.11a). Mice with similar tumours and administered doxorubicin at a high dose (10 mg/kg) on two days, either side of a day without treatment had all died by day 11 after the initial treatment (Fig 6.11b). However, if tumour bearing mice were injected with rapamycin (2 mg/kg), immediately after i.p. injection with a high dose of doxorubicin (10 mg/kg), then the survival of these mice was prolonged compared to those not receiving a rapamycin injection.

4   Discussion

Although little data on the subject exists, it appears as though short term starvation prior to or during chemotherapy can result in a differential protection of normal and cancer cells to the cytoxic effects of some drugs. The remarkable success from the few cell culture, animal and human studies performed to date has been promising. If proven to be reproducible and safe, then this differential starvation therapy could be easily utilized to improve the quality of life and perhaps even prevent some of the more serious consequences and side effects in patients receiving conventional chemotherapy. No studies to date have investigated autophagy in the context of short term starvation therapy during anticancer treatment regimes. Previous experimental data (chapter 4) has demonstrated that a metastatic cancer cell line with high basal autophagy displays increased signs of apoptosis if cells are starved of amino acids during doxorubicin treatment. Furthermore, a non-tumourogenic cell line exposed to similar conditions and treatments displayed a relative protection to the cytotoxic effects of doxorubicin if simultaneously starved of amino acids. Increased autophagy levels were indirectly implicated in this increased tolerance to doxorubicin cytotoxicity (chapter 4). As cancers are heterogenous masses composed of metastatic as well as stromal cells that are vital for continued growth and survival of these neoplasms, protection of non-cancer cells or cancer cells within the tumour mass could potentially confer a survival advantage onto these treated cancers. Furthermore, few models exist for the analysis of autophagy in solid tumours during either cancer treatment or starvation interventions.

As interest in modulation of autophagy during cancer treatment increases and novel strategies such as fasting therapy during high-dose cancer treatment are explored, it is imperative that studies are undertaken to understand the underlying mechanisms driving these beneficial observations before use in a clinical setting begins in earnest.

This chapter describes the first study to assess short term complete protein starvation during chemotherapy in a tumour model. Using a novel mammary tumour model (described in chapter 5), it was shown that high-dose doxorubicin treatment (10 mg/kg for a cumulative dose of 20 mg/kg over three days) resulted in low survival rates of rodents possessing large, aggressive tumours (Fig 6.1a). Remarkably, probability of survival was significantly improved if mice in this model were placed on protein free diets immediately after drug administration (Fig 6.1b). Although evidently extremely toxic to the tumour bearing mice in this model, the dose of doxorubicin used here was sufficient to significantly reduce tumour size after only 8 days. Crucially, these reductions in tumour sizes were not diminished in those mice starved of proteins during treatment (Fig 6.3a and Fig 6.3b). These results reflect previous findings from a cell culture based model (described in chapter 4). Although few similar studies exist, it has been proposed that changes in circulating hormone and glucose levels could be partly responsible for the differential protection of non-cancer cells from the cytotoxic impact of certain chemotherapy drugs in the *in vivo* setting. An aim of this study was to assess the role of autophagy in this apparent protection, a mechanistic aspect not yet explored in the literature, in this context.

As protection of the non-cancer subpopulation within these tumours is an important concern, a novel *in vivo* model exploiting the design of a mouse with a systematic expression of GFP fused to LC3 was designed (described in chapter 5). Using this model, it was found that although tumour size did not appear to be influenced by protein starvation therapy during doxorubicin treatment, whole tumours displayed decreased caspase activity (Fig 6.4). This decreased caspase activity was correlated with a significant increase in autophagy flux in the non-cancer subpopulation of these tumours during the combined treatment regime (Fig 6.6). Previous experimental data has described a phenomenon and an associated mechanism whereby increased autophagy flux can contribute to the tolerance of doxorubicin (described in

273

chapter 1, chapter 2, chapter 3 and chapter 4). This data represents a caveat to researchers aiming to utilize fasting or starvation diets in combination with conventional chemotherapy, and illustrates that additional mechanistic data is required in order to better understand the indirect consequences of such treatment strategies.

In order to further investigate these processes, tumour bearing mice were administered smaller single doses (5 mg/kg), but an equivalent cumulative dose (20 mg/kg), over a more prolonged treatment period (16 days). This treatment schedule was better tolerated by the treatment animals, and no pattern of decreased survival due to treatment was noted (data not shown). Importantly, although tumours in animals treated with doxorubicin displayed significant decreases in overall volume, mice starved of protein for 24 hours after doxorubicin injection did not experience similar reductions in tumour size. As in the tumours of mice treated with higher doses of doxorubicin (10 mg/kg), tumours from mice starved of protein during drug treatment displayed decreased caspase activity. Furthermore, significant increases in autophagy flux in the non-cancer population of these tumours were noted. It is proposed here that increased autophagy flux in this subpopulation of these tumours is protective and increases tolerance to lower doses of doxorubicin. Although this represents a promising avenue for differential protection from the well-documented off target consequences of doxorubicin treatment, caution must be taken as indirect protection of the neoplastic system could occur.

To further assess the possible role of autophagy in protection during doxorubicin treatment, tumour bearing mice treated with doxorubicin (10 mg/kg) were simultaneously injected with the well described autophagy inducer rapamycin (2 mg/kg). Although, rapamycin did not influence tumour growth patterns, either in association with drug treatment or when administered alone (Fig 6.10), a significantly increased probability of survival during

doxorubicin treatment was noted (Fig 6.11). Together with previous experimental data, these promising findings imply a role for autophagy in the differential protection during doxorubicin treatment, and require further investigation.

4.1   Conclusions

This is the first study to assess the role of autophagy in the non-cancer cell population within a solid mammary tumour mass during chemotherapy. Cell culture based studies (chapter 4) demonstrated a promising differential protection of non-cancer cells and increased signs of apoptosis in cancer cells during chemotherapy when these cell lines were starved of amino acids. However, translation of this model *in vivo* has shown that although protein deprivation appears to increase survival rates without impacting on reductions in tumour volumes during high dose doxorubicin treatment, a potentially increased protection may be occurring in cells within these tumours. The model established here, and the related findings, have presented a novel and unique platform for further research into this remarkable phenomenon, and particularly the role of autophagy therein.

5 References

LEE, C. & LONGO, V. D. 2011. Fasting vs dietary restriction in cellular protection and cancer treatment: from model organisms to patients. *Oncogene,* 30**,** 3305-16.

LEE, C., SAFDIE, F. M., RAFFAGHELLO, L., WEI, M., MADIA, F., PARRELLA, E., HWANG, D., COHEN, P., BIANCHI, G. & LONGO, V. D. 2010. Reduced levels of IGF-I mediate differential protection of normal and cancer cells in response to fasting and improve chemotherapeutic index. *Cancer Res,* 70**,** 1564-72.

MARTINET, W., DE MEYER, G. R., ANDRIES, L., HERMAN, A. G. & KOCKX, M. M. 2006. In situ detection of starvation-induced autophagy. *J Histochem Cytochem,* 54**,** 85-96.

MUELLER, M. M. & FUSENIG, N. E. 2004. Friends or foes - bipolar effects of the tumour stroma in cancer. *Nat Rev Cancer,* 4**,** 839-49.

RAFFAGHELLO, L., LEE, C., SAFDIE, F. M., WEI, M., MADIA, F., BIANCHI, G. & LONGO, V. D. 2008. Starvation-dependent differential stress resistance protects normal but not cancer cells against high-dose chemotherapy. *Proc Natl Acad Sci U S A,* 105**,** 8215-20.

SAFDIE, F. M., DORFF, T., QUINN, D., FONTANA, L., WEI, M., LEE, C., COHEN, P. & LONGO, V. D. 2009. Fasting and cancer treatment in humans: A case series report. *Aging (Albany NY),* 1**,** 988-1007.

SHVETS, E., FASS, E. & ELAZAR, Z. 2008. Utilizing flow cytometry to monitor autophagy in living mammalian cells. *Autophagy,* 4**,** 621-8.

7 _____

Synthesis

Novel research investigating approaches aimed specifically at targeting characteristics common to a broad range of malignancies are becoming increasingly necessary. However, the safety and effectiveness of many emerging therapeutic strategies remains poorly understood. Many neoplasms appear to have the ability to circumvent the deleterious consequences of a chaotic blood supply (due to abnormal vascularisation) and the resulting transient episodes of nutrient limitation. Understanding how cancer cells are able to avoid and tolerate the effects of a short term cessation of nutrient supply could prove vital if future anticancer strategies are to be successfully developed based on this premise. Indeed, current research has already begun to investigate these avenues, and the recent employment of controlled amino acid starvation of cancer patients has exposed a potentially feasible and reproducible therapeutic approach. In a series of studies, this manuscript presents an investigation into the ability of a commonly used cancer cell line (MDAMB231), in comparison to a non-tumourogenic control line (MCF12A), to tolerate a short term bout of amino acid restriction. Using this model, additional experiments were designed to provide mechanistic insight into these initial findings. Thereafter, using this knowledge, studies were undertaken in an attempt to exploit the novel anticancer potential of using amino acid starvation in conjunction with chemotherapy *in vitro*. A new and innovative cancer model was then developed to expand these findings into the *in vivo* setting.

Initial experiments (presented in chapter 1) established that a fast growing, metastatic cancer cell line (MDAMB231) was more sensitive to a dearth of amino acids than a non-tumourogenic line (MCF12A). It was shown that a short term deprivation of amino acids

resulted in increased cell death and a proliferation arrest in these cells. Most cells are known to possess proficient intracellular mechanisms that are able to maintain amino acid levels during times of starvation. The autophagosomal-lysosomal pathway is predominant among these and MDAMB231 cells are known to have high basal levels of autophagy, even in nutrient rich conditions. Recently published findings have revealed that human cancers with mutations in H-*ras* or K-*ras* may require autophagy for tumour survival and for sustained growth. Although, these mutations are not common in breast cancer, genetic modifications in regions coding for proteins elsewhere in the RAS pathway results in high RAS activation in a large percentage of breast malignancies. As the MDAMB231 breast cancer cell line is a known K-*ras* mutant, it was speculated that autophagy is crucial for this tolerance to acute amino starvation. Experimental evidence (chapter 2) demonstrated that autophagy inhibition resulted in decreased cell survival and reduced proliferation levels during acute amino acid starvation in the MDAMB231 cell line. After a few hours without exposure to amino acids protection was lost and intracellular cell death programs initiated. Surprisingly, the slower growing, non-cancer cell line was more tolerant to these short term alterations in amino acid levels.

Autophagy has been frequently implicated as a potential survival mechanism in cancerous tumours, based on the premise that the degradation products released following autophagy-mediated breakdown of cytoplasmic materials can be utilized for protein synthesis or as substrates for ATP production. Unfortunately, there is little direct evidence to support this hypothesis in cancer cells. Based on evidence from previous experiments, the subsequent study (chapter 3) attempted to provide a rare insight into the autophagy-mediated changes in amino acid levels that occur during a short term starvation event and supply some mechanistic support to explain the finding that autophagy protects MDAMB231 and MCF12A cells during amino acid starvation. Unlike most existing studies into this

278

phenomenon, the model design used here allowed for the delineation of the impact of amino acid starvation alone (a known trigger for increased autophagy) while all other nutrients remained constant. It was successfully demonstrated, by inhibiting autophagy pharmacologically (bafilomycin A1) or biologically (ATG5 siRNA), that autophagy is a vital process for tolerance to amino acid deprivation. Interestingly, it was shown that both cell lines utilized in these studies exhibited a short lived autophagy-mediated surge in amino acid levels. While amino acid levels quickly decreased in the MDAMB231 cells thereafter, presumably due to the high metabolic and biosynthesis needs of these cells, they remained elevated in the slower growing MCF12A cells. As autophagy inhibition blunted this protective response, it was inferred that generation of amino acids by autophagy is a vital mechanism during adaptive tolerance to short term amino acid starvation. The discovery of an analogous elevation in free fatty acid levels during similar conditions (which could be blunted by autophagy inhibition) strengthened the hypothesis that increased autophagy results in the increased intracellular availability of basic protein and organelle constituents for reuse elsewhere in the cell. In an attempt to understand how these basic cellular building blocks were being utilized by the cell, changes in ATP levels were examined during starvation in the presence or absence of autophagy inhibition. Surprisingly, autophagy related processes were implicated in the maintenance of ATP levels within these cell lines during amino acid starvation. MDAMB231 cells were revealed to be particularly reliant on the ATP homeostasis conferred by increased autophagy, during the first hours of amino acid deprivation. Together, these three studies demonstrate how a cancer cell line that depends on autophagy for survival is able to avoid cell death during short term starvation by generating basic cellular building blocks and utilizing them for cellular processes such as ATP maintenance.

Many clinical trials are beginning to assess the effectiveness of compounds known to regulate autophagy in patients receiving anticancer therapy, and short term starvation has shown promise in alleviating some of the symptoms associated with chemotherapy in some studies. Previous results demonstrated that complete amino acid deprivation elicited specific and dynamic alterations to acidic compartmentalization in MDAMB231 cells. Using this data as a platform, the next study was designed to establish if lysosomal acidity levels, associated with amino acid starvation in these cells, correlated with cell survival during doxorubicin treatment (chapter 4). Interestingly, a sustained elevation of autophagy (and lysosomal acidity) in MCF12A cells during similar treatment was associated with a relative protection from cell death during doxorubicin treatment as well.

 Much of the solid tumour is typically made up of a variety of cell subpopulations that are required for continued growth and invasion. As these heterogeneous neoplasms are comprised of cancer and stromal elements, it is therefore essential that *in vitro* studies are translated *in vivo*. The next study was successful in establishing a novel mammary tumour model in a GFP-LC3 transgenic mouse (chapter 5). A reproducible method to study autophagy in the non-cancer subpopulation of tumours was established, for the first time.

As data showed that a non-cancer cell line experienced protection if starved of amino acids during doxorubicin treatment, but a cancer cell line with high basal autophagy activity had increased cell death, the final study reproduced here was undertaken in order to establish if tumours are protected or display decreased survival if mice are starved of proteins during doxorubicin treatment. Evidence in this chapter shows that while protein deprivation of mice receiving a high cumulative dose doxorubicin treatment increases survival it also decreases intratumour caspase activity. Increased intratumour autophagy flux in the non-cancer cell population of these tumours was implicated in this protection.

Appendix

Chapter one

Caspase-Glo® 3/7 assay
(MCF7/MDA-MB-231/MCF12-A cells in a 96-well format)

Preparation of working reagent solution and storage:

1. Mix the Caspase-Glo® 3/7 buffer reagent gently and allow to equilibrate at room temperature.

2. Transfer the lyophilized substrate to the buffer and mix by swirling

3. Store at -20°C. (Note that reconstituted reagent that is freeze thawed will display diminished signal over time – approximately 60% compared to freshly prepared reagent after 4 weeks according to the manufacturer. However, little reduction in signal intensity was noticed over longer time periods of freeze thawing in our experiments.)

Assay protocol:

1. Allow the working buffer reagent to equilibrate at room temperature for at least 30 minutes.

2. Remove plates containing cells from 37°C growing conditions to allow them to equilibrate at room temperature. (At least 10 minutes).

3. Transfer 50 µl (1:1) of working reagent to each well containing cells.

4. Mix plates on a shaker for 30 seconds.

5. Incubate plates in the dark for 1 hour at *constant* room temperature. (Can incubate for up to 3 hours).

6. Measure the luminescence in a luminometer.

Cell cycle analysis (CycleTEST™ PLUS DNA Reagent Kit)
(MCF7/MDA-MB-231/MCF12-A cells in a T25 flask format)

1.   Add 3 ml Trypsin/EDTA (0.25%) to each flask and place on the cell shaker for 5 minutes or until the cells have detached from the surface of the flask.

2.   Add 6 ml of appropriate culture medium to each flask.

3.   Transfer each resulting cell suspension to a separate, sterile 15 ml falcon tube.

4.   Centrifuge at 400 x g for 5 minutes at room temperature.

5.   Carefully decant all the supernatant, and tap off the last drop onto a tissue.

6.   Wash the pellet with sterile room temperature PBS.

7.   Centrifuge at 400 x g for 5 minutes at room temperature.

8.   Add 250 µl of trypsin buffer (Solution A) to each tube and mix by tapping. (Do not vortex).

9.   Allow solution A to react for 10 minutes at room temperature.

10.   Do not remove solution A.

11.   Add 200 µl of trypsin inhibitor and RNase buffer was added to each tube and mix gently by hand tapping. (Do not vortex).

12.   Incubate for 10 minutes at room temperature.

13.   Add 200 µl of ice cold propidium iodide stain solution was added to each tube and incubated on ice in the dark for a further 10 minutes.

14.   Filter samples through a 50 µm nylon mesh into 12x75 mm tubes.

15.   Analyse using flow cytometry

MTT activity assay
(MCF7/MDA-MB-231/MCF12-A cells in 96-well plate format)

Solutions and reagents

Solution A

Component	Final percentage
Isopropanol (propan-2-ol)	99%
conce. HCl	1%

Solution B

Component	Final percentage
Triton-X-100	0.1%
dH$_2$O	99.9%

1. Prepare a 1% MTT working solution in PBS (0.01 g MTT/ml PBS).

2. Remove culture medium from cells. (Do not rinse cells with PBS).

3. Add 150 µl of warm PBS and then 50 µl of MTT working solution to each well containing the cell monolayer.

4. Incubate at 37ºC for two hours.

5. In the meantime, mix together a working stock of solution A and solution B in a 50:1 ratio. 50 ml should be sufficient

6. Remove cells from the incubator and examine under the microscope. The solution is light sensitive so do not expose for too long

7. Discard the supernatant and add 200 µl of the solution A/solution B mixture

8. Protect cells from light by covering with foil and shake vigorously for 5 minutes

9. Read the absorbance of the supernatant using a platereader (wavelength of 540 nm). Use the solution A/solution B mixture as a blank.

RIPA buffer
100 ml RIPA buffer (***final concentration in bold***)

Add the reagents in the following order. Protect the solution from light and prepare while stirring on ice.

1. Tris-HCl pH 7.4 (790 mg Tris + 900 mg NaCl) *(50 mM)*

2. 10 ml of 10% NP-40

3. 2.5 ml Na-deoxycholate *(0.25%)*

4. 1 ml of 100 mM EDTA pH 7.4 *(1 mM)*

5. 100 µl of 1 mg/ml Leupeptin *(1 µg/ml)*

6. 80 µl of 5 mg/ml SBT1 *(4 µg/ml)*

7. 100 µl of 1M Benzamadine *(1 mM)*

8. 500 µl of 200 mM NaF *(1 mM)* Toxic!

9. 500 ul of 200 mM Na3VO4 *(1 mM)*

10. Mix briefly.

11. Allow to incubate until the cells are ready to treat and assay.

12. Add 1 ml of Triton X-100. Viscous!

13. Aliquot into practical amounts to avoid freeze thawing

Bradford Assay

Bradford reagent (5X concentrated)
Dilute 500 mg of Coomassie Brilliant blue G in 250 ml 95% ethanol
Add 500 ml of phosphoric acid before mixing thoroughly
Make up to one litre with dH_2O
Filter and store at 4°C

Bradford working solution
Dilute stock in a 1:5 ratio with dH_2O
Filter using 2 filter papers (at the same time)
Solution should be a light brown colour

1. Thaw 1 mg/ml BSA stock solution

2. Thaw protein samples if in -80°C freezer. *Keep on ice at all times*

3. Make up a working solution of 100 µl BSA:400µl dH_2O. *Vortex mixture*

4. Mark 7 Eppendorf tubes for the standards as well as tubes for the samples to be tested

5. Now add BSA and water to marked Eppendorf tubes as followed:

Blank:	0 µl BSA	100 µl dH_2O	
2 µg protein:	10 µl BSA	90 µl H_2O	
4 µg protein:	20 µl BSA	80 µl H_2O	
8 µg protein:	40 µl BSA	60 µl H_2O	
12 µg protein:	60 µl BSA	40 µl H_2O	
16 µg protein:	80 µl BSA	20 µl H_2O	
20 µg protein:	100 µl BSA	0 µl H_2O	
Each sample:	0 µl BSA	95 µl H_2O	5 µl of sample protein

6. Vortex all the tubes for a moment

7. Now add 900µl of Bradford reagent to each Eppendorf tube. *Vortex again*

8. Let the solutions stand for ~5min (*switch on the spectrophotometer in the meantime*)

9. Read absorbencies, twice each, at 595nm

    a. If sample values fall outside the range of the highest standard then dilute with RIPA buffer.

10. Make use of excel to make a linear plot of absorbencies and then calculate the amount of each sample to be added to aliquots.

Sample preparation (Western blot-SDS-PAGE)

1. Set heating block to 99°C

    a. Remember to keep protein samples on ice at this point

2. Make up a stock solution containing 850 µl of sample buffer and 150 µl of mercaptoethanol

3. Vortex the solution

4. Calculate the number of sample sets needed, each containing one representative of each protein sample

5. Add sample buffer to each aliquot. *Do so under the fume hood*

6. Add a volume of sample buffer equal to 1/3 of the final volume

7. Now add the amount of sample calculated previously to each respective Eppendorf tube

8. Punch small pin size holes in each tube then place in boiling water to stand for a period of 5min.

9. Spin tubes for a moment (~5sec) using the tabletop centrifuge

10. Samples can now be stored at -80°C

In the case that samples have been stored in the -80°C freezer:

1. Start by bringing a beaker of water to the boil

2. Remove samples from the freezer

3. Make sure that small pin size holes have been punched in the top of each tube

4. Place in boiling water for a period of 5min

5. Spin down momentarily (20sec) on the tabletop centrifuge (*take care not to over centrifuge, especially if samples have been obtained from tissue*)

6. Samples can now be used

SDS-PAGE -Western blotting

1. Clean pairs of large and small glass plates with methanol and a paper towel.

2. Place the small glass plate onto the large plate and slide these into the green assembly.

3. Tighten the assembly by pushing the green clips outward.

4. Place the assembly onto the rubber base, pushing down gently.

5. Prepare two small beakers, two Pasteur pipettes and a small stirring bar.

6. Fill one beaker with H_2O and prepare isobutanol.

7. Gel recipe for 10% 0.75mm gels:

	2 gels:	4 gels:
	µl	µl
dH_2O	3850	7700
1.5M Tris-HCl pH 8.8	2500	5000
10% SDS (stock)	100	200
10% APS (0.1g/ml)	20	40
Acrylamide 40%	2500	5000
Temed	5	10

8. Mix the solution momentarily.

9. Quickly pour the mixture between the glass plates using a Pasteur pipette leaving enough space for the stacking gel.

10. Add a layer of isobutanol using a fresh Pasteur pipette.

11. Allow to set for 45 minutes - 1 hour.

12. In the meantime prepare running buffer in a 1:10 dilution.

13. After 30- 45 minutes has passed begin to prepare the stacking gel (4% recipe):

287

	2 gels:	4 gels:
	µl	µl
dH$_2$O	3050	6100
0.5M Tris-HCl pH 6.8	1250	2500
10% SDS (stock)	50	100
10% APS (0.1g/ml)	50	100
Acrylamide 40%	500	1000
Temed	10	10

14. Once the gels are set (after ~1 hour), wash off the isobutanol and ensure the plates are dry.

15. Add Temed to the stacking solution, mix quickly and add stack between the plates.

16. Gently push combs (of the correct width) into the stacking gel.

17. Allow to set for 30 minutes.

18. Switch on the heating block (set to a temperature of 95°C).

19. Retrieve prepared samples from the -80°C freezer and allow them to thaw (on ice).

20. Ready the electrophoresis apparatus for use.

21. Once thawed, vortex each sample briefly before denaturing on the heating block for 5 minutes.

22. In the mean time, carefully remove the combs from the gels and wash gently with dH$_2$0 being careful not to damage the wells.

23. Vortex each sample briefly before centrifuging rapidly for a few seconds.

24. Take the gel plates out of the assembly stand and place them into the U-shaped adaptor cassette. The small plates must be facing inwards.

25. Place the U-shaped adaptor into the loading system and push the latches closed, away from your body.

26. Carefully pour running buffer into the middle compartment between the gel plates, allowing the buffer to flow over into the wells.

27. Add 10 µl of molecular weight marker into the first well on the left of each gel.

28. Add your samples into each well using a micropipette and loading tips. Use a clean tip for every sample.

29. Place the system into the outer running chamber, and add running buffer until ~1 cm below the wells.

30. Place the green lid with electrical leads onto the cell system, making sure to attach the electrodes correctly (red to red and black to black).

31. Perform an initial ten minute run at 100 V (constant) and 400 mA.

32. Thereafter, perform a longer run (usually ~50 minutes) at 200 V (constant)

33. Turn off the power and disconnect the electrodes before removing the gel plates from the system.

34. Place the gel in transfer buffer two for at least 15 minutes.

35. **Electrotransfer** can now be performed using the semi-dry apparatus (Bio-Rad).

36. Cut two chromatography filter papers and one 0.2 micron PVDF membrane per gel.

37. Soak filter papers in transfer buffer.

38. Soak one PVDF membrane in methanol for 15 seconds and then rinse with water before leaving to soak in transfer buffer.

39. Place one filter paper onto the semi-dry apparatus.

40. Carefully place PVDF membranes onto lower filter paper. Role with a wet tube to remove any bubbles that may have formed.

41. Place gels onto the membranes. Role with a wet tube to remove any bubbles.

42. Place filter paper onto gel to complete the membrane sandwich.

43. Close the system and run at limit 0.5 A and 15 V for ~1 hour.

44. Wash the membranes three times for 5 minutes in copious amounts of previously prepared TBS-Tween (allow foam to develop by vigorous mixing).

45. Block the membranes in suitable blocking reagent.

46. Prepare the primary antibody as per manufactures instructions (usually 5 μl in 5 ml TBS-T).

47. Mix at 4°C overnight.

48. Wash membranes in TBS-T with agitation. Three times for five minutes each is sufficient.

49. Place the membranes in the HRP-conjugated secondary antibody (1.25 μl in 5ml TBS-T). Incubate with agitation for one hour at room temperature.

50. **Exposure** requires an enhanced chemi-luminescent reagent (e.g. ECL/ECL+ detection kit (Amersham biosciences) or LumiGLO Reserve™ CL substrate kit (KPL, Inc., USA).).

51. Add 500 μl of each of the ECL cocktails provided in a ratio corresponding to the manufacturer˚s instructions. (Usually 1:1.) Cover a falcon tube with foiland mix for a few seconds.

52. Cover the area of the membrane known to have the bands that you are looking for and leave to incubate for ~one minute.

53. Expose membranes to x-ray film in a dark room.

Chapter two

Reverse transfection protocol
(siRNA into MCF7/MDA-MB-231/MCF12-A cells in a 60 mm^2 petri format)

For each petri dish to be transfected, prepare RNAi duplex-Lipofectamine RNAiMAX complexes in the following way:

1. Prepare mastermix by diluting 20 pmol of duplex into 250 ul of transfection medium (medium containing no antibiotics or serum).

2. Mix lipofectamine RNAiMAX gently and add 2 ul per 250 ul of mix.

3. Resuspend and add 250 ul to each petri dish.

4. Allow to incubate for 20 minutes.

5. Split and dilute cells in growth medium (must contain no antibiotics) to have a final volume of 2 ml in each petri.

6. Add 1.5 ml of diluted cell suspension to each well containing the RNAi duplex-Lipofectamine RNAiMAX complexes.

7. Mix gently

8. Allow to incubate until cells are ready to treat (24-48 hours later).

488 nm laser and 610LP, 616/23BP emission filters.

Lysotracker™ (Flow cytometry)
(MCF7/MDA-MB-231/MCF12-A cells in a T25 flask format)

1. Following completion of the treatment protocol, remove culture media and wash cells in 5 ml PBS.

2. Add 3 ml Trypsin/EDTA (0.25%) to each flask and place on the cell shaker for 5 minutes or until the cells have detached from the surface of the flask.

3. Add 6 ml of appropriate culture medium to each flask.

4. Transfer each resulting cell suspension to a separate, sterile 15 ml falcon tube.

5. Centrifuge at 6000xg for 3 minutes.

6. Pour off the media-trypsin.

Preparation of Samples for Analysis

7. Re-suspend each cell pellet in 0.5 ml LysoTracker™ red (Invitrogen/Molecular Probes) working solution (final concentration of 100 nmol/L).

8. Incubate the suspension for 15 minutes at 37ºC

9. Gently re-suspend cell suspension 10x directly before filtering through into FACS tube

10. Analyse on the flow cytometer (BD FACSAria I) immediately

11. Collect a minimum of 10000 events using 488 nm laser and 610LP, 616/23BP emission filters.

Hoescht and Lysotracker™ (Cell imaging)
(MCF7/MDA-MB-231/MCF12-A cells in a 60 mm^2 petri dish format)

1. Prepare a warm solution of PBS/LysoTracker™ red (Invitrogen/Molecular Probes) working solution (final concentration of 100 nmol/L).

2. Remove this solution from the cells and wash twice with sterile 0.1M PBS.

3. Add cold fixative (1:1 methanol/acetone) and incubate for 10 minutes at 4°C.

4. Remove fixative using a micropipette and leave to air dry for approximately 20 minutes

    - Prepare a 1:200 Hoechst solution and centrifuge momentarily before use.

5. Rinse the cell monolayer 3 times with sterile PBS.

6. Add enough Hoechst dye (1:200) to cover the cell monolayer completely (100 µl) and then incubate for a further 10 minutes.

7. Wash the cell monolayer 5 times.

8. Cells can now be stored at -20°C for ~2 weeks. *Wrap in foil to avoid exposure to UV radiation.*

Chapter three

Lowry protein determination
(MDA-MB-231/MCF12-A cells in 60mm^2 petri dishes)

1. Prepare the working standards (albumin (0.5 g/10 ml) in 0.5 M NaOH):

   1:400 (0.5 ml 200 ml), 1:100 (1 ml 100 ml) and 1:200 (0.5 ml 100 ml)

2. Prepare a cold NaK-Tartrate-CuSO$_4$ solution: (49 ml 2% Na$_2$CO$_3$, 0.5 ml 1% CuSO$_4$.5H$_2$O and 0.5 ml 2% NaK-Tartrate).

3. Add 1 ml of cold NaK-Tartrate-CuSO$_4$ to the following groups in 10 second intervals:

   • 1x 50 µl 0.5 M NaOH as blank

   • 3x 50 µl working standard 1, 2 and 3

   • 2x sample lysate

4. After 10 minutes add 100 µl cold 1:3 Folin Ciocult:dH$_2$O solution to each sample in 15 second intervals.

5. After 30 minutes the absorbencies were measured on a spectrophotometer at 750 nm.

ATP analysis (ENLITEN® ATP assay system)
(MCF7/MDA-MB-231/MCF12-A cells in 60 mm^2 petri dishes)

Preparation of working reagent solution and storage:

1. It is important to use clean glassware and equipment that are free of trace amounts of ATP. (e.g. don't touch the outside of gloves with skin).

2. Transfer the rL/L lyophilized substrate to the reconstitution buffer and mix by swirling. (Don't shake the bottle.)

3. Store in single use aliquots at -20°C. (Note that reconstituted reagent that is freeze thawed will display diminished signal over time – approximately 50% compared to freshly prepared reagent after 2 weeks according to the manufacturer.)

ATP extraction:

1. Allow the working buffer reagent to equilibrate at room temperature for at least 60 minutes. (Stable at room temperature for 8 hours.)

2. Remove plates containing cells from 37°C growing conditions to allow them to equilibrate at room temperature. (At least 10 minutes).

3. Detach cells using trypsin and then centrifuge at 4°C.

4. Wash pellets in PBS.

5. Centrifuge the cell suspension at 4°C to pellet.

Assay protocol:

1. Prepare standard solutions by performing a 10x serial dilution of the ATP standard (1×10^{-7} M) assay buffer in lysis buffer(100 mM Tris-HCl and 4 mM EDTA, pH 7.75). (Four such dilutions will dilute the standard to 1×10^{-11} M – the lowest standard will have a final concentration of 1×10^{-16} mol/100 µl).

2. Resuspsend the cell pellet in 50 µl of ice-cold lysis buffer and transfer to 1.5 ml tubes.

295

2. Add 150 µl of boiling lysis buffer to each sample.

3. Incubate samples for 2 minutes at 99°C.

4. Centrifuge the lysates at 10 000 rpm at 4°C for 1 minute.

5. Transfer 50 µl of the supernatant of working reagent and sample (or blank assay buffer) to a luminometer plate (1:1).

6. Measure the luminescence in a luminometer. (Delay period = 2 sec. Integrate period = 10 sec. Replicates = 1)

Preparation for amino acid quantification by means of a mass spectroscopy based proteomics method
(MCF7/MDA-MB-231/MCF12-A cells in a 60 mm^2 petri format)

1. Seed cells in 60 mm petri dishes and treat once they have reached 75% confluence.

2. Scrape cells in 400 µl of saline (0.9mM Sodium Chloride) and transfer to previously labelled tubes.

3. Sonicate samples for 10 seconds.

4. Transfer 5 µl of each sample to a separate tube. (This will be used for protein quantification.)

5. Following sonication, transfer each sample to a tube-centrifugal filter unit (AMICON ULTRA 0.5ML 10K; Millipore; UFC501024).

6. Centrifuge the tubes for 10 minutes @ 1400 rpm.

7. Retain the filtrate for the amino acid quantification process.

Waters API Quattro Micro. Mass Spec (Capillary voltage: 3.5 kV, Cone voltage: 1 V, Source: 100ºC, Desolvation Temp: 350ºC, Desolvation gas: 350 L/h, Cone gas: 50 L/h)

Table A1 Mean amino acid content in MDAMB231 cells. Mean amino acid levels are expressed in mg/ml.

	0 hrs		6 hrs		12 hrs		24 hrs	
	mean	±SD	mean	±SD	mean	±SD	mean	±SD
His	0.002028	0.000214	0	0	0	0	0	0
Ser	0.003151	0.000632	0.000293	5.18E-06	8.23E-05	3.73E-05	0.000109	8.48E-05
Arg	0.0062	0.001406	0.000439	2.18E-05	0.000249	9.7E-05	0.000235	1.4E-05
Gly	0.007843	0.001903	0.001989	6.47E-05	0.002116	0.000702	0.002795	0.000349
Asp	0.001029	0.00037	0.000775	4.33E-05	0.000865	0.00032	0.001131	7.4E-05
Glu	0.013315	0.004561	0.005237	0.000389	0.004711	0.00102	0.005179	0.000324
Thr	0.013237	0.002625	0.001381	3.48E-05	0.000915	0.000353	0.001078	6.89E-05
Ala	0.052328	0.010936	0.00668	0.000148	0.004738	0.001937	0.006039	0.000223
Pro	0.003504	0.000961	0.000691	4.18E-05	0.000735	0.00034	0.000973	5.85E-05
Cys	0	0	0	0	0	0	0	0
Lys	0.012497	0.003119	0.001235	6.7E-05	0.00076	0.000282	0.000786	3.15E-06
Tyr	0.00934	0.001224	0.000754	7.25E-05	0.000442	0.000207	0.000527	5.18E-05
Met	0.003152	0.000519	0.00023	2.55E-05	8.23E-05	3.7E-05	5.27E-05	5.18E-06
Val	0.009746	0.002123	0.001046	4.07E-05	0.000471	0.000118	0.00047	2.79E-05
ILe	0.008849	0.001951	0.000774	7.51E-05	0.000264	4.89E-05	0.000207	5.38E-05
Leu	0.008796	0.002009	0.000837	4.44E-05	0.000346	8.44E-05	0.000288	8.78E-06
Phe	0.009832	0.001634	0.001067	7E-05	0.000675	0.000352	0.000709	3.26E-05
Asn	0	0	0	0	0	0	0	0
Gln	0.131706	0.027194	0.008763	0.001	0.003286	0.000945	0.002826	9.29E-05
Trp	0.002755	0.000528	0.000272	3.44E-05	0.000166	6.45E-05	0.000183	1.91E-05
Total:	0.305155	0.063483	0.032465	0.000581	0.020903	0.006368	0.023587	0.001058

	ATG5 siRNA + BCKDH siRNA							
	0 hrs		6 hrs		12 hrs		24 hrs	
	mean	±SD	mean	±SD	mean	±SD	mean	±SD
His	0.002642	0.000398			0.00029	6.22E-05	0.000371	3.1E-05
Ser	0.002299	0.00049	0.000429	5.26E-05	0.000213	2.15E-05	0.000226	2.25E-06
Arg	0.002657	0.00037	0.000417	5.03E-05	0.000316	6.31E-05	0.000306	6.64E-05
Gly	0.004471	0.000998	0.002045	0.000235	0.002481	0.000889	0.002181	0.000288
Asp	0.000762	0.000241	0.000699	0.000126	0.000608	4.53E-06	0.000549	2.87E-05
Glu	0.008707	0.002086	0.005138	0.001078	0.004472	0.000244	0.003295	0.00038
Thr	0.007807	0.00123	0.001304	0.000165	0.00112	7.24E-05	0.001018	5.85E-05
Ala	0.031266	0.004661	0.006814	0.000688	0.006272	0.000306	0.006157	0.000521
Pro	0.00132	0.000399	0.000712	0.000186	0.000716	5.06E-05	0.000808	9.51E-05
Cys	0	0	0	0	0	0	0	0
Lys	0.008483	0.000676	0.001497	2.5E-05	0.001207	0.000162	0.001116	5.69E-05
Tyr	0.006353	0.001088	0.000892	2.42E-05	0.000772	4.47E-05	0.000743	2.7E-05
Met	0.002216	0.000344	0.000253	4.19E-05	0.00015	4.92E-05	4.85E-05	5.61E-07
Val	0.007666	0.001027	0.001141	5.56E-06	0.00082	9.93E-05	0.000636	7.3E-06
ILe	0.007092	0.000947	0.000836	1.75E-05	0.000522	0.000102	0.000294	3.37E-06
Leu	0.007259	0.000929	0.001018	1.22E-06	0.000635	0.000121	0.00044	5.05E-06
Phe	0.006943	0.001297	0.00113	4.01E-05	0.00104	0.000178	0.001066	4.55E-05
Asn	0.000654	0.000147	0	0	0.00056	3.62E-05	0.000645	0.000167
Gln	0.094915	0.016587	0.009585	0.000254	0.007146	0.001708	0.003604	0.000659
Trp	0.001993	0.000392	0.000314	1.19E-05	0.000273	3.11E-06	0.000242	3.21E-05
Total:	0.202864	0.031411	0.03392	0.002335		0.001735		0.000826

Table A2 Mean amino acid content in MDAMB231 cells. Mean amino acid levels are expressed in mg/ml.

	Bafilomycin (10 mM)									BCKDH siRNA							
	0 hrs		6 hrs		12 hrs		24 hrs			0 hrs		6 hrs		12 hrs		24 hrs	
	mean	±SD	mean	±SD	mean	±SD	mean	±SD		mean	±SD	mean	±SD	mean	±SD	mean	±SD
His					0.000271	6.04E-06	0.000248	1.26E-05	His	0.00316	0.000596	0.000472	0.000115	0	0		
Ser			0.00024	0.000194	0.00027	3.97E-05	0.000109	4.15E-05	Ser	0.002531	0.000467	0.000534	4.22E-05	0.00013	3.89E-05	0.000113	3.95E-05
Arg			0.0004	0.00029	0.000256	2.84E-05	0.000167	4.96E-05	Arg	0.002738	0.000494	0.000669	4.55E-05	0.000232	5.61E-05	0.000195	2.5E-05
Gly			0.002242	0.001857	0.002199	0.00028	0.001846	1.8E-05	Gly	0.005237	0.001049	0.002577	1.15E-05	0.001777	0.00024	0.001756	0.000129
Asp			0.000961	0.00079	0.00089	0.000157	0.000844	0.00012	Asp	0.000793	0.000161	0.000791	1.44E-05	0.000601	0.000114	0.000499	6.12E-05
Glu			0.006206	0.005071	0.005974	0.001207	0.004598	7.7E-05	Glu	0.01004	0.002243	0.005723	0.000256	0.004236	0.00077	0.002797	8.97E-05
Thr			0.001041	0.000888	0.001176	0.00018	0.001003	8.03E-05	Thr	0.009213	0.001925	0.001677	0.000121	0.000901	0.00017	0.000802	2.11E-05
Ala			0.005485	0.004617	0.006441	0.001257	0.005735	0.00025	Ala	0.037068	0.008785	0.00865	0.000785	0.005217	0.001238	0.00493	0.000194
Pro			0.000721	0.000582	0.000725	0.000179	0.000801	6.2E-05	Pro	0.001653	0.000376	0.000766	7.83E-05	0.000616	0.000132	0.000629	3.37E-05
Cys			0	0	0	0	0	0	Cys	0	0	0	0	0	0	0	0
Lys			0.001081	0.000843	0.001189	0.000139	0.000909	6.73E-05	Lys	0.009921	0.002471	0.00188	0.000208	0.001042	0.000329	0.000948	0.00015
Tyr			0.000641	0.000526	0.000708	8.01E-05	0.000661	8.83E-06	Tyr	0.007179	0.001091	0.001176	7E-06	0.000599	0.00018	0.000529	7.02E-05
Met			0.00012	9.69E-05	9.03E-05	2.01E-06	6.83E-05	2.17E-05	Met	0.002503	0.00049	0.00033	2.34E-05	4.58E-05	4.72E-05	1.52E-05	3.22E-05
Val			0.000681	0.000554	0.00078	0.000137	0.000466	9.85E-05	Val	0.009592	0.001907	0.001652	6.28E-05	0.00067	0.000186	0.000612	0.000102
ILe			0.0004	0.00032	0.000513	8.27E-05	0.000254	5.06E-05	ILe	0.008853	0.001713	0.001256	7.82E-06	0.000398	0.000144	0.000235	5.49E-05
Leu			0.000561	0.000426	0.000602	6.96E-05	0.00034	1.04E-05	Leu	0.008992	0.00179	0.001454	3.53E-05	0.000529	0.000136	0.0004	7.99E-05
Phe			0.000801	0.000665	0.000858	8.62E-05	0.000756	5.38E-05	Phe	0.007582	0.001354	0.001512	3.11E-05	0.000816	0.000168	0.000785	0.000123
Asn			0	0	0	0	0	0	Asn	0.000696	0.000172	0.000217	0.000461	0.000157	0.000272	0.000369	0.000387
Gln			0.004965	0.003896	0.006093	0.001522	0.003756	0.001355	Gln	0.097635	0.021042	0.012403	0.000667	0.00501	0.00283	0.00206	0.002999
Trp			0.00024	0.000194	0.000226	4.95E-05	0.000164	3.3E-05	Trp	0.002151	0.000323	0.000399	2.34E-05	0.000201	3.63E-05	0.00016	9.64E-06
Total:			0.026784	0.019495	0.027075	0.004781	0.0216	0.000796	Total:	0.222028	0.047751	0.042987	0.002644	0.023178	0.005632	0.017641	0.004014

Table A3 Mean amino acid content in MCF12A cells. Mean amino acid levels are expressed in mg/ml.

	0 hrs		6 hrs		12 hrs		24 hrs	
	mean	±SD	mean	±SD	mean	±SD	mean	±SD
His	0.007	0.003105	0.000379	0.000379			0.00075	7.07E-05
Ser	0.0123	0.002425	0.000551	0.000551			0.00035	7.07E-05
Arg	0.022033	0.003164	0.012231	0.012231			0.0061	0.008202
Gly	0.017667	0.00206	0.002616	0.002616			0.0058	0.001131
Asp	0.003433	0.000451	0.000896	0.000896			0.00155	0.000212
Glu	0.065333	0.013123	0.008535	0.008535			0.01185	0.000212
Thr	0.0266	0.003604	0.000896	0.000896			0.00165	0.000354
Ala	0.0953	0.012934	0.003436	0.003436			0.0065	0.002263
Pro	0.002133	0.000153	0.000577	0.000577			0.00155	7.07E-05
Cys	0.0061	0.001039	5.77E-05	5.77E-05			0.0001	0
Lys	0.0294	0.002666	0.000493	0.000493			0.00175	0.000354
Tyr	0.0201	0.0021	0.000379	0.000379			0.00135	0.000212
Met	0.007967	0.001102	0.000208	0.000208			0.00025	7.07E-05
Val	0.027933	0.003653	0.000751	0.000751			0.0014	0.000283
ILe	0.027667	0.003332	0.000404	0.000404			0.0006	0.000141
Leu	0.028633	0.003386	0.000608	0.000608			0.00115	7.07E-05
Phe	0.0191	0.002066	0.000436	0.000436			0.0014	0.000141
Asn	0.002367	0.000321	0.000115	0.000115			0.0002	0
Gln	0.1196	0.01317	0.001833	0.001833			0.0012	0
Trp	0.004	0.0004	0.000231	0.000231			0.0004	#DIV/0!

	Bafilomycin (10 mM)							
	0 hrs		6 hrs		12 hrs		24 hrs	
	mean	±SD	mean	±SD	mean	±SD	mean	±SD
His	0.0089	0.002616	0.00065	7.07E-05			0.0008	0.0001
Ser	0.0123	0.003748	0.000867	0.000416			0.000667	0.000115
Arg	0.0206	0.004384	0.009033	0.007477			0.000567	0.000115
Gly	0.0196	0.005445	0.005933	0.000802			0.005667	0.000473
Asp	0.0047	0.001838	0.001567	0.000252			0.001367	5.77E-05
Glu	0.0762	0.029416	0.016133	0.002155			0.011633	0.000611
Thr	0.0269	0.007425	0.001833	0.000153			0.001767	0.000321
Ala	0.0968	0.026234	0.006833	0.000351			0.0076	0.001386
Pro	0.0025	0.000778	0.001167	0.000153			0.001433	5.77E-05
Cys	0.0043	0.000707	0.000267	0.000153			0	0
Lys	0.0312	0.006788	0.0023	0.000173			0.002033	0.000379
Tyr	0.0209	0.005374	0.002	1E-04			0.001433	0.000208
Met	0.0079	0.001838	0.000467	5.77E-05			0.000267	5.77E-05
Val	0.0278	0.007283	0.0017	1E-04			0.0015	0.000346
ILe	0.0275	0.006859	0.001267	0.000115			0.000633	0.000208
Leu	0.0286	0.007212	0.001833	0.000153			0.001133	0.000289
Phe	0.0194	0.00495	0.0014	0.0001			0.001433	0.000208
Asn	0.0023	0.000919	0	0			0	0
Gln	0.1156	0.020648	0.003333	0.001222			0.001467	0.000231
Trp	0.0044	0.001131	0.0004	0			0.0004	0

Table A4 Mean amino acid content in MCF12A cells. Mean amino acid levels are expressed in mg/ml.

	BCKDH siRNA									ATG5 siRNA + BCKDH siRNA							
	0 hrs		6 hrs		12 hrs		24 hrs			0 hrs		6 hrs		12 hrs		24 hrs	
	mean	±SD	mean	±SD	mean	±SD	mean	±SD		mean	±SD	mean	±SD	mean	±SD	mean	±SD
His	0.0069	0.001852	0.000767	0.000153			0.00115	0.000212	His	0.005667	0.000551	0.000733	0.000153			0.000933	0.000321
Ser	0.009067	0.002601	0.001033	0.000153			0.00095	0.000212	Ser	0.007533	0.000987	0.000833	0.000321			0.000467	0.000115
Arg	0.0156	0.00418	0.0014	0.000265			0.001	0.000283	Arg	0.012867	0.000777	0.001133	0.000321			0.000633	0.000153
Gly	0.0132	0.003305	0.005267	0.000802			0.0069	0.000424	Gly	0.0109	0.001735	0.005133	0.001137			0.0057	0.001
Asp	0.002833	0.000702	0.001633	0.000351			0.00335	7.07E-05	Asp	0.002433	0.000306	0.0016	0.000346			0.002367	0.000603
Glu	0.0455	0.013379	0.013533	0.003201			0.01885	0.000354	Glu	0.036267	0.006585	0.014567	0.00445			0.014333	0.003917
Thr	0.0201	0.005667	0.0019	0.000361			0.0022	0.000283	Thr	0.0167	0.002022	0.001933	0.000404			0.001933	0.000777
Ala	0.074367	0.022504	0.007333	0.001436			0.01065	0.000919	Ala	0.061167	0.007893	0.007733	0.001882			0.009533	0.003828
Pro	0.001833	0.000451	0.0011	0.0002			0.0022	0.000141	Pro	0.0015	0.000173	0.001133	0.000321			0.0017	0.000458
Cys	0.0031	0.000872	0.0001	0			0.0001	0	Cys	0.002867	0.000666	0.000133	5.77E-05			0.000133	5.77E-05
Lys	0.021867	0.004907	0.002367	0.000351			0.0021	0.000283	Lys	0.0205	0.003315	0.002267	0.000666			0.0021	0.000964
Tyr	0.0161	0.00336	0.001933	0.000404			0.0018	0.000283	Tyr	0.013533	0.001415	0.001867	0.000404			0.001567	0.000643
Met	0.0061	0.0015	0.0005	0			0.00035	7.07E-05	Met	0.005067	0.000586	0.000467	0.000115			0.000267	0.000115
Val	0.021267	0.005597	0.002247	0.000344			0.00185	0.000354	Val	0.0177	0.002078	0.0018	0.000346			0.0016	0.0007
ILe	0.0207	0.005209	0.00188	0.000574			0.00085	0.000212	ILe	0.017467	0.002228	0.001267	0.000289			0.0007	0.000361
Leu	0.021533	0.005193	0.002277	0.000322			0.0015	0.000283	Leu	0.018233	0.002376	0.001833	0.000404			0.001267	0.000569
Phe	0.0151	0.003119	0.001567	0.000252			0.0017	0.000283	Phe	0.012733	0.001332	0.001467	0.000289			0.0015	0.000529
Asn	0.002267	0.000321	0.000167	0.000153			0.00015	7.07E-05	Asn	0.0019	0.000458	0.000133	5.77E-05			0.0001	0
Gln	0.096933	0.029484	0.004667	0.001405			0.0034	0.000849	Gln	0.0836	0.00799	0.0048	0.001058			0.0032	0.001442
Trp	0.003333	0.000611	0.000267	0.000231			0.0004	0	Trp	0.002933	0.000462	0.0004	0			0.000267	0.000231

Table A5 Mean fatty acid content in MDAMB231 cells. Mean fatty acid levels are expressed in µg FA /mg protein. SD = standard deviation.

Free Fatty Acids : Quantitative Composition : µg FA / mg protein

| | | 14:0 | | 16:0 | | n-7 16:1 | | 18:0 | | n-9 18:1 | | n-7 18:1 | |
FA		Mean	±SD	Mean	±SD	Mean	±SD	Mean	±SD	Mean	±SD	Mean	±SD
Sample	Hours (n=#)	Mean	±SD	Mean	±SD	Mean	±SD	Mean	±SD	Mean	±SD	Mean	±SD
- amino acids + ATG5 siRNA + Etomoxir	24 (n=2)	0.10	0.09	1.41	1.25	0.04	0.03	1.55	1.62	0.88	0.73	0.22	0.16
	6 (n=3)	0.09	0.03	1.44	0.45	0.06	0.02	1.37	0.40	0.83	0.27	0.28	0.07
	0 (n=3)	0.03	0.01	1.12	0.14	0.05	0.00	1.44	0.07	1.18	0.16	0.35	0.06
- amino acids + Etomoxir	24 (n=3)	0.09	0.05	1.31	0.14	0.06	0.02	1.17	0.04	0.96	0.12	0.29	0.02
	6 (n=3)	0.08	0.05	1.28	0.15	0.04	0.00	1.15	0.16	0.73	0.24	0.19	0.02
	0 (n=2)	0.11	0.02	1.13	0.13	0.06	0.02	1.02	0.16	1.02	0.25	0.28	0.07
- amino acids + ATG5 siRNA	24 (n=3)	0.10	0.04	1.66	0.34	0.08	0.01	1.79	0.52	1.26	0.09	0.39	0.04
	6 (n=3)	0.10	0.04	1.25	0.41	0.05	0.03	1.14	0.20	0.82	0.34	0.23	0.06
	o (n=3)	0.07	0.02	1.23	0.34	0.07	0.01	1.20	0.33	1.07	0.24	0.35	0.08
- amino acids + bafilomycin (10 nM)	24 (n=3)	0.20	0.03	3.06	1.56	0.12	0.05	2.54	1.50	2.22	1.35	0.51	0.26
	6 (n=3)	0.07	0.02	0.99	0.21	0.03	0.01	0.87	0.08	0.62	0.12	0.12	0.01
	0 (n=2)	0.15	0.15	1.62	0.75	0.07	0.02	1.60	0.65	1.22	0.45	0.21	0.19
- amino acids	24 (n=2)	0.19	0.10	1.96	0.27	0.09	0.02	1.89	0.25	1.70	0.22	0.41	0.09
	6 (n=3)	0.17	0.05	2.38	0.18	0.08	0.03	2.73	0.61	1.55	0.20	0.33	0.03
Control n(=4)		0.09	0.02	1.63	0.47	0.06	0.02	1.49	0.51	1.13	0.36	0.24	0.05
siRNA control (n=3)		0.12	0.05	1.45	0.30	0.07	0.01	1.33	0.34	1.23	0.19	0.32	0.04

| | | n-6 18:2 | | n-6 20:3 | | n-6 20:4 | | 24:0 | | n-3 22:5 | | n-3 22:6 | | Total | |
FA		Mean	±SD	Mean	±SD	Mean	±SD	Mean	±SD	Mean	±SD	Mean	±SD	Mean	±SD
Sample	Hours (n=#)	Mean	±SD	Mean	±SD	Mean	±SD	Mean	±SD	Mean	±SD	Mean	±SD	Mean	±SD
- amino acids + ATG5 siRNA + Etomoxir	24 (n=2)	0.14	0.07	0.07	0.08	0.66	0.80	0.03	0.02	0.15	0.04	0.16	0.11	5.86	5.42
	6 (n=3)	0.14	0.03	0.06	0.03	0.10	0.08	0.06	0.03	0.10	0.02	0.13	0.03	5.27	1.84
	0 (n=3)	0.31	0.07	0.07	0.02	0.38	0.08	0.05	0.00	0.25	0.07	0.26	0.08	5.90	0.50
- amino acids + Etomoxir	24 (n=3)	0.23	0.07	0.06	0.00	0.28	0.05	0.05	0.00	0.18	0.04	0.21	0.05	5.14	0.58
	6 (n=3)	0.26	0.19	0.02	0.00	0.12	0.03	0.06	0.02	0.12	0.01	0.13	0.02	4.51	0.62
	0 (n=2)	0.23	0.04	0.05	0.02	0.22	0.07	0.04	0.01	0.15	0.03	0.17	0.03	4.72	0.68
- amino acids + ATG5 siRNA	24 (n=3)	0.30	0.07	0.08	0.00	0.41	0.02	0.07	0.02	0.37	0.06	0.38	0.02	7.30	1.10
	6 (n=3)	0.21	0.12	0.05	0.02	0.19	0.06	0.04	0.01	0.13	0.03	0.18	0.03	4.63	1.46
	o (n=3)	0.29	0.10	0.07	0.02	0.34	0.07	0.05	0.02	0.25	0.06	0.27	0.07	5.69	1.34
- amino acids + bafilomycin (10 nM)	24 (n=3)	0.54	0.40	0.11	0.05	0.52	0.33	0.11	0.07	0.41	0.26	0.46	0.29	11.46	6.51
	6 (n=3)	0.20	0.13	0.03	0.00	0.12	0.02	0.03	0.01	0.08	0.01	0.11	0.01	3.45	0.61
	0 (n=2)	0.27	0.01	0.07	0.00	0.28	0.01	0.08	0.04	0.19	0.03	0.23	0.01	6.74	2.69
- amino acids	24 (n=2)	0.38	0.18	0.09	0.02	0.38	0.13	0.09	0.01	0.27	0.15	0.30	0.11	8.64	0.01
	6 (n=3)	0.42	0.10	0.10	0.05	0.28	0.03	0.07	0.01	0.16	0.02	0.22	0.01	9.18	1.00
Control n(=4)		0.37	0.10	0.06	0.03	0.22	0.05	0.06	0.02	0.15	0.07	0.18	0.04	6.10	1.76
siRNA control (n=3)		0.38	0.06	0.08	0.03	0.28	0.06	0.06	0.02	0.22	0.06	0.25	0.06	6.23	1.19

303